ALTERRA

Long-term effects of climate change on carbon budgets of forests in Europe

K. Kramer & G.M.J. Mohren

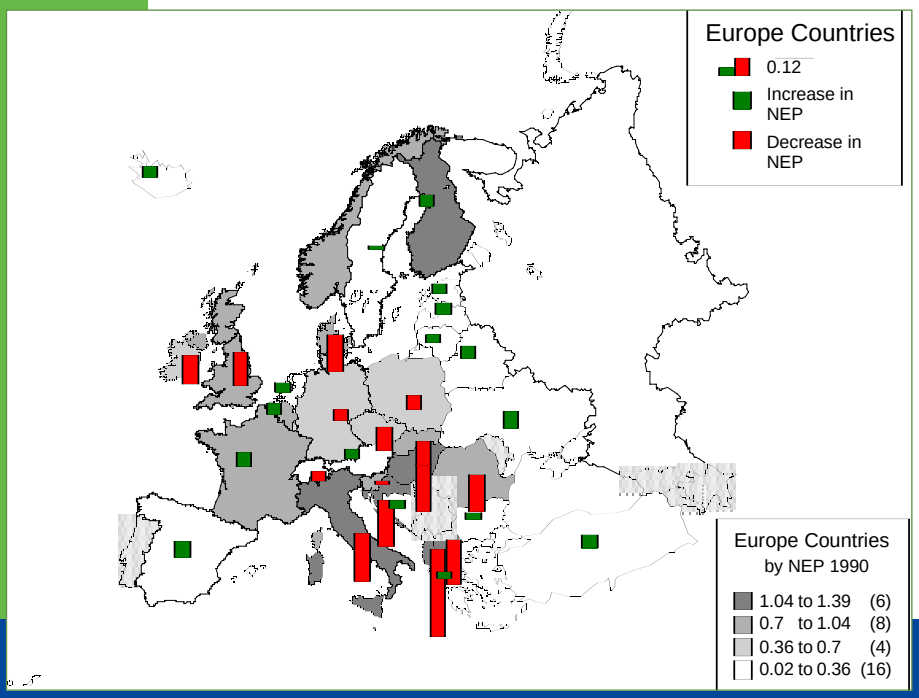

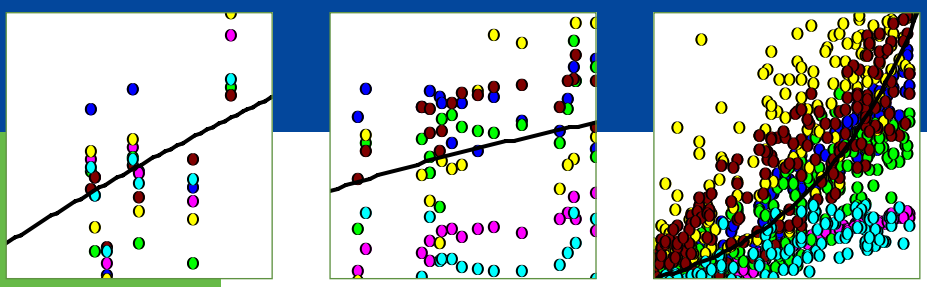

Alterra-report 194, ISSN 1566-7197

WAGENINGENUR

Long-term effects of climate change on carbon budgets of forests in Europe

Long-term effects of climate change on carbon budgets of forests in Europe

K. Kramer
G.M.J. Mohren

Alterra-report 194

Alterra, Green World Research, Wageningen, 2001

ABSTRACT

Kramer, K. & Mohren, G.M.J., 2001. Long-term effects of climate change on carbon budgets of forests in Europe. Wageningen, ALTERRA, Green World Research. report 194.

The EU-funded project *Long-term regional effects of climate change on European forests: impact assessment and consequenses for carbon budgets* (LTEEF-II, ENV4-CT97-0577) aimed to: i) assess likely responses of European forests to climate change; ii) quantify the fluxes of carbon and water between the vegetation and the atmosphere; iii) assess acclimation mechanisms of forests to climate change; iv) identify optimal regional forest management strategies; and v) to assess the carbon balance of the forest sector in Europe.
Several process-based models on forest growth at the stand scale were able to accurately represent both short-term flux data and long-term growth and yield data. However, the models diverged in their assessment of possible effects of climate change. Three approaches were applied to scale up to from the regional to the European scale and to assess the carbon budget of the European forests. Evaluation of different forest management strategies at the European scale was performed using the forest inventory approch. Remaining uncertainties include that currently available forest cover maps from different sources are inconsistent and that the different large scale model diverge in their assessment of the contribution of carbon stocks in trees versus soils and in their assessment of the magnitude of net primary production and heterotroph respiration.

Keywords: climate change, European carbon budget, forests, boreal, temperate, Mediterranean zone, model validation, process-based modeling, uncertainty analysis, upscaling, remote sensing, forest inventory data, biome scale modelling

P.O. Box 47, NL-6700 AA Wageningen (The Netherlands).
Phone: +31 317 474700; fax: +31 317 419000; e-mail: postkamer@alterra.wag-ur.nl

Alterra is the amalgamation of the Institute for Forestry and Nature Research (IBN) and the Winand Staring Centre for Integrated Land, Soil and Water Research (SC). The merger took place on 1 January 2000.

Project 344.36602.07 Alterra-rapport 194/HM/01-2001]

Contents

Summary

Forests are especially vulnerable to climate change, due to the longevity of trees and the expected climate change within their life span. Through its impact on forest growth, climate change will affect both long-term wood supply and carbon sequestration in trees, forest soils and wood products. The central objective of the LTEEF-II project was to assess climate change impacts on European forests with respect to water and carbon fluxes, regional differences, long-term effects and overall carbon budget for the forests in Europe. The results of this assessment is aimed to be used to identify sustainable forest management strategies that account for these impacts, and that maximise carbon sequestration. Extensive research has been performed over the last decades: i) determination how climate affects plant physiological processes and forest growth, both by experiments and by process-based models; ii) compilation and analysis of forest inventory data throughout Europe; iii) analysis and use of remote sensing data for NPP studies at the European scale; and iv) downscaling of climate change prediction to the regional scale. Using results of this, it is now feasible to make future projection of long-term impacts of climate change based on the main forest types of Europe (boreal, temperate, Mediterranean) , and to scale up from local to regional, national and European level. This was done by: A) assessment and process-based modelling of the long-term regional effects of climate change on European forests; and B) upscaling of such regional responses to the European scale by forest inventory data, biome scale modelling and remote sensing data.

The results include:

i) an assessment of the likely responses of forest to climate change in the main regions in Europe. Due to differences in the mechanisms driving forest growth in the boreal, temperate and Mediterranean region, differences in response between the forests are forecasted. There appears to be a regional differences, and the highest increase in the carbon sequestration is predicted for the boreal region. quantification of changes in fluxes of carbon and water between vegetation and the atmosphere, in both timing and magnitude. Most of the process-based models are able to accurately predict net fluxes of carbon and water. However, the analysis of the contribution of the different processes revealed that the models diverged in their results. Also models that do accurately predict the components contributing to the net fluxes, may strongly differ in their assessment to climate change response of the forest.

ii) assessment of possibilities of acclimation by means of self-regulating processes of existing forests. Long-term impacts responses to forests to climate change were analysed with respect to acclimation to water stress at different regions of Europe.

iii) identification of response strategies for forest management. The effects of different management strategies under the conditions climatic change on wood production at site level were analysed in the Mediterranean zone.

iv) assessment of the carbon balance for the forest sector. Four approaches were applied to assess the current stocks of carbon and the net annual change in thereof in the European forest. Three of these approaches were able to make

future projections. The results showed large uncertainty in the model predictions, indicated by the variation both in the estimates for the initial conditions and climatic change responses. Based on the forest inventory approach it can be concluded that if management of European forests were to change from its current use to a more multifunctional forest use, including an increase in harvesting due to an increased need of forest products in the future and allowing forests to increase in biodiversity and recreational values, also the carbon sequestration will increase. However, this effect is minor compared to the effects of the climatic change.

1 Introduction: forest growth and forest ecosystem carbon budgets in relation to climate change

G.M.J. Mohren & K. Kramer

The central objective of the LTEEF-II project was to assess climate change impacts on European forests, in terms of water and carbon fluxes, regional differences, long-term effects, and the overall carbon budget for forests in Europe. The results of this assessment were used to identify forest management strategies that account for these impacts, and that maximise carbon sequestration. The LTEEF-II project mainly consisted of A) assessment and modelling of the long-term regional impacts of climate change on European forests, and B) upscaling of these regional responses to the European scale, to quantify the overall carbon budget and sustainable wood supply of European forests. As part of the long-term impact assessment, emphasis was on growth rates and water relations (drought), and on possible adaptive strategies for forest management. The overall forest sector carbon budget was quantified under present climate and under expected future climate change.

The LTEEF-II project (1998-2000) comprised the second phase of a major research effort undertaken as part of the EU Environment and Climate research program under the 4th Framework Program of the European Commission. In the first phase of LTEEF (1994-1997), existing forest models where extended and applied to conditions representative of a range of sites throughout Europe, under present-day and future climate scenario's. In this part of the project, emphasis was on model development and model comparison (Mohren, 1999; Mohren & Kramer 1997). In the second phase of the LTEEF project (LTEEF-II), model performance was evaluated by application to the EUROFLUX sites, by comparing model output with the eddy-covariance flux estimates. (EUROFLUX was a largely EU-funded European flux network, in which carbon and water fluxes over forests were monitored using eddy-covariance techniques, at more than 15 sites in a range of forest types from northern Sweden to Italy). The model comparison was done in close collaboration with the EUROFLUX consortium, and the most recent experimental data, such as from the ECOCRAFT project (Jarvis, 1998), was used as input data to parameterise the process descriptions in the models. In addition to the comparison against flux data, the models were evaluated against long-term growth and yield data from permanent plots as used in traditional growth and yield research. Based on this model evaluation, regional impact studies were carried out to assess potential climate change impacts for a range of forest ecosystems throughout Europe. Using the models in combination with climate scenarios as identified from global climate modelling, forest management response strategies were identified, and evaluated with respect to the consequences for forest ecosystem carbon budgets. The regional impacts assessments were scaled up to a European level, using a) national forest inventory data and b) remote sensing techniques (Karjalainen *et al.*, 1997; Grace *et al.*, 1999; Veroustraete, 1994; Veroustraete *et al.* 1996). This resulted in estimates of the current carbon balance for the European forest sector, as well as assessments of

timber production and forest carbon budgets per country under future climate scenarios, including estimates of carbon sink strength.

1.1 Model evaluation

The proces models used were tested using the same site and species information so that differences as a consequence of differences in parametrisation is ruled out as much as possible. The criteria for the comparison and selection of models included: 1) model evaluation against short-term flux data; 2) model evaluation against long-term growth & yield data; 3) a sensitivity analysis, to determine the response of selected model output to climate change scenario's (temperature, CO_2 and precipitation, independently and jointly); 4) an uncertainty analysis to attribute uncertainties in the model output to uncertainties in model input; and 5) availability of technical documentation of the model.

1.2 Forest ecosystem carbon budgets

The components of the forest carbon budget include: the above- and below ground biomass, the soil organic matter and the forest products. A typical carbon budget of a managed forest is presented in Figure 1. A total of 15 Mg C $ha^{-1}yr^{-1}$ is annually fixed by gross photosynthesis. 7 Mg C $ha^{-1}yr^{-1}$ of this amount is transferred to the soil organic matter pool through litter fall and root turnover, 6 Mg C $ha^{-1}yr^{-1}$ of biomass C is respired, and an average annual increment of 2 Mg C $ha^{-1}yr^{-1}$, equivalent to some 8-10 m^3 $ha^{-1}yr^{-1}$ is harvested. The soil organic matter pool in this example releases somewhat less carbon as compared to the inputs through litter and root turnover, resulting in a net accumulation of 0.5 Mg C $ha^{-1}yr^{-1}$. The carbon in wood products that leave the forest is in the long-term brought back to the atmosphere by product decomposition. Consequently, the measured Net Ecosystem Exchange (NEE) of 2.5 Mg C $ha^{-1}yr^{-1}$ (15 Mg C $ha^{-1}yr^{-1}$ uptake by plant photosynthesis minus 12.5 Mg C $ha^{-1}yr^{-1}$ by ecosystem respiration) decreases to 0.5 Mg C $ha^{-1}yr^{-1}$ when product decomposition outside the forest is taken into account.

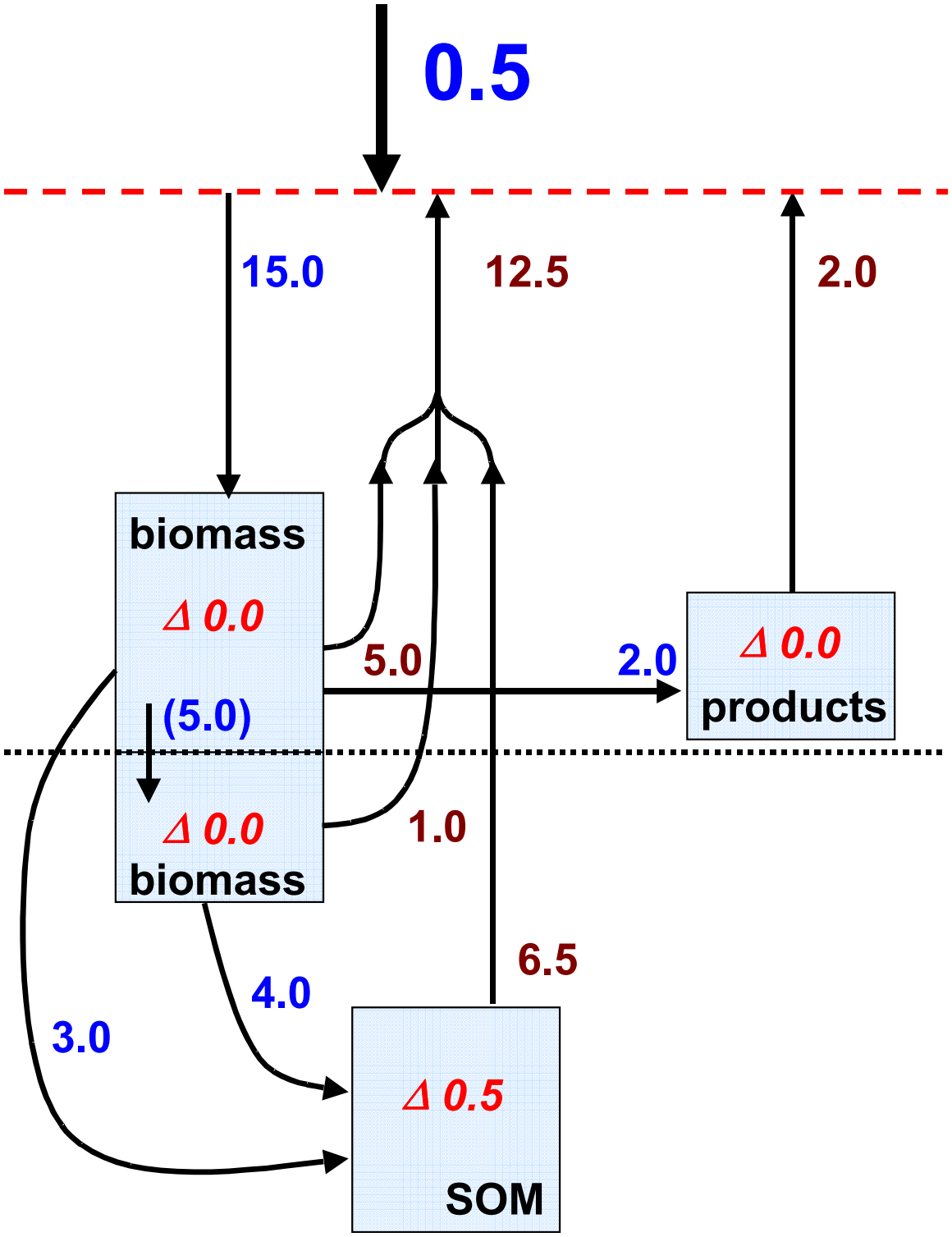

Figure 1.1: A general carbon budget for managed forest, accounting for wood harvest and product decay. All values refer to annual rates, in Mg C ha^{-1}yr^{-1}. Of the total annual uptake of 15 Mg C ha^{-1}yr^{-1}, 5 Mg C (35 %) is assumed to be allocated to below-ground biomass. Litter fall is assumed to be 3 Mg C ha^{-1}yr^{-1}, and root turnover is assumed to be equal to 4 Mg C ha^{-1}yr^{-1}. Average annual wood harvest is assumed to be equal to annual increment, i.e. 2 Mg C ha^{-1}yr^{-1}. The amount of carbon in soil organic matter (SOM) is assumed to accumulate at a rate of 0.5 Mg C ha^{-1}yr^{-1}. The total amount of carbon in products is assumed to be constant, hence the average amount of carbon harvested is equal to the amount of carbon released in product decomposition, i.e. 2 Mg C ha^{-1}yr^{-1}.

To assess the impacts of climate change on overall carbon budgets one needs to take into account all components described above, including the role of forest management. Changes in temperature, atmospheric CO_2 concentrations and precipitation directly affect the rates of gross photosynthesis and the decomposition of organic matter in the soil, which can be evaluated by process-based forest growth models. Forest management plays and important factor as it controls the rate at which carbon in woody products leaves the forest, and as it affects, through thinning and harvesting, also the growth rates of the remaining trees. Other disturbances of the forest ecosystem such as fires, storm, flooding and landslides need also be taken into account to quantify the carbon budget at the regional scale, but are outside the scope of this project.

1.3 Discussion and conclusions

The availability of fluxes of CO_2 and H_2O at the stand level provides an unprecedented opportunity to test stand-level forest growth models. Earlier attempts of this have been made (e.g. Vermetten et al, 1994), but the flux data currently collected by the EUROFLUX project and elsewhere in the world provide high resolution data that make model testing over a wide climatic range and over different forest types possible. In an earlier model comparison the different models showed highly divers results because of differences in model assumptions and description of processes (Sonntag, 1997). The availability of independent data now allowed selection of those models that are most relevant for specific climatic regions and forest types. This selection was critical to assess the sensitivity of the different forest types in Europe to changes in climatic parameters like temperature and precipitation, and atmospheric CO_2 concentration. Carefully formulated and validated models are the only means to do this as large scale experiments over long time horizons are impossible to perform. Sensitivity of model output to changes in climatic parameters provided insight into the relevance of the mechanisms involved in the impact of climate change on forests. The first of such sensitivity analyses have evaluated the importance of water and water-stress (Van Wijk *et al.*, 1999; Loustau *et al.* 1997), and the importance of differences between species in phenological response to temperature (Kramer, 1995; Kramer & Mohren, 1996).

The selection of models was also critical for the scaling up from the stand to the regional level in a future climate. The principle ways of scaling up were aplied in the LTEEF project: 1) by the adjustment of growth and yield tables of many forest types based on the sensitivity to climatic parameters of the selected forest growth models, combined with a large database of the distribution of these forest types over Europe; 2) by formulating simple models that adjust the radiation use efficiency (Bartelink *et al.*, 1997) also based on the sensitivity to climatic parameters of the selected forest growth models; and 3) simplified process models. These approaches allowed to assess the sink strength of European forests in the coming decades (Nabuurs & Mohren, 1995; Nabuurs *et al.*, 1997; Martin *et al.*, 1998).

1.4 References

Bartelink, H.H., K. Kramer & G.M.J. Mohren, 1997. Applicability of the radiation-use efficiency concept for simulating growth of mixed forest stands. *Agricultural and Forest Meteorology* **88**: 169-179.

Grace, J., F. Veroustraete & T. Karjalainen, 1999. A methodologies for estimating the forest carbon budget for Europe (in press, these proceedings).

Jansen M.J.W & Withagen J.C.M., 1997. USAGE: uncertainty and sensitivity analysis in a Genstat environment. *Manual. Report CBW*, 14 pp.

Jansen M.J.W., Rossing W.A.H. & R.A. Daamen, 1994. Monte Carlo estimation of uncertainty contributions from several independent multivariate sources. In: *J. Grasman & G. Verstraten (Eds.) Predictability and nonlinear modelling in natural sciences and economics.* Kluwer, Dordrecht, The Netherlands, pp. 334-343.

Jarvis, P.G. (ed.), 1998. European forests and global change. The likely impacts of rising CO_2 and temperature. *Cambridge University Press*, 380 pp.

Karjalainen, T., G.-J. Nabuurs & S. Kellomäki, 1997. Carbon sequestration in the forest sector under climate change: upscaling from the plot level to the European forest level. In: *G.M.J. Mohren, K. Kramer & S. Sabaté (eds.): Impacts of Global Change on Tree Physiology and Forest Ecosystems. Proceedings of an International Conference held* 26-29 November 1996, Wageningen, The Netherlands. Dordrecht, Kluwer Academic Publishers, p. 351-361.

Kramer, K., 1995. A modelling comparison to evaluate the importance of phenology on the effects of climate change on growth of temperate-zone deciduous trees. *Climate Research* **5**: 119-130.

Kramer, K. & G.M.J. Mohren, 1996. Sensitivity of FORGRO to climatic change scenarios. A case study on *Betula pubescens*, *Fagus sylvatica* and *Quercus robur* in The Netherlands. *Climate Change* **34**: 231-237.

Kramer, K., M.T. van Wijk, M.J.W. Jansen, E.M. Falge & G.M.J. Mohren, 1999. Application of the model FORGRO to 7 EUROFLUX sites: evaluation of climate change scenarios, long-term effects and uncertainty analysis. *Agricultural and Forest Meteorology*, submitted.

Loustau, D., P. Berbigier & K. Kramer, 1997. Sensitivity of the water balance of South-western France maritime pine forests to climate. In: *G.M.J. Mohren, K. Kramer & S. Sabaté (eds.): Impacts of Global Change on Tree Physiology and Forest Ecosystems.* Proceedings of an International Conference held 26-29 November 1996, Wageningen, The Netherlands. Dordrecht, Kluwer Academic Publishers, p. 193-205.

Magnani F., Borghetti M. & J. Grace, 1996. Carbon allocations and tree growth under hydraulic constraints in *Pinus sylvestris* L. In *Miglietta F., van Laar G. & J. Goudriaan (eds.): System Analysis and Simulation for Agricultural Science: a contribution of the RAISA Project.* CABO-DLO.

Magnani F., Leonardi S., Tognetti R., Grace J. & M. Borghetti 1998. Modelling the surface conductance of a road-leaf canopy: effects of partial decoupling from the atmosphere. *Plant Cell and Environment* **21**: 867-879.

Magnani F., Mencuccini M. & J. Grace, 1999. Age-related decline in stand productivity: the role of structural acclimation under hydraulic constraints. Submitted.

Martin, Ph. *et al.*, 1998. New estimate of the carbon sink strength of EU forests integrating flux measurements, field surveys, and space observations. *Ambio* **27**: 582-584.

Mohren, G.M.J., 1994. Modelling Norway spruce growth in relation to site conditions and atmospheric CO_2. In: *F. Veroustraete, R. Ceulemans et al. (eds.): Vegetation, Modelling and Climate Change Effects. SPB Academic Publishing,* The Hague, Netherlands, pp. 7-22.

Mohren, G.M.J., 1999. Long-Term Effects of CO2-Increase and Climate Change on European Forests (LTEEF: EV5V-CT94-0468). Proceedings EU-Climate Conference, *Orvieto*, in press.

Mohren, G.M.J., H.H. Bartelink, I.T.M. Jorritsma & K. Kramer 1993. A process-based growth model (FORGRO) for analysing forest dynamics in relation to environmental factors. In: *M.E.A. Broekmeyer, W. Vos & H. Koop (eds): European Forest Reserves.* Proceedings of the European Forest Reserves Workshop, 6-8 May 1992, The Netherlands. PUDOC, Wageningen, p. 273-279.

Mohren, G.M.J. & K. Kramer, 1997. Simulation of direct effects of CO_2 and temperature increase on forest growth: the LTEEF project. In: *G.M.J. Mohren, K. Kramer & S. Sabaté (eds.): Impacts of Global Change on Tree Physiology and Forest Ecosystems.* Proceedings of an International Conference held 26-29 November 1996, Wageningen, The Netherlands. Dordrecht, Kluwer Academic Publishers, p. 307-316.

Nabuurs, G.J., A.J. Dolman, E. Verkaik, A.P. Whitmore, W.P. Daamen, O. Oenema, P. Kabat, G.M.J. Mohren, 1999. Resolving the issues on terrestrial biospheric sinks in the Kyoto protocol. *Dutch National Research Programme on Global Air Pollution and Climate Change*, Report No. **410 200 030**, 100 pp.

Nabuurs, G.J. & G.M.J. Mohren, 1995. Carbon sequestering potential of selected world forest ecosystems. *Canadian Journal of Forest Research* **25**: 1157-1172.

Nabuurs, G.J., R. Päivinen, R. Sikkema & G.M.J. Mohren, 1997. The role of European forests in the global carbon cycle - a review. *Biomass and Bioenergy* **13**: 345-358.

Sonntag, M., 1997. Comparison of forest growth models at the leaf and canopy scale. In: *G.M.J. Mohren, K. Kramer & S. Sabaté (eds.): Impacts of Global Change on Tree Physiology and Forest Ecosystems*. Proceedings of an International Conference held 26-29 November 1996, Wageningen, The Netherlands. Dordrecht, Kluwer Academic Publishers, p. 299-306.

Van der Voet, H. & G.M.J. Mohren, 1994. An uncertainty analysis of the process-based growth model FORGRO. *Forest Ecology and Management* **69**: 157-166.

Van Wijk, M., S.C. Dekker, W. Bouten, F.C. Bosveld, W. Kohsiek, K. Kramer & G.M.J. Mohren, 1999. Evaluation of possibilities to incorporate water stress effects in three stomatal conductance models when modelling daily ecosystem fluxes of a Douglas fir forest. Submitted.

Vermetten, A., L. Ganzevel, A. Jeuken, P. Hofschreuder & G.M.J. Mohren, 1994. CO2 uptake by a stand of Douglas-fir: Flux measurements compared to model calculations. *Agricultural and Forest Meteorology* **72**: 57-80.

Veroustraete F., 1994. On the use of a simple deciduous forest model for the interpretation of climate change effects at the level of carbon dynamics. *Ecological Modelling* **75-76**: 221-237.

Veroustraete, F.,R. B. Myneni & J. Patyn, 1996. Estimating Net Ecosystem Exchange of Carbon Using the NDVI and an Ecosystem Model. *Remote Sensing of Environment* **58**: 115-130.

2 Representing the impact of climate change on physiological and ecosystem processes

Federico Magnani, Koen Kramer, Illka Leinonen, Giorgio Matteucci & Marco Borghetti

2.1 Introduction

The objective of the present chapter is to review the state of the art in representing and modeling the response of some key plant and ecosystem processes to atmospheric carbon dioxide and climatic variables, highlighting existing gaps in our understanding and pointing to the need for further research and model refinement.

As outilined in the previous chapter, it is widely accepted that the long-term effects of CO_2 increase and climate change on forest ecosystems can only be predicted through the application of process growth models, as we are asked to extrapolate our predictions outside the range of environmental conditions the forests have experienced yet and, due to their long life cycles and properties, forest trees and ecosystems cannot be easily subjected to long-term experimental manipulations. Based on our best understanding of basic physiological processes, process growth models have been greatly refined from the early reviews by Thornley (1976) and Landsberg (1986). In recent years, a number of models have been proposed, validated and challenged as tools for assessing the response of forests to CO_2 increase and climate change at the stand (Ryan *et al.* 1996, Thornley & Cannell 1996, Kirschbaum *et al.* 1998a, Peng & Apps 1999, Kirschbaum 1999, Magnani *et al.* 2000) and at the regional/global scale as well (Kimball *et al.* 1997, Cao & Woodward 1998, Cramer *et al.* 1999). In the following chapters a throughout application of process growth models to predict the long-term impact of CO_2 increase and climate change on European forest is going to be presented.

However, despite their widespread application, it is known that several key physiological processes still escape a full mechanistic understanding (Luo *et al.* 1999) and it is recognised that to develop operational models at the system level it is still necessary to accept that they may include both causal and empirical components (Makela *et al.* 2000).

Our analysis will concentrate on how models are currently dealing with the response to environmental factors of the following processes: leaf gas exchanges, carbon allocation, growth rates and age-related processes, respiration and decomposition, phenology.

2.2 Leaf gas exchange

The representation of the impact of climate change on leaf gas exchanges may require a good understanding on how photosynthesis and stomatal conductance are singularly regulated but even more on how their coordination is triggered by climatic factors and on how regulatory feed-backs are going on. From the first observation reported by Wong *et al.* (1979) of a constant linear relationship between stomatal conductance and photosynthesis, the hypothesis of a coordination in leaf gas exchanges has been confirmed by the observation that photosynthesis and stomatal conductance behave in such a way as to maintain the ratio of intercellular-to-atmospheric CO_2 concentration (c_i/c_a) at a constant value close to 0.7 for C_3 species (Leuning 1995, Jarvis *et al.* 1999). A recent review of the long-term effects of elevated CO_2 has confirmed that c_i/c_a is almost identical in plants grown in ambient and doubled c_a (Drake, Gonzalez-Meler & Long 1997). On the other hand, the trade-off between assimilation and transpiration, which is captured by the concept of plant water use efficiency (amount of CO_2 absorbed per unit of H_2O transpired), is largely determined by the shape and value of the stomatal response so that the absorption of carbon is largely limited by the constraints imposed by soil water deficits on stomatal conductance and transpiration.

As we are going to see, current models are dealing conveniently with a number of aspects, but we still lack a general mechanistic representation of the coordinated response of photosynthesis and stomatal conductance to combined environmental stimuli.

2.2.1 Photosynthesis and leaf properties

After the mechanistic representation proposed by Farquhar *et al.* (1980), which is now assumed as a standard, modeling the effects of CO_2 intercellular concentration and temperature on plant assimilation in C_3 species is a task that can be answered with a good degree of confidence.

In the Farquhar's model, plant assimilation is assumed to be limited by either the rate of ribulose 1-5 biphosphate (Rubp) regeneration through the photosynthetic carbon reduction cycle, i.e. by light availability and electron transport rate, or by the capacity of the enzyme Rubp carboxylase-oxygenase (Rubisco). According to these constraints, leaf net photosynthesis A can be expressed as:

$$A = V_c - 0.5 \cdot V_o - R_d = V_c \cdot \left| 1 - \frac{0.5 \cdot O}{\tau \cdot C_c} \right| - R_d \qquad (2.1)$$

where V_c and V_o are rates of carboxylation and oxygenation of Rubisco, R_d is leaf dark respiration, τ is a specificity factor for Rubisco and O and C_c are the partial pressures of O_2 and CO_2 in equilibrium with their dissolved concentrations at the site of oxygenation and carboxylation.

The rate of carboxylation is assumed to be limited alternatively by two co-occurring processes:

$$V_c = \min\{W_c, W_j\} \tag{2.2}$$

where W_c is the rate of carboxylation limited solely by the amount, activation state and kinetic properties of Rubisco and obeys Michaelis-Menten kinetics with two competing substrates, O_2 and CO_2:

$$W_c = \frac{V_{c\,max} \cdot C_c}{C_c + K_c \cdot \left(1 + \frac{O}{K_o}\right)} \tag{2.3}$$

where V_{cmax} is maximum carboxylation rate and K_c and K_o are Michaelis-Menten constants for carboxylation and oxygenation, respectively.

The rate of carboxylation limited solely by the rate of Rubisco regeneration in the Calvin cycle (W_j) is a function of the rate of electron transport J:

$$W_j = \frac{J \cdot C_c}{4 \cdot (C_c + O/\tau)} \tag{2.4}$$

Unique relationships can be used to estimate the dependence of Farquhar's photosynthetic parameters (electron transport rate, Rubisco activity, dark respiration rate) on nitrogen content per unit leaf area in a large number of species (Wullschleger 1993, Leuning 1997, Le Roux 1999). Nitrogen content and leaf mass per unit leaf area have been successfully used as covariables to describe photosynthetic capacity in multilayers models of canopy photosynthesis based on the Farquhar's representation (Raulier *et al.* 1999, Carswell *et al.* 2000).

Partly as a result of the increasing confidence in the representation proposed by Farquhar *et al.* (1980), the simplistic assumption has been often made that the response of plant growth to CO_2 is just a reflection of the photosynthetic response, although in this way the effects of important interactions may go missed (Lloyd & Farquhar 1996).

The interaction between CO_2, temperature and light should be properly accounted for when modeling photosynthesis. Under both 'light limited' and 'enzyme-limited' conditions, the dependence of assimilation on CO_2 concentrations is described by a hyperbolic function: after an almost linear increase at low CO_2 concentrations, assimilation levels off at a value of c_a that depends on leaf temperature, generally increasing under warmer conditions. As a result, assimilation appears to be most sensitive to elevated CO_2 under warm conditions (Morison & Lawlor 1999). As a rule, under given environmental conditions assimilation rates increase until an optimum temperature is reached and then decline as a result of the negative effects

of high temperatures on enzymatic activity; Day (2000) reports, in *Picea rubens*, a flat response of net photosynthesis to temperatures in the range 16-32 ^{0}C, whilst temperatures between 32 and 36 ^{0}C markedly decreased photosynthesis. Using a model of C_3 photosynthesis and assuming a constant c_i/c_a ratio, Long (1991) has shown that the temperature optimum for light-saturated photosynthesis increases by 5 °C with an increase in c_a from 35 to 65 Pa. The photosynthetic response to light is also affected by temperature and CO_2: the decline of maximum quantum yield of photosynthesis with increasing temperature is reduced at elevated CO_2, as is the increase with temperature in the light compensation point. Compensating effects are likely to be found, on the other hand, at the canopy level: modeling the influence of temperature on canopy photosynthesis by a coupled leaf photosynthesis-stomatal conductance model, Raulier *et al.* (2000) found that within a broad range of values temperature had a minor effect on canopy assimilation.

Leaf assimilation can be limited by the accumulation of photosynthetic products inside the cell and, ultimately, by the rate of carbon export from the leaf through the phloem (Sharkey 1985). Such a limitation could have an important role in the down-regulation of photosynthesis under elevated CO_2, if higher photosynthetic rates were not matched by an increased utilisation of carbohydrates in growth. This 'end product inhibition' of photosynthesis, however, is not generally assumed to be a long-term regulator of carbon metabolism, because the plant eventually adjusts the concentration of photosynthetic enzymes and other factors to bring carbon assimilation and utilisation into balance (Wolfe *et al.* 1998). Detailed dynamic models of leaf photosynthesis have been proposed by Pearcy *et al.* (1997) and Kirschbaum *et al.* (1998b), which explicitely considers the build up of photosynthetic intermediates and can therefore account for the rapid response of photosynthesis under conditions of fluctuating light, such as would be experienced by understorey plants or by leaves deep down in the canopy.

Over the long-term, leaf photosynthetic response does not play in isolation, as other processes such as carbon export and respiration, nutrient uptake and ultimately growth lead to a complex acclimation of plant structure and function to environmental conditions.

A prolonged exposure to elevated CO_2 results in a profound modification of plant biochemical and structural properties (Wolfe *et al.* 1998). At the leaf level, it has been often observed that the short-term stimulatory effect of elevated CO_2 on photosynthesis is followed by a partial down-regulation of photosynthetic processes. In a meta-analysis of experimental results from 15 field-based elevated CO_2 experiments, Medlyn *et al.* (1999) concluded that a down-regulation of both potential electron transport rate and maximum Rubisco activity of the order of 10% is commonly observed; in these experiments plants were not constrained by pot dimensions so that the possibility of an experimental artifact can be excluded, confirming the view that some level of downward acclimation should be expected even in plants with unrestricted root growth in the field (Wolfe *et al.* 1998). Photosynthetic down-regulation could be interpreted as the result of a decline in leaf nitrogen concentration, as the same tight relationship with nitrogen content of

electron transport capacity and Rubisco activity, reported for a large number of species under ambient conditions (Wullschleger 1993, Leuning 1997, Le Roux 1999), was observed in plants grown under elevated CO_2 (Medlyn *et al.* 1999). On the other hand, the expected reallocation of leaf nitrogen away from Rubisco and towards light-utilisation complexes (Wolfe *et al.* 1998), that would respond to the principle of optimal use of limited resources, was not generally observed (Rey & Jarvis 1998, Medlyn *et al.* 1999). Poorter *et al.* (1997) concluded that the main effect of elevated CO_2 on the chemical composition of C_3 species was an increase in leaf non-structural carbohydrates, together with a minor decline in the leaf content of organic nitrogen compounds and nutrients.

Such a variation in leaf biochemical composition can be readily explained in terms of carbon and nitrogen budgets at the leaf and plant level. Dewar *et al.* (1998) presented a simple model of leaf biochemical processes, based on the assumption that a variable fraction of leaf carbohydrates is exported from the leaf, the remaining being used to provide the substrate and energy needed for the maintenance of leaf proteins. Once it is recognised that photosynthesis is a direct function of leaf nitrogen content and that exported carbohydrates are needed for nutrient uptake by the roots, the model shows that growth is maximised under elevated CO_2 by increasing the fraction of carbon exported to the roots, so as to increase nitrogen uptake and prevent an excessive reduction of carboxylation rates, but that nevertheless the nitrogen content of the leaf is bound to decline. This is accompanied by a marked increase in the content of non-structural carbohydrates, in good agreement with experimental evidence (Poorter *et al.* 1997). The same general pattern is predicted by the Thornley transport-resistance model of carbon and nitrogen allocation (Thornley 1972). A more detailed qualitative model of photosynthetic acclimation to elevated CO_2 that tries to explicitely account for all the metabolic pathways involved has recently been proposed by Moore *et al.* (1999), but a quantitative mathematical formulation is still missing.

Leaf morphology and specific leaf area are also known to be affected by elevated CO_2 (Wolfe *et al.* 1998); thicker leaves are generally produced, with profound effects on the return, in terms of light interception, coming from carbon investment in foliage growth. This could be simply related to the reduction in leaf nitrogen content under elevated CO_2 . Reich *et al.* (1999) have recently observed a consistent link across species and biomes between leaf structural characteristics and nitrogen content. Schulze *et al.* (1994), however, reported that such a broad relationship between specific leaf area and leaf nitrogen concentration at the global scale breaks down when intra-specific variation in response to environmental conditions is considered.

Overall, existing models appear to be able to account properly for the downward acclimation of leaf biochemical characteristics to elevated CO_2, as long as the interaction between carbon and nitrogen cycles is duly considered at a whole plant level. We are still unable to account for structural acclimation, on the contrary, at a more than just empirical level.

2.2.2 Stomatal conductance

A full description of the response of leaf gas exchange to atmospheric carbon dioxide and temperature requires an understanding of the parallel response of stomata, which determines the concentration of CO_2 in the leaf intercellular spaces and sets transpiration rates. However, despite the relevance of stomatal control in the regulation of both photosynthesis and transpiration, no mechanistic understanding of stomatal behaviour has been reached so far (Monteith 1995, Assmann 1999). Models are generally based on either an empirical or a goal-seeking approach; in particular, phenomenolgical models have been widely used to predict diurnal and seasonal variability of stomatal conductance as a function of environmental factors and multiplicative environmental-constraint functions of stomatal conductance are often applied at the canopy level (Whitehead 1998).

In recent years models that couple stomatal conductance to photosynthesis at the leaf scale are being used more widely and have been reported to be superior to climate-only related models in describing conductances across species and structural properties (Moren 1999). Time constants have also been added to static models to construct dynamic models that explained better the stomatal response to rapidly changing environmental conditions (Rayment *et al.* 2000).

The semi-empirical models proposed by Ball *et al.* (1987) and Leuning (1995) are most commonly applied. The two models differ only in their representation of the effects of air humidity, but both assume that the stomatal response to CO_2 is mediated by photosynthetic rates, in agreement with experimental evidence (Wong *et al.* 1979). A functional explaination for such a link is provided by the hypothesis that the regulation of anion channels in the guard cell membrane, which is largely responsible for stomatal opening, is triggered by malate concentration in the guard cell apoplast, which is itself a function of leaf assimilation rates (Hedrich *et al.* 1994). A comparison of the Ball-Berry and Leuning models for their suitability to incorporate a soil water stress function in their formulation and for their performance in modeling forest ecosystem fluxes is provided by Van-Wijk *et al.* (2000).

A regulatory function on stomatal opening of ATP mesophyll concentration, presumably because of its putative role in active ion pumping at the guard cell plasmalemma, and of a carbon-fixation substrate, whose pool in the mesophyll is modulated by photosynthetic rates, are assumed in the stomatal models proposed by Farquhar and Wong (1984) and Jarvis and Davies (1998), respectively. In both models the concentration of regulatory compounds is increased by photosynthetic light reactions and depleted by dark reactions, so that they capture rather well the response of stomatal conductance and photosynthesis to the environment. However, the involvement of mesophyll reactions in stomatal control is not supported by the observation that the response of guard cells to CO_2 is maintained in detached epidermal strips, where no photosynthesis takes place, and would suggest the co-existance of more than one mechanism of action (Assmann 1999).

An alternative way of representing gas exchange response to the environment has been based on the optimality approach first proposed by Cowan (1977): the hypothesis is made that transpiration, which comes with stomatal opening, represents a cost for the plant, and that stomata are regulated in such a way as to balance such a cost with the advantage of increased photosynthesis. Such a goal-seeking approach has indeed successfully predicted leaf gas exchange under present environmental conditions (Berninger, Mäkelä & Hari 1996; Hari, Mäkelä & Pohja 2000), although Thomas *et al.* (1999) warned that stomatal optimization was only partial in a number of tropical species. It should be noted, moreover, that existing analytical solutions to the problem of gas exchange optimisation are based on the assumption of a linear response of assimilation to intercellular CO_2 concentration, which runs contrary both to detailed photosynthetic models and to a large body of experimental evidence. Such an assumption could lead to considerable errors when applied to the prediction of plant response to climate change. Friend (1991), on the other hand, resorted to numerical means to couple a model of optimal stomatal behaviour to the Farquhar model of photosynthesis, so predicting in a convenient way the saturating response of assimilation to elevated CO_2, as well as the maintenance of the ratio of intercellular to ambient CO_2 concentrations under a wide range of C_a and environmental conditions that is the basis of the empirical models described above. One would therefore expect these empirical models to imply a quasi-optimal stomatal response.

Overall, there seems to be a general agreement on how to represent the effects of CO_2 on stomatal conductance, although no full physiological understanding has been reached of the mechanisms involved.

The stomatal response to air and soil humidity, on the contrary, is still a matter of debate. Air vapour pressure deficit is expected to increase under climate change scenarios as a result of the predicted rise in temperature, although the effect could be partly counterbalanced by an increase in ocean and terrestrial evapotranspiration. Such an indirect effect of temperature is particularly important for stomata, which are known to be highly sensitive to atmospheric humidity (Grantz 1990).

A linear decline in stomatal conductance with a reduction in relative humidity is assumed in the model of Ball *et al.* (1987). Despite the model ability to represent the stomatal behaviour of a number of species, however, a direct effect of relative humidity has been experimentally disproved (Aphalo & Jarvis 1991). Elegant work by Mott and Parkhurst (1991) demonstrated that stomata respond to transpiration rates rather than air humidity *per se*. This is captured by the model proposed by Monteith (1995), which predicts a linear decline in stomatal conductance with increasing leaf transpiration. Since transpiration is itself the product of stomatal conductance and leaf-to-air vapour pressure deficit, however, such a linear response to transpiration is fully equivalent to assuming an hyperbolic decline of stomatal conductance with increasing vapour pressure deficit, as first proposed by Lohammar *et al.* (1980) and implemented in the semi-empirical model of Leuning (1995). A functional interpretation of Leuning's model based on the representation of the gradients in

water potential and of water transport between guard cells and epidermal cells has been proposed by Dewar (1995).

The implications for forest hydrology of such a stomatal response is relevant: in response to increasing vapour pressure deficits, leaf transpiration would increase asymptotically to a constant value, that would be reached at a value of vapour pressure deficit of about 2 kPa. As a result, any reductions in air humidity brought about by climate change would most strongly affect plants growing under moist conditions, whose leaf transpiration is still highly sensitive to vapour pressure deficit, but would have only a marginal effect under drier climates where maximum transpiration rates are already reached under present conditions. Under these conditions, soil water availability would play a far more important role than air humidity.

A recent meta-analysis of literature data (Oren *et al.* 1999) suggests that relative stomatal sensitivity to air vapour pressure deficit could be rather conservative, changing little between species and as a result of growing conditions. As a result, leaf transpiration should approach its maximum at a constant vapour pressure deficit of about 2 kPa, irrespective of species or environment. Bunce (1998), on the other hand, reported significant differences in relative stomatal sensitivity to vapour pressure deficit between plants grown at a range of temperatures, carbon dioxide concentrations and light conditions. Even more interesting, for scaling purposes across species and environments, is the report (Franks & Farquhar 1999) of a linear relationship across species between stomatal sensitivity to vapour pressure deficit and the ratio of intercellular-to-ambient carbon dioxide concentration, that is determined, as already discussed, by stomatal sensitivity to ambient CO_2 concentration and photosynthesis. Whether this holds true also in response to a change in growth conditions remains to be seen.

Overall, the semi-empirical models described above prouved to be able to describe succesfully the response of stomata to environmental stimuli in well-watered plants, whilst no general solution has been reached so far to incorporate the influence of plant water status and soil water deficits on stomatal conductance.

Recent studies have suggested that the effect of transpiration on stomata could be mediated by leaf water potential (Saliendra, Sperry & Comstock 1995; Fuchs & Livingston 1996; Comstock & Mencuccini 1998). The movement of water across a series of hydraulic resistances in the soil-plant continuum can induce very negative leaf water potentials, with detrimental effects on xylem integrity, foliage growth and survival (Tyree & Sperry 1989).

It has been suggested that, in order to prevent an excessive dehydration, the plant would close stomata in dry air, so limiting xylem cavitation and loss of hydraulic conductivity (Jones & Sutherland 1991); on the other hand experimental evidence is available that short term changes in stomatal conductance and the sensitivity of stomatal closure to increasing vapour pressure deficit are linked to the hydraulic properties of the conducting system (Comstock 2000). Therefore, homeostatic

mechanisms are suggested that operate to ensure the long-term balance between evaporative demand and the potential hydraulic conductivity of trees growing in different environments (Whitehead 1998). Such an homeostatic response constitutes the basis of the canopy gas exchange model of Williams *et al.* (1996), which assumes that stomatal conductance throughout the canopy is jointly regulated by light, nitrogen availability, air humidity and soil-plant hydraulic properties.

The role of soil-to-leaf hydraulic resistance in stomatal control could help explain the different response of stomatal conductance and assimilation to soil spring temperatures observed under boreal conditions. The hydraulic resistance of the soil-plant continuum is known to be strongly affected by root and soil temperature (Pavel and Fereres 1998), and to increase dramatically when soil water freezes during the winter. By carefully warming the soil in a *Picea abies* stand, Bergh and Linder (1999) were able to demonstrate that stomatal conductance can be limthited by the availability of liquid water in the soil, independently of leaf photosynthetic potential. Soil warming early in the spring induced a quick recovery of plant transpiration, but had only a limited effect on photosynthesis.

Limitations of plant water use and transpiration imposed by rhizosphere and xylematic conductance have been explored with a model by Sperry et al. (1998) and Bond and Kavanagh (1999) succesfully predicted stomatal conductance in four woody species with a model linking leaf-specific hydraulic conductance and a threshold leaf water potential.

Uncertainty also exists about the response of stomata to soil water availability, which is also expected to be affected by climate change. Other than the direct effects of leaf water potential, stomata do also respond to soil water status (Schulze 1993), as already recognized in early empirical stomatal models (Jarvis 1976), presumably via a chemical messenger produced in the roots in response to dehydration. Abscisic acid (ABA) is regarded as the most likely candidate. A role of abscisic acid has also been suggested in the response of stomata to air humidity and transpiration rates, through its accumulation in mesophyll cells in proximity of the guard cells (Jarvis & Davies 1997). The latest experimental evidence, however, points to an interacting regulation of stomatal conductance by hydraulic and chemical signals, possibly mediated by the effects of leaf water potential on apoplastic pH and ABA sequestration (Netting 2000). In large woody plants the short-term response of stomata may be brought about by hydraulic signals that affect stomatal conductance by triggering the release of ABA in the leaves. Tardieu and Davis (1993) and Tardieu and Simonneau (1998) developed an interactive model that incorporates, although in a semi-empirical way, hydraulic and chemical effects to describe the response of stomatal to soil drying and evaporative demand.

On the other hand, in a field study on several temperate deciduous species, stomatal conducance was generally better correlated with environmental variables than with plant variables (xylem sap ABA concentration, xylem sap pH) and response surface models incorporating environmental variables were more succesfull at explaining the variation of stomatal conductance across species (Auge *et al.* 2000).

2.2.3 Water use efficiency: an analysis of its dependence on the climate

Under conditions of high light availability and low soil water content, resulting in partial stomatal closure, conditions of Rubp-limited photosynthesis would prevail and the amount of carbon absorbed by the plant will be constrained by the availability of water for transpiration (Dewar 1997). Water use efficiency (WUE) should viewed as a key plant functional trait under water-limited conditions and its response to environmental conditions worth to be explored.

The response of water use efficiency to the environment is strongly affected by the shape and value of the stomatal response to the environment. This can be exemplified by the comparison of the implications of two alternative stomatal models.

Jones (1992) explored the implications for water use efficiency of the assumption of a constant ratio between intercellular and atmospheric CO_2 concentrations (Wong *et al.* 1979). From the mass-balance equation, assimilation rate A can be expressed as:

$$A = \frac{g_s^c \cdot \left(c_a - c_i\right)}{P} = \frac{g_s^c \cdot c_a \cdot \left| 1 - \frac{c_i}{c_a} \right|}{P} \tag{2.5}$$

where g_s^c is stomatal conductance to CO_2, c_a and c_i are atmospheric and internal CO_2 concentration and P is atmospheric pressure. If a constant value of 0.7 is assumed for the ratio c_i / c_a in C_3 species (Wong *et al.* 1979), Eq. 5 can be expressed as:

$$A \approx \frac{g_s^c \cdot c_a \cdot 0.3}{P} \tag{2.6}$$

Transpiration from well-coupled leaves can be assumed to equal imposed transpiration and can be therefore expressed as:

$$E \approx 1.6 \cdot g_s^c \cdot \frac{D}{P} \tag{2.7}$$

When Eqs. 6 and 7 are combined, the dependency of water use efficiency upon air vapour pressure D can be expressed as:

$$WUE = \frac{A}{E} = \frac{c_a \cdot 0.3}{1.6 \cdot D} \tag{2.8a}$$

$$WUE = \mathrm{b}_1 \cdot \frac{1}{D} \tag{2.8b}$$

Equation 2.8b predicts a hyperbolic decline of water use efficiency, tending to zero in very dry air; that is, extreme air dryness would limit assimilation much more than transpiration rates.

However, a different picture emerges when other state-of-the-art stomatal models are applied. Leuning (1995), for example, suggested that the linear relationship between stomatal conductance and photosynthesis is modulated by air vapour pressure deficit:

$$g_s^c = \mathrm{a}_1 \cdot \frac{A}{c_a - \Gamma} \cdot \frac{D_0}{D + D_0} \tag{2.9}$$

where Γ is the CO_2 compensation point and a_1 and D_0 are empirical coefficients. Leaf transpiration can be therefore expressed as:

$$E \approx 1.6 \cdot \mathrm{a}_1 \cdot \frac{A}{P \cdot \left(c_a - \Gamma\right)} \cdot \frac{D_0 \cdot D}{D + D_0} \tag{2.10}$$

and the dependence of water use efficiency upon air vapour pressure deficit can be represented as:

$$WUE = \frac{A}{E} = \frac{P \cdot \left(c_a - \Gamma\right)}{1.6 \cdot \mathrm{a}_1} \cdot \frac{D + D_0}{D_0 \cdot D} \tag{2.11a}$$

$$WUE = \mathrm{b}_2 \cdot \left| \frac{1}{D} + \frac{1}{D_0} \right| \tag{2.11b}$$

As in Eq. 2.8b, WUE is expected to decline hyperbolically; however, it would not tend to zero but to a finite value. Based on experimental values of the parameter D_0 (Leuning 1995), the limit of WUE in very dry air would be just half the value at a vapor pressure deficit of 1 kPa.

Long-term eddy covariance records (e.g. Valentini *et al.* 2000) provides concurrent data of canopy transpiration and photosynthesis under variable conditions of air and soil humidity that could allow to depict the response of WUE to the climate and test alternative models of canopy stomatal conductance. It is worth remembering that year-to-year changes in water use efficiency (WUE) can be estimated in trees from the measurement of carbon isotope discrimination ($\Delta^{13}C$) among annual growth rings (Francey & Farquhar 1982; Dupouey *et al.*1993) and that the seasonal development of WUE can also be derived from within-ring variations in $\Delta^{13}C$, combined with the continuous measurement of tree radial increments (MacFarlane & Adams 1998; Walcroft *et al.*1997; Livingston & Spittlehouse 1996).

The availability and application of simple functional models of water use efficiency would result in the production of look-up tables depicting the response of WUE to the climate for the most important forest types, as a useful predictive tool for climate change research.

2.3 Respiration and decomposition processes

Approximately equal amounts of CO_2 are exchanged every year between the terrestrial higher plants and the atmosphere through photosynthesis and respiration processes (Amthor 1995). The major role of ecosystem respiration in determining the geographic pattern of net ecosystem exchange (*NEE*) has been recently documented in a number of forests growing across a latitudinal gradient in Europe (Valentini *et al.* 2000). Hence, respiration has the potential to be as important as photosynthesis in determining the carbon balance of trees and forests and any model aimed to predict the long-term impact of climate change on forest ecosystems and their carbon balance should include a proper representation of respiration and decomposition. In the following paragraphs, the current way of representing, in process models, respiration processes and the impact on them of climate change is briefly reviewed.

2.3.1 Plant respiration

There is still no a mechanistic model for plant respiration (*R*) equivalent to the one proposed by Farquhar for photosynthesis. This may sound as rather surprising, given the ubiquitous nature of respiration in both plants and animals. Most workers still accept and apply the modelling approach of McCree (1974), distinguishing between the growth and the maintenance components of plant respiration. However, Thornley & Cannell (2000) recently explored alternative approaches to modelling plant respiration.

Growth respiration is related to plant biomass increment: it can be viewed as a 'construction cost', which may depend on the compounds synthesized; however the construction cost per unit of biomass is generally rather constant (Cannell & Thornley 2000). Growth respiration is commonly held to be insensitive to temperature; environmental factors can influence growth respiration by limiting growth itself or inducing changes in allocation patterns that distribute carbon to tissues with different construction costs. The maintenance component of respiration is assumed, on the contrary, to respond exponentially to temperature, generally according to the Arrhenius model which, over the 0-50 °C temperature range, mimics the Q_{10} relationship (Ryan 1991). Maintenance coefficients are different for different plant organs (leaves, stem, roots) and a careful evaluation of parameters is necessary to increase model performance (Cannell & Thornley 2000).

Plant respiration can be also represented as the sum of different component processes; for a number of these processes the 'specific unit cost' (i.e. the respiratory cost per unit of process) has been measured or defined, paving the road towards

more detailed models where the single components of respiration are accounted for quantitatively (Cannell & Thornley 2000). For instance, better representations are obtained when maintenance respiration is related to carbohydrates supply and the rates of energy-requiring processes (Thornley & Cannell 2000); due to its sensitivity to environmental factors, a detailed representation of the maintenance component should provide better estimates of plant respiration in a changing environment (Ryan 1991). In a promising approach, regulation and limitations to respiratory fluxes have been linked to the rate of supply of photosynthetic carbohydrates (Dewar *et al.* 1999, Thornley & Cannell 2000). Nitrogen content has been also reported to be linearly related to maintenance respiration, often being a better predictor of respiration rates than plant biomass or volume (Ryan 1991, Ryan *et al.* 1996b).

Based on short-term experiments, tissue respiration is generally expected to increase with temperature, whilst photosynthesis is known to decline beyond an optimal temperature value. Due to this contrasting response, climate change and the expected temperature increase may result in an increase in the respiration/assimilation (R/A) ratio. However, long-term experimental evidence does not support this view. Respiration seems to track photosynthesis, which provides the substrate for respiration, so that the R/A ratio keeps remarkably constant when temperature is artificially changed (Gifford 1995). Most available information comes from annual crops. Also in *Eucalyptus pauciflora*, however, Atkin *et al.* (2000) reported a significant acclimation of leaf respiration to temperature even on a seasonal basis, so that relatively little difference was observed in total daily respiration in winter and summer; interestingly, acclimation of respiration to temperature occurred in as little as 1-3 days, and was associated with a change in the concentration of soluble sugars, under controlled conditions but not in the field. Respiration rates of tree stems were found to change over the season independently from temperature, probably as a result of variable contribution of maintenance and growth components but possibly involving acclimation processes (Lavigne & Ryan 1997). Respiration rates of vegetation grown in warm environments are often lower than those measured in cooler environments, particularly when measured at warm temperatures (Ryan 1991). The acclimation of respiration to temperature may account for the observation that forest stands growing under widely different climates show similar or quasi-constant R/A ratios (Waring, Landsberg & Williams 1998). Anyhow, in some situations and developmental stages R/A ratio do change, so that Cannell & Thornley (2000) suggest that it should be treated in models as a constrained function more than as a constant.

Some insight into the homeostasis of the R/A ratio comes from a recently proposed leaf biochemical model (Dewar *et al.* 1998, 1999). In the model, leaf photosynthesis and maintenance respiration are proposed to be intimately linked, since respiration is assumed to use a constant fraction of available carbohydrates to continuously repair the photosynthetic apparatus. As a result, any reduction in maintenance respiration would lead to a reduction in leaf photosynthetic potential, whilst an increase of assimilation would result in a parallel increase of maintenance respiration. Even if different temperature responses are assumed for carboxylation and labile carbon utilisation, the R/A ratio is predicted to return to its initial value after a short-term

increase following a step increase in leaf temperature. The short-term positive temperature response of R/A is linked to a transient dynamics of carbon and proteins pools, whilst, in the long-term, the homeostasis of R/A with temperature occurs as these pools come to a steady-state (Dewar *et al.* 1999).

Such an homeostasis in the *R/A* ratio is not expected, on the contrary, in response to an increase in atmospheric CO_2 concentration, which exerts both direct and indirect effects on respiratory processes (Amthor 1995, Dewar *et al.* 1998). Indirect effects are related to changes in plant tissue composition that often occur under elevated C_a. In the model developed by Dewar *et al.* (1998), optimal growth under elevated C_a can only be achieved by increasing the fraction of carbohydrates allocated to nutrient uptake, whilst reducing leaf protein turnover and the associated maintenance respiration. Assuming an optimal acclimation to elevated C_a, maintenance respiration is therefore expected to decline in parallel with leaf protein content. A review of available experimental evidence (Drake *et al.* 1999) suggests indeed a general decline in tissue respiration under elevated CO_2. Over the long-term an average 5% decline is observed (Drake *et al.* 1997), which often closely matches the reduction in tissue nitrogen content and increase in soluble carbohydrates in plants grown at elevated CO_2. This is in good agreement with the general assumption that maintenance respiration per unit biomass is proportional to tissue nitrogen content (Ryan *et al.* 1996b), and is well captured by models based on the transport-resistance approach of Thornley (1972). The response of mitochondrial respiration to CO_2, however, seems to involve several components. In the short-term, a rather large reduction of up to 20% in specific respiration rate is supposed to result from the inhibition of two mitochondrial electron transport enzymes (Gonzàlez-Meyer *et al.* 1996, Drake *et al.* 1999). This is not taken into account by simulation models yet.

Overall, it seems that representing respiration rates as coupled to substrate concentrations and availability could make plant respiration models more realistic. Also, accounting for the different components of maintenance respiration into models could increase their capacity to represent the impact of climate change, as far as the inceasing experimental evidence will result in a more reliable model parametrization.

2.3.2 Soil respiration and decomposition

The emission of CO_2 by soils, related to both root respiration and soil organic matter (SOM) decomposition, has been reported to make up 60-70% of total ecosystem respiration (Janssens *et al.* 2000). Thus, respiratory processes in the soil are known to be just as important as plant net productivity in determining the potential of carbon sequestration by natural ecosystems.

In process models root and and heterotrophic respiration can be represented separately: this option is frequently followed in models with a long-term perspective, where net primary production has to be allocated to the different plant parts and litter contributes to the dinamics of carbon in the soil. Alternatively, soil CO_2

emission can be modelled as a whole: this option is frequently used in models aimed to simulate the carbon flux at the ecosystem level.

In process models SOM decomposition rates and total soil CO_2 emission are generally assumed to increase exponentially with temperature, and to be variously affected by soil water content and soil organic matter composition (Parton *et al.* 1987, Raich & Schlesinger 1992, Lloyd and Taylor 1994, Schimel *et al.* 1994, Davidson, Belk & Boone 1998, Epron *et al.* 1999a, Leiròs *et al.* 1999). As a result, soil decomposition rates and CO_2 emission have been widely expected to increase as a result of climate change, largely offsetting any increase in plant carbon sequestration induced by increased atmospheric CO_2 (Jenkinson *et al.* 1991, Kirschbaum 1995). However, recent evidence suggest this expectation may be questionable (Grace & Rayment 2000). Soil heating experiments have shown an increase of soil respiration in heated plots in the short-term, whilst over longer periods minor or no differences were found (Peterjohn *et al.* 1993, McHale *et al.* 1998, Jarvis & Linder 2000). From a metanalysis of published data Giardina and Ryan (2000) argue that soil decomposition rates are remarkably constant irrespective of average temperature, suggesting a process of downward acclimation to elevated temperature that could largely offset the predicted impact of climate change. Whilst temperature was found to represent the main control factor of soil respiration at a given site, at the geographic scale soil respiration rates of 18 forest ecosystems across Europe showed no significant relationship with site mean annual temperature (Janssens *et al.* 2000). Liski *et al.* (1999) suggested that the acclimation of soil respiration to temperature could result from the weak sensitivity of old organic to decompose; as a consequence soil carbon would slowly accumulate in boreal forest soils, rather than be depleted as generally expected. To date, no functional model is able to fully account for the acclimation process to temperature. Lloyd and Taylor (1994), moving from a review of datasets from a variety of biomes, suggested an empirical model that partly accounts for this acclimation of respiration to temperature, hinting that the Q_{10} coefficient of soil respiration should be expected to decline with increasing average soil temperature

Elevated atmospheric CO_2 concentrations have been reported to increase the allocation of carbon to below-ground, both in roots and in exudates (Canadell, Pitelka & Ingram 1996). In closed forest ecosystems, roots are generally contributing between 30 and 60% to total soil respiration (Bowden *et al.* 1993, Kelting *et al.* 1998, Epron *et al.* 1999b, Matteucci *et al.* 2000), strongly influencing the temperature sensitivity of soil respiration (Boone *et al.* 1998). This is generally reflected in an enhanced soil respiration in ecosystems exposed to increased atmospheric [CO_2] (Canadell, Pitelka & Ingram 1996). To take these factors into account, process models should represent properly carbon allocation, as we are going to discuss in the next paragraph.

2.4 Carbon allocation

In process growth models the description of assimilate allocation play a central role, as the partitioning of carbon between foliage, sapwood and fine root has crucial consequences for plant function and its growth potential. Production of new leaves and fine roots increase light interception and nutrient uptake, whilst the production of new sapwood has a key role in water transport and plant stability.

The allometry of the plant is known to be affected by a variety of environmental factors and changes in resource allocation in response to CO_2 increase have been recognised. Temperature, water and nutrient availability are known to alter the balance between foliage and fine roots (Wilson 1988, Santantonio 1990, Dewar *et al.* 1994). The leaf-to-sapwood area ratio has also been demonstrated to be affected by environmental conditions (Mencuccini & Grace 1995; Palmroth *et al.* 1999) and by changing the value of such a ratio in a process model Berninger and Nikinmaa (1997) depicted the implications of a change in carbon allocation for forest productivity along a climatic gradient.

On the other hand, climate-driven differences in biomass allocation and physiological traits may results in compensatory effects: in ponderosa pine trees growing in contrasting climates the reduction of leaf-to-sapwood area ratio with increasing air vapour deficit has been found to be associated with an increase of the specific conductivity of the xylem, contributing to the maintenance of transpiration rates and to the homeostasis in leaf water potential (Maherali & DeLucia 2000).

The modelling analysis of Medlyn and Dewar (1996) also demonstrates that the long-term response of forest productivity to CO_2 and nitrogen deposition strongly depends on the extent to which stem allocation and foliage allocation are coupled. At the global scale, the effect of alternative carbon allocation schemes on biosphere productivity was demonstrated by Friedlingstein *et al.* (1999), who proposed a semi-empirical approach by which allocation changes could be included in a global biosphere model.

Nevertheless, modelling carbon allocation is still a difficult subject (Cannell & Dewar 1994). First, a full quantitative understanding of the mechanisms involved, such as phloem loading, unloading and carbon fluxes, is still lacking. Second, although theoretical concepts and mechanistic models of allocation have been proposed (Thornley 1972), they include many parameters that cannot be quantified. Therefore, in many process growth model the assumption is made that tree structure is dictated by the need of a functional balance and carbon allocation is performed as to maintain this balance.

Whitehead *et al.* (1984) argued that a balance must exist between transpiring foliage, sapwood conducting area, tree height and humidity of soil and in the air. The balance should therefore change as a function of the environment, rather than being constant as in the pipe model theory. Givnish (1986) predicted that optimal growth can only be achieved if the balance between foliage and fine roots is tuned to the environment

experienced by the plant. The observation of functional homeostasis in tissue biochemical composition led to the hypothesis that a functional balance exists between leaf assimilation and root nutrient uptake (Davidson 1969). As we are going to see below in some detail, the hypothesis of functional balance in water transport has been recently extended to take into account the role of fine roots in plant hydraulic conductance (Magnani, Mencuccini & Grace 2000).

The hypothesis of functional balance in carbon and nutrient uptake is consistent with the transport-resistance model of resource allocation proposed by Thornley (1972). The approach, already implemented in some forest growth models (Rastetter *et al.* 1991, Thornley & Cannell 1996), tries to capture in a simple way the dynamics of phloem transport, assuming that both the flux of carbon from leaves and the flux of nutrients from the roots to other sinks are driven by concentration gradients divided by resistances to flow. The main limitation of such a mechanistic approach is the impossibility to obtain an independent measure of model parameters. A more complete mechanistic model, which expands the original Thornley's approach but takes into account both nutrient and water limitations, has been proposed by Dewar (1993). Tissue growth is assumed to be limited not only by local carbon and nutrient availability, but also by tissue water potential, itself a function of plant functional allometry. A preliminary analysis (Magnani & Grace 1999) demonstrates that the model, which at present only includes a leaf and a shoot compartment, could account for the observed functional homeostasis in both nutrient and water relations.

The nutrient- and water-based approaches differ in their predictions of elevated CO_2 effects on the balance between foliage and absorbing roots. An increase in foliage photosynthetic efficiency, as would be expected under elevated CO_2, would be expected to increase belowground allocation, so as to balance the increased availability of carbohydrates with additional nutrients. Under an hydraulic perspective, on the contrary, the partial closure of stomata that is commonly observed in response to increasing C_a would be expected to maintain a lower foliage-to-fine root ratio. However, experimental data of CO_2 effects on root-shoot (*R*:*S*) ratios show no convergent trend. Rogers, Runion & Krupa 1994) found the *R*:*S* ratios to increase in 41% of cases, whilst several studies with forest tree species showed little response. Eamus and Jarvis (1989) also found no evidence of an increase in the root-to-shoot ratio of temperate tree saplings grown at elevated C_a, although in some cases *R*:*S* declined. In model ecosystems of spruce, biomass allocation to roots has been found to increase under elevated CO_2 (Hattenschwiler & Korner 1998). What role nutrients and water played in these experiments is not known; moreover, the direct effect of C_a could have been confounded by ontogenetic changes and the faster plant development commonly observed under elevated C_a.

2.4.1 Optimal carbon allocation and functional homeostasis in water transport

Here we describe a new approach (Magnani, Borghetti & Grace 2000b) aimed to interprete formally the hydraulic constraints on carbon allocation in trees. The analysis is based on the hypothesis of optimal growth and functional homeostasis in water transport (Magnani, Mencuccini & Grace 2000). The assumption is made that minimum leaf water potentials are constrained by the risk of destructive xylem embolism and that foliage production and tree growth are maximized within the limits imposed by this hydraulic constraint. Any factors leading to a decline in leaf transpiration (such as stomatal closure under elevated CO_2) or in water viscosity (such as a temperature increase) would be expected to allocate resources preferentially away from sapwood and fine roots and towards foliage, so decreasing leaf-specific hydraulic conductance whilst maintaining leaf water potentials within a safety range.

The constraint on leaf water potential requires that plant hydraulic resistance per unit foliage area (R_{tot}) be inversely related to leaf transpiration E_f:

$$R_{tot} = \frac{\Psi_{soil} - \Psi_{leaf}}{E_f} \tag{2.12}$$

where the shoot (R_{shoot}) and root (R_{root}) components of plant hydraulic resistance are a function of fine root biomass W_r, stem length h and sapwood area A_s :

$$R_{shoot} = \frac{r_s \cdot \eta \cdot h}{A_s} \tag{2.13a}$$

$$R_{root} = \frac{r_r \cdot \eta}{W_r} \tag{2.13b}$$

where r_s and r_r are unit permeabilities and η is water viscosity.

The assumption of optimal growth under hydraulic constraint requires an equal return from investment into fine root or sapwood production, once discounted for different fine root and sapwood longevities l_r and l_s:

$$\frac{\partial R_{tot}}{\partial W_r} \Big/ \frac{1}{l_r} = \frac{\partial R_{tot}}{\partial W_s} \Big/ \frac{1}{l_s} \tag{2.14}$$

which implies a constant ratio of fine root biomass per sapwood area. Once combined with the hydraulic constraint (Eq. 1), optimal allocation for water transport requires that the ratio between leaf biomass and sapwood, often assumed to be constant according to the pipe model theory, be proportional to total plant

resistance per unit leaf area (*i.e.* inversely proportional to leaf transpiration; see Eq. 2.8) and inversely related to plant height and to water viscosity:

$$\frac{W_f}{A_s} = \frac{R_{tot}^f}{\sigma \cdot \eta \cdot r_s} \cdot \left| h + \frac{l_s}{c \cdot l_r} \right|^{-1} \tag{2.15}$$

The implications of this hypothesis for tree structural acclimation to the environment has been explored by Magnani, Borghetti and Grace (2000a). Such an approach to modeling carbon allocation is applied in the HYDRALL model (Magnani, Borghetti and Grace 1996, Magnani, Borghetti & Grace (2000b).

2.5 Growth rates and age-related processes

With the present and successive paragraph we will move progressively from the the plant to the population and to the ecosystem perspective.

Plant growth is commonly observed to decline with age and, in particular, forest net primary productivity (NPP) is known to vary to a great extent over the lifetime of the stand: after a peak at polestage, NPP has been often observed to decline by more than 50% in ageing forests. Although the age-related decline in productivity has long been known to foresters and forest ecologists, the mechanisms underlying such dynamics are not well understood and probably vary with local environmental conditions and ecosystem properties (Ryan, Binkley & Fownes 1997, Hunt *et al.* 1999).

Allometric, nutrient and hydraulic and constraints have been suggested to be involved in the age-related decline and in most cases they appear the result of plant dimensions rather than of age *per se*. A reduction in net productivity with age/dimension is predicted by the pipe-model (Shinozaki *et al.* 1964), as resources would be diverted from photosynthesizing foliage towards respiring sapwood in tall trees. A decline with age in photosynthetic light use efficiency could be the result of nitrogen limitations and reduced leaf protein content, as nitrogen is increasingly immobilized in undecomposed organic matter in ageing stands (Murty, McMurtrie and Ryan 1996). Lower photosynthetic rates could be also the result of hydraulic limitations and partial stomatal closure in tall trees as found by Mencuccini & Grace 1996) in *Pinus sylvestris* and by Schafer *et al.* (2000) in *Fagus sylvatica*, where stomatal conductance of individual tree crowns decreased by some 60% with 30 m increase in tree height, driving a marked reduction in carbon uptake. In ageing Norway spruce managed stands an effect on canopy conductance through a change in the clumping of needles and their light exposure has been documented by Falge *et al.* (2000). With increasing plant height, the decline in aboveground hydraulic conductivity would have to be counterbalanced either by stomatal closure (Hubbard, Bond & Ryan 1999) or by an increased allocation to transport tissues, mainly sapwood (Schafer *et al.* 2000) and fine roots (Magnani, Mencuccini and Grace 2000). As recently shown (Magnani, Mencuccini and Borghetti 2000) ontogenetic changes in plant hydraulic

architecture, imposing a constraint on leaf gas exchange, may explain the age-related trends of leaf carbon balance and, ultimately, of plant population productivity.

The negative effects of plant dimensions on growth rates clearly interacts with the response of plant growth to elevated CO_2 and temperature: the faster initial growth under more favourable conditions may hasten the onset of age-related limitations. Centritto *et al.* (1999), for instance, reported that when potted seedlings of *Picea sitchensis* and *Prunus avium* were grown for up to three years in open-top chambers, the main effect of elevated CO_2 was a faster initial growth. When comparing plants of the same dimensions, however, there was no difference in relative growth rate among treatments. Hättenschwiler *et al.* (1997), moving from a dendroecological analysis of *Quercus ilex* increments at a natural CO_2 spring, also suggested that the main effect of high CO_2 concentrations could be a faster initial tree growth. This would point to an internal feed-back leading to a more precocious age-related decline in tree productivity. This result was confirmed by Idso (1999), who re-analysed these and other data from long-term CO_2 enrichment studies under field conditions, comparing them with results from potted plants. The field datasets showed a startling agreement. After a very strong growth enhancement at the seedling stage, the positive effect of elevated CO_2 was observed to decline, albeit at a slower rate than in experiments on potted seedlings. Such an effect of plant dimensions has been recognised by Norby *et al.* (1999), who suggested that dimensional effects should be first screened before data from elevated CO_2 experiments can be analysed.

The ecosystem implications of age-related trends in growth rates appears to depend upon some questions: are limitations reducing gross primary productivity (GPP) or increasing the fraction of NPP that is allocated belowground? The total amount of carbon stored in the ecosystem (as opposed to the harvestable stock) would be greater in the latter case, as carbon would accumulate in the soil, under boreal conditions in particular, and be only released after harvesting; are changes in GPP and allocation related to nitrogen availability or to hydraulic limitations? In the first case, one could expect the understorey to be affected to a similar extent, whilst in the second case it could be released from competition for light, better exploit site resources and compensate for the reduction in overstorey NPP. This could lead to a functional homeostasis in above-ground productivity at the community level; how are soil decomposition rates affected by changes in light environment, water balance and litter quality induced by above-ground dynamics?

Some existing process models of tree growth and forest function are including the key hypotheses outlined above and could be tested and falsified using measurements collected on forest chronosequences under different environmental conditions. A comparison of the behaviour of the different models under various environmental conditions may yield significant insight into the relevance of the proposed mechanisms for the age-related decline and even into the consequences at the ecosystem level under climate change scenarios.

2.5.1 Age-related decline in forest productivity: the interaction between stomatal limitations and structural changes

Here we briefly introduce the rationale of a new mathematical model (Magnani & Borghetti 2000) conceived to explain the dynamic trade-off among between stomatal conductance, assimilation rates and structural acclimation in growing trees.

As we have seen above, both the hydraulic structure of the plant and maximum stomatal conductances have been reported to vary in ageing stands. Hydraulic limitations have been invoked to explain both phenomena, since extremely negative (and potentially harmful) water potentials could be prevented both by stomatal limitations and by a shift of resources from transpiring foliage to transport tissues in the shoot and in the roots. The assumption is made that the plant has evolved an optimal strategy in order to maximize growth whilst preventing xylem cavitation and foliage die-back, through a combination of stomatal regulation and structural adjustments. Stomatal closure could prevent extreme water potentials, but at the cost of lower intercellular CO_2 concentrations and reduced photosynthesis. The assimilation per unit foliage that can be achieved under given environmental conditions is an increasing function of stomatal conductance. This can be viewed as an "assimilation constraint" on stomatal opening. The construction of additional transport tissues could allow greater stomatal conductances and assimilation rates, but would divert resources from foliage growth. The amount of sapwood and fine roots that has to be produced to supply with water a unit of foliage, in order to prevent extreme water potentials, will be itself an increasing function of stomatal conductance. The production and maintenance cost of this transport structure determines a second "hydraulic constraint" on stomatal opening. An optimal strategy of cavitation avoidance requires to maximize the net return per unit foliage, i.e. the difference between carbon gain and carbon costs of cavitation avoidance. This will require a combination of both mechanisms of stomatal and structural acclimation: as the plant grows taller both stomatal conductance and the ratio between transpiring foliage and conducting tissues will have to be reduced (Magnani & Borghetti 2000).

2.6 Phenology and growing season length

The phenology of trees relates the timing of the onset and cessation of growth to seasonality in the local climate. It is generally assumed that a correct timing has a high adaptive value, especially for the onset of growth. In the boreal and temperate zone this is because a too early onset of growth may have severe costs for a tree due to late frost damage. On the other hand, a too late onset of growth may reduce its competitive ability as the growing season is not optimally used and a neighboring tree may take better advantage of the available resources, and thereby win the competition for space. It can be expected that the cessation is less precisely synchronised with the prevailing climate as the costs thereof are less severe. Daily incoming light is less in autumn during leaf fall than in spring during bud break, and due to a usually higher cloudiness there is also less direct incoming radiation. Moreover, for a decidous tree early autumn frost does not lead to significant costs

because it will lose its foliage anyway. So there is not a second investment required which is the case if foliage is lost during spring. However, valuable mobile nutrients must be redistributed from the leaf to the tree before abscission. For conifereous trees it is important that a save level frost hardiness is attained before strong night frosts occur. However, the mature needles are less prone to frost damage than the young needles in spring.

Phenology of mediterranean trees is not only driven by seasonality temperature, but also in water availability. Water availability affects not only the timing of the onset and cessation of growth and the abcission of foliage. It also affects the development of leaf area during the growing season and the longevity of foliage for evergreen tree species.

In the following, current theories and models concerning the environmental control of the phenological features of trees will be described. For boreal conifereous trees this includes seasonality in photosynthetic capacity (and the onset and cessation of growth). For deciduous trees, both in the boreal and temperate zone, this includes the moment of bud break and leaf senescence.

2.6.1 Boreal coniferous trees

The photosynthetic capacity of boreal evergreen conifers is strongly limited during winter, mainly due to the reduced photochemical efficiency (e.g. Öquist 1983, Ottander and Öquist 1991, Bauer et al. 1994). The photochemical down regulation of photosynthesis has been seen at least partly to be caused by acclimation against unfavorable winter conditions by protecting the photosynthetic machinery from damage caused by the combination of low temperatures and light energy (e.g. Gillies and Vidaver 1990, Huner et al. 1993). The timing and rate of spring recovery of photosynthesis determines strongly the amount of annual carbon sequestration of boreal forests. It has been generally observed that the recovery of photosynhetic capacity from negligible winter level to its summertime maximum is a gradual process and may take several weeks (Pharis et al. 1970, Öquist 1983, Ottander and Öquist 1991). Furthermore, this recovery is known to be strongly dependent on air temperature (e.g. Lundmark et al. 1988).

Dynamic modelling approaches have been utilized to predict the winter recovery and autumn cessation of photosynthetic capacity of boreal conifers. Pelkonen and Hari (1980) developed a model for the seasonal photosynthetic activity of Scots pine. In their model, the rate of change (increase or decrease) of the photosynthetic capacity depended on air temperature and on the prevailing state of development. According to the model, warm spring temperatures caused a gradual recovery of photosynthesis from winter depression, while the occurrence of low temperatures caused a drawback of this development.

Bergh et al. (1998) modelled the seasonality of photosynthetic capacity of boreal Norway spruce. The main principles of their model were basically similar as in the

model of Pelkonen and Hari (1980). The spring recovery of photosynthesis was modelled according to the temperature sum approach, and frost temperatures were assumed to reduce or reverse the development. In addition to the air temperature, also soil temperature was included to their model, and the photosynthetic recovery was assumed to be hastened after soil thawing in spring. Thus, according to the both modelling approaches described above, the relationship between the seasonality and the photosynthetic parameters, for example the light saturated rate of photosynthesis, A_{max}, in conifers can be described as follows:

$$A_{max} = K \cdot A_{max}(opt) \tag{2.16}$$

$$K = f(T, t) \tag{2.17}$$

Where $A_{max}(opt)$ is maximum rate of photosynthesis at optimum (summertime) conditions, K is the seasonally changing scaling factor (ranging from 0 to 1), T is temperature and t is time.

2.6.2 Temperate and boreal deciduous trees

In the deciduous temperate and boreal trees, the duration of the photosynthetically active period is determined by the timing of spring bud burst and autumn leaf senescence. The dynamic modelling of the timing of bud burst is based on the fact that the rate of spring bud development is strongly dependent on air temperature. Usually the models include certain threshold temperature, below which the rate of development is zero, and above this threshold a quantitative temperature response (either linear or non-linear) is assumed. The state of development at each time instant is determined by integrating the rate of development over time, and the bud burst occurs when certain critical value of the developmental state is attained.

The oldest and probably most widely used approach for modelling the timing of phenological events, so called temperature sum or thermal time method, can be seen analogous to the dynamic modelling approach described above. In this method, accumulated daily or hourly mean temperatures above certain threshold are used as an independent variable to predict, for example, the occurrence of bud burst of trees. In this case, the momentary temperature can be seen to be directly related to the rate of bud development, whilst the accumulated temperature sum represents the developmental state of the bud.

According to the traditional temperature sum approach, the rate bud development is assumed to be linearly dependent on temperature. However, also different response functions have been presented. Sarvas (1972) measured the developmental rate at different constant temperatures and found a logistic temperature response function, which was applicable for several tree species and both vegetative and flower buds. In later dynamic bud burst models, this response has been sometimes used to replace the linear temperature sum function (Hänninen 1990, Häkkinen et al. 1998).

In addition to the important role of spring temperatures, other driving variables have also been included in the phenological models. The occurrence of dormancy breaking chilling temperatures has been suggested to play an important role in the bud development of several temperate tree species. Amongst different modelling approaches describing the chilling effects, a model including two sequential phases of bud development, called *rest* and *quiescence*, was found to be the most suitable for 11 European deciduous tree species (Kramer 1994). In the model, the rate of chilling, R_c, during the rest phase is modelled by a piece-wise linear temperature response function, which includes the maximum, minimum and optimum temperatures, T_i, T_o, T_m, as parameters. After rest completion, the tree enters the quiescence phase, during which the rate of bud development, R_f, is modelled according to a logistic temperature function. This sequential model can be described as follows:

$$\begin{aligned} S_c &= \int_{t_1}^{t_2} R_c(T) \\ S_f &= \int_{t_2}^{t_3} R_f(T) \end{aligned} \tag{2.18}$$

$$R_c = \begin{cases} 0 & T \le T_i \\ \dfrac{T - T_i}{T_o - T_i} & T_i < T \le T_o \\ \dfrac{T - T_a}{T_o - T_a} & T_o < T < T_a \\ 0 & T \ge T_a \end{cases} \tag{2.19}$$

$$R_f = \begin{cases} 0 & T \le T_b \\ \dfrac{1}{1 + e^{-b(T-c)}} & T > T_b \end{cases} \tag{2.20}$$

In which S_c is the state of chilling during rest, and S_f the state of forcing during quiescense. Rest ends (t_2) when the state of chilling exceeds its critical value, C^*. Similarly, quiescence ends (t_3) when the state of forcing exceeds its critical value, F^*. The duration of the rest and quiescence phase is defined as the number of days between t_1 and t_2, and t_2 and t_3, respectively. T_b is the base temperature below which no ontogenetic development occurs.

An alternative approach to model the chilling effect was presented by Cannell and Smith (1983). In their model, the accumulated chilling, i.e. number of hours when temperature is below a certain threshold, was assumed to reduce the temperature sum required for bud burst according to decreasing exponential function:

$$F^* = \alpha + \beta r^{-S_c} \tag{2.21}$$

Where F* is the critical state of forcing, S_c is the state of chilling (number of chilling hours), and α, β and r are parameters.

This approach has been found to be applicable especially for some temperate tree species which have high chilling requirement for dormancy release (e.g. Murray et al. 1989). The original model of Cannell and Smith (1983) was modified by Hänninen (1990) according to the dynamic modelling approach. He assumed that the quantitative relationship between chilling and high spring temperatures can be interpreted in a way that increased chilling gradually increases the competence of bud to respond to temperatures which drive the ontogenetic development towards the bud burst. In this approach, the rate is chilling is modelled as described above (Eqn. 2.19), and the rate of forcing as follows:

$$R_f = K\, R_{f(pot)}, \tag{2.22}$$

Where the potential rate of forcing, $R_{f(pot)}$, is analogous to the rate of forcing in Eqn. 2.20, and K is the competence function, determined by the state of chilling.
Photoperiod is known to control the timing of phenological events of various tree species. The role of photoperiod is pronounced in events such as growth cessation and bud set in autumn (e.g. Heide 1974, Koski and Sievänen 1985). In the case of the timing of bud burst in spring, the effect of photoperiod is, however, less understood, although some evidence indicate that photoperidic response is involved also in this event (e.g. Heide 1993). The photoperiodic effect can be interpreted to be included indirectly in some models predicting bud burst by using a fixed calendar date (i.e. threshold day length) as a starting point of the accumulation of spring temperature sum (Häkkinen et al. 1998, Wielgolaski, 1999).

The models including the photoperiodic effect have been found to be applicable to predict the timing of spring bud burst especially at boreal forest trees. Under the conditions with long and cold winter, the chilling requirement of buds have been observed to be fulfilled relatively rapidly, and therefore insufficient chilling does not limit the springtime bud development. Bud burst models including only the response to spring temperatures have been found to be suitable for boreal tree species, and accuracy of such models may be further improved by including the fotoperiodic effect rather than the chilling effect as an additional environmental variable (Hakkinen et al. 1998).

2.7 Final remarks

Models, be they conceptual or mathematical, still are the best available tool for system analysis and understanding of complex systems as forests are. However, as we have seen, several processes that play a key role in plant function and growth, such as stomatal conductance, respiration, resource allocation, phenology, can only be represented in a very empirical way. Other processes, not considered here, such as nutrient uptake, tissue mortality, fruiting and competition face us with similar problems. To some respects, it has to be recognized that modellers are somewhat

slow to include in their representation the latest knowledge gained at the cellular and molecular level.

In the refining and improving of process growth models some directions may be suggested. On the one hand, quite obviously the empirical assumptions still in use should be challenged, pointing to more functional representations. This may be done both by filling the gap between detailed physiology and ecophysiology as well as by using the models in a more euristic way, *i.e.* to provide testable hypotheses to be addressed by experiments. On the other hand, whilst a tendency can be recognized to continuously refine models, leading to an increasing model complexity, both theoretical and experimental studies suggest that even complex systems composed of many interacting units could behave in a simple way, displaying linear or homeostatic behaviour. Looking at plant self-organization and conservative properties (Kaufmann 1993, Waring *et al.* 1998, Magnani & Grace 1999) may provide the basis from which the behaviour of complex ecosystems may be represented and predicted, greatly contributing to the semplification of process growth models.

2.8 References

Amthor J.S. (1995). Terrestrial higher-plant response to increasing atmospheric [CO_2] in relation to the global carbon cycle. *Global Change Biology* **1**, 243-274.

Aphalo P.J. & Jarvis P.G. (1991) Do stomata respond to relative-humidity? *Plant Cell and Environment* **14**, 127-132.

Assmann E. (1970) *The Principles of Forest Yield Study.* Pergamon Press, Oxford.

Assmann S.M. (1999) The cellular basis of guard cell sensing of rising CO_2. *Plant Cell and Environment* **22**, 629-637.

Atkin O.K., Holly C. & Ball M.C. (2000) Acclimation of snow gum (*Eucalyptus pauciflora*) leaf respiration to seasonal and diurnal variations in temperature: the importance of changes in the capacity and temperature sensitivity of respiration. *Plant Cell and Environment* **23**, 15-26.

Atkinson C.J. & Taylor J.M. (1996) Effects of elevated CO2 on stem growth, vessel area and hydraulic conductivity of oak and cherry seedlings. *New Phytologist* **133**, 617-626.

Auge R.M., Green C.D., Stodola A.J.W.,Saxton A.M., Olinik J.B., Evans R.M. (2000) Correlations of stomatal conductance with hydraulic and chemical factors in several deciduous tree species in a natural habitat. *New Phytologist* **145**, 483-500.

Ball J.T., Woodrow I.E. & Berry J.A. (1987) A model predicting stomatal conductance and its contribution to the control of photosynthesis under different

environmental conditions. In *Progress in Photosynthesis Research* (ed. J.Biggens), pp. 221-224. Martinus Nijhoff, The Netherlands.

Bartelink H.H. (1998) A model of dry matter partitioning in trees. *Tree Physiology* **18**, 91-1010.

Bauer H., Nagele M., Comploj M., Galler V., Mair M. & Unterpertinger E. (1994) Photosynthesis in cold acclimated leaves of plants with various degrees of freezing tolerance. *Physiologia Plantarum* **91**, 403-412.

Bergh J. & Linder S. (1999) Effects of soil warming during spring on photosynthetic recovery in boreal Norway spruce stands. *Global Change Biology* **5**, 245-253.

Bergh J., McMurtrie R.E. & Linder S. (1998) Climatic factors controlling the productivity of Norway spruce: a model-based analysis. *Forest Ecology and Management* **110**, 127-139.

Berninger F. & Nikinmaa E. (1997) Implications of varying pipe model relationships on Scots pine growth in different climates. *Functional Ecology* **11**, 146-156.

Berninger F., Mäkelä A. & Hari P. (1996) Optimal control of gas exchange during drought: empirical evidence. *Annals of Botany* **77**, 469-476.

Bond B.J., Kavanagh K.L. (1999) Stomatal behavior of four woody species in relation to leaf-specific hydraulic conductance and threshold water potential. *Tree Phisiology* **19**, 503-510.

Boone R.D., Nadelhoffer K.J., Canary J.D. & Kaye J.P. (1998). Root exert a strong influence on the temperature sensitivity of soil respiration. *Nature* **396**, 570-572.

Bossel H. (1994) *Modeling and Simulation*. Peters-Vieweg, Wiesbaden.

Bowden R.D, Nadelhoffer K.J, Boone R.D, Melillo J.M. & Garrison J.B. (1993) Contributions of aboveground litter, belowground litter, and root respiration to total soil respiration in a temperate mixed hardwood forest. *Canadian Journal of Forest Research* **23**, 1402-1407.

Bunce J.A. (1996) Growth at elevated carbon dioxide concentration reduces hydraulic conductance in alfalfa and soybean. *Global Change Biology* **2**, 155-158.

Bunce J.A. (1998) Effects of environment during growth on the sensitivity of leaf conductance to changes in humidity. *Global Change Biology* **4**, 269-274.

Canadell J.G., Pitelka L.F. & Ingram J.S.I. (1996). The effects of elevated [CO2] on plant-soil carbon below-ground: a summary and synthesis. *Plant and Soil* **187**, 391-400.

Cannell M.G.R. & Dewar R.C. (1994) Carbon allocation in trees: a review of concepts for modelling. *Advances in Ecological Research* **25**, 50-104.

Cannell M.G.R. & Smith R.I. (1983) Thermal time, chill days and prediction of budburst in Picea sitchensis. *Journal of Applied Ecology* **20**, 951-963.

Cannell M.G.R. & Thornley J.H.M. (2000) Modelling the components of plant respiration. Some guiding principles. *Annals of Botany* **85**, 45-54.

Cao M. & Woodward F.I. (1998) Dynamic responses of terrestrial ecosystem carbon cycling to global climate change. *Nature* **393**, 249-252.

Carswell F.E., Meir P., Wandelli E.V., Bonates L.C.M., Kruijt B., Barbosa E.M., Nobre A.D., Grace J., Jarvis P.G. (2000) Photosynthetic capacity in a central Amazonian rain forest. *Tree Physiology* **20**, 179-186.

Centritto M., Lee H.S.J. & Jarvis P.G. (1999) Increased growth in elevated [CO_2]: an early, short-term response? *Global Change Biology* **5**, 623-633.

Comstock J.P. & Mencuccini M. (1998) Control of stomatal conductance by leaf water potential in *Hymenoclea salsola* (T. & G.), a desert subshrub. *Plant Cell and Environment* **21**, 1029-1038.

Comstock J.P. (2000) Variation in hydraulic architecture and gas-exchange in two desert sub-shrubs, *Hymenoclea salsola* (T & G) and *Ambrosia dumosa* (Payne). Oecologia **125**: 1-10.

Cowan I.R. (1977) Stomatal behaviour and environment. *Advances in Botanical Research* **4**, 117-227.

Cramer W., Kicklighter D.W., Bondeau A., Moore B., Churkina C., Nemry B., Ruimy A. & Schloss A.L. (1999) Comparing global models of terrestrial net primary productivity (NPP): overview and key results. *Global Change Biology* **5**, 1-15.

Dang Q.L., Margolis H.A., Collatz G.J. (1998) Parameterization and testin of a coupled photosynthesis-stomatal conductance model for oreal trees. Tree Physioloy **18**, 141-153.

Davidson E.A., Belk E. & Boone R.D. (1998). Soil water content and temperature as independent or confounded factors controlling soil respiration in a temperate mixed hardwood forest. *Global Change Biology* **4**, 217-227.

Davidson R.L. (1969) Effect of root/leaf temperature differentials on root/shoot ratios in some pasture grasses and clover. *Annals of Botany* **33**, 561-569.

Day M.E. (2000) Influence of temperature and leaf-to-air vapor pressure deficit on net photosynthesis and stomatal conductance in red spruce (*Picea rubens*). *Tree Physiology* **20**, 57-63.

Dewar R.C. (1993) A root-shoot partitioning model based on carbon-nitrogen-water interactions and Münch phloem flow. *Functional Ecology* **7**, 356-368.

Dewar R.C. (1995) Interpretation of an empirical model for stomatal conductance in terms of guard cell function. *Plant, Cell and Environment* **18**, 365-372.

Dewar R.C., Medlyn B.E. & McMurtrie R.E. (1998) A mechanistic analysis of light and carbon use efficiencies. *Plant Cell and Environment* **21**, 573-588.

Dewar R.C., Medlyn B.E. & McMurtrie R.E. (1999) Acclimation of the respiration-photosynthesis ratio to temperature: insights from a model. *Global Change Biology* **5**, 615-622.

Drake B.G., Azcon-Bieto J., Berry J., Bunce J., Dijkstra P., Farrar J., Gifford R.M., Gonzalez-Meler M.A., Koch G., Lambers H. *et al.* (1999) Does elevated atmospheric CO_2 concentration inhibit mitochondrial respiration in green plants? *Plant Cell and Environment* **22**, 649-657.

Drake B.G., Gonzalez-Meler M.A. & Long S.P. (1997) More efficient plants: a consequence of rising atmospheric CO_2? *Annual Review of Plant Physiology and Plant Molecular Biology* **48**, 609-639.

Eamus D. & Jarvis P.G. (1989) The direct effects of increase in the global atmospheric CO_2 concentration on natural and commercial temperate trees and forests. *Advances in Ecological Research* **19**, 1-55.

Epron D., Farque L., Lucot É. & Badot P.-M. (1999b). Soil CO_2 efflux in a beech forest: the contribution of root respiration. *Annals of Forest Sciences* **56**, 221-226.

Epron D., Farque L., Lucot E. & Badot. P.-M. (1999a). Soil CO2 efflux in a beech forest: dependence on soil temperature and soil water content. *Annals of Forest Sciences* **56**, 221-226.

Falge E., Tenhunen J.D., Ryel R., Alsheimer M., Kostner B. (2000) Modelling age- and density related gas exchange of Picea abies canopies in the Fitchelbegirge. *Annals of Forest Science* **57**, 229-243.

Farquhar G.D. & Wong S.C. (1984) An empirical model of stomatal conductance. *Australian Journal of Plant Physiology* **11**, 191-210.

Farquhar G.D., von Caemmerer S. & Berry J.A. (1980) A biochemical model of photosynthetic CO_2 assimilation in leaves of C_3 species. *Planta* **149**, 78-90.

Franks P.J. & Farquhar G.D. (1999) A relationship between humidity response, growth form and photosynthetic operating point in C_3 plants. *Plant Cell and Environment* **22**, 1337-1349.

Friedlingstein P., Joel G., Field C.B. & Fungs I.Y. (1999) Toward an allocation scheme for global terrestrial carbon models. *Global Change Biology* **5**, 755-770.

Friend A.D. (1991) Use of a model of photosynthesis and leaf microenvironment to predict optimal stomatal conductance and leaf nitrogen partitioning. *Plant Cell and Environment* **14**, 895-905.

Fuchs E.E. & Livingston N.J. (1996) Hydraulic control of stomatal conductance in Douglas fir [*Pseudotsuga menziesii* (Mirb.) Franco] and alder [*Alnus rubra* (Bong)] seedlings. *Plant Cell and Environment* **19**, 1091-1098.

Giardina C.P. & Ryan M.G. (2000) Evidence that decomposition rates of organic carbon in mineral soil do not vary with temperature. *Nature* **404**, 858-861.

Gifford R.M. (1995) Whole plant respiration and photosynthesis of wheat under increased CO_2 concentration and temperature: long-term vs short-term distinctions for modelling. *Global Change Biology* **1**, 385-396.

Gillies S.L. & Vidaver W. (1990) Resistance to photodamage in evergreen conifers. *Physiologia Plantarum* **80**, 148-153.

Givnish T.J. (1986) Optimal stomatal conductance, allocation of energy between leaves and roots, and the marginal cost of transpiration. In *On the Economy of Plant Form and Function* (ed. T.J.Givnish), pp. 171-213. Cambridge University Press, Cambridge.

Gonzàlez-Meler M.A., Ribas-Carbó M., Siedow J.N. & Drake B.G. (1996). Direct inhibition of plant mitochondrial respiration by elevated CO_2. *Plant Physiology* **112**, 1349-1355.

Grace J. & Rayment M. (2000). Respiration in the balance. *Nature* **404**, 819-820.

Grantz D.A. (1990) Plant response to atmospheric humidity. *Plant Cell and Environment* **13**, 667-679.

Häkkinen R., Linkosalo T., and Hari P. (1998) Effects of dormancy and environmental factors on timing of bud burst in *Betula pendula*. *Tree Physiology* **18**, 707-712.

Hänninen H. (1990) Modelling bud dormancy release in trees from cool and temperate regions. *Acta Forestalia Fennica* **213**, 1-47.

Hänninen H. (1995) Effects of climatic change on trees from cool and temperate regions. An ecophysiological approach to modeling of bud burst phenology. *Canadian Journal of Botany* **73**, 183-199.

Hari P., Mäkelä A. & Pohja T. (2000) Surprising implications of the optimality hypothesis of stomatal regulation gain support in a field test. *Australian Journal of Plant Physiology* **27**, 77-80.

Hattendchwiler S., Korner C. (1998) Biomass allocation and canopy development in spruce model ecosystems under elevated CO2 and increased N deposition. Oecologia **113**, 104-114.

Hättenschwiler S., Miglietta F., Raschi A. & Körner C. (1997) Thirty years of in situ tree growth under elevated CO_2 : a model for future forest responses? *Global Change Biology* **3**, 463-471.

Hedrich R., Marten I., Lohse G., Dietrich P., Winter H., Lohaus G. & Heldt H.W. (1994) Malate-sensitive anion channels enable guard cells to sense changes in the ambient CO_2 concentration. *Plant Journal* **6**, 741-748.

Heide O.M. (1974) Growth and dormancy in Norway spruce (*Picea abies*). I. Interaction of photoperiod and temperature. *Physiologia Plantarum* **30**, 1-12.

Heide O.M. (1993) Daylength and thermal time responses of budburst during dormancy release in some northern deciduous trees. *Physiologia Plantarum* **88**, 531-540.

Hubbard R.M., Bond B.J. & Ryan M.G. (1999) Evidence that hydraulic conductance limits photosynthesis in old *Pinus ponderosa* trees. *Tree Physiology* **19**, 165-172.

Hunt E.R., Lavigne M.B., Franklin S.E. (1999) Factors controlling the decline of net primary production with stand age for balsam fir in Newfoundland assessed using an ecosystem simulation model. *Ecological modelling* **122**, 151-164.

Huner N.P.A., Öquist G., Hurry V.M., Krol M. Falk, S. & Griffith, M. (1993) Photosynthesis, photoinhibition and low temperature acclimation in cold tolerant plants. *Photosynthesis Research* **37**, 19-39.

Idso S.B. (1999) The long-term response of trees to atmospheric CO_2 enrichment. *Global Change Biology* **5**, 493-495.

IPCC (1995) *Climate Change 1994. Radiative Forcing of Climate Change and an Evaluation of the IPCC IS92 Emission Scenario.* Cambridge Univ. Press, Cambridge.

Janssens I.A., Lankreijer H., Matteucci G., Kowalski A.S., Buchmann N., Epron D., Pilegaard K., Kutsch W., Longdoz B., Grünwald T *et al.* (2000). Productivity overshadows temperature in determining soil and ecosystem respiration across European forests. *Global Change Biology* (in press)

Jarvis A.J. & Davies W.J. (1997) Whole-plant ABA flux and the regulation of water loss in *Cedrella odorata*. *Plant Cell and Environment* **20**, 521-527.

Jarvis A.J. & Davies W.J. (1998) The coupled response of stomatal conductance to photosynthesis and transpiration. *Journal of Experimental Botany* **49**, 399-406.

Jarvis A.J., Mansfield T.A. & Davies W.J. (1999) Stomatal behaviour, photosynthesis and transpiration under rising CO_2. *Plant Cell and Environment* **22**, 639-648.

Jarvis P.G. & Linder S. (2000). Constraints to growth of boreal forests. *Nature* **405**, 904-905.

Jarvis P.G. (1976) The interpretation of the variations in leaf water potential and stomatal conductance found in canopies in the field. *Philosophical Transactions of the Royal Society of London Series B- Biological Sciences* **273**, 593-610.

Jenkinson D.S., Adams D.E. & Wild A. (1991). Model estimates of CO2 emissions from soil in response to global warming. *Nature* **351**, 304-306.

Jones H.G., Sutherland R.A. (1991) Stomatal control of xylem embolism. *Plant, Cell & Environment* **14**: 607-612.

Kaufmann S.A. (1993) *The Origins of Order. Self-Organization and Selection in Evolution.* Oxford University Press, Oxford.

Kelting D.L., Burger J.A. & Edwards G.S. (1998). Estimating root respiration, microbial respiration in the rhizosphere, and root-free soil respiration in forest soils. *Soil Biology & Biochemistry* **30**, 961-968.

Kimball J.S., Thornton P.E., White M.A., Running S.W. (1997) Simulating forest productivity and surface-atmosphere carbon exchange in the BOREAS study region. *Tree Physiology* **17**, 589-599.

Kirschbaum M.U.F. (1995). The temperature dependence of soil organic matter decomposition, and the effect of global warming on soil organic C storage. *Soil Biology and Biochemistry* **6**, 753-760.

Kirschbaum M.U.F. (1999) Modelling forest growth and carbon storage in response to increasing CO2 and temperature. *Tellus Series B Chemical and Physical Meteorology* **51(5),** 871-888.

Kirschbaum M.U.F., Küppers M., Schneider H., Giersch C. & Noe S. (1998b) Modelling photosynthesis in fluctuating light with inclusion of stomatal conductance, biochemical activation and pools of key photosynthetic parameters. *Planta* **204**, 16-26.

Kirschbaum M.U.F., Medlyn B.E., King D.A., Pongracic S., Murty D., Keith H., Khanna P.K., Snowdon P. & Raison R.J. (1998a) Modelling forest-growth response to increasing CO_2 concentration in relation to various factors affecting nutrient supply. *Global Change Biology* **4**, 23-41.

Koski V. & Sievänen R. (1985) Timing of growth cessation in relation to the variations in the growing season. In: Tigerstedt P.M.A., Puttonen P. and Koski V. (eds.), *Crop Physiology of Forest Trees*. Helsinki University Press, Helsinki, pp. 167-193.

Kramer K. (1994) A modelling analysis of the effects of climatic warming on the probability of spring frost damage to tree species in The Netherlands and Germany. *Plant Cell and Environment* **17**, 367-377.

Landsberg J.J. (1986) *Physiological Ecology of Forest Production.* Academic Press, London.

Landsberg J.J., Waring R.H. (1997) A generalised model of forest productivity using simplified concepts of radiation-use efficiency, carbon balance and partitioning. *Forest Ecology and Management* **95**, 209-228

Lavigne M.B. & Ryan M.G. (1997). Growth and maintenance respiration rates of aspen, black spruce and jack pine at northern and southern BOREAS site. *Tree Physiology* **17**: 543-551.

Le Roux X., Grand S., Dreyer E., Daudet F.A. (1999) Parameterization and testing of a biochemically based photosynthesis model for walnut (*Juglans regia*) trees and seedlings. Tree Physiology **19**, 481-492.

Leinonen I. (1996) A simulation model for the annual frost hardiness and freeze damage of Scots pine. *Annals of Botany* **78**, 687-693.

Leirós M.C., Trasar-Cepeda C., Seoane S. & Gil-Sotres F. (1999). Dependence of mineralization of soil organic matter on temperature and moisture. *Soil Biology & Biochemistry* **31**, 327-335.

Leuning R. (1995) A critical appraisal of a combined stomatal-photosynthesis model for C_3 plants. *Plant Cell and Environment* **18**, 339-355.

Leuning R. (1997) Scaling to a common temperature improves the correlation between the photosynthesis parameters J_{max} and V_{cmax}. *Journal of Experimental Botany* **48**, 345-347.

Liski J., Ilvesniemi H., Mäkelä A. & Westman C.J. (1999) CO_2 emissions from soil in response to climatic warming are overestimated. The decomposition of old soil organic matter is tolerant of temperature. *Ambio* **28**, 171-174.

Lloyd J. & Farquhar G.D. (1996) The CO_2 dependence of photosynthesis, plant growth responses to elevated CO_2 concentrations and their interaction with soil nutrient status. I. General principles and forest ecosystems. *Functional Ecology* **10**, 4-32.

Lloyd J. & Taylor J.A. (1994) On the temperature dependence of soil respiration. *Functional Ecology* **8**, 315-323.

Lohammar T., Larsson S., Linder S. & Falk S.O. (1980) FAST - Simulation models of gaseous exchange in Scots pine. In *Ecological Bulletins. Structure and Function of Northern Coniferous Forests. An Ecosystem Study.* (ed. T.Persson), pp. 505-523. Stockholm.

Long S.P. (1991) Modification of the response of photosynthetic productivity to rising temperature by atmospheric CO_2 concentration: has its importance been underestimated? *Plant Cell and Environment* **14**, 729-739.

Lundmark T., Hällgren J-E. & Hedén J. (1988) Recovery from winter depression of photosynthesis in pine and spruce. *Trees* **2**, 110-114.

Luo Y.Q., Reynolds J., Wang Y.P. & Wolfe D. (1999) A search for predictive understanding of plant responses to elevated [CO_2]. *Global Change Biology* **5**, 143-156.

Lutze J.L., Roden J.S., Holly C.J., Wolfe J., Egerton J.J.G. & Ball M.C. (1998) Elevated atmospheric [CO_2] promotes frost damage in evergreen tree seedlings. *Plant Cell and Environment* **21**, 631-635.

Magnani F. & Grace J. (1999) Plants as self-organising systems. In *Leaf Development and Canopy Growth* (eds. B.Marshall & J.Roberts) Sheffield Academic Press, Sheffield.

Magnani F., Borghetti M. & Grace J. (2000) Acclimation of coniferous tree structure to the environment under hydraulic constraints. Submitted to *Functional Ecology*

Magnani F., Mencuccini M. & Grace J. (2000) Age-related decline in stand productivity: the role of structural acclimation under hydraulic constraints. *Plant Cell and Environment* **23**, 251-263.

Maherali H., DeLucia E.H. (2000) Xylem conductivity and vulnerability to cavitation of ponderosa pine growing in constrasting climates. *Tree Physiology* **20**, 859-867.

Makela A. (1997) A carbon balance model of growth and self-pruning based on structural relationships. *Forest Science* **43**, 7-24.

Makela A., Landsberg J., Ek A.R., Burk T.E., Ter-Mikaelian M., Agren G.I., Oliver C.D., Puttonen P. (2000) Process-based models for forest ecosystem management: current state of the art for practical implementation. *Tree Physiolgy* **20**, 289-298.

Matteucci G., Dore S., Stivanello S., Rebmann C. & Buchmann N. (2000). Soil respiration in beech and spruce forests in Europe: trends, controlling factors, annual

budgets and implications for the ecosystem carbon balance. In: *Carbon and Nitrogen Cycling in European forest Ecosystems*, (edit. Schulze E.-D..) *Ecological Studies 142*, Springer Verlag, Heidelberg. Pp. 217-236.

McCree K.J. (1974) Equations for the rate of dark respiration of white clover and grain sorghum as functions of dry weight, photosynthetic rate and temperature. *Crop Science* **14**, 509-514.

McHale P.J., Mitchell M.J. & Bowles F.P. (1998). Soil warming in a northern hardwood forest: trace gas fluxes and leaf litter decomposition. *Canadian Journal of Forest Research* **28**, 1365-1372.

Medlyn B.E. & Dewar R.C. (1996) A model of the long-term response of carbon allocation and productivity of forests to increased CO_2 concentration and nitrogen deposition. *Global Change Biology* **2**, 367-376.

Medlyn B.E., Badeck F.W., De Pury D.G.G., Barton C.V.M., Broadmeadow M., Ceulemans R., De Angelis P., Forstreuter M., Jach M.E., Kellomäki S. *et al.* (1999) Effects of elevated [CO_2] on photosynthesis in European forest species: a meta-analysis of model parameters. *Plant Cell and Environment* **22**, 1475-1495.

Mencuccini M. & Grace J. (1995) Climate influences the leaf area-sapwood area ratio in Scots pine. *Tree Physiology* **15**, 1-10.

Menzel A. & Fabian P. (1999) Growing season extended in Europe. *Nature* **397**, 659

Monteith J.L. (1995) A reinterpretation of stomatal responses to humidity. *Plant Cell and Environment* **18**, 357-364.

Moore B.D., Cheng S.H., Sims D. & Seemann J.R. (1999) The biochemical and molecular basis for photosynthetic acclimation to elevated atmospheric CO_2. *Plant Cell and Environment* **22**, 567-582.

Moren A.S. (1999) Modelling branch conductance of Norway spruce and Scots pine in relation to climate. Agricultural and Forest Meteorology 98-9 Special Iss. SI, 579-593.

Morison J.I.L. & Lawlor D.W. (1999) Interactions between increasing CO_2 concentration and temperature on plant growth. *Plant Cell and Environment* **22**, 659-682.

Mott K.A. & Parkhurst D.F. (1991) Stomatal responses to humidity in air and helox. *Plant Cell and Environment* **14**, 509-515.

Murray M.B., Cannell M.G.R. & Smith R.I. (1989) Date of budburst of fifteen tree species in Britain following climatic warming. *Journal of Applied Ecology* **26**, 693-700.

Murty D., McMurtrie R.E. & Ryan M.G. (1996) Declining forest productivity in aging forest stands: a modeling analysis of alternative hypotheses. *Tree Physiology* **16**, 187-200.

Neftel A., Oescheger H., Schwander J., Stauffer B. & Zumbrunn R. (1982) Ice core sample measurements give atmospheric CO_2 content during the past 40000 years. *Nature* **327**, 477-482.

Netting A.G. (2000) pH, abscisic acid and the integration of metabolism in plants under stressed and non-stressed conditions: cellular responses to stress and their implication for plant water relations. *Journal of Experimental Botany* **51**, 147-158.

Norby R.J., Wullschleger S.D., Gunderson C.A., Johnson D.W. & Ceulemans R. (1999) Tree responses to rising CO_2 in field experiments: implications for the future forest. *Plant Cell and Environment* **22**, 683-714.

Öquist G. (1983) Effects of low temperature on photosynthesis. *Plant Cell and Environment* **6**, 281-300.

Oren R., Sperry J.S., Katul G.G., Pataki D.E., Ewers F.W., Phillips N. & Schäfer K.V.R. (1999) Survey and synthesis of intra- and interspecific variation in stomatal sensitivity to vapour pressure deficit. *Plant Cell and Environment* **22**, 1515-1526.

Ottander C. & Öquist G. (1991) Recovery of photosynthesis in winter-stressed Scots pine, *Plant Cell and Environment* **14**, 345-349.

Palmroth S., Berninger F., Nikinmaa E., Lloyd J., Pulkkinen P. & Hari P. (1999) Structural adaptation rather than water conservation was observed in Scots pine over a range of wet to dry climates. *Oecologia* **121**, 302-309.

Parton W.H., Schimel D.S., Cole C.V. & Ojima D.S. (1987) Analysis of factors controlling sol organic matter levels in Great Plains grasslands. *Soil Science Society of America Journal* **51**, 1173-1179.

Pavel E.W., Fereres E. (1998) Low soil temperatures induce water deficits in olve (Olea europaea) trees. Physiologia Plantarum **104**, 525-532.

Pearcy R.W., Gross L.J. & He D. (1997) An improved dynamic model of photosynthesis for estimation of carbon gain in sunfleck light regimes. *Plant Cell and Environment* **20**, 411-424.

Pelkonen P. & Hari P. (1980) The dependence of the springtime recovery of CO_2 uptake in Scots pine on temperature and internal factors. *Flora* **169**, 398-404.

Peterjohn W.T., Melillo J.M., Bowles F.P. & Steudler P.A. (1993). Soil warming and trace fluxes: experimental design and preliminary flux results. *Oecologia* **110**, 93:18-24.

Pharis R.P., Hellmers H. & Schuurmans E. (1970) Effects of subfreezing temperatures on photosynthesis of evergreen conifers under controlled environment conditions. *Photosynthetica* **4**, 273-279.

Poorter H., van Berkel Y., Baxter R., den Hertog J., Dijkstra P., Gifford R.M., Griffin K.L., Roumet C., Roy J. & Wong S.C. (1997) The effect of elevated CO_2 on the chemical composition and construction costs of leaves of 27 C_3 species. *Plant Cell and Environment* **20**, 472-482.

Porte A. Loustau D. (1998) Variability of the photosynthetic characteristics of mature needles within the crown of a 25-year-old Pinus pinaster. *Tree Physiology* **18**, 223-232.

Raich J.W. & Schlesinger W.H. (1992). The global carbon dioxide flux in soil respiration and its relationship to vegetation and climate. *Tellus* **44B**, 81-99.

Rastetter E.B., Ryan M.G., Shaver G.R., Melillo J.M., Nadelhoffer K.J., Hobbie J.E. & Aber J.D. (1991) A general biogeochemical model describing the response of the C and N cycles in terrestrial ecosystems to changes in CO_2, climate, and N deposition. *Tree Physiology* **9**, 101-126.

Raulier F., Bernier P.Y., Ung C.H. (1999) Canopy photosynthesis of sugar maple (Acer saccharum): comparing big-leaf and multilayer extrapolations of leaf-level measurements. *Tree Physiology* **19**, 407-420.

Raulier F., Bernier P.Y., Ung C.H. (2000) Modeling the influence of temperature on monthly gross primary productivity of sugar maple stands. *Tree Physiology* **20**, 333-345.

Rayment M.B., Loustau D., Jarvis P.G. (2000) Measuring and modeling conductances of black spruce at three organizational scales: shoot, branch and canopy. *Tree Physiology* **20**, 713-723.

Reich P.B., Ellsworth D.S., Walters M.B., Vose J.M., Gresham C., Volin J.C. & Bowman W.D. (1999) Generality of leaf trait relationships: a test across six biomes. *Ecology* **80**, 1955-1969.

Repo T., Hänninen H. & Kellomäki S. (1996) The effects of long-term elevation of air temperature and CO_2 on the frost hardiness of Scots pine. *Plant Cell and Environment* **19**, 209-216.

Rey A., Jarvis P.G. (1998) Long-term photosynthetic acclimation to increased atmospheric CO2 concentration in young birch (Betula pendula) trees. *Tree Physiology* **18**, 441-450.

Rogers H.H., Runion G.B. & Krupa S.V. (1994) Plant responses to atmospheric CO_2 enrichment with emphasis on roots and rhizosphere. *Environmental Pollution* **83**, 155-189.

Ryan M.G. (1991) Effects of climate change on plant respiration. *Ecological Applications* **1**, 157-167.

Ryan M.G., Binkley D. & Fownes J.H. (1997) Age-related decline in forest productivity: pattern and processes. *Advances in Ecological Research* **27**, 213-262.

Ryan M.G., Hubbard R.M., Pongracic S., Raison R.J. & McMurtrie R.E. (1996b) Foliage, fine-root, woody tissue and stand respiration in *Pinus radiata* in relation to nitrogen status. *Tree Physiology* **16**, 333-343.

Ryan M.G., Hunt E.R., McMurtrie R.E., Ågren G.I., Aber J.D., Friend A.D., Rastetter E.B., Pulliam W.M., Raison R.J. & Linder S. (1996a) Comparing models of ecosystem function for temperate conifer forests. I. Model description and validation. In *Global Change: Effects on Coniferous Forests and Grasslands* (eds. A.I.Breymeyer, D.O.Hall, J.M.Melillo & G.I.Ågren), pp. 313-362. J. Wiley, Chichester.

Saliendra N.Z., Sperry J.S. & Comstock J.P. (1995) Influence of leaf water status on stomatal response to humidity, hydraulic conductance, and soil drought in *Betula occidentalis*. *Planta* **196**, 357-366.

Sarvas R. (1972) Investigations on the annual cycle of development of forest trees. Active period. *Communicationes Instituti Forestalis Fenniae* **76(3)**, 1-110.

Schafer K.V.R., Oren R., Tenhunen J.D. (2000) The effect of tree height on crown level stomatal conducance. *Plant, Cell. & Env.* **23**, 365-375.

Schimel D.S., Braswell B.H., Holland E.A., McKeown R., Ojima D.S., Painter T.H., Parton W.J. & Townsend A.R. (1994). Climatic, edaphic, and biotic controls over storage and turnover of carbon in soils. *Global Biogeochemical Cycles* **8**, 279-293.

Schulze E.-D. (1993) Soil water deficits and atmospheric humidity as environmental signals. In *Water Deficits. Plant Responses from Cell to Community.* (eds. J.A.C.Smith & H.Griffiths), pp. 129-145. Bios Scientific Publishers, Oxford.

Schulze E.-D., Kelliher F.M., Korner C., Lloyd J. & Leuning R. (1994) Relationships among maximum stomatal conductance, ecosystem surface conductance, carbon assimilation rate, and plant nitrogen nutrition: a global ecology scaling exercise. *Annual Review Ecology Systematics* **25**, 629-660.

Sharkey T.D. (1985) Photosynthesis in intact leaves of C_3 plants:physics, physiology and rate limitations. *Botanical Review* **51**, 53-105.

Sperry J.S., Alder F.R., Campbell G.S., Comstock J.P. (1998) Limitation of plant water use by rhizosphere and xylem conductance: results from a model. *Plant, Cell and Environment* **21**, 37-35.

Tardieu F. & Simonneau T. (1998) Variability among species of stomatal control under fluctuating soil water status and evaporative demand: modelling isohydric and anisohydric behaviours. *Journal of Experimental Botany* **49**, 419-432.

Thomas D.S., Eamus D. & Bell D. (1999) Optimization theory of stomatal behaviour. II. Stomatal responses of several tree species of north Australia to changes in light, soil and atmospheric water content and temperature. *Journal of Experimental Botany* **50**, 393-400.

Thornley J.H.M. & Cannell M.G.R. (1996) Temperate forest responses to carbon dioxide, temperature and nitrogen: a model analysis. *Plant Cell and Environment* **19**, 1331-1348.

Thornley J.H.M. & Cannell M.G.R. (2000) Modelling the components of plant respiration. Representation and realism. *Annals of Botany* **85**, 55-67.

Thornley J.H.M. (1972) A balanced quantitative model for root:shoot ratios in vegetative plants. *Annals of Botany* **36**, 431-441.

Thornley J.H.M. (1976) *Mathematical Models in Plant Physiology*. Academic Press, London.

Valentini R., Matteucci G., Dolman A.J., Schulze E.-D., Rebmann C., Moors E.J., Granier A., Gross P., Jensen N.O., Pilegaard K. *et al.* (2000) Respiration as the main determinant of carbon balance in European forests. *Nature* **404**, 861-865.

Van-WijK M.T., Dekker S.C., Bouten W., Bosveld F.C., Kohsiek. W., Kramer K., Mohren G.M.J. (2000) Modeling daily gas exchange of a Douglas-fir forest: comparison of three stomatal coductance models with and without a soil water stress function. *Tree Physiology* **20**, 115-122.

Waring R.H., Landsberg J.J., Williams M. (1998) Net primary production of forests:a constant fraction of gross primary production? *Tree Physiology* **18**, 129-134.

Whitehead D. (1998) Regulation of stomatal conductance and transpiration in forest canopies. *Tree Physiology* **18**, 633-644.

Whitehead D., Jarvis P.G. & Waring R.H. (1984) Stomatal conductance, transpiration, and resistance to water uptake in a *Pinus sylvestris* spacing experiment. *Canadian Journal of Forest Research* **14**, 692-700.

Wielgolaski F-E. (1999) Starting dates and basic temperatures in phenological observations of plants. *International Journal of Biometeorology* **42**, 158-168.

Williams M., Rastetter E.B., Fernandes D.N., Goulden M.L., Wofsy S.C., Shaver G.R., Melillo J.M., Munger J.W., Fan S.-M. & Nadelhoffer K.J. (1996) Modelling the

soil-plant-atmosphere continuum in a *Quercus-Acer* stand at Harvard Forest: the regulation of stomatal conductance by light, nitrogen and soil-plant hydraulic properties. *Plant Cell and Environment* **19**, 911-927.

Wilson J.B. (1988) A review of evidence on the control of shoot:root ratio, in relation to models. *Annals of Botany* **61**, 433-449.

Wolfe D.W., Gifford R.M., Hilbert D. & Luo Y. (1998) Integration of photosynthetic acclimation to CO_2 at the whole-plant level. *Global Change Biology* **4**, 879-893.

Wong S.C., Cowan I.R. & Farquhar G.D. (1979) Stomatal conductance correlates with photosynthetic capacity. *Nature* **282**, 424-426.

Wullschleger S.D. (1993) Biochemical limitations to carbon assimilation in C_3 plants. A retrospective analysis of the A/C_i curves from 109 species. *Journal of Experimental Botany* **44**, 907-920.

3 Process-based models for scaling up to tree and stand level

Koen Kramer

3.1 Introduction

The previous chapter presents an overview of the processes that determine forest growth and describes how these processes are affected by environmental variables. The focus of this chapter is on how these processes are integrated in the process-based models that are used in LTEEF. In this chapter, firstly the general modelling concepts that are used for process-based modelling at the stand scale will be presented. Secondly, the principles of integration will be described, and how the rates of change of different state variables change at different time scales. This will be done based on examples of output of the model FORGRO. Thirdly, the key-features of the different models that were used for the regional impact assessment and that provided information for the upscaling from stand to the European scale will be shortly outlined.

3.2 Modelling concepts

The process-based models that are used in LTEEF aim to assess the long-term dynamics of growth of managed forest stands. Stand characteristics, expressed per hectare, include: tree density, stem volume, tree height, stem diameter at breast height (DBH), canopy dimensions, biomass of foliage, branches, stem (hardwood and sapwood) coarse roots and fine roots. The stand characteristics are based either on individual trees, cohorts of trees of different diameter classes, or average trees (i.e. all trees of a species in the stand are identical), depending on the model. Forest management strategies affect these features by thinning or harvesting.

The models describe the physical environment (light, temperature, vapour or water) in the vegetation and in the soil in detail. Figure 3.1 gives a general scheme on how the processes are interrelated for the model GOTILWA, which is representative for the other models used in this study. Table 3.1 gives an overview of the features of each of the models. Much effort is paid to the interception and attenuation of light in the canopy because of the non-linear relationship between photosynthesis and available light. Most models include a leaf energy balance, thus a vertical temperature gradient, as photosynthesis is strongly affected by temperature. None of the models include vertical gradients in either CO_2 or H_2O-concentration. Maintenance respiration is proportional to the amount of respiring biomass, and increases exponentially with increasing temperature. In many models it depends on the nitrogen concentration in the plant tissue. Growth respiration is proportional to total growth but is not temperature dependent. Phenology, i.e. the timing of bud burst and foliage loss, is usually described as temperature dependent only. Also root turnover may depend on temperature and in some models also on water availability. The

LTEEF models use different approaches for the allocation of assimilates to plant components (e.g. pipe model, allometric relationships, hydraulic constrains). This is especially important for long-term dynamics of forest growth, however, it is not important for the comparison of predicted and observed exchange of CO_2 and H_2O. The LTEEF-models also differ significantly in the degree of detail in which the dynamics of carbon and temperature of the soil is described, and hence heterotroph respiration.

The hydrological aspect of most models includes interception and evaporation of rain by the canopy and transpiration of water through the vegetation taken from the soil. Some models include evaporation from the soil. The links between carbon and water cycles in the soil and the vegetation are through the effects of soil moisture on conductance. Either directly using an empirical relationship or through the effect of soil water potential on leaf water potential based on a series of resistances between the soil and the atmosphere through the tree for the transport of water.

The required climatic variables, expressed as daily values, include: global radiation, minimum and maximum temperature, relative humidity or early morning vapour pressure, wind speed and rainfall.

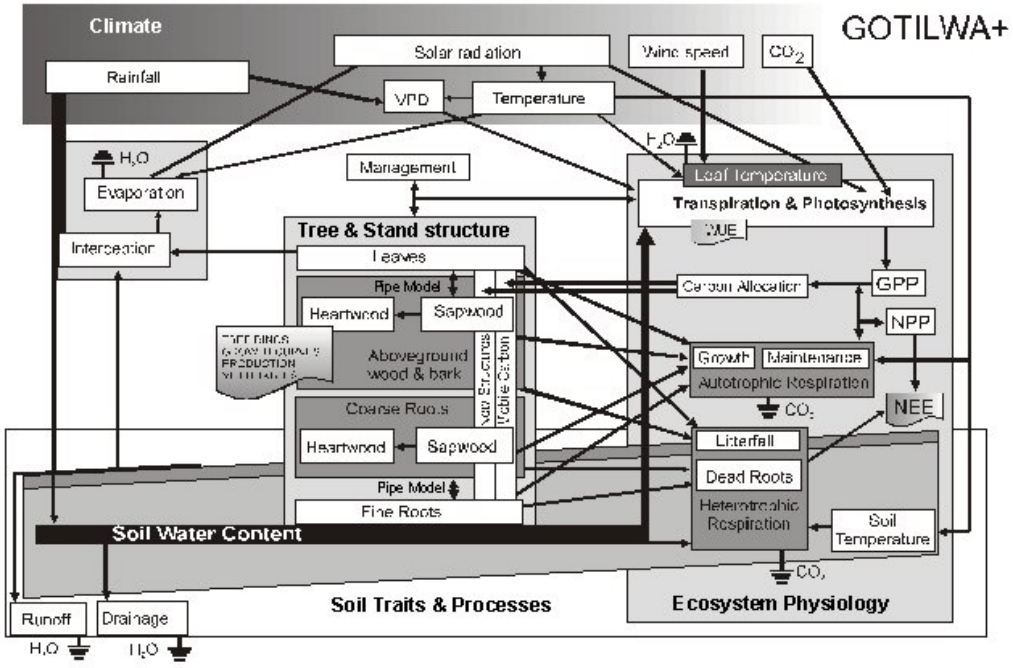

Figure 3.1. General scheme of processes and their interrelationships for GOTILWA, which is representative for the other process-based models that are used in LTEEF

Table 3.1 Characteristics of LTEEF-models

	COCA/FEF	FINNFOR	FORGRO	GOTILWA	HYDRALL	TREEDYN
Range of applicability in Europe						
Species	Coniferous	coniferous	coniferous/deciduous	coniferous/deciduous	coniferous	coniferous/deciduous
Climate	Boreal	boreal	boreal/temperate/Mediterranean	boreal/temperate/Mediterranean	boreal/temperate/Mediterranean	boreal/not water-stressed temperate
Canopy structure						
Vertical	needle distribution	Homogeneous, ellipsoid leaf density	LAI layers. Homogeneous or ellipsoid leaf density	Two LAI layers (sun and shade). Ellipsoid leaf density	Different leaf density per layer dependent on diameter class	LAI layers
Horizontal Architecture	Homogeneous size classes of trees; description of tree structure in each class	Homogeneous Cohorts of trees; description of tree structure in each class	Homogeneous identical trees	Homogeneous size classes of trees	Homogeneous identical trees	Homogeneous individual
Clumping	Y	n	y	n	y	n
Radiation interception						
Direct/diffuse	Y	y	y	y	y	y
Scattering	Y	y	y	y	y	n
Photosynthesis						
Model	Solution of optimum stomatal control problem	Biochemical (Farquhar type)	Biochemical (Farquhar type)	Biochemical (Farquhar type)	Biochemical (Farquhar type)	Biochemical (Farquhar type)
Control variables	I,T	I, T,CO2	I, T,CO2	I, T,CO2	I, T,CO2	I, T,CO2,RH
Conductance						
Model	Optimal stomatal control	Jarvis-type stomatal control	Ball & Berry	Leuning (1995)	Optimal stomatal conductance	Ball & Berry
Control variables*	-	T, VPD	RH	RH	T, VPD	RH
Phenology	Pelkonen & Hari 1980	Pelkonen & Hari 1980	Hänninen 1990; Kramer 1994; Leinonen 1996	Pelkonen & Hari 1980		Sonntag 1998;Kramer 1994**;** Leinonen 1996
Energy balance / water flux						
Canopy temperature	N	n	y	y	y	n
Transpiration	N	y	y	y	y	n
Rainfall interception	N	y	y	y	y	n
soil evaporation	N	y	n	n	n	n
Soil water balance	N	n	y	y	y	n

Respiration	Foliage, fine roots, sapwood, soil	Foliage, fine &coarse roots, branches, sapwood, soil	Foliage, fine root, sapwood, soil	Leaves, fine & coarse roots, live xylem, soil	Foliage, fine roots, sapwood, soil	Leaf, fruit, fine root, sapwood; soil
Autotroph	Y	y	y	y	y	y
Growth/Maintenance	Y	y	y	y	y	y
Temperature dependency	Q10	Q10	Q10	Q10	Exponential	Quadratic
Heterotroph						
Temperature dependency	Q10	Q10	Exponential	Q10	Q10	Quadratic
Smallest time step	COCA: seconds FEF: years	hours	hours	hours	half hour	hours
Principal literature	Hari et al. 1999; Vesala *et al.* 1999	Kellomäki&Väisänen 1997; Kellomäki *et al.* 1993	Mohren 1987; Kramer 1996	Gracia et al, 1997,1999	Magnani *et al*; 1999a, b,c	Sonntag 1998; Bossel 1996

* abbreviations used: T: temperature; I: radiation, CO2: CO2 concentration, RH: relative humidity, VPD: vapour pressure deficit

3.3 Scaling-up in space

The integration in space for process-based forest models means the integration of assimilates and transpired water over the foliage layers in the canopy. Thus, the fluxes of CO_2 and H_2O per unit foliage area are accumulated over the foliage layers and expressed per unit ground area. Figure 3.2 shows how the integration over the canopy is performed by the model FORGRO. The amount of absorbed radiation at different depths of the canopy depends on the incoming direct and diffuse shortwave radiation. The downward attenuation and scattering of light results in a declining fraction of sunlit and an increasing fraction of shaded foliage. A detailed estimate of the amount of radiation intercepted at different layers in the canopy is very important because of photsynthesis depends non-linearly on light level (see also chapter 2). The integration of assimilation and transpiration over the foliage layers is performed using a nested Gaussian integration technique (Goudriaan & van Laar, 1994). For the shaded foliage, 3 foliage layers, hence light-intensities, are considered. For the sunlit foliage, 5 layers are distinguished within these 3 layers, resulting in an integration over 15 light intensities. The foliage temperature is calculated for each of the 15 foliage layers based on the absorbed photosynthetic active radiation (PAR) and near infra-red radiation (NIR) and the amount of water transpired (Goudriaan & van Laar 1994). Both the absorbed shortwave radiation (PAR) and foliage temperature determine photosynthesis, stomatal conductance and transpiration, and thereby the internal CO_2-concentration (Figure 3.2, see also Chapter 2).

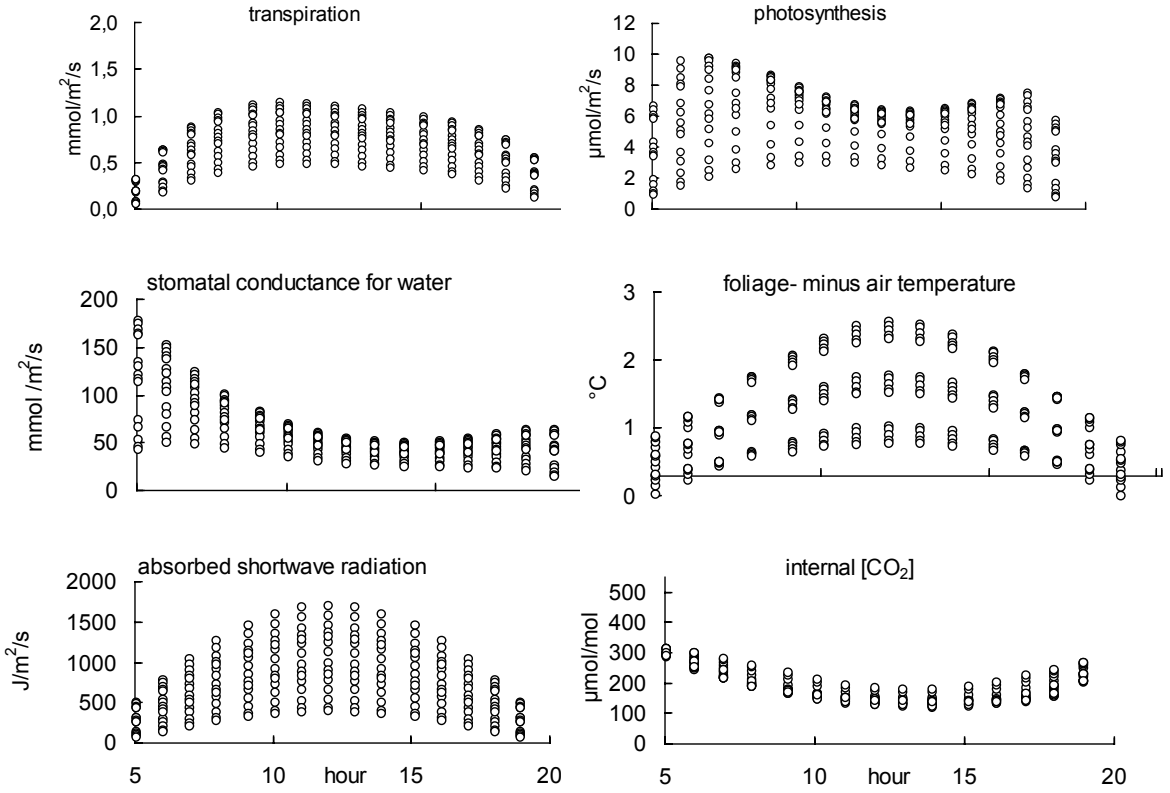

Figure 3.2. Integration of instantaneous rates of transpiration and photosynthesis over foliage layers as performed by the model FORGRO. Temperature and radiation vary over the day and over the canopy, thus affecting stomatal conductance and CO2-concentration in the stomatal cavity

FORGRO requires input of daily values of meteorological variables, including incoming radiation, minimum temperature, maximum temperature, vapour pressure and precipitation. However, the integration over the day is performed based on an hourly time-step. Therefore, the evolution over the day for radiation, air temperature and vapour pressure deficit is calculated. This is done based on an approach presented in Goudriaan & van Laar (1994).

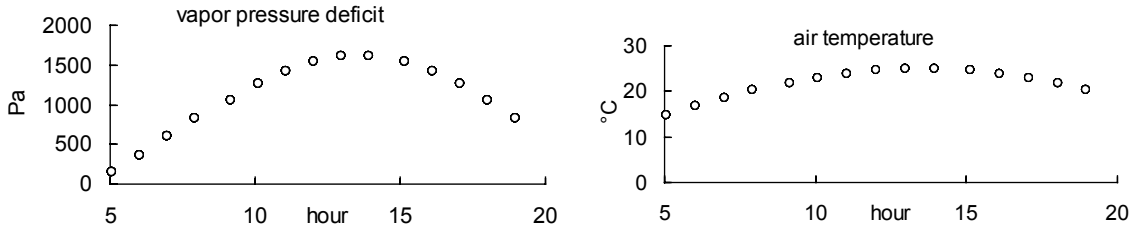

Figure 3.3. Evolution of vapor pressure deficit and air temperature over the day, based on a daily input value.

Most of the models take a similar approach for the integration as presented here for FORGRO. However, they may differ in details considering the number of foliage layers over which the integration is performed, and the calculation of the fraction sunlit and shaded leaf area.

3.4 Scaling-up in time

Integration in time means for forest growth the daily and annual accumulation of above- and below ground biomass, as well as soil organic matter and soil moisture. This integration is first done by accumulating the instantaneous values for photosynthesis, transpiration and stomatal conductance (per second and per unit ground area) to daily values (per day and unit ground area). In FORGRO, 24 hourly values are accumulated to attain a daily value, thus assuming that the instantaneous values are constant at an hourly base.

Figure 3.4 shows examples of daily output for a two-year period for *Pinus pinaster* forest with a *Molinia caerulea* understorey in Bray, France. Daily incoming global radiation (in red) determines the absorbed PAR and NIR by both *P. pinaster* (in green) and *Molinia* (in yellow), and thus net radiation as the balance between incoming short-wave radiation and outgoing long-wave radiation. There is a feedback between stomatal conductance, soil moisture content and transpiration, because transpiration reduces the soil moisture content, this increases the soil moisture deficit which causes the stomates to close thereby reducing transpiration.

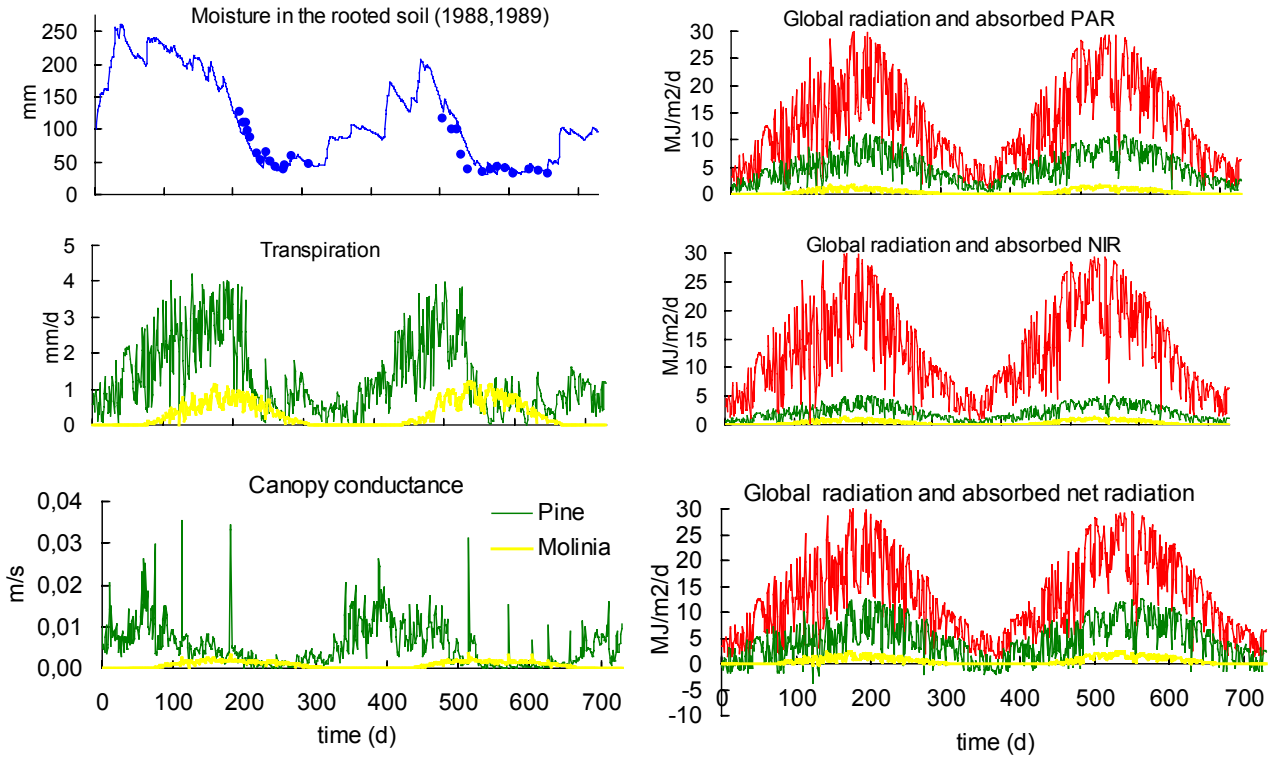

Figure 3.4. Daily output of a Pinus pinaster forest with Molinia understorey in Bray, France, as calculated by the model FORGRO

Figure 3.5 shows results on the accumulation of daily values to attain annual value for the Bray site. It shows large variability in annual precipitation. The transpiration by the pine also shows strong differences between years, whereas the transpiration by the understorey appears to be relatively constant, and is on average responsible for 20% of the total transpiration. The net primairy production (NPP) is the difference between gross photosynthesis (GPP) and both growth and maintenance respiration. NPP is allocated to the different tree components, resulting in the change of biomass of foliage, branches, stem, coarse roots and fine roots. Thinnings performed by management periodically reduces the amount of biomass. Tree growth can also be expressed as annual volume increment, which provides an output that can be tested against independent observations.

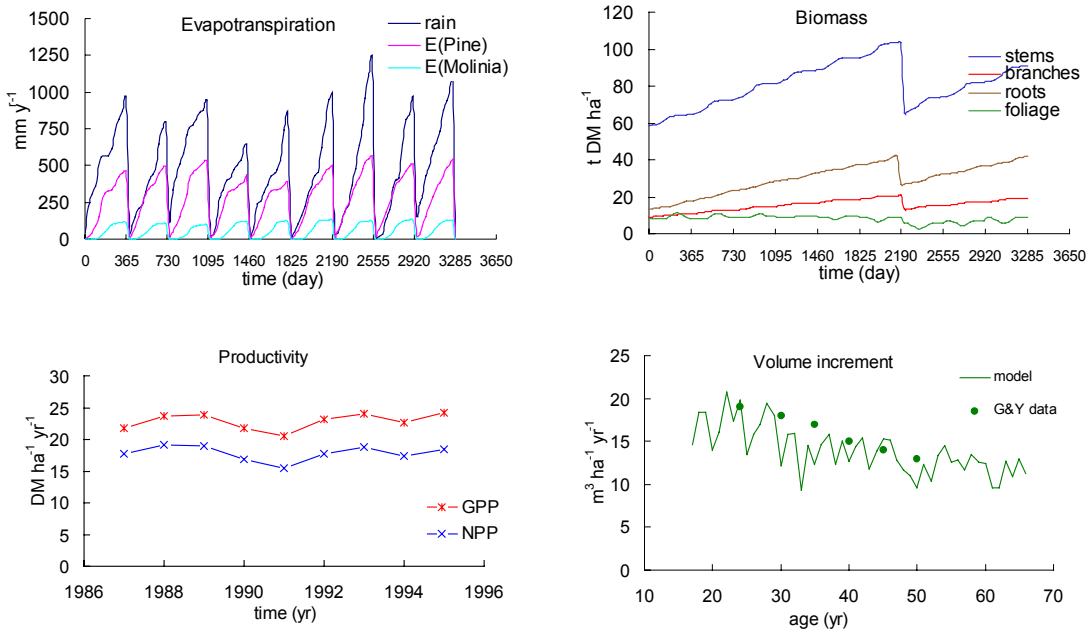

Figure 3.5. Accumulation of daily values to attain annual values

Once a process model has been validated at both the daily and the annual scale, it can produce output that can either be used for upscaling to larger spatial scales, or to evaluate the long-term consequences of climate change scenarios. The model validation will be discussed in detail in chapter 4**.** The radiation use efficiency (amount of dry matter or carbon fixed per MJoule absorbed radiation, Figure 3.6) provides a simple statistic that can be used to for the upscaling of annual variability in productivity over a very large spatial scale, e.g. by linking this to remotely sensed information. Figure 3.6 further shows the effects of different climate change scenarios (2°C increase in temperature; transient doubling in atmospheric CO_2 concentration; 10% reduction in precipitation, and combinations of these) on stemweight of *Pinus pinaster* at the Bray site. The responses of growth and yield to climate change scenarios, as determined by process-based models can be used to adjust observed growth and yield tables for a given species and location, and thus assess the possible impacts of climate change on large spatial scales. Both methods for upscaling based on process-based models output will be described in more detail in chapter 5.

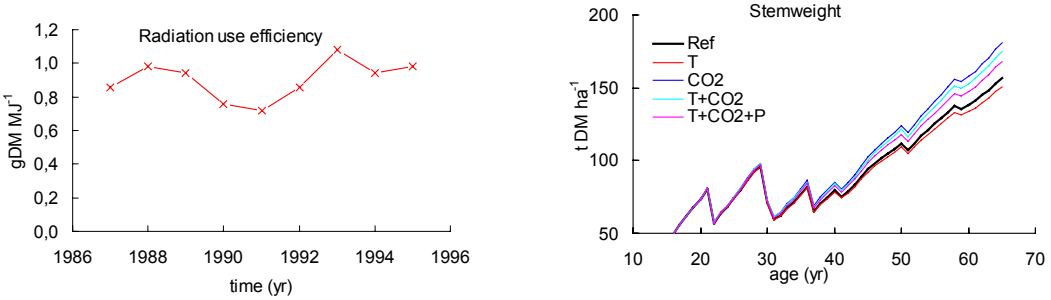

Figure 3.6. Output for upscaling and scenario analysis

3.5 Outline of the process-based models used in LTEEF

3.5.1 COCA/FEF

The model COCA (Complex Canopy Model) consists of three main elements (Hari et al., 1999): (i) calculation of momentary radiation (PAR) distributions within a canopy, (ii) integration of photosynthetic production in a canopy, which is based on the PAR distributions and solution for an optimal stomatal action problem, and (iii) determination of respiration in leaves, woody components (branches, stem, large roots) and fine roots, and heterotrophic respiration in soil.

The PAR distributions are determined separately for cloudy and sunny weather. The solar elevation, the needle area above, and the path length of the solar beam in the canopy determine the distribution of PAR at each height. The photosynthesis depends on irradiance and stomatal conductance that is determined by irradiance, temperature and water vapour concentration in air (Hari et al. 1999). The respiration terms depend exponentially on the temperature.

For the soil, the temperature is modelled using air temperature and snow cover. Respiration of heterotrophs, large roots and fine roots depends on soil temperature. Furthermore, the chemical reactions of major ions (by concentration) are taken into account, as well as leaching of nutrients in runoff. These soilt features subsequently affect the amount of fine roots.

The models FEF (Forest Element Fluxes) and COCA (Complex Canopy model) deal with different time resolutions, COCA with instantaneous and FEF with annual phenomena. COCA consists of three main elements: (i) determination of instantaneous PAR distributions within a canopy, (ii) utilisation of the optimal stomatal control model of photosynthesis (Hari et al., 1999) and (iii) scaling over canopy and growing season. The obtained annual photosynthetic productions as function of shading leaf area are utilised in FEF.

The pine stand is formed by size classes in FEF, the structure of a tree and the number of tree in each size class is treated. The tree is formed by worls which are the functional units of the model. The photosynthetic production, obtained with COCA, is used to the maintenance and growth of the whorl and for the top of the tree. The water transport for the new needles generates a close link between needle and branch and stem growth. The carbon-balance equation is formed stating that the photosynthetic production is used to maintenance and growth of needles, water pipes and fine roots.

The soil component of FEF includes description of the dynamics organic component and soil chemistry. The organic component is separated into rapidly, slowly and extremely slowly decaying components. The litter fall is the source of new organic material for soil. It is decomposed by microbes and the carbon flows from rapidly via slowly to extremely slowly decaying component of released into the atmosphere. The nutrients in the decaying organic matter are either released to the

soil nutrient pool or moved to the next organic component. The kation exchange between soil surfaces and matrix water is the most important chemical reaction.

The fine roots take nutrients from the surfaces of soil particles and from matrix water. The uptake is assumed to be proportional to the product of fine root mass and concentration on soil particles. All new tissues have their specific nutrient concentrations thus the need of additional nutrients is obtained as the product of the mass of each tissue type and its specific concentration. The nutrient balance equation states that the need of additional nutrients and nutrient uptake must be equal. The carbon and nutrient balance equations are the core of FEF. They include two unknown, the needle and fine root growth. These two is solved from the two balance equations and the growth of woody components is determined (Nissinen and Hari, 1998 and Hari, 1999).

3.5.2 FINNFOR

Finnfor is developed by Kellomäki & Väisänen (1997) (see also Kellomäki et al. 1993), in which the dynamics of the ecosystem are directly linked to climate through photosynthesis, respiration and transpiration and indirectly through the hydrological and nitrogen cycles. The hourly computations cover an entire year or several years, representing both the active and dormant seasons.

The tree stand calculation updates the density of the stand, the height and diameter of stems, the weight of the foliage age classes in the crown layers and the weight of the branches, stems, coarse roots and fine roots, based on the allocation of net photosynthates to different organs as constant fractions and converted into dry matter. The density of the tree stand is determined by the regeneration (natural or planting) and the mortality of the trees, which are treated as cohorts in the calculations. Initialisation of the tree cohort calculations requires the number, diameter and age of the trees in each cohort. These factors are used to calculate the structure of the crown (length, width, needle area density). Tree crowns are assumed to be ellipsoids over the lifetime of the tree. The foliage area is distributed uniformly within the crown layers, and the foliage representing each crown layer is formed by the four needle age classes typical of Scots pine. The crown layer areas are determined by the allocation of photosynthates to the foliage and by reference to the life expectancy of each age class in the layer. One tree cohort is shading others and, thus reduces the available radiation, which is given in terms of hourly values for diffuse and direct radiation. The trees are assumed to follow a Poisson distribution within the stand.

Soil conditions are represented in the calculations of photosynthesis by soil T, soil moisture and nitrogen, as detailed by Kellomäki et al. (1993) and Kellomäki and Väisänen (1997). The T and moisture gradients between the soil surface and lower soil layers drives the transfer of water and heat into the soil utilising an hourly time step. The heat and water conditions are computed by means of the partial differential equations, solved using Euler integration. The soil surface forms the upper boundary conditions for the equations, while the lower boundary conditions are obtained from

the heat flow and percolation from the lowest soil layer. The downward flow of heat is the sum of heat conduction and convection. The water on the soil surface represents direct precipitation, precipitation through the canopy and water produced by melting snow. Daily evaporation from the surface pool is calculated as the daily latent heat flow divided by the latent heat of evaporation. Daily infiltration into the soil indicates the outflow of deeper water into the soil profile. The processes related to soil moisture and T are interlinked in such a way that the volumetric water content depends on the freezing T and evaporation of water from the soil. Similarly, the water in the soil influences soil T through its heat content and heat capacity relative to the physical properties of the soil. The soil moisture conditions are given layer by layer in terms of volumetric water content and water tension. The layers are assumed to be horizontally homogeneous.

The decomposition of litter and humus makes the nitrogen bound in the humus available to trees. Litter represents dead organic material from any mass compartment (foliage, branches, stem, course roots and fine roots). Any litter cohort will contain several types of litter, which decay separately under the control of T and precipitation, the determinants of actual evapotranspiration, which is the main force behind the decay. Furthermore, the quality of the litter (lignin and nitrogen content) will affect the rate of decay and the subsequent rate of nitrogen mineralisation. The availability of nitrogen from the soil and from the internal nitrogen cycle determines the nitrogen content of the needles and other organs of living trees (Kellomäki et al. 1993, Kellomäki and Väisänen 1997).

3.5.3 GOTILWA

Gotilwa model simulates carbon and water uptake and fluxes through forests in different environments (from North boreal Europe to Mediterranean), for different single tree species stands (coniferous or broad-leaved, evergreen or deciduous) and in changing environmental conditions, either due to climate or to management regimes (Gracia et al., 1999, 1997).

The input data includes: climate (max. and min. temperatures, rainfall, VPD, wind speed, global radiation); stand characteristics (tree structure; DBH class distribution); tree physiology (photosynthetic and stomatal conductance parameters), site conditions including soil characteristics and hydrological parameters and also forest management criteria. Results of GOTILWA are computed for each DBH class and they are integrated at the stand level. The processes are described with different sub-models that interact and integrate the results of simulated growth and evolution of the whole tree stand through time (hourly calculations integrated at a daily time step). Horizontal space is assumed homogeneous and vertical profile distinguishes two canopy layers (sun and shade conditions).

Light extinction coefficient is estimated by Campbell's approach, based on an ellipsoidal leaf angle distribution. The photosynthesis equations are based on Farquhar and co-workers approach (Farquhar and Von Caemmerer 1982). Stomatal conductance uses Leuning's approach that modifies Ball, Woodrow and Berry model

(Leuning 1995). Leaf temperature is determined based on leaf energy balance and transpiration is estimated according to the Penman-Monteith equation. Autotrophic respiration is separated in maintenance and growth respiration. Maintenance respiration is calculated as a proportion of total respiring biomass (structural and non-structural components distinguished), with rates that depend on temperature according to a Q_{10} approach. Growth respiration is a fraction of available carbohydrates for growth consumed when transformed into new tissues. A constant efficiency of 0.68 is assumed (g of new tissue / g of carbohydrate). NPP is allocated first to form new leaves and fine roots to compensate their turnover. The remaining is allocated to the pool of mobile carbon in leaves and woody tissues. The surplus is invested in new tissues (leaves, fine roots and sapwood) according to the pipe model (Shinozaki et al. 1964). Soil is divided in two layers, organic and inorganic horizons. Soil organic matter (OM) is originated by plant litter: leaves, branches, stems and reproductive organs aboveground and coarse and fine roots belowground. OM is decomposed depending on soil temperature (according to a Q_{10} approach) and soil moisture (optimal at 60% of the maximum soil water-filled porosity). Soil moisture is calculated based on water inputs and outputs and soil traits. Temperature also affects leaf shedding through a Q_{10} approach. Root mortality that is also dependent on temperature (Q_{10} approach), soil moisture and the length of the growing period.

3.5.4 FORGRO

Forgro is a process-based forest growth model at the stand scale. The stand can consist of different species including an understorey that compete for light and water. Central in Forgro is the description of the attenuation of light in a horizontally homogeneous canopy. The amount of light intercepted by a species in the canopy is weighted by the amount of foliage the species has in each foliage layer (Kropf & Van Laar 1993). The absorption of diffuse and direct fluxes of PAR and NIR, daily gross photosynthesis and transpiration is calculated by integrating hourly over both sunlit and shaded leaf layers using a Gaussian integration scheme (Goudriaan 1986) dividing the canopy into shaded and sunlit leaf layers (Goudriaan & Van Laar 1994). The costs of maintenance respiration are based on the costs of biosynthetic processes and the biochemical composition of the structural biomass (Penning de Vries *et al.* 1974). Maintenance respiration depends on temperature according to a Q_{10} approach, whilst growth respiration is assumed to be insensitive to changes in temperature (Goudriaan & Van Laar 1994).

The photosynthesis equations are based on the approach developed by Farquhar and co-workers (Farquhar & Von Caemmerer 1982), whilst the stomatal conductance model was developed by Ball, Woodrow & Berry (1987). The coupled photosynthesis-conductance approach presented by Baldocchi (1994) was used.
Two-layer soil water balance: rooted soil, subsoil; interception of water by canopy; through fall, stem flow; evaporation based on Penman-Montheith eqn. transpiration by integration over foliage layers.

3.5.5 HYDRALL

The HYDRALL (HYDRaulic constraints on ALLocation) model simulates the growth of a coniferous forest stand over a whole rotation. A complete description of the model can be found in Magnani, Borghetti & Grace (1999b). In comparison with other existing forest growth models, model generality is considerably improved by the recognition that growth allocation among tree organs is not fixed, but responds dynamically to the environment, resulting in the acclimation of plant's functional structure to local climatic conditions. The hypothesis of functional homeostasis in water transport (Magnani, Mencuccini & Grace 1999; Magnani, Borghetti & Grace1999a) constitutes the basis to represent the changes in growth allocation both over the lifetime of the forest and in response to the environment.

The representation of global radiation absorption by the sunlit and the shaded portion of the coniferous canopy and by the understorey is based on the two-leaf model of Wang & Leuning (1998). Leaf photosynthetic parameters are integrated over sunlit and shaded foliage and adjusted as a function of absorbed photosynthetically active radiation and leaf temperature. The up-scaling of photosynthetic properties over the canopy is based on the approach of De Pury & Farquhar (1997) and Wang & Leuning (1998). Whilst the effects of aerodynamic decoupling are most strongly felt in broadleaf canopies, the gas-exchange of short, dense coniferous forests could also be affected (Shaw & Pereira 1982). Stand aerodynamic conductance is therefore computed iteratively in the model, following Monteith & Unsworth (1990) and Garratt (1992).

The conductance and gas-exchange of sunlit and shaded foliage are computed separately on a half-hourly basis and summed up to a total value for the canopy. The representation of leaf assimilation is based on the Farquhar model (Farquhar, von Caemmerer & Berry 1980). The dependence of stomatal conductance upon assimilation and air vapour pressure deficit is captured by the Leuning (1995) model, whilst a simple linear dependence of stomatal conductance upon soil water potential is assumed. The representation of transpiration and net carbon exchange from a generic understorey is based on the approach proposed by Dewar (1997). Canopy interception is assumed to be a fixed proportion of incoming precipitation.

The respiration of sapwood and fine roots, on the contrary, are computed on a daily basis as a function of average daily temperature, tissue biomass and nitrogen content, as suggested by Ryan (1991). The two-compartment model of Andrén & Kätterer (1997) has been chosen to represent soil respiration and the transition from young to old soil carbon pools. The empirical model presented by Lloyd & Taylor (1994) is used to represent the dependence of tissue and soil respiration upon temperature.

3.5.6 TREEDYN3

TREEDYN3 simulates the carbon and nitrogen dynamics of an average tree depending on stand density, climate, nitrogen deposition and soil processes. Stand structure is described with height, diameter, carbon mass of tree components. Assimilates are allocated hierarchically and a simple functional balance between leaf

area and fine root mass. The biochemical leaf photosynthesis model of Harley and Tenhunen (1991) combined with the analytical approach of Baldocchi (1994) is linked to TREEDYN3 (Sonntag 1998).

3.6 References

Andrén O. & Kätterer T. (1997) ICBM: the introductory carbon balance model for exploration of soil carbon balances. *Ecological Applications* **7,** 1226-1236.

Aubinet, M., Grelle, A., Ibrom, A., Rannik, Ü., Moncrieff, J., Foken, T., Kowalski, A.S., Martin, P.H., Berbigier, P., Bernhofer, Ch., Clement, R., Elbers, J., Granier, A., Grünwald, T., Morgenstern, K., Pilegaard, K., Rebmann, C., Snijders, W., Valentini, R. and Vesala, T., 2000. Estimates of the annual net carbon and water exchange of European forests: the EUROFLUX methodology. *Advances in Ecological Research*, **30**, 113-175.

Baldocchi, D. 1994. An analytical solution for coupled leaf photosynthesis and stomatal conductance models. *Tree Physiology* **14** : pp 1069-1079.

Ball J.T., Woodward I.E. & Berry.J.A., 1987. A model predicting stomatal conductance and its contribution to the control of photosynthesis under different environmental conditions. In: I, Biggins (Ed.) Progress in Photosynthesis research, Martinus Nijhoff Publishers, The Netherland, pp. 221-224.

Berbigier P., Bonnefond J.M., Loustau D., Ferreira M.I., David J.S., Pereira J.S., 1996. Transpiration of a 64-year old maritime pine stand in Portugal. II : Evapotranspiration and canopy stomatal conductance measured by an eddy covariance technique. *Oecologia*, **107**: 43-52.

Bernhofer, Ch., Feigenwinter, C., Grünwald, T., Vogt, R.: A modified spectral correction method for damping loss of water and carbon flux using displaced sensors for EC measurements. Submitted to "Annales Forestriere"

Bossel, H. 1996. TREEDYN3 forest simulation model. *Ecological Modelling* **90** : pp 187-227.

Cutini A., Matteucci G., Scarascia Mugnozza G. (1998). Estimation of leaf area index with the Li-Cor LAI 2000 in deciduous forests. *Forest Ecology and Management* **105**: 55-65.

De Pury D.G.G. & Farquhar G.D. (1997) Simple scaling of photosynthesis from leaves to canopies without the errors of big-leaf models. *Plant Cell and Environment* **20,** 537-557.

Dewar R.C. (1997) A simple model of light and water use evaluated for *Pinus radiata.*

Tree Physiology **17,** 259-265.

Diawara A., Loustau D., Berbigier P., 1991. Comparison of two methods for estimating the evaporation of a Pinus pinaster (Ait.) stand: sap flow and energy balance with sensible heat measurements by eddy covariance. Agric. For. Meteorol., 54:49-66.

Epron D., Farque L., Lucot E., Badot P.M., 1999. Soil CO_2 efflux in a beech forest: dependence on soil temperature and soil water content. Ann. Sci. For., in press.

Epron D., Farque L., Lucot E., Badot P.M., 1999. Soil CO_2 efflux in a beech forest: the contribution of root respiration, Ann. Sci. For., in press.

Farquhar G.D., von Caemmerer S. & Berry J.A. (1980) A biochemical model of photosynthetic CO_2 assimilation in leaves of C_3 species. *Planta* **149,** 78-90.

Farquhar G.D. and Von Caemmerer S., 1982. Modelling of photosynthetic response to environmental conditions. In: *Physiological Plant Ecology II: Water Relations and Carbon Assimilation*, 12B, O.L. Lange, P.S. Nobel, C.B. Osmond and H. Ziegler (eds.) Springer-Verlag, Berlin, pp. 549-587.

Garratt J.R. (1992) *The Atmospheric Boundary Layer*. Cambridge Univ. Press, Cambridge.

Goudriaan J. and Van Laar H.H., 1994. Modelling potential crop growth processes, Kluwer Academic Publishers, Dordrecht, 238 pp.

Gracia C.A., E. Tello, S. Sabaté, J. Bellot 1999. GOTILWA: An integrated model of water dynamics and forest growth. In: Rodà, F., J.Retana, , C.A. Gracia, J. Bellot, (eds) Ecology of Mediterranean evergreen oak forests. Springer-Verlag, Berlin.

Gracia C.A., S. Sabaté, E. Tello. 1997. Modelling the responses to climate change of a Mediterranean forest managed at different thinning intensities: effects on growth and water fluxes. In: *Mohren, G.M.J., K. Kramer, S. Sabaté (eds) Impacts of global change on tree physiology and forest ecosystems.* Kluwer, Dordrecht, pp. 243-252.

Granier A., Biron P., Lemoine D., 1999. Transpiration and water balance in two beech stands over a two-years experiment. Agric. For. Meteorol., submitted.

Granier A., Ceschia E., Damesin C., Dufrêne E., Epron D., Gross P., Lebaube S., Le Dantec V., Le Goff N., Lemoine D., Lucot E., Ottorini J.M., Pontailler J.Y., Saugier B., 1999. Carbon balance of a young beech forest over a two-year experiment. Funct. Ecology, submitted.

Grünwald, Th., and Ch. Bernhofer, (1998): Data gap filling with regression modelling. Proceedings of the LTEEF-EUROFLUX Conference in Antwerp, Belgium, **21**.-25.9.1998.

Hänninen, H (1990) Modelling bud dormancy release in trees from cool and temperate regions. *Acta Forestalia Fennica,* 47 pp.

Hari, P., 1999. Towards a quantitative theory in the research of plant production. In: *Agro's Annual Review of Plant Physiology IV*. Eds. Purohit, S., Agarwal, S., Vyas, S. and Gehlot, H. Agrobios (India), pp. 1-45.

Hari, P., Mäkelä, A., Berninger, F. and Pohja, T., 1999. Field evidence for the optimality hypthesis of gas exchange in plants. *Australian Journal of Plant Physiology* **26**: 169-175.

Hari, P., Mäkelä, A., Berninger, F. and Pohja, T. 1999. Field evidence for the optimality hypothesis of gas exchange in plants. *Australian Journal of Plant Physiology* **26:** 239-244.

Harley, P.C. & J.D. Tenhunen, 1991. Modelling the photosynthetic response of C3 leaves to environmental factors. In: *Modelling crop photosynthesis from biochemistry to canopy*. American Society of Agronomy, Madison, WI, pp 17-39.

Kellomäki S, Väisänen H, (1997) Modelling the dynamics of the forest ecosystem fro climate change studies in the boreal conditions. *Ecological Modelling* **97**, 121-140.

Kellomäki S, Väisänen H, Strandman H (1993) FINNFOR: a model for calculating the response of boreal forest ecosystem to climate change. Version 1. University of Joensuu, Faculty of Forestry, Research Notes **6**, 120 pp.

Kramer K (1994) A modelling analysis of the effects of climatic warming on the probability of spring frost damage to trees species in The Netherlands and Germany. *Plant, Cell and Environment*, **17**, 367-377.

Kramer K (1996) Phenology and growth of European trees in relation to climate change. Thesis, Wageningen Agricultural University, The Netherlands, 210 pp.

Kropff M.J. and Van Laar H.H. (eds.), 1993 . Modelling crop-weed interactions. CAB International, 274 pp.

Lamaud E., Brunet Y., Berbigier P., 1996. Radiation and water use efficiencies of two coniferous forest canopies. *Phys. Chem. Earth,* **21**: 361-365.

Lankreijer, H., A. Lindroth, A. Grelle, Ch. Bernhofer, T. Vesala (1998): Simulation of Carbon and Water Fluxes from Three Coniferus Forests: Application of 'OUR MODEL' to EUROFLUX Data. To be submitted to Agric.Forest Meteorology

Leinonen I (1996) A simulation model for the frost hardiness and freeze damage of Scots pine. *Annals of Botany*, **78**: 687-693.

Leuning R. (1995) A critical appraisal of a combined stomatal-photosynthesis model

for C_3 plants. *Plant Cell and Environment* **18,** 339-355.

Lloyd J. & Taylor J.A. (1994) On the temperature dependence of soil respiration. *Functional Ecology* **8**, 315-323.

López, B., S. Sabaté, C.A. Gracia. 1998. Fine roots dynamics in a mediterranean forest: effects of drought and stem density. *Tree Physiology*, **18**: 601-606.

López, B., S. Sabaté, I. Ruiz, C.A. Gracia. 1997. Effects of Elevated CO2 and Decreased Water Availability on Holm-Oak Seedlings in Controlled Environment Chambers. In: Mohren, G.M.J., K. Kramer, S. Sabaté (eds) Impacts of global change on tree physiology and forest ecosystems. Kluwer, Dordrecht, pp. 125-133.

Magnani F., Borghetti M. & Grace J. (1999a) Acclimation of coniferous tree structure to the environment under hydraulic constraints. Submitted to *Functional Ecology*.

Magnani F., Borghetti M. & Grace J. (1999b) Growth patterns of *Pinus sylvestris* across Europe. A functional analysis using the Hydrall model. Submitted to *Tree Physiology*.

Magnani F., Mencuccini M. & Grace J. (1999) Age-related decline in stand productivity: the role of structural acclimation under hydraulic constraints. *Plant Cell and Environment*, in press.

Matteucci G. (1998). Bilancio del carbonio in una faggeta dell'Italia Centro-Meridionale: determinanti ecofisiologici, integrazione a livello di copertura e simulazione dell'impatto dei cambiamenti ambientali. PhD Thesis, Università degli Studi di Padova. Padova, 28 Febbraio 1998, Italy.

Mayer DG, Butler DG (1993) Statistical validation. Ecol Model 68: 21-32

Miller DR (1974) Sensitivity analysis and validation of simulation models. J Theor Biol 48: 354-360

Mohren, GMJ (1997) Simulation of forest growth, applied to Douglas fir stands in the Netherlands. Thesis, Wageningen Agricultural University, The Netherlands, 184 pp.

Monteith J.L. & Unsworth M.H. (1990) *Principles of Environmental Phisics*. Edward Arnold, London.

Nissinen, A. and Hari, P., 1998. Effects of nitrogen deposition on tree growth and soil nutrients in boreal Sctos pine stands. *Environmental Pollution* **102**: 61-68.

Pelkonen, P. and Hari, P. 1980. The dependence of the spring time recovery of CO2 uptake in Scots pine on temperature and internal factors. *Flora* **169**: 389-404.

Penning de Vries F.W.T., Brunsting A, and Van Laar H.H., 1974. Products, requirements and efficiency of biosynthesis; a quantitative approach. *Journal of Theoretical Biology* **45**: 339-377.

Power M (1993) The predictive validation of ecological and environmental models. *Ecol Model* **68**: 33-50

Rannik, U., 1998a, Turbulent atmosphere: Vertical fluxes above a forest and particle growth. Ph.D. Thesis (Department of Physics, University of Helsinki). Report Series in Aerosol Sience 35.

Rannik, U., 1998b, On the surface layer similarity at a complex forest site. J. Geophys. Res. 103, 8685-8697

Ryan M.G. (1991) A simple method for estimating gross carbon budgets for vegetation in forest ecosystems. *Tree Physiology* **9,** 255-266.

Shaw R.H. & Pereira A.R. (1982) Aerodynamic roughness of a plant canopy: a numerical experiment. *Agricultural Meteorology* 26, 51-65.

Sonntag, M. 1998. Klimaveraenderungen und Waldwachstum: TREEDYN3-Simulationen mit einer Analyse modellstruktureller Unsicherheiten. Verlag Mainz, Aachen. Dissertation, Univ. of Kassel, Germany,160 p.

Valentini R., De Angelis P., Matteucci G., Monaco R., Dore S., Scarascia Mugnozza G.E. (1996). Seasonal net carbon dioxide exchange of a Beech forest with the atmosphere. *Global Change Biology* **2**: 199-207.

Vesala, T. et al., 1999. Long-term field measurements of atmosphere-surface interactions in boreal forest combining forest ecology, micrometeorology, aerosol physics and atmospheric chemistry. Trends in Heat, Mass and Momentum Transfer (in press)

Wallach D, Goffinet B (1987) Mean squared error of prediction in models for studying ecological and agronomic systems. Biometrics 43: 561-573

Wallach D, Goffinet B (1989) Mean squared error of prediction as a criterion for evaluating and comparing system models. Ecol Model 44: 299-306.

Wang Y.P. & Leuning R. (1998) A two-leaf model for canopy conductance, photosynthesis and partitioning of available energy. I. Model description and comparison with a multi-layered model. *Agricultural and Forest Meteorology* **91,** 89-111.

4 Model evaluation

K. Kramer, I. Leinonen & S. Sabate

4.1 Introduction

Process-based models are essential tools to assess the likely consequences of climate change on growth and functioning of forest ecosystems (Houghton *et al.* 1990; Troen 1993). However, a rigorous testing of these models under current climatic conditions is critical if they were to be used to scale up from the stand to the regional scale in order to assess the role of forests for a regional carbon-balance. The models used were tested using the same site and species information so that differences as a consequence of differences in parametrisation is ruled out as much as possible. The criteria for the comparison and selection of models include: *i*) model validation against short-term flux data; *ii*) model validation against long-term growth & yield data; *iii*) a sensitivity analysis, to determine the response of selected model output to climate change scenario's (temperature, CO_2 and precipitation, independently and jointly); *iv*) an uncertainty analysis to attribute uncertainties in the model output to uncertainties in model input.

4.2 Material and Methods

4.2.1 Model validation

To compare the accuracy of the models, the goodness-of-fit of the models was expressed both as the variance explained (r^2) and as mean square error (MSE). Wallach & Goffinet (1987, 1989) conclude that the evaluation of two models should not be based on R^2 values alone, but also on the analysis of mean squared errors (MSE):

$$MSE = \frac{\left(y_o - y_p\right)^2}{N} \tag{4.1}$$

Where y_o and y_p are the observed and predicted values of the dependent variable, and N is the total number of observations. The use of MSE makes it possible to discriminate between systematic (MSE_s) and unsystematic error (MSE_u). If predicted values are linearly regressed on observed values, let the equation of the regression line be: $\hat{y} = a + by_o$. In case of a perfect model fit it would be:

$$a = 0;\ b = 1;\ \ y_p = \hat{y}. \tag{4.2}$$

In case of an unsystematic error, the modeled points would be scattered around the regression line, while a systematic error would result in values of the parameters that

are different from those above. The systematic and unsystematic error can thus be quantified as:

$$MSE_s = \frac{\sum\left(\hat{y} - y_o\right)^2}{N} \tag{4.3}$$

$$MSE_u = \frac{\sum\left(\hat{y} - y_p\right)^2}{N} \tag{4.4}$$

respectively. In case of a perfect model fit both $MSE_s = 0$ and $MSE_u = 0$. This approach will be followed for the comparison of the model results both to measured CO_2 and H_2O fluxes, and to growth and yield data.

4.2.1.1 CO_2 and H_2O flux data

In the EUROFLUX project emphasis was paid to a unified protocol and instrumentation to obtain CO_2 and H_2O fluxes of 14 sites in Europe (Valentini 1999). In the following a brief qualitative description of this approach is presented. A full description of the system is given by Moncrieff *et al.* (1997) and Aubinet *et al.* (2000). See Table 4.1 for an overview of the characteristics of the EUROFLUX sites.

The eddy-correlation technique is used to obtain the turbulent fluxes. The measurements system is based on a 3D ultrasonic anemometer in combination with a fast infrared gas analyzer placed on the top of a tower reaching 10-20m above the forest. Additionally profiles were measured of CO_2 and H_2O concentrations as well as wind speed and temperature. To determine net radiation, the four components of the radiation balance were measured simultaneously using a net radiometer. Both incoming and reflected short wave radiation was measured with pyranometers. The long wave components were estimated as the difference between global and net radiation.

At the top of the tower, standard meteorological measurements of precipitation, horizontal wind speed, wind-direction, relative humidity and air temperature were made. The soil heat flux was measured using heat flux sensors under the litter layer in the mineral soil. Soil moisture and temperature was measured in one or more profiles at several depths.

The flux data consist of half-hourly values of the exchange of CO2 and H2O between the vegetation and the atmosphere. The output interval of the models is typically 1 day, although the smallest time interval for the calculations is also 1 hour for most models (see Chapter 3). To compare the measurements to the simulated values, the half-hourly values thus need to be accumulated to a daily value. In case of missing measurements, a linear interpolation between adjacent observations is used based on the following criteria: maximally 2 consecutive values are missing during daytime, or maximally 4 consecutive values are missing during night-time. If more

consecutive values are missing then this day is not used for the comparison to the simulated fluxes. No other adjustments than these were performed on the data as provided by the principal investigator of the Euroflux site. See the references for each of the sites (Tabel 4.1) for the correction of the nighttime fluxes. See Chapter 3 for a description for each of the models used.

In this section, the short-term validation was carried out *i*) by analyzing the generality and accuracy of the different models in producing the carbon and water fluxes of different forests, and *ii*) by analyzing the contribution of processes and their environmental determinants in the daily fluxes of carbon and water between different European forests and the atmosphere, indicating possible differences in model realism. This was done by comparing the results of 6 LTEEF models to the independent EUROFLUX data of CO_2 and H_2O fluxes of 6 forest sites in Europe, and by taking advantage of the values of parameters compiled in the ECOCRAFT database.

For the analysis of the carbon fluxes (all in gC m^{-2} soil d^{-1}) the following definitions were used:

$$GPP = A + R_d \tag{4.5}$$

$$NPP = A - R_f - R_w - R_r - \Delta W + d_1 + d_r + c_{II} \tag{4.6}$$

$$NEP = NEE = A - R_f - R_w - R_r - R_h = \Delta W + \Delta S \tag{4.7}$$

where:

Symbol	Explanation
ΔS	rate of change in soil carbon content
ΔW	rate of change in plant carbon content
A	net assimilation rate per unit soil area (= gross assimilation - daytime leaf respiration)
C_{II}	rate of consumption by secondary producers
D_l	rate of litter production
D_r	rate of root turnover
GPP	Gross primary production
NEP	net ecosystem production (= NEE: net ecosystem exchange): net carbon immobilisation rate per unit ground area
NPP	net primary production is the net carbon assimilation rate per unit ground area
R_d	Daytime leaf respiration
R_f	Nighttime leaf respiration rate per unit soil area
R_h	Heterotrophic respiration
R_r	Respiration of the root tissues
R_w	Respiration of the other aerial plant tissues , e.g. branch stem and reproductive organs

The water fluxes include transpiration (T) and evaporation (E), both in kg H_2O m^{-2} yr^{-1}.

Table 4.1 Characteristics of EUROFLUX sites.

Site/stand/climate	Bray	Collelongo	Hesse	Hyytiala	Loobos	Tharandt
Location	44°46'N,+0°42'E	41°52'N,13°38'E	48°40'N,7°05'E	61°51'N,24°18'E	52°10'N,5°44'E	50°58'N,13°38'E
Elevation (m)	62.5	1550	305	170	25	380
Species	Pinus pinaster	Fagus sylvatica	Fagus sylvatica	Pinus sylvestris	Pinus sylvestris	Picea abies
Understorey	Molinia caerulea	Herbs, cf. Gallium	Carpinus betulus	Calluna vulgaris Vaccinium vitis-idaea Vaccinium myrtillus	Deschampsia flexuosa	Deschampsia flexuosa
Soil type	sandy podzol	Calcareous brown earth		Haplic podzol	Podzol	Podzol brown earth
Age (in 1996)	27	100	25-30	34 (30-35)	100	95
Height (m)	18.0	22	13	13	15	25
Tree density (n ha^{-1})	526	890	4000	2500	362	783
Basal area (m^2 ha^{-1})	31.8	32.1		21.9	24.8	33.9
LAI (m^2m-2) (projected)	2.6-3.1	3.5	5.5	5	3.0	7.2
Wood biomass (kg m^{-2})	12.3	21.1	8.0	5.4	7.3	20.1
Mean temperature (°C)	13.5	7	9.2	3	12	7.5
Precipitation (mm y^{-1})	930	1180	820	700	800	820
Data used						
Period	30-6-96 / 30-6 –97	1-1-97 / 31 -12 -97	1-1-97 / 31 -12 -97	1-1-97 / 31 -12 -97	1-1-97 / 31 -12 -97	1-1-97 / 31 -12 -97
Site responsible	Berbigier	Matteucci	Granier	Vesala	Dolman	Bernhofer
Reference	Aubinet *et al* 1999; Berbigier (submitted)	Valentini *et al.* 1996; Matteucci 1998	Granier *et al.* 1999 a,b; Epron *et al.*1999a,b	Vesala *et al.* 1999; Rannik 1998a,b		Bernhofer *et al* 1998; Grünwald & Bernhofer 1998
Measurements						
Radiation balance*	Rn, Rg, PAR (i, r, d/d)	Rn, Rg, PAR (i, r,d/d)	Rn, Rg, PAR (i, r)	Rn, Rg	Rn, Rg, PAR (i, r, d/d)	Rn, Rg, PAR (i, r, d/d)
Scalar fluxes	CO2, H2O; Heat	CO2, H2O; Heat	CO2, H2O; Heat	CO2, H2O; Heat	CO2, H2O; Heat	CO2, H2O; Heat
Soil moisture	Y	y	y	y	y	y

* abbreviations used: *R*n: net radiation, *R*g: global radiation, PAR: visible radation, NIR: near infra red, FIR: far infra red, i:incident, r:reflected, d/d:direct/diffuse

4.2.1.2 Growth and yield data

The process-based models BIOMASS, COCA-FEF, FORGRO, GOTILWA and HYDRALL long-term predictions are evaluated in this section. Model runs were performed in the same EUROFLUX sites than in the previous section (short-term analysis) were detailed information about the site characteristics was available (Valentini 1999). In this case, appropriate growth and yield tables for each of the EUROFLUX sites were selected based on either local observations (Hyytiälä, Flakkaliden, Bray, Collelongo) or using the database of the European Forest Institute (EFI, Joensuu, Finland). A list of variables considered in the analysis is presented in Table 4.2. The meteorological series used as model input were the long-term daily measurements for stations near the Loobos and Bray sites. For the other sites used within the LTEEF-II project, synthetic weather series generated by the weather generator of the Potsdam Institut für Klimafolgenforschung (PIK, Potsdam) were used. The simulations were performed using an equivalent management to those reflected in the growth and yield tables by leaving at each site and age the stem volume provided by the table. The other variables were obtained as outputs derived from model assumptions on processes determining growth patterns.

Table 4.2. Growth and yield characteristics used to test long term model outputs.

Name	Symbol	Units	Explanation
Stand density	N	stems·ha^{-1}	Number of trees per stand area
Diameter at breast height	DBH	cm	tree trunk diameter at 1.3 m from the ground
Tree height*	H	m	Distance from bottom to top of the trees
Basal area	BA	m^2·ha^{-1}	total trunks section area at 1.3 m per stand area
Stem Volume	STVOL	m^3·ha^{-1}	total volume of trees per stand area
Current annual increment	CAI	m^3·ha^{-1}·y^{-1}	Volume production per stand area and year

*Height has been tested for Hydrall model instead of DBH.

4.2.2 Short-term sensitivity analyses

Fluxes of CO_2 and H_2O and meteorological observations were provided for days without water stress. Furthermore, the characteristics describing the stand (LAI, standing biomass, tree density etc.) are known for each site. The leaf photosynthesis model LeafPhot developed by Falge *et al.* (1996) was coupled to Forgro (Mohren 1987, 1994; Kramer 1996a,b). The parameter values required for this model were made available to the participants for each of the species considered (*Fagus sylvatica* L.*, Picea abies* (L.) Karst.*, Pinus sylvestris* L. *and Pseudotsuga menziessi* (Mirb.) Franco). Insufficient information was available to use the standard way of calculating maintenance respiration of Forgro for all sites. Therefore the night-time CO_2 fluxes were used to estimate a respiration coefficient and used to calculate the day-time maintenance respiration at the prevailing temperature. Otherwise, only observed parameter values were used without any calibration of parameters of the flux data.

For the analyses, data was available for 7 EUROFLUX sites considering: *i*) meteorological variables; *ii*) parameter values for both the photosynthesis and stomatal conductance model; *iii*) structural stand information; and *iv*) CO_2 and H_2O fluxes to compare the model output against. This was done for days at which it can reasonably be assumed that there was no water

stress. Table 4.3 provides some basic information for each of the sites considered in this study.

Table 4.3 Information of the sites

Site	Species	Country	Age	No of days with data
Flakaliden	*Picea abies*	Sweden	34	18
Weiden Brunnen	*Picea abies*	Germany	44	20
Hyytialla	*Pinus sylvestris*	Finland	34	47
Loobos	*Pinus sylvestris*	The Netherlands	100	49
Collelongo	*Fagus sylvatica*	Italy	100	9
Hesse	*Fagus sylvatica*	France	25-20	23
Vielsalm	*Pseudotsuga menziesii*	Belgium	60-90	20

For the evaluation of climate change scenarios, response surfaces of CO_2 and H_2O fluxes for each site were determined by altering the observed temperature series by 0-5°C, and the ambient CO_2-concentration by 0-350 ppm. Thus, the response surfaces are based on days with flux measurements only and hence differ in number of days and period of the growing season, depending on the site of observation. In the figures presented the responses are expressed relative to the CO_2 and H_2O fluxes that are based on the unaltered weather series.

4.2.3 Long-term sensitivity analyses

The response of stand growth to changes in ambient CO_2 concentration, temperature and precipitation was analysed at the stand level. In these analyses, two sensitivity indices were considered:

$$S_1 = \frac{O_1}{O_0} \tag{4.8}$$

indicating the response relative to the baseline scenario without climate change, and

$$S_2 = \frac{(O_1 - O_0)/|O_0|}{|(p_1 - p_0)/p_0|} \tag{4.9}$$

indicating the response relative to a change in the climate parameters.

O_i: model output with i=1: changed parameter value increased (or decreased) and i=0: default parameter value

p_i: climate parameter ([CO_2], temperature, precipitation), with i=1: parameter value increased (or decreased) and i=0: default parameter value

The climate changes imposed on the weather series were: [CO_2] = 400 and 700 ppm; change +/- 10% e in precipitation; temperature + 2° C. The reference [CO_2] = 350 ppm.

The model output evaluated was: gross primary productivity (GPP, gC $m^{-2}y^{-1}$) Net primary productivity (NPP, gC $m^{-2}y^{-1}$); Evapotranspiration (ET, kgH_2O $m^{-2}y^{-1}$), and CAI. To evaluate the possible effects of acclimation as represented by the models the average response was taken for the 1-5 years period, 16-20 years period and 46-50 years period, after the start of the simulation.

4.2.4 Process-level uncertainty analyses

An uncertainty analysis studies the accuracy of model prediction with current knowledge, and the prospects to improve accuracy by gaining new knowledge (Jansen *et al.,* 1994). Sources of uncertainty include initial values, parameter values, exogenous variables, model structure, noise, etc. An uncertainty analysis aims at gaining insight into which sources of uncertainty contribute most to the overall output uncertainty. It provides an impression on the quality of the model predictions, indicates necessary additional experiments and research priorities, studies the effect of ignoring some source of uncertainty, and may lead to simplification of complex models. The method of uncertainty analysis developed by Jansen (Jansen *et al.* 1994; Jansen & Withagen 1997) and the software of uncertainty analysis was used. It allows analysis of the uncertainty contributions of aggregated sources based on an efficient sampling design. The aggregated sources may consist of a number of dependent scalar sources however the different aggregated sources must be independent. Here only an outline of the method is presented, whereas a full account of the method can be found in the literature cited.

Let Y be a scalar model output, depending on a number of input vectors, A, B, C. Y can be obtained by evaluating the deterministic function f(A,B,C) by simulation. The input vectors have independent distributions, F_A, F_B, F_C. They may have different lengths, and the elements of a vector may be dependent. The total output variability is characterised by its variance, VTOT, that is induced by all sources collectively. The method aims at quantifying the contribution of the various sources to VTOT. Let U denote a group of one or more sources of uncertainty, then, by assumption, U is independent of the complementary sources, which are collectively denoted by V. Two variances are of interest: i) the top marginal variance of U, TMV(U), which is defined as the expected reduction of the variance of Y in case U should become fully known, and ii) the bottom marginal variance of U, BMV(U), defined as the remaining variance of Y in case all inputs except U should become fully known, U remaining as variable as before (Figure 4.1). These two variance components thus constitute the limits to what may be achieved by new research: the top marginal variance is the maximal variance reduction, whereas the bottom marginal variance is the minimal residual variance. The analysis of the so-called winding stairs samples of the model output is described in detail in Jansen *et al.* (1994).

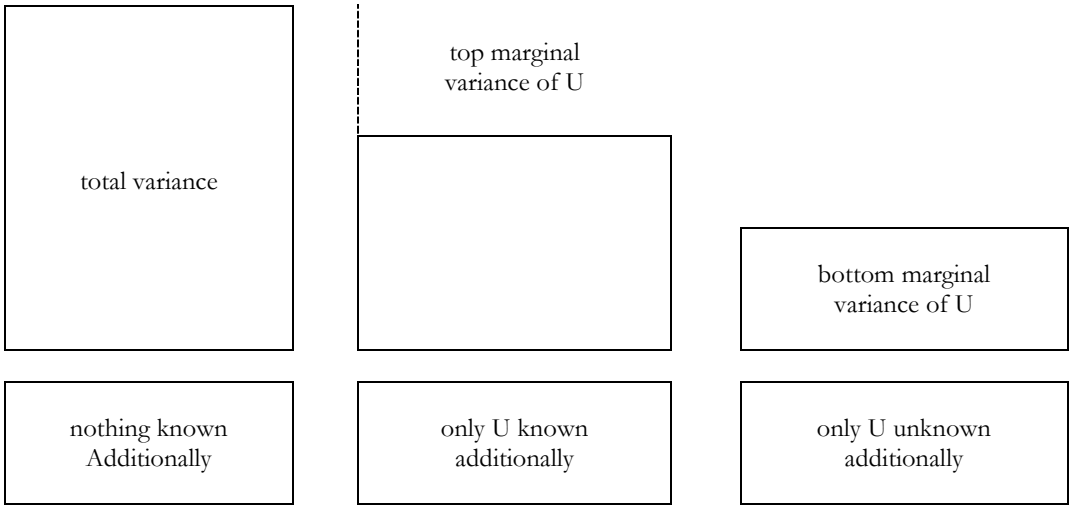

Figure 4.1 Graphical presentation of the variances considered in uncertainty analysis. Total output variance VTOT; top-marginal variance of U TMV(U); bottom marginal variance of U BMV(U).

4.3 Results

4.3.1 Goodness-of-fit of short-term carbon flux predictions

A visual comparison of the model output and the data over time showed that all models accurately predicted the beginning of carbon uptake in spring and the seasonal patterns in NEE. The highest differences between measured and modelled daily values of NEE occurred in summertime. For some models a systematic trend was found when the model residuals where plotted against summertime values of environmental variables, such as radiation and temperature. These responses of the model output during the growing season are analysed in more detail below.

There was a good correlation between the measured NEE fluxes and the daily predictions of most of the models. The r^2 varied between 0.29 (TREEDYN for Tharandt) and 0.93 (FORGRO for Collelongo) (Table 4.4) However, for some models and sites, there were considerable systematic errors between the model predictions and the EUROFLUX estimates (Table 4.1). This leads to an under- or overestimation of the annual fluxes.

Table 4.1. Goodness-of-fit of the model predictions expressed as explained variance (r^2), systematic mean square error (MSE_s) total mean square error (MSE) of Net Ecosystem Exchange (both in gC m^{-2} d^{-1}) compared to estimates based on EUROFLUX measurements at different sites

	COCA/FEF	FINNFOR	FORGRO	GOTILWA	HYDRALL	TREEDYN
Bray (n=259)						
r^2			0.37	0.48	0.56	0.58
MSE_s			4.43	0.90	0.56	0.95
MSE			10.56	2.40	2.07	2.03
Collelongo (n=319)						
r^2			0.93	0.91		
MSE_s			0.81	0.34		
MSE			1.59	1.73		
Hesse (n=365)						
r^2			0.71	0.74		0.81
MSE_s			0.69	0.05		1.24
MSE			2.14	2.34		1.82
Hyytiala (n=357)						
r^2	0.77	0.86	0.83	0.68	0.81	0.80
MSE_s	0.07	0.15	0.40	0.05	0.00	0.07
MSE	1.08	0.62	1.43	1.61	0.61	0.83
Loobos (n=282)						
r^2			0.46	0.62	0.67	0.66
MSE_s			1.95	0.61	0.34	0.56
MSE			3.99	1.29	1.18	1.18
Tharandt (n=282)						
r^2			0.47			0.29
MSE_s			3.91			3.43
MSE			5.86			8.44

4.3.2 Disaggregation of carbon fluxes and responses to environmental variables

To better understand the differences between models, the models predictions were analysed in more detail for the Scots pine forest in Hyytiälä and the beech forest in Hesse. This analysis includes the disaggregation of the annual NEP into gross primairy production and ecosystem respiration, and their responses to temperature, and for GPP also to incoming radiation

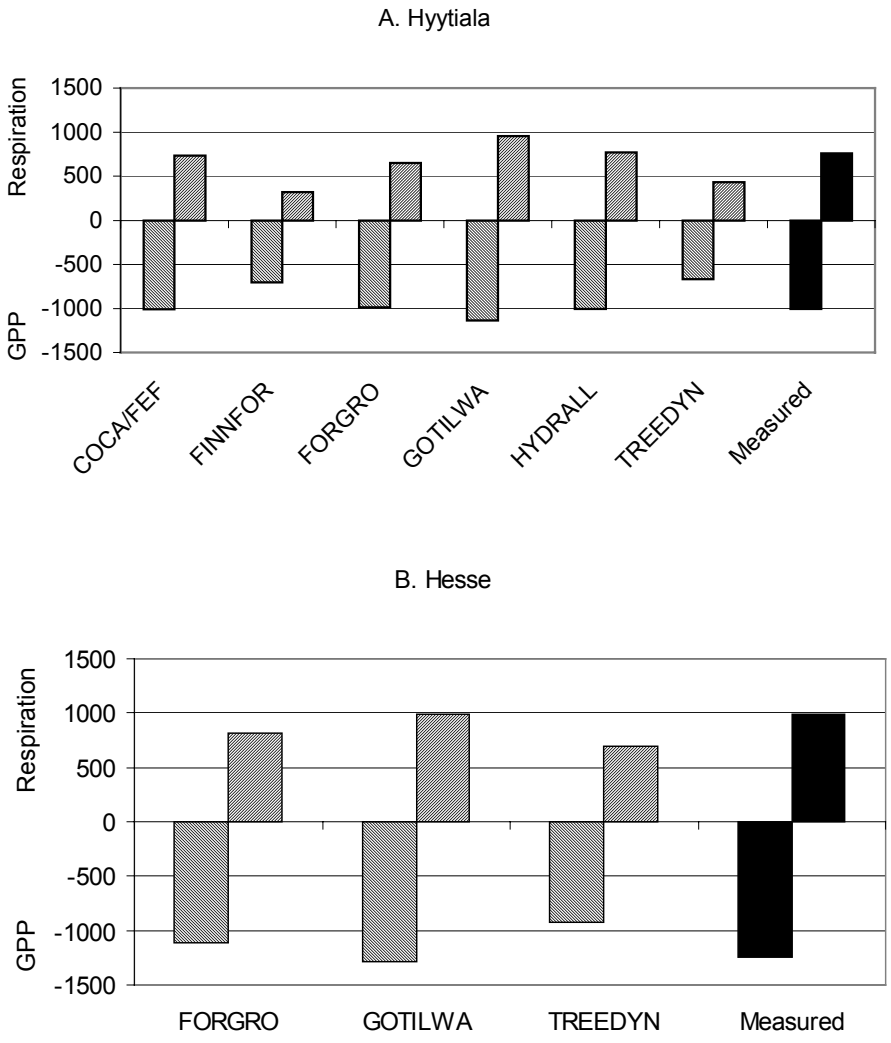

Figure 4.2. Annual carbon fluxes (gC m-2 yr-1) of gross primairy production (GPP) and ecosystem respiration for Scots pine in Hyytiälä, Finland (A) and beech in Hesse, France (B).

The daily values of gross primary production and ecosystem respiration predicted by the models were compared to the estimations from the EUROFLUX data (Valentini et al. 2000). Figure 4.2A shows that for Hyytiälä, COCA/FEF, FORGRO and HYDRALL predicted accurately the annual GPP, while GOTILWA gave a slight overestimate (13%) and FINNFOR and TREEDYN underestimated the EUROFLUX results (30% and 34%, respectively). For Hesse, the most precise prediction for GPP was given by GOTILWA (Figure 4.2B). For this site, FORGRO underestimated GPP by 11% and TREEDYN by 26%. The major differences between the model output occurred in their predictions of ecosystem respiration. For Hyytiälä, HYDRALL and COCA predicted the annual respiration accurately compared to the EUROFLUX estimate (Figure 4.2A). GOTILWA overestimated the respiration by 26% and FORGRO, TREEDYN and FINNFOR underestimated by 14%, 57% and 58%, respectively. For Hesse, GOTILWA predicted the annual respiration accurately and both FORGRO and TREEDYN underestimated it by 18% and 29%, respectively (Figure 4.2B).

The goodness-of-fit of the predicted daily values of GPP and ecosystem respiration were determined for Hyytiälä. For this site daily estimates for these variables were available. Hyytiälä was also the only site where all models where applied. Generally the models showed a higher goodness-of-fit for the separate processes compared to the total net ecosystem exchange (cf. r^2 in Table 4.4 and Table 4.5 for Hytiälä). However, those models that simultaneously under- or overestimated both GPP and respiration, showed systematic errors of single processes that were considerable higher compared to the errors in NEE (cf MSE_s in Table 4.4 and Tabel 4.5 for Hytiälä).

Table 4.5 Goodness-of-fit of model prediction expressed as explained variance (r^2), systematic mean square error (MSE_s) total mean square error (MSE) gross primary production (GPP) and ecosystem respiration (both in $gCm^{-2}d^{-1}$) compared to estimates based on EUROFLUX measurements at Hyytiälä

	COCA/FEF	FINNFOR	FORGRO	GOTILWA	HYDRALL	TREEDYN
GPP						
(n=357)						
r^2	0.92	0.91	0.94	0.90	0.93	0.85
MSE_s	0.04	1.07	0.02	0.92	0.02	1.30
MSE	0.97	1.66	0.81	2.73	0.75	2.40
Respiration						
(n=357)						
r^2	0.93	0.94	0.84	0.87	0.86	0.83
MSE_s	0.03	2.27	0.39	0.59	0.02	2.54
MSE	0.26	2.31	0.71	1.41	0.63	2.67

The differences in the model outputs for the Hyytiälä site were analysed further by plotting the predicted daily values of GPP versus temperature and radiation, and ecosystem respiration versus temperature (Figure 4.3). Figure 4.3A shows the temperature response of the GPP predicted by the models during days with high radiation level (above 20 MJ m^{-2}). All models showed a similar pattern at low temperatures. However, at high temperatures (>15°C), FINNFOR and TREEDYN showed a stronger reduction of GPP compered to both the other models and the EUROFLUX data. GOTILWA predicted higher level of GPP and showed also higher temperature optimum.

Figure 4.3B show the response of GPP to radiation during the Finnish summer time (June-September). The models showed rather similar responses, however, GOTILWA overestimated the GPP at high radiation levels and FINNFOR and TREEDYN underestimated it at low radiation levels. In addition, these two models showed the lowest scatter, which indicates a stricter radiation response compared to other models.

Figure 4.3C shows the differences in the response of ecosystem respiration to air temperature. Two models (COCA/FEF and HYDRALL) have a similar exponential response, which was close to the response estimated from the EUROFLUX data . GOTILWA overestimated respiration when the temprature exceeded 20°C. FORGRO slightly overestimated the respiration at low temperatures (<0°C), and underestimates this at high temperature (>20°C). Both FINNFOR and TREEDYN showed a nearly linear temperature response, thereby underestimating ecosystem respiration at high temperatures.

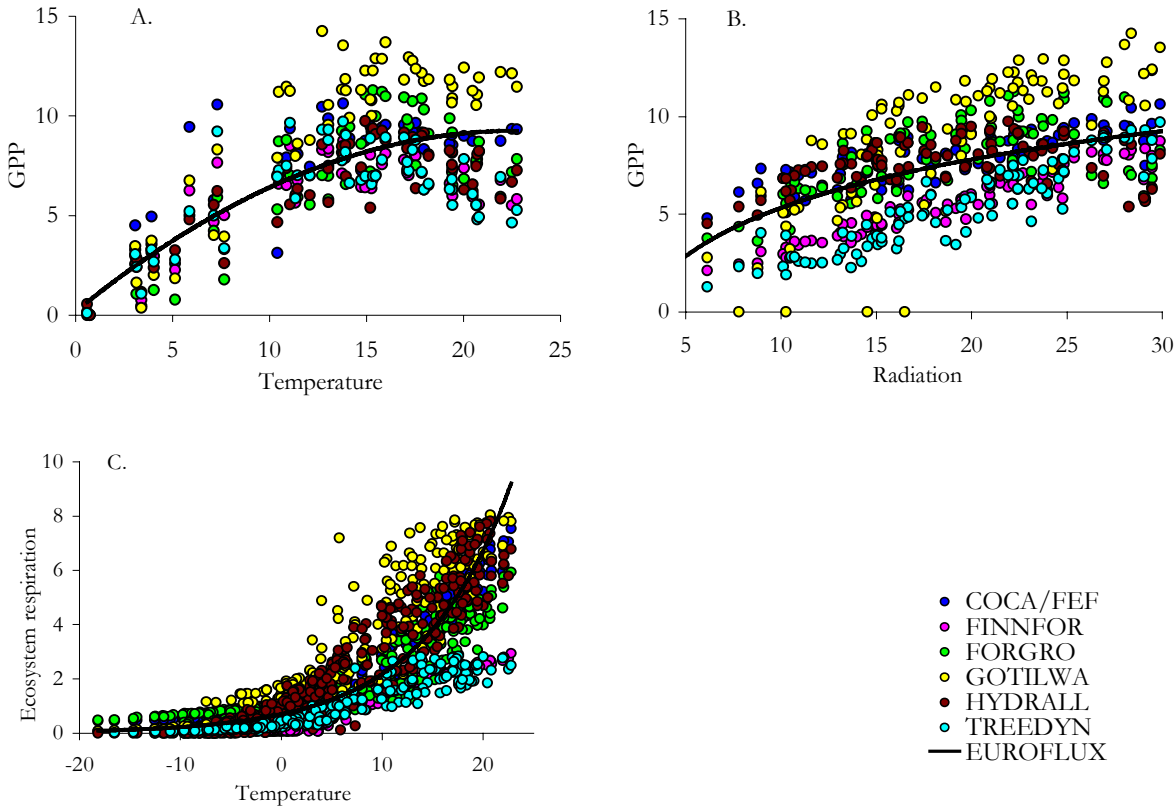

Figure 4.3 Responses of gross primairy production to temperature (A), and radiation (B), and of ecosystem respiration to temperature (C). The EUROFLUX-line is a fitted trendline through the EUROFLUX data.

Since transpiration and carbon sequestration are linked through stomatal conductance, the comparison of measured and predicted transpiration can be used to analyze the modelled carbon fluxes. In the EUROFLUX data, transpiration values were not separated from the total water fluxes. However, during dry days, interception and soil evaporation will be negligable in forest stands. Therefore, the model output was analysed for data during the growing season at days without precipitation. This was done for two sites, Hyytiala and Hesse, and four models (FINNFOR, FORGRO, GOTILWA and HYDRALL), which all provide daily transpiration as an output.

For Hyytiala, the transpiration predicted by HYDRALL fitted most closely to the data (Tabel 4.6). Also FORGRO and GOTILWA showed low systematic error, but more unsystematic variation. FINNFOR systematically underestimated the transpiration for values exceeding 1 mm d^{-1}. Only the models FORGRO and GOTILWA were applied to the beech forest at Hesse. Both models gave accurate estimates of transpiration, but FORGRO gave a larger systematically error (Tabel 4.6).

Tabel 4.6 Goodness-of-fit of predicted transpiration (kg H_2O m^{-2} d^{-1}) at dry days during the growing season compared to estimates based on EUROFLUX measurements at Hyytiälä and Hesse.

		FINNFOR	FORGRO	GOTILWA	HYDRALL
Hyytiälä (n=43)					
	r^2	0.02	0.57	0.52	0.73
	MSE_s	3.33	0.09	0.03	0.01
	MSE	3.55	0.37	0.60	0.25
Hesse (n=56)					
	r^2		0.75	0.79	
	MSE_s		0.24	0.16	
	MSE		0.32	0.32	

Figure 4.4 shows the responses of transpiration at dry days during the growing season to radiation and temperature. For Hyytiälä (Figure 4.4A.B) HYDRALL most closely represents the observed responses. Both FORGRO and GOTILWA show a somewhat wider scatter of the modelled responses, but also accurately represent the observed response. FINNFOR underestimates the higher values of daily transpiration both at high radiation and temperature compared to the EUROFLUX reference.

For Hesse, both FORGRO and GOTILWA represent the observed responses reasonably good (Figure 4.4C,D) FORGRO underestimates high transpiration values at high levels of radiation and temperature. GOTILWA somewhat underestimates the transpiration at high radiation levels (Figure 4.4C) and at low temperature (Figure 4.4D).).

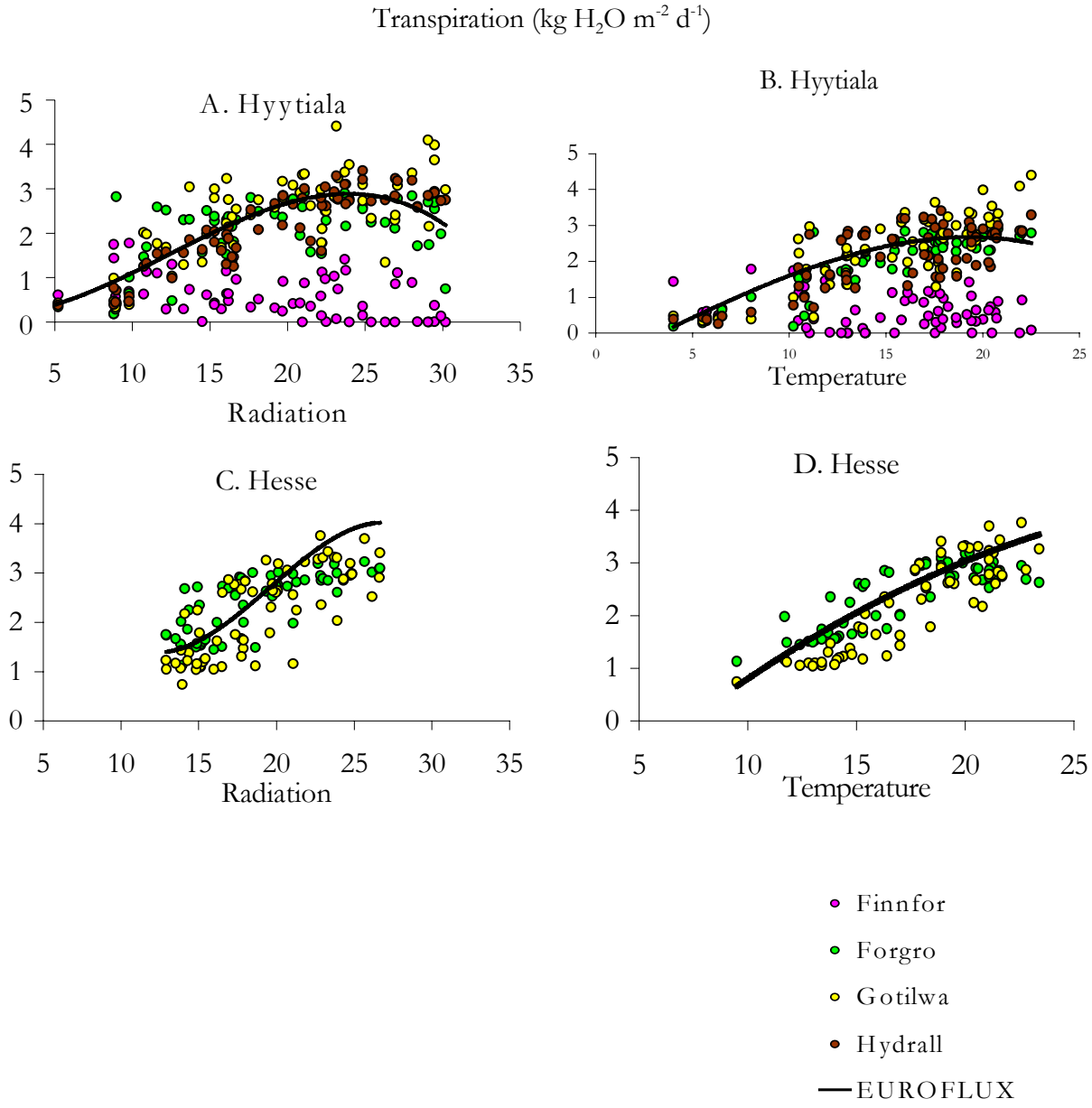

Figure 4.4 Responses of transpiration (kg H_2O m^{-2} d^{-1}) at dry days during the growing season to temperature and radiation in Hyytiälä and Hesse. Hyytiälä represents a boreal Scots pine forest site. Hesse represents a temperate beech forest site. The EUROFLUX-line is a fitted trendline through the EUROFLUX data.

4.3.3 Model comparison to growth and yield data

Annual values of stand density (N), stem diameter (DBH), height (H) (only in the case of Hydrall), stand basal area (BA), stand volume (STVOL) and current annual increment (CAI) obtained with the different process-based models were compared with the growth and yield table values suitable for the each site. Table 4.7 presents the goodness-of-fit of

the models in Hyytiala (table from Koivisto 1959). In general for most of variables, all models output show a good correlation. Only, the explained variance (r^2) for COCA/FEF basal area output, and FORGRO CAI output are very low (0.02). In these cases the tendency of these variables with increasing stand age is rather flat differently than the pattern shown by growth and yield tables (see Figure 4.5).

Table 4.7. Goodness-of-fit of the model predictions expressed as explained variance (r^2), systematic mean square error (MSE_s) total mean square error (MSE) of N (trees ha^{-1}), DBH (cm), H (m), BA ($m^2\ ha^{-1}$), standing volume ($m^3 ha^{-1}$) and CAI ($m^3 ha^{-1} yr^{-1}$) compared to data from growth and yield tables for Hyytiälä site (Koivisto 1959).

	COCA/FEF	BIOMASS	FORGRO	GOTILWA	HYDRALL
N					
(n=10)					
r^2	0.96	1.00	0.94	0.90	
MSE_s	101.53	0.00	607.32	82.63	
MSE	198.76	0.00	736.79	256.14	
DBH					
(n=10)					
r^2			0.99	0.98	
MSE_s			1.85	1.94	
MSE			2.21	2.59	
H					
(n=11)					
r^2					0.95
MSE_s					0.79
MSE					1.87
BA					
(n=10**)**					
r^2	0.02		0.98	0.82	
MSE_s	11.19		19.43	1.87	
MSE	22.00		20.65	3.16	
STVOL					
(n=10)					
r^2	0.88	1.00	0.98	0.99	0.99
MSE_s	22.41	0.00	11.91	0.03	9.06
MSE	42.74	0.00	20.03	0.09	12.33
CAI					
(n=10)					
r^2	0.68	0.81	0.02	0.56	0.13
MSE_s	0.65	0.37	1.88	0.34	1.30
MSE	1.65	1.16	2.60	2.50	2.41

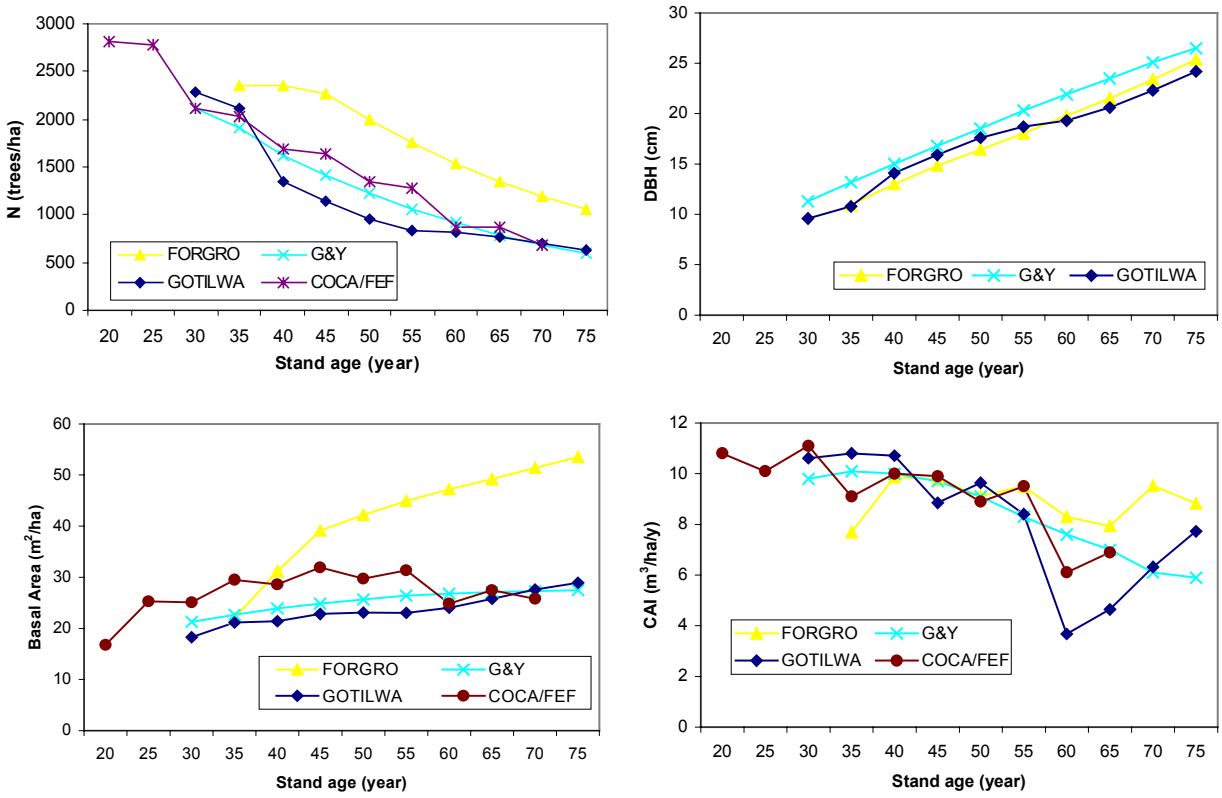

Figure 4.5. Stand density (N), Stem diameter (DBH), Basal Area and Current Annual Increment (CAI) of Pinus sylvestris in Hyytiala obtained with the models COCA/FEF, FORGRO and GOTILWA and growth and yield tables (G&Y, Koivisto 1959) predicted at different stand ages.

Looking at table 4.7, N systematic (MSE_s) is high in the case of FORGRO. This is also shown in figure 4.5 where FORGRO values of stand density are parallel but higher that values of growth and yield table. BIOMASS followed the same values than growth and yield table, and COCA/FEF and GOTILWA were closely around those values. DBH values predicted by the models FORGRO and GOTILWA are good, but slightly lower that growth and yield table ones. The same can be stated for HYDRALL predictions of H. Explained variance of BA in the case of FORGRO is high, but it presents a relatively high systematic error. This is also shown in figure 4.5 where FORGRO BA values are systematically higher than growth and yield table ones. GOTILWA presents very close values of BA to growth and yield ones, thus showing the lower systematic error. It was agreed that performing the simulations, stand volume was the criteria to cut the forest throughout time according to the table values, at different stand ages. Thus, most of the models followed the same volume values than the tables (not shown). Only COCA/FEF and FORGRO show some deviation from that but minor differences. In general, CAI presents the lower r^2 values for most of the models. As presented in Figure 4.5 it can be seen that model predictions fluctuate around growth and yield table values. Since most of the models present a strong variation between 55 and 70 years of stand age, this is probably due to the pattern of the meteorological file applied.

Table 4.8. Goodness-of-fit of GOTILWA model predictions expressed as explained variance (r^2), systematic mean square error (MSE_s) total mean square error (MSE) of N (trees ha^{-1}), DBH (cm), BA ($m^2\ ha^{-1}$), standing volume ($m^3 ha^{-1}$) and CAI ($m^3 ha^{-1} yr^{-1}$) compared to data from growth and yield tables for EUROFLUX sites. (Hyytiälä: Koivisto 1959, Bray: Lemoine and Decourt 1969, Collelongo: Cantiani 1957, Loobos: Jansen et al. 1996, Sarrebourg: Mendlik 1985).

	Hyytiälä (n=10)	Bray (n=6)	Collelongo (n=4)	Loobos (n=10)	Sarrebourg (n=5)
N					
r^2	0.90	0.98	0.99	0.99	0.90
MSE_s	82.63	67.60	310.46	105.70	518.92
MSE	256.14	79.04	551.76	138.01	740.50
DBH					
r^2	0.98	0.99	0.99	0.98	0.91
MSE_s	1.94	1.35	0.62	0.59	2.69
MSE	2.59	1.72	0.73	1.13	3.87
BA					
r^2	0.82	0.99	0.93	0.95	0.98
MSE_s	1.87	7.32	0.88	2.90	11.26
MSE	3.16	8.02	2.59	3.60	12.49
STVOL					
r^2	0.99	0.99	0.99	1.00	0.99
MSE_s	0.03	4.97	0.17	0.00	18.95
MSE	0.09	9.49	0.26	0.00	28.29
CAI					
r^2	0.56	0.92	0.66	0.65	0.96
MSE_s	0.34	0.69	9.37	2.89	23.08
MSE	2.50	1.12	18.53	4.09	45.74

Table 4.8 shows the long-term goodness-of-fit of GOTILWA model in the different EUROFLUX sites. Other models were also applied in some of these sites (data not shown here) but GOTILWA illustrates what was obtained. In general the results of this table can be explained similarly to the previous table (table 4.7). Nevertheless, the objective of presenting this table is to show that the models (in this case GOTILWA) were applied to different species in different environmental conditions. Of course, depending of the species and sites the availability of values at a given stand age of growth and yield tables were limited (see n= in each site), constraining the applicability of this type of comparison analysis. This situation of the long-term model comparisons was not the case of the short-term comparisons (presented above) where more values, several days, were compared.

4.3.4 Short-term model sensitivity

The results for each site of the observed and predicted CO_2-fluxes, and the observed and predicted H_2O fluxes are presented in Figures 4.6A1-7 and 4.6X1-7, respectively. The response surfaces of the CO_2 and H_2O fluxes of the climate change scenarios are presented in Figures 4.6B1-7 and 4.6D12-7, respectively. To understand the differences in the response surfaces between species and between sites for similar species, the responses of both net photosynthesis and stomatal conductance to light, temperature and CO_2 are

required. These responses are presented in Figures 4.7a1-6 for net photosynthesis and in Figures 4.7b1-6 for stomatal conductance for each species. The assumed conditions for these figures are T= 20°C, CO2= 350 ppm; radiation= 500 μmol m^{-2} s^{-2} PAR, unless stated otherwise.

In general it can be seen in Figures 4.6B1-7 and 4.6D1-7 that the responses of the H_2O fluxes to the climate change scenarios is more similar over species and sites than the responses of the CO_2 fluxes. Interesting differences between species and sites include: i) The response surfaces of the CO_2 flux of Fagus and Pseudotsuga are less sensitive to CO_2 than that of Picea and Pines (Figs 4.6B1-7) The light responses of these species show that Fagus and Pseudotsuga are under the conditions considered only light-limited; whereas Picea and Pinus are also CO_2-limited at high light conditions (Figs. 4.7B1-4) The parameter values of these species result in higher net photosynthesis of the former two species compared to the latter two at CO_2=350 ppm, and a less pronounced increase of net photosynthesis to a doubling of CO_2. ii) The response surface of the CO_2 flux of Pinus in Hyytialla is much more sensitive to temperature than that of Pinus in Loobos (Figs. 4.6B4 vs 4.6B5). Figures 4.7A5 shows that the optimum temperature for net photosynthesis for Pinus is rather low and with a distinctive peak at 15°C. The prevailing temperature in Hyytiälä will be less than in Loobos and therefore net photosynthesis will respond more to a temperature increase in Hyytiälä compared to Loobos. iii) The sensitivity of response surface of the H_2O flux to CO_2 is similar for all species (Figs. 4.6D1-7). In Fig. 4.7B6 it can be seen that the response of stomatal conductance to CO_2 is indeed very similar for the 4 species. iv) The response surface of the H_2O flux of Pseudotsuga and Picea at Weiden Brunnen is much more sensitive to temperature than that of the other species and sites. Fig. 4.7B5 shows that the stomatal conductance of Pseudotsuga is indeed much more sensitive to temperature than the other species. For Picea this is due to the low absolute values of the stomatal conductance (Fig. 4.7B1) so that even a small absolute change results in a large relative response (Fig. 4.6D7).

A4 Figuur 4.6 (= figuur 3 Excel)

A4 Figuur 4.7 (figuur 4 Excel)

4.3.5 Long-term model sensitivity

Model sensitivity indexes for *Pinus sylvestris* at Hyytiälä site are shown in tables 4.9 and 4.10 (S1 and S2 respectively). In general models show a positive response to the increase of CO_2 concentration, presenting higher values of GPP, NPP and CAI than the reference (S1 is greater than 1 and S2 has positive values). Despite 700 represent 1.75 times 400, the response at 700 of these variables was in a lower proportion. This is evidenced in both S1 and S2. S1 at 700 is not 1.75 times S1 at 400 and S2 values at 700 are smaller than at 400. The effects of increased CO2 on ET values depend on the models and stand age. Looking at precipitation, all models are responsive. In most of the cases they show negative responses in terms of GPP, NPP, CAI and ET, to 10 percent decrease in precipitation and a slightly positive responses to 10 percent increase of precipitation.

The response to the temperature increase depends of the models and stand age. Growth could be positively affected by the increase in temperature by means enhancement of photosynthetic activity, that is expected in cold areas as Hyytiala. Nevertheless this positive effect may be counter balanced by the increase in respiration activity. This happens to be more important in older (bigger) trees, so the most common pattern shown by the models is a negative effects in the older period despite the positive effects in the first period when the stand is younger (and trees smaller). ET is also enhanced by T+2 except in the case of HYDRALL.

Some models are less responsive to stand age. This is the case of FORGRO, which does not show different responses or only slightly different at the different periods of the stand development.

The sensitivity analysis was performed by some of the models in other sites and with other species. As an example table 4.11 presents the results of S1 index performed by GOTILWA model in different sites and species. The pattern observed in the other sites is very similar to the one obtained in Hyytiala. Thus, the of results and their explanations are mostly equivalent.

Table 4.9 Sensitivity index S1 for some output variables for Pinus sylvestris at Hyytiälä site

		GOTILWA					FORGRO			COCA-FEF			HYDRALL					BIOMASS		
Variables	Years	400	700	P-10	P+10	T+2	400	700	T+2	400	700	T+2	400	700	P-10	P+10	T+2	400	700	T+2
GPP	1 - 5	1.10	1.47	0.99	1.00	1.05	1.06	1.29	1.00				1.24	1.38	0.95	1.04	0.86	1.06	1.29	1.09
$GCm^{-2}y^{-1}$	16 - 20	1.09	1.37	0.97	1.02	0.96	1.06	1.29	0.99				1.32	1.32	0.98	1.02	0.87	1.08	1.36	1.06
	46 - 50	1.10	1.40	0.97	1.03	0.97	1.06	1.29	0.98									1.11	1.56	1.05
NPP	1 - 5	1.11	1.53	0.99	1.00	1.01	1.06	1.29	1.00				1.24	1.38	0.95	1.04	0.86	1.08	1.37	1.01
$GCm^{-2}y^{-1}$	16 - 20	1.09	1.32	0.98	1.02	0.94	1.06	1.29	0.99				1.32	1.32	0.98	1.02	0.87	1.09	1.42	0.99
	46 - 50	1.07	1.22	0.97	1.02	0.91	1.06	1.29	0.98									1.14	1.68	0.97
CAI	1 - 5	1.17	1.81	0.99	1.00	0.95	1.10	1.47	0.94	1.23	2.73	1.08	1.36	1.48	0.91	1.07	0.76	1.09	1.43	1.01
$M3\ ha^{-1}y^{-1}$	16 - 20	1.09	1.13	1.02	0.99	0.98	1.09	1.40	0.93	1.21	2.97	1.10	1.24	1.21	0.91	1.07	0.84	1.11	1.52	0.98
	46 - 50	1.12	0.84	0.92	0.95	0.63	1.08	1.35	0.91	1.27	2.14	1.11						1.21	2.06	0.96
ET	1 - 5	0.99	0.92	0.97	1.03	1.18	0.99	1.01	1.09				1.23	2.11	0.83	1.18	0.93	0.99	0.93	1.18
$KgH_2O\ m^{-2}y^{-1}$	16 - 20	1.00	0.98	0.94	1.05	1.07	1.00	1.00	1.09				1.15	1.15	0.82	1.18	1.00	1.01	1.03	1.12
	46 - 50	1.00	0.98	0.94	1.05	1.09	1.00	0.99	1.07									1.05	1.20	1.12

Table 4.10 Sensitivity index S2 for some output variables for Pinus sylvestris at Hyytiälä site

		GOTILWA					FORGRO			COCA-FEF			HYDRALL					BIOMASS		
Variables	Years	400	700	P-10	P+10	T+2	400	700	T+2	400	700	T+2	400	700	P-10	P+10	T+2	400	700	T+2
GPP	1 - 5	0.68	0.47	-0.09	0.04	0.06	0.45	0.29	-0.01				1.13	0.34	-0.50	0.41	-0.62	0.43	0.29	0.10
$GCm^{-2}y^{-1}$	16 - 20	0.66	0.37	-0.30	0.23	-0.07	0.45	0.29	-0.02				0.67	0.29	-0.24	0.15	-0.56	0.54	0.36	0.08
	46 - 50	0.69	0.40	-0.33	0.28	-0.05	0.45	0.29	-0.03									0.80	0.56	0.09
NPP	1 - 5	0.79	0.53	-0.10	0.03	0.02	0.45	0.29	-0.01				1.13	0.34	-0.50	0.41	-0.62	0.54	0.37	0.01
$GCm^{-2}y^{-1}$	16 - 20	0.63	0.32	-0.25	0.21	-0.10	0.45	0.29	-0.02				0.67	0.29	-0.24	0.15	-0.56	0.62	0.42	-0.02
	46 - 50	0.48	0.22	-0.33	0.20	-0.17	0.45	0.29	-0.03									0.95	0.68	-0.05
CAI	1 - 5	1.22	0.81	-0.12	0.00	-0.06	0.72	0.47	-0.07	1.63	12.11	0.13	1.69	0.42	-0.88	0.70	-1.05	0.62	0.43	0.01
$M3\ ha^{-1}y^{-1}$	16 - 20	0.66	0.13	0.16	-0.11	-0.03	0.63	0.40	-0.10	1.46	13.80	0.18	1.15	0.18	-0.88	0.67	-0.70	0.77	0.52	-0.02
	46 - 50	0.87	-0.16	-0.84	-0.48	-0.66	0.56	0.35	-0.17	1.87	7.98	0.15						1.48	1.06	-0.07
ET	1 - 5	-0.07	-0.08	-0.30	0.26	0.22	-0.09	0.01	0.11				1.09	0.99	-1.68	1.79	-0.29	-0.09	-0.07	0.21
$KgH_2O\ m^{-2}y^{-1}$	16 - 20	0.01	-0.02	-0.59	0.51	0.10	0.02	0.00	0.13				0.69	0.14	-1.77	1.83	-0.01	0.09	0.03	0.18
	46 - 50	0.03	-0.02	-0.58	0.53	0.17	-0.02	-0.01	0.12									0.36	0.20	0.21

Table 4.11 . Sensitivity index S1 for some output variables at other sites different that Hyytiala also simulated by GOTILWA model

Site		GPP $gCm^{-2}y^{-1}$					NPP $gCm^{-2}y^{-1}$					CAI $m3\ ha^{-1}y^{-1}$					ET $KgH2O\ m^{-2}y^{-1}$				
Species	Years	400	700	P-10	P+10	T+2	400	P-10	P+10	700	T+2	400	700	P-10	P+10	T+2	400	700	P-10	P+10	T+2
LOOBOS	1 - 5	1.11	1.56	0.96	1.03	0.90	1.13	1.70	0.95	1.03	0.84	1.26	2.37	0.92	1.05	0.66	0.99	0.96	0.94	1.05	1.04
Pinus	16 - 20	1.10	1.43	0.96	1.02	0.90	1.07	1.28	0.97	1.02	0.91	0.95	0.63	0.99	0.97	0.92	1.00	0.98	0.94	1.05	1.04
sylvestris	46 - 50	1.12	1.56	0.97	1.03	0.88	1.10	1.53	0.97	1.03	0.87	1.05	2.23	0.97	1.02	0.78	1.01	0.97	0.95	1.05	1.06
BRAY	1 - 5	1.12	1.72	0.98	1.01	0.96	1.13	1.78	0.98	1.02	0.94	1.20	2.14	0.97	1.02	0.83	1.00	0.98	0.97	1.03	1.11
Pinus	16 - 20	1.12	1.59	0.97	1.03	0.94	1.12	1.58	0.97	1.03	0.93	1.17	1.82	0.96	1.04	0.86	1.01	1.00	0.95	1.04	1.07
pinastser	46 - 50	1.10	1.42	0.97	1.02	0.92	1.09	1.31	0.97	1.02	0.93	0.85	0.05	0.97	0.97	1.23	1.01	1.01	0.95	1.04	1.02
SARREBOURG	1 - 5	1.10	1.47	0.98	1.01	1.06	1.12	1.56	0.98	1.02	1.04	1.21	1.96	0.97	1.02	1.05	1.00	0.95	0.95	1.04	1.11
Fagus	16 - 20	1.05	1.18	0.98	1.01	1.05	1.02	1.04	0.99	1.00	1.05	0.78	0.32	1.08	0.93	1.24	1.00	0.97	0.94	1.05	1.10
sylvatica	46 - 50	1.09	1.27	0.99	1.01	1.07	1.11	1.25	0.99	1.02	1.02	1.53	2.58	1.12	1.02	0.64	0.99	0.97	0.95	1.04	1.14
COLLELONGO	1 - 5	1.16	1.99	0.95	1.05	1.00	1.17	1.99	0.94	1.05	0.97	1.18	2.11	0.96	1.04	1.00	1.01	1.06	0.95	1.05	1.06
Fagus	16 - 20	1.14	1.43	0.98	1.02	0.95	1.14	1.29	0.99	1.01	0.88	1.16	1.10	1.03	1.03	0.80	1.00	0.98	0.95	1.04	1.06
sylvatica	46 - 50	1.19	1.71	0.95	1.04	0.94	1.23	2.01	0.96	1.04	0.79	1.25	4.04	0.36	0.95	0.33	1.00	0.99	0.94	1.05	1.06
PRADES	1 - 5	1.14	1.85	0.96	1.03	0.99	1.25	2.50	0.94	1.06	0.87	1.44	3.59	0.89	1.10	0.73	1.00	1.00	0.95	1.05	1.05
Quercus	16 - 20	1.15	1.71	0.95	1.04	0.96	1.14	1.64	0.95	1.05	1.00	1.18	1.71	1.03	1.63	1.46	1.02	1.02	0.94	1.05	1.03
ilex	46 - 50	1.15	1.82	0.96	1.04	0.97	1.15	2.03	0.97	1.04	0.99	0.99	3.27	1.05	1.04	1.27	1.01	1.01	0.96	1.05	1.05

4.3.6 Process-level uncertainty

The key-difficulty of performing an uncertainty analysis is the quantification of the uncertainty of the input values. In this study it was decided to treat only those source of uncertainty that could be quantified, thereby accepting the risk that other, not quantified, sources of uncertainty that may determine the output uncertainty, are missed. The sources of input uncertainty that could be quantified for this study consider the parameters of LeafPhot and the parameters of the climate change scenarios. For LeafPhot, five aggregated groups of parameters were discerned: *i*) the light-reaction; *ii*) the CO_2-reaction; *iii*) dark respiration; *iv*) the temperature response of the parameters and *v*) stomatal conductance. The output variables considered were the CO_2 and H_2O fluxes for the site where the model predictions most closely match the observations. This was *Picea abies* at the Weiden Brunnen-site. The groups of parameters and their ranges are indicated in table 4.12. A uniform distribution over the ranges was assumed, as no information was available on the distribution of the values within these ranges. For each group of parameters 1000 samples was drawn while keeping the other parameter fixed. Hence the estimation of the variances of the uncertainty analysis is based on 5000 model runs.

Table 4.12 Parameter values for each of the sites, and the range used for 5 groups of parameters (indicated in bold) for the uncertainty analysis. The uncertainty analysis was performed for Picea abies at Weiden Brunnen.

	Default value	*Min*	*Max*	*Description*	*Unit*
			Light		
α	0.015	0.015	0.018	light use efficiency	µmol CO2 µmol photons-1
J_{max}	14	12	14	Electron transport rate at 298K	µmol CO2 m-2 s-1
			CO2		
K_c	299			MM-constant for carboxylation at 298K	µl l-1
K_o	160			MM-constant for oxygenation at 298K	ml l-1
τ	2339.53			specifity at 298K	-
$V_{c,max}$	19.7	19.7	37.1	carboxylation at 298K	µmol CO2 m-2 s-1
			Respiration		
R_d	0.53	0.53	0.72	respiration at 298K	µmol CO2 m-2 s-1
			Temperture		
$\Delta S(J_{max})$	643			entropy term	J mol-1 K-1
$\Delta S(V_{c,max})$	656			entropy term	J mol-1 K-1
$H_a(R_d)$	63500	56050	63500	energy of activation	J mol-1
$H_a(K_C)$	65000			energy of activation	J mol-1
$H_a(K_O)$	36000			energy of activation	J mol-1
$H_a(\tau)$	-28990			energy of activation	J mol-1
$H_a(V_{c,max})$	75750	75250	75750	energy of activation	J mol-1
$H_a(J_{max})$	47170	44898	47170	energy of activation	J mol-1
$H_d(J_{max})$	200000	190000	200000	energy of deactivation	J mol-1
$H_d(V_{c,max})$	200000	200000	230000	energy of deactivation	J mol-1
			Conducance		
C_g	9.8	9.8	12.8	Ball-factor	-
$G_{s,max}$	60	60	350	maximum conductance	mmol H2O m-2 s-1
$G_{s,min}$	0	0	1	minimum conductance	mmol H2O m-2 s-1

The percentage of total output variance that is attributable to the parameter groups discerned in the coupled photosynthesis-stomatal conductance model LeafPhot are presented inTable 4.13. For the CO_2 fluxes it was found that 94% of the output uncertainty is due to the variability of the parameters involved in the photosynthesis calculation. However, for the H_2O fluxes 59% of the output uncertainty is attributable to the conductance parameters. For both the CO_2 and H_2O fluxes the variability of the temperature and dark respiration parameters considered attribute only a minor part to the total output variance (4+8=12% for the CO_2 flux; 2+4=6% for the H_2O flux). Both fluxes are also consistent in that the uncertainty in parameters involved in carboxylation (72% for CO_2; 34% for H_2O) attribute more to the total output variance compared to the parameters involved in the light reaction (20% for CO_2; 9% for H_2O).

Table 4.13 Percentage of variance of CO_2-fluxes (NEE, gC m^{-2} y^{-1}) and H_2O-fluxes (E, kg H_2O m^{-2} y^{-1}) attributed to variance of groups of input parameters by the model FORGRO (Kramer et al., 1999). The groups are composed into larger groups, e.g. the first result column for each flux compares the parameter groups Light, CO_2, Dark respiration, Temperature with Conductance, etc. (standard deviation between brackets).

<table>
<tr><th>Parameter group</th><th colspan="3">CO_2-fluxes</th><th colspan="3">H_2O-fluxes</th></tr>
<tr><td>Light</td><td rowspan="4">94 (4)</td><td rowspan="3">89 (4)</td><td>20 (3)</td><td rowspan="4">42 (4)</td><td rowspan="3">41 (3)</td><td>9 (3)</td></tr>
<tr><td>CO_2</td><td>72 (3)</td><td>34 (3)</td></tr>
<tr><td>Dark respiration</td><td>4 (3)</td><td>2 (3)</td></tr>
<tr><td>Temperature</td><td>8 (3)</td><td>8 (3)</td><td>4 (3)</td><td>4 (3)</td></tr>
<tr><td>Conductance</td><td>5 (3)</td><td>5 (3)</td><td>5 (3)</td><td>59 (3)</td><td>59 (3)</td><td>59 (3)</td></tr>
</table>

4.4 Discussion

4.4.1 Model validation

In this study, the first step to evaluate the ability of different models to produce reliable predictions of short-term carbon fluxes was the analysis of the goodness-of-fit, where the model-predicted daily values of NEE were compared to those estimated at the EUROFLUX project. This analysis showed that generally the model

results fitted well to the observed data, but also that the goodness-of-fit systematically varied between different sites.

The applications of the models under changing environmental conditions requires that the environmental response of both components of net ecosystem exchange, namely gross primary production and respiration, must be represented realistically in the models. The comparison of modelled annual values of these variables to the EUROFLUX estimates showed that in the case of most models, accurate estimates of GPP and respiration were produced. However, in some models, considerable over- or underestimates were found for both components of carbon flux. This discrepancy required further analyses.

The comparison to the environmental responses of these processes, estimated on the basis of the EUROFLUX results, showed that the main causes for the systematic model errors were in the radiation response of GPP and in the temperature response of respiration. In the case of respiration, different type of response functions were applied in different models. Due to the lack of empirical data on the environmental response of the respiration of different components in trees and soil, the model assumptions may differ considerable, and therefore various results are excepted. In the predictions of photosynthesis, differences between models may occur in the assumptions and parametrization at the process level, and in the scaling up to the canopy level. In the case of most of the models used in this study, similar approach was used in modelling the leaf photosynthesis (Farquhar and von Caemmerer 1982), and also the model parametrization was made uniform as far as possible by utilizing the ECOCRAFT database. Instead, the assumptions concerning the environmental regulation of stomatal conductance differed between the models. The EUROFLUX data allowed indirect methods for evaluating the modelled stomatal conductance through the measurements of evapotranspiration. The comparison of the environmental responses of the dry day evapotranspiration to the modelled transpiration values (in the case of those models, which could produce this variable) indicates that major part of the differences between the model predictions of photosynthesis is caused by the differences in the modelled stomatal conductance.

Precise data is required for the testing of models. The reliability of the flux data itself was not under discussion in this study. The data provided by the researchers of the EUROFLUX sites were used with a minor gap-filling procedure to avoid the loss of many days with observations (see Material and Methods). However, the quality and methods of correction of flux data is a much-discussed topic in this area of research (*e.g.* Wofsy *et al.* 1993; Goulden *et al.* 1996; Lavigne *et al.* 1997). Therefore a lack of correspondence between model output and data may partly be due to fact that such corrections have not been applied to the data used.

Furthermore, it should be realized that the data sets used are quite limited and do not represent all climatic conditions encountered in Europe. Especially, there was no strong water stress influence in the data sets used. Although some models track the responses of transpiration to respiration and temperature accurately, the effects of water limitation on growth are not tested in this study. Thus, the conclusion drawn

from this exercise is limited to boreal and northern temperate forests, *i.e.* not water-stressed conditions.

As a conclusion, several process-based models are available which are able to produce accurate estimates of carbon and water fluxes at several forest sites of Europe. This considerable accuracy fulfills one requirement of models to be able to predict the impacts of climate change on the carbon balance of European forests. However, the variable behavior of the models at the process level indicates requirement of further model testing with special emphasis on model realism.

4.4.2 Short-term model sensitivity

The relative responses of the CO_2 fluxes to the climate change scenarios differ strongly between the species and sites (Fig 2b). A large relative response can be either due to a strong sensitivity of photosynthesis to a driving factor, or due to a small change of a low absolute value. This is *e.g.* the case for Picea at the Weiden Brunnen site. Vice versa, a small relative response can be either due to a low sensitivity of photosynthesis to a driving factor, or due to a high absolute value even with a significant sensitivity. This is *e.g.* the case for Pseudotsuga for the Vielsalm site. However, presenting absolute responses make results difficult to compare if the scales are very different. Therefore the responses of the underlying processes such as net photosynthesis and stomatal conductance to light, temperature and CO_2, are required to understand the responses of fluxes of CO_2 and H_2O at the stand level to climate change scenarios.

4.4.3 Long-term model testing and sensitivity analysis

The models analysed at long-term time scale are able to mimic forest growth patterns. Nevertheless it is difficult to perform good comparisons due to the few amount of reference values to compare. Since growth and yield tables provide values every 5 or 10 years the set of values taken into account for comparisons is rather small. On the other hand models took into account the 50 years of meteorological data, with specific events throughout the time series. Thus, variations of growth at a certain age may be stimulated by certain conditions due to the meteorological data utilised at each site.

Despite the models are suitable to mimic forest growth, it would be good to check models with other independent long term data with at least annual values and longer time series. Nevertheless, the approach utilised here is encouraging for further analysis. Another point of concern about the limitation of this long term comparison is that the models performance may apparently behave worse that they really do. This comes after the assumption that the chosen growth and yield tables are valid for the specific stands of EUROFLUX sites, while the tables were built based on values obtained over larger areas.

All models have shown that are responsive to changes in environmental variables as temperature, precipitation and CO_2 concentration, which are important to define climate conditions. The type of responses is in relatively good agreement with the expected responses obtained by experimental studies. Despite it is difficult to quantify the proper amount of response in each condition, the models are able to deal with new conditions and explore the likely effects of climate change. This is shown in the sensitivity analysis performed in Hyytiälä, but also in the other sites where other species and environmental conditions were considered.

4.4.4 Uncertainty analyses

The aim of performing an uncertainty analysis is to attribute the uncertainty of the model prediction to different sources of uncertainty. For some sources such as parameters the uncertainty can be reduced by more accurate measurements, and hence the reduction in uncertainty of the model prediction can be evaluated (Rossing *et al.* 1994a, b). Other sources such as the climate are inherently uncertain and constitute the remaining model uncertainty if the other sources of uncertainty are quantified in perfection. Thus the analysis can focus research to those sources of uncertainty from which the largest reduction in model uncertainty is expected. The critical step in this analysis is however the quantification of the uncertainty of the different sources. Preferably both the distribution and the correlation structure of the parameters is determined based on the data from which the parameters are estimated. In this study a method to perform an uncertainty analysis is outlined, and the first results are presented. It is based on observed ranges of parameters that are assumed the most important for short-term responses of CO_2 and H_2O to climate change scenarios. It can be argued that the chosen ranges of the parameters are rather narrow compared to other values presented in the literature (e.g. Wullschleger 1993). Nevertheless the results are sufficiently outspoken that for the coupled leaf photosynthesis-stomatal conductance model LeafPhot it can be concluded that the uncertainty of flux of H_2O is to a large extend attributable to the stomatal conductance model, whereas this is hardly the case for the CO_2 flux. Furthermore, the parameters of the CO_2-reaction contribute most for the uncertainty of both fluxes compared to the other parameters of the photosynthesis model. Thus, the output uncertainty can be much reduced by an accurate quantification of the parameters of the photosynthesis model.

4.5 References

Aubinet, M., Grelle, A., Ibrom, A., Rannik, Ü., Moncrieff, J., Foken, T., Kowalski, A.S., Martin, P.H., Berbigier, P., Bernhofer, Ch., Clement, R., Elbers, J., Granier, A., Grünwald, T., Morgenstern, K., Pilegaard, K., Rebmann, C., Snijders, W., Valentini, R. and Vesala, T., 2000. Estimates of the annual net carbon and water exchange of European forests: the EUROFLUX methodology. Advances in Ecological Research, 30, 113-175.

Baldocchi D., 1994. An analytical solution for coupled leaf photosynthesis and stomatal conductance models. *Tree Physiology*, **14**: 1069-1079.

Ball J.T., Woodward I.E. & Berry.J.A., 1987. A model predicting stomatal conductance and its contribution to the control of photosynthesis under different environmental conditions. In: *I, Biggins (Ed.) Progress in Photosynthesis research,* Martinus Nijhoff Publishers, The Netherland, pp. 221-224.

Bernhofer Ch, Feigenwinter C, Grünwald T, Vogt R (1998) A modified spectral correction method for damping loss of water and carbon flux using displaced sensors for EC measurements. Submitted to *Annales des Sciènce Forestrière*

Cantiani, M. 1957. Yield tables for low fertility beech stands in Irpinia (Region: Campania; Province: Avellino, Southern Italy).

Epron D, Farque L, Lucot E, Badot PM (1999) Soil CO_2 efflux in a beech forest: dependence on soil temperature and soil water content. *Annales des Sciènce Forestrière*, in press.

Falge E.M., Graber W., Siegwolf R., Tenhunen, J.D., 1996. A model of the gas exchange response of Picea abies to habitat conditions. *Trees* **10**: 277 - 287

Falge, E.M., Ryel, R.J., Alsheimer M., Tenhunen, J.D., 1997. Effects of stand structure and physiology on forest gas exchange: a simulation study for Norway spruce. *Trees* **11**: 436 - 448

Farquhar G.D. and Von Caemmerer S., 1982. Modelling of photosynthetic response to environmental conditions. In: *Physiological Plant Ecology II: Water Relations and Carbon Assimilation*, 12B, O.L. Lange, P.S. Nobel, C.B. Osmond and H. Ziegler (eds.) Springer-Verlag, Berlin, pp. 549-587.

Goudriaan J., 1986. A simple and fast numerical method for the computation of daily totals of crop photosynthesis. *Agricultural and Forest Meteorology* **38**: 249-254.

Goudriaan J. and Van Laar H.H., 1994. Modelling potential crop growth processes, Kluwer Academic Publishers, Dordrecht, 238 pp.

Granier A, Biron P, Lemoine D (2000a) Water balance, transpiration and canopy conductance in two beech stands over a two-years experiment. *Agricultural and Forest Meteorology*, in press.

Granier A, Ceschia E, Damesin C, Dufrêne E, Epron D, Gross P, Lebaube S, Le Dantec V, Le Goff N, Lemoine D, Lucot E, Ottorini JM, Pontailler JY, Saugier B (2000b) Carbon balance of a young beech forest. *Functional Ecology*, in press

Goulden ML, Munger JW, Fan SM, Daube BC, Wofsy SC (1996) Measurements of carbon sequestration by long-term eddy covariance: Methods and a critical evaluation of accuracy. *Global Change Biology*, 2, 169-182.

Grünwald, Th, Bernhofer Ch (1998) Data gap filling with regression modelling. Proceedings of the LTEEF-EUROFLUX Conference in Antwerp, Belgium, 21-25.9.1998.

Houghton, JT, Filho LGM, Callander BA, Harris N, Kattenberg A, Maskell (eds) (1996) Climate Change. The science of climate change. Contribution of working group I to the second assessment report of the intergovernemental panel on climate change. Technical summary. Cambridge University Press, Cambridge, pp 4-47.

Houghton J.T., Jenkins G.J. and Ephraums J.J. (eds.), 1990. Climate change. The IPCC scientific assessment. Cambridge University Press, 365 pp.

Jansen M.J.W & Withagen J.C.M., 1997. USAGE: uncertainty and sensitivity analysis in a Genstat environment. Manual. Report CBW, 14 pp

Jansen M.J.W., Rossing W.A.H. & Daamen R.A., 1994. Monte Carlo estimation of uncertainty contributions from several independent multivariate sources. In: J. Grasman & G. Verstraten (Eds.) Predictability and nonlinear modelling in natural sciences and economics. Kluwer, Dordrecht, The Netherlands, pp. 334-343.

Jansen, J.J., J. Sevenster en P.J. Faber (eds.) 1996 Opbrengsttabellen voor belangrijke boomsoorten in Nederland. Yield tables for important tree species in the Netherlands. IBN Rapport 221, Hinkeloord Report No 17. *(compilation of all species)*

Koivisto, P. 1959. Growth and yield tables. Communications Instituti Forestalis Fenniae. 51: 1-44. Finnish Forest Research Insitute. Helsinki, Finland. *(compilation of all species)*

Kramer K., 1996a. Modelling comparison to evaluate the importance of phenology and spring frost damage for the effects of climate change on growth of mixed temperate-zone deciduous trees. *Climate Research* **7**: 31-41.

Kramer, K., 1996b. Phenology and growth of European trees in relation to climate change. Thesis Agricultural University Wageningen, 210 pp.

Kropff M.J. and Van Laar H.H. (eds.), 1993 . Modelling crop-weed interactions. CAB International, 274 pp.

Lavigne, MB, Ryan, MG, Anderson, DE, Baldocchi, DD, Crill, PM, Fitzjarrald, DR, Goulden, ML, Gower, ST, Massheder, JM, McCaughey, JH, Rayment, M, Striegl, RG, (1997) Comparing nocturnal eddy covariance measurements to estimates of ecosystem respiration made by scaling chamber measurements at six coniferous boreal sites. *J Geophys Res Atm*, 102, 28977-28985

Lemoine, B. and N. Decourt 1969 Yield tables for Maritime pine in the South-east of France Revue Forestiere Francaise 21(1): 5-17.

Matteucci G (1998) Bilancio del carbonio in una faggeta dell'Italia Centro-Meridionale: determinanti ecofisiologici, integrazione a livello di copertura e simulazione dell'impatto dei cambiamenti ambientali. PhD Thesis, Università degli Studi di Padova. Padova, 28 Febbraio 1998, Italy.

Medlyn, B.E. & Jarvis, P.G., 1997. Integration of results from elevated CO2 experiments on European forest species: the ECOCRAFT project. In: G.M.J. Mohren, K. Kramer & S. Sabaté: Impacts of Global Change on Tree Physiology and Forest Ecosystems. Proceedings of the International Conference on Impacts of Global change on Tree Physiology and Forest Ecosystems, held 26-29 November 1996, Wageningen, The Netherlands, pp. 273-279.

Mendlik, G. 1985 Beech yield table. Erdeszeti-Kutatasok 75: 189-198.

Mohren G.M.J., 1987. Simulation of forest growth, applied to Douglas fir stands in the Netherlands. Thesis, Wageningen Agricultural University, The Netherlands, 184 pp.

Mohren G.M.J., 1994. Modelling Norway spruce growth in relation to site conditions and atmospheric CO2. In: *Vegetation, Modelling and Climate Change Effects*, F. Veroustraete and R. Ceulemans (eds.), SPB Academic Publishing bv. The Hague, The Netherlands, pp. 7-22.

Mohren, G.M.J. & Kramer, K., 1997. Simulation of direct effects of CO2 and temperature increase on forest growth: the LTEEF project. In: G.M.J. Mohren, K. Kramer & S. Sabaté: Impacts of Global Change on Tree Physiology and Forest Ecosystems. Proceedings of the International Conference on Impacts of Global change on Tree Physiology and Forest Ecosystems, held 26-29 November 1996, Wageningen, The Netherlands, pp. 307-317.

Penning de Vries F.W.T., Brunsting A, and Van Laar H.H., 1974. Products, requirements and efficiency of biosynthesis; a quantitative approach. *Journal of Theoretical Biology* **45**: 339-377.

Rannik U (1998a) Turbulent atmosphere: Vertical fluxes above a forest and particle growth. Thesis Department of Physics, University of Helsinki. Report Series in Aerosol Sience 35.

Rannik U (1998b) On the surface layer similarity at a complex forest site. *Journal of Geophysical Research,* 103, 8685-8697.

Redei, K. and J. Gal 1986 Yield of robinia stands. Erdeszeti-Kutatasok 76-77: 195-203.

Rossing W.A.H, Daamen R.A. & Jansen M.J.W., 1994a. Uncertainty analysis applied to supervised control of aphids and brown rust in winter wheat. Part 1. Quantification of cost-benefit calculations. *Agricultural Systems* **44**: 419-448.

Rossing W.A.H, Daamen R.A. & Jansen M.J.W., 1994b. Uncertainty analysis applied to supervised control of aphids and brown rust in winter wheat. Part 2. Relative importance of different components of uncertainty. *Agricultural Systems* **44**: 449-460.

Troen I.,1993 (Ed.). Global change: climate change and climate and climate change impacts. Focussing of European research. Proceedings of the symposium held in Copenhagen, Denmark 6-10 September 1993. European Commission, Brussels, Belgium, 796 pp.

Valentini R (1999) The role of flux monitoring networks in carbon dioxide source/sinks estimation in terrestrial ecosystems. In: Valentini R, Brüning C (eds) Greenhouse gases and their role in climate change: the status of research in Europe. European Commission DG XII/B.I EUR (19085 EN, pp. 1-6.

Valentini R, De Angelis P, Matteucci G, Monaco R, Dore S, Scarascia Mugnozza GE (1996) Seasonal net carbon dioxide exchange of a beech forest with the atmosphere. *Global Change Biology* 2, 199-207.

Valentini R, Matteucci, G, Dolman AJ, Schulze E-D, Rebmann C, Moors EJ, Granier A, Gross P, Jensen NO, Pilegaard K, Lindroth A, Grelle A, Bernhofer C, Grünwald T, Aubient M, Ceulemans R, Kowalski AS, Vesala T, Rannik Ü, Berbigier P, Loustau D, Guđmundsson J, Thorgeirsson H, Ibrom A, Morgenstern K, Clement R, Moncrieff J, Montagnani L, Minerbi S, Jarvis PG (2000) Respiration as the main determinant of carbon balance in European forests. *Nature* 404, 861-865.

Vesala T, Markkanen L ,Palva E, Siivola, Palmroth S, Hari P (1999) Effect of variations of PAR on CO_2 exchange estimation for Scots pine. *Agricultural and Forest Meteorology,* 2747, 1-11.

Wallach D, Goffinet B (1987) Mean squared error of prediction in models for studying ecological and agronomic systems. *Biometrics,* 43, 561-573.

Wallach D, Goffinet B (1989) Mean squared error of prediction as a criterion for evaluating and comparing system models. *Ecological Modeling*, 4, 299-306.

Wofsy SC, Goulden ML, Munger JW, Fan SM, Bakwin PS, Daube BC, Bassow SL, Bazzaz FA, (1993) Net exchange of CO_2 in a mid-latitude forest. Science 260, 1314-1317.

Wullschleger S.D., 1993. Biochemical limitations to carbon assimilation in C_3 plants - a retrospective analysis of the A/C_i curves from 109 species. *Journal of Experimental Botany* **44**: 907-920.

5 Large-scale approaches

5.1 Introduction

In the LTEEF-II project three different types of large scale models had been applied for estimating the overall forest carbon pools and fluxes on European level. The large scale forest scenario model EFISCEN uses forest inventory data as input. Long - term dynamics of forest ecosystems under present and future climate projections, including soil carbon budget and forest management can be simulated with the model on a highly aggregated spatial and temporal level. The remote sensing based carbon budgeting tool C-Fix allows the simulation of the carbon fluxes in years with dedicated climatic conditions. The spatial explicit distribution of carbon fluxes can be studied in 1 x 1 km spatial and daily temporal resolution. The large scale vegetation models Eurobiota and Hybrid simulate long term dynamics of vegetation with generalized growth processes on a intermediate temporal and spatial resolution. So competition between different ecosystems under climate change can also be investigated. In this chapter we describe the different model types and approaches. Results will be presented and discussed in Chapter 9.

5.2 Forest inventory-based approach

G-J. Nabuurs, A. Pussinen, J. Liski & T. Karjalainen

A straightforward scaling-up method is based on forest inventory data and a large scale forestry model EFISCEN (European Forest Information Scenario Model) at the European Forest Institute (EFI). EFISCEN is a forest resource model, especially suitable for large scale (> 10 000 ha) and long term (20-70 years) analysis. It is suitable for assessments of the future state of forests under assumptions of future felling levels. The projections carried out with EFISCEN provide insight in increment, growing stock, age class distribution and actual felling per tree species. EFISCEN is an area-based forest matrix model and is based on earlier work of Sallnäs (1990) and Nilsson et al. (1992). This model has been further improved, and the current version, EFISCEN 2.0, is described in Pussinen et al. (2000). Analyses of the future development of forest resources in Europe and Russia have been carried out (for e.g. Nabuurs & Päivinen 1996, Nabuurs et al. 1998, Päivinen et al. 1999). Possibility to include transient changes in forest growth has been incorporated into the model, as well as conversion of stem wood volumes to whole tree biomass and carbon, litter production, and dynamic soil carbon and wood product submodels. Information from process based models, described in earlier chapters, have been used to convert stem wood volumes to whole tree biomass and litter production. Also forest growth under changing climate is based on the process based model output through modifying current forest growth in the model. A carbon book-keeping has been included in order to calculate carbon budgets of forests and wood products. Following subchapters provides details of the approach.

5.2.1 Description of the model

5.2.1.1 Input data and calculation of growth

State of a forest is depicted as an area distribution over age and volume classes in volume - age matrixes (Figure 5.1.1). Growth is described as area changes to higher volume classes and ageing of forest is incorporated as a function of time up to the point of regeneration. Fellings are specified for the whole country for each species group for each time period. The basic input data include forest area, growing stock and increment by age-classes, i.e. the data gathered in the national forest inventories. Separate matrix is set up for each forest type provided in the inventory data. Forest types are distinguished by region, by owner class, by site class and by tree species, depending of the aggregation level of the provided data. The projection of the growth in the model is based on growth fuctions that are calibrated based on the inventory data.

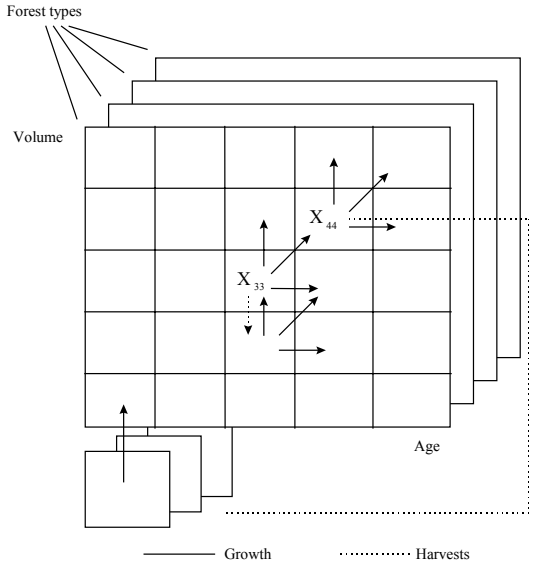

Figure 5.1.1. In EFISCEN state of forest is depicted as an area distribution over age and volume classes in volume - age matrixes (Nilsson et al. 1992). Growth is described as area changes to higher volume classes and ageing of forest is incorporated as a function of time up to the regeneration. Separate matrix is provided for each forest type provided in the inventory data used in the model.

European wide forest resource database, the EFISCEN European Forest Resource Database (EEFR) at the European Forest Institute (Nabuurs et al. 1996, Schelhaas et al. 1999) provides forest areas, the initial standing stemwood stock as well as the growth of the standing stock under past environmental conditions. This database contains information of the forest resources in 30 European countries. The information is provided by country, region, owner class, site class, tree species, and age class. Detail of information varies between countries. Figure 5.1.2 shows an example of the input data. Forest area that is covered in the database is 146.5 mill. Ha, distributed to 2527 forest types. In this project, three of the 30 countries are excluded from the analysis due to incomplete data. These countries are Greece, Russia and Turkey.

REGION	1
OWNER CLASS	1
SITECLASS	2
SPECIES	1

AGE, years	AREA, ha	VOLUME, m^3/ha	INCREMENT, m^3/ha/year
10	667718	14	1.63
30	410370	89	6.88
50	194522	158	7.33
70	258085	183	6.21
90	100000	200	5.32
110	167714	199	4.35
130	63182	180	3.34
150	20814	181	2.76
160	9015	226	2.55

Figure 5.1.2. *An example of the input data. The data of one forest type of Scots pine (species 1) on* Myrtillus *type forest on mineral soils (site class 2) in Southern Finland (region 1) is presented above. The Finnish input data of EFISCEN consists of 64 tables like this one.*

The projections carried out with EFISCEN provide insight in increment, growing stock, age class distribution, actual fellings per tree species and region. These are, however, only stem wood volume data. Therefore data are then converted to whole tree biomass using allocation coefficients per age class and species as provided by the process based models described in earlier chapters.

5.2.1.2 Change of growth rate and calculation of biomass allocation and litter

EFISCEN simulates the development of the forest for decades. It can be expected that growth rates might change during such long periods, due to changes in the environment and in the LTEEF-II project as a consequence of climate change. Therefore the model has been modified to simulate the impact of such changes on growth rate. The basis of the growth calculation is the growth in the inventory data which are currently based on the inventory data of the early 1990s. The growth is used to calculate the transitions of area to higher volume classes in the matrixes (see Figure 5.1.1). If changes in the growth occur, the transitions of area in the matrixes are adapted accordingly.

In the LTEEF-II project, the evaluation of climate induced changes in the growth rates are based on process model outputs. Process models simulate photosynthesis and respiration of trees in hourly or daily timesteps and calculate consequent biomass increment of trees and stands. Because of the high needs of initialisation data and computing capacity simulations can only be performed at a very limited number of sites. Therefore sites were selected which should be representative in relation to climate, tree species and forest inventory data (see Chapter 6). The performance of process models in relation to the short and long term dynamics of carbon exchange and forest growth rates have been evaluated (Kramer *et al.* 2000) against the available forest ecosystem gas exchange data (short term performance) and growth and yield

data (long term performance). Table 5.1.1 provies an example how growth in the EFISCEN can be modified based on information from process based models.

Table 5.1.1. *An example showing how growth in the EFISCEN model can be modified based on information from process based models (FORGRO model, site in Slovakia, tree species is beech) as a consequence of climate change. Growth of stemwood by stand age under current climatic conditions is provided for year 1990 and change in growth (ratio) compared to current growth by 2010, 2030, 2050 and 2070 under changing climatic conditions. Provided ratios are then used to modify growth in EFISCEN*

Growth of stem wood

		Change from current climate			
Stand Age	Year 1990	2010	2030	2050	2070
	m3/ha/a	ratio	ratio	Ratio	ratio
0-20	5.10	1.071	1.118	1.154	1.182
21-40	11.62	1.071	1.118	1.154	1.182
41-60	11.81	1.070	1.116	1.150	1.180
61-80	11.83	1.069	1.115	1.149	1.180
81-100	11.82	1.069	1.115	1.149	1.179
101-120	11.80	1.068	1.116	1.149	1.179
>120	11.76	1.068	1.115	1.148	1.179

Based on the standing stem wood volumes the model calculates the biomass of branches, coarse roots, fine roots and foliage. For these calculations the model requires dry wood density and biomass distribution tables by age class (Table 5.1.2). The biomass distribution can be defined by regions and tree species. It is also possible to change the biomass distributions in time due to for example climate change. The carbon content of biomass is assumed to be 50%.

Table 5.1.2. *Example of a biomass distribution table that is needed to calculate biomass in the EFISCEN model. Such tables have been provided by process based models.*

Distribution of standing (living) biomass Current climate

Year 1990

	dry weight					
Stand Age	Total tree biomass	Stem	Branches	Coarse roots	Fine roots	Foliage
	Mg /ha	share	share	share	share	share
0-20	17.28	0.764	0.135	0.058	0.015	0.028
21-40	101.38	0.764	0.135	0.058	0.015	0.028
41-60	179.96	0.835	0.104	0.037	0.009	0.016
61-80	273.00	0.866	0.088	0.030	0.006	0.010
81-100	359.45	0.886	0.076	0.025	0.005	0.008
101-120	428.30	0.901	0.067	0.022	0.004	0.007
>120	477.66	0.910	0.060	0.020	0.003	0.006

Each year a proportion of the stems, branches, roots and leaves of the trees die, resulting in litter production. This litter production is also calculated, and it is possible to change the proportions of litter production in time, due to for instance climate change. Also, when a thinning or final felling is carried out, all biomass of the other tree components are added to the litter production and thus litter production depends on the harvest level in the region. Table 5.1.3 provides an example of a table

that is required for litter production calculations. Proportions in the table are provided by the process based models.

Table 5.1.3. *An example of a litter production table providing proportions of annual litterfall of the standing biomass. This information is used in EFISCEN for calculating litter production.*

Litter production Current climate, managed stands

Year 1990

Stand Age	Share of annual litterfall of the standing biomass in that compartment				
	Stem	Branches	Coarse roots	Fine roots	Foliage
	share	share	share	share	share
0-20	0.000	0.030	0.030	0.948	1.000
21-40	0.000	0.030	0.030	0.948	1.000
41-60	0.000	0.030	0.030	0.938	1.000
61-80	0.000	0.030	0.030	0.933	1.000
81-100	0.000	0.030	0.030	0.931	1.000
101-120	0.000	0.030	0.030	0.931	1.000
>120	0.000	0.030	0.030	0.930	1.000

5.2.1.3 Dynamic soil module

The EFISCEN model contains a dynamic soil carbon submodel that calculates the amount of carbon in dead organic matter. The submodel consists of three litter compartments describing physical fractionation of litter and five compartments describing microbiological decomposition in soil (Figure 5.1.3). Of the litter compartments, one is for stem litter, one for branch and coarse root litter and one for foliage and fine root litter. Of the soil compartments, one is for the soluble compounds of litter, one for holocellulose, one for lignin-like compounds and the other two for humus compounds. Each of the litter compartments has a specific fractionation rate (ai) and each of the soil compartments a specific decomposition rate (ki). These rates determine fractions that are removed from the contents of the compartments each year. Carbon removed from the litter compartments is divided into the soluble, holocellulose and lignin-like soil compartments according to the chemical composition of the litter (ci). A part of carbon removed from the soil compartments (pi) is tranferred to the subsequent compartment and the rest out of the system; from the second humus compartment, carbon is only transferred out of the system. The used Parameters in soil module are in Table 4.1.4. Carbon input into the soil module is litter production calculated in the tree module.

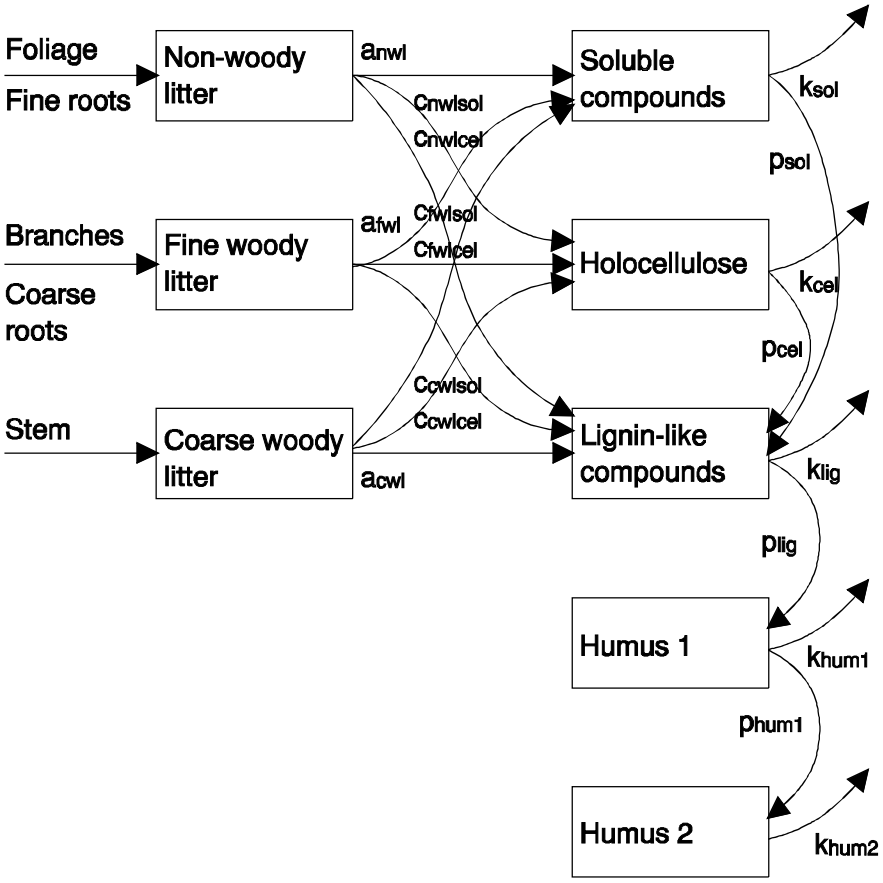

Figure 5.1.3*. Flow chart of the soil carbon submodel in EFISCEN. The boxes represent carbon compartments, the arrows carbon fluxes, and the text by the arrows parameters controlling the fluxes.*

Table 5.1.4. *Parameters of the soil carbon submodule at the reference conditions (annual mean temperature 4 °C, the difference between precipitation and potential evaporation 50 mm between May-September). The fractionation and decomposition rates were dependent on climate according to equations (1) and (2), the other parameters were similar for all conditions.*

Parameter	Value
Fractionation rates	
a_{nwl}	1 yr^{-1}
a_{fwl}	0.5 yr^{-1}
a_{cwl}	0.05 yr^{-1}
Litter composition	
c_{nwlsol} for conifers	0.27
c_{nwlcel} for conifers	0.51
c_{fwlsol} for conifers	0.03
c_{fwlcel} for conifers	0.65
c_{cwlsol} for conifers	0.03
c_{cwlcel} for conifers	0.69
c_{nwlsol} for deciduous trees	0.38
c_{nwlcel} for deciduous trees	0.36
c_{fwlsol} for deciduous trees	0.03
c_{fwlcel} for deciduous trees	0.65
c_{cwlsol} for deciduous trees	0.03
c_{cwlcel} for deciduous trees	0.75
Decomposition rates	
k_{sol} for conifers	0.5 yr^{-1}
k_{sol} for deciduous trees	0.8 yr^{-1}
k_{cel}	0.3 yr^{-1}
k_{lig}	0.15 yr^{-1}
k_{hum1}	0.013 yr^{-1}
k_{hum2}	0.0012 yr^{-1}
Transfer proportions	
p_{sol}	0.15
p_{cel}	0.15
p_{lig}	0.18
p_{hum1}	0.18

The fractionation rates (ai) and the decomposition rates (ki) depend on annual mean temperature (T) and the difference between precipitation and potential evaporation from May to September (P-E):

$$ai(T, P\text{-}E) = 1 + (0.0937 * (T - 4)) + 0.00229((P - E) - (-50)) * a0 \quad (5.1)$$

$$ki(T, P\text{-}E) = 1 + s * (0.0937 * (T - 4)) + 0.00229((P - E) - (-50)) * k0 \quad (5.2)$$

These dependencies were established by reanalysing data on the decomposition of Scots pine needles across Europe (Berg *et al.* 1993). The reference rates, a0 and k0, were determined for conditions where T = 4°C and P-E = -50 mm by adjusting model-calculated mass loss rates to litter bag experiments (Berg. *et al.* 1982, Berg *et al.* 1984) and model-calculated steady state amounts and accumulation rates of soil carbon to measured values (Liski and Westman 1995, Liski *et al.* 1998). Parameter s decreases the temperature dependence of humus decompostion (Liski et *al.* 1999,

Giardina and Ryan 2000). It was set equal to 0.6 for the first humus compartment and 0.36 for the second one; it was equal to 1 for the other compartments.

The soil submodel operates on a yearly time step. It was initialized in this study by setting the compartments to steady state with the input of the first studied year 1990.

5.2.1.4 Forest management

Forest management in EFISCEN is described in terms of thinning and final felling regimes, and total volumes to be thinned and clearcut by tree species group. Final felling regime is expressed as a probability, dependent on the stand age, actual standing volume and forest type. These probabilities are converted into a proportion of the area in each cell that can be felled. The actual area felled in a cell depends on the requested volume to be harvested and volume available in the species group. A clear felled area is moved to a bare-forest-land class (see Figure 4.1.1). Regeneration is regarded as transition of area from the bare-forest-land class to the first volume and age class. Forest management can be modified and impacts on forest resource (tree species composition, age class structure and standing volume) can be assessed. Forest management also influences soil carbon through litter input. Thinnings and final fellings provide raw material for manufacturing wood products and therefore also influences wood product carbon stocks.

5.2.1.5 Wood products module

Harvested wood in EFISCEN is processed into wood products in the wood product model (Karjalainen *et al.* 1994). Coniferous and non-coniferous timber is transferred separately into several production lines like sawn timber, wood pulp (chemical and mechanical pulp, paper), wood-based panels (plywood, veneer, and particle board) and fuelwood. The model follows those production lines with country- or region-specific parameters for the wood processing industry and shares in consumption until the products are removed from use and the stored carbon is released back into the atmosphere. Manufactured products are divided into seven usage categories (short life paper products, long life paper products, packing materials, furnishing, structural support materials, building materials and other building materials) with four different lifespan options to separate the different usage of wood products and their possible later re-use. At the end of its primary use, products can be either recycled, or burned for energy production or disposed to landfills. In landfills, the disposed products decompose slowly, releasing carbon into the atmosphere. In this project, however, landfills are excluded since there was not enough data available to initialise carbon stocks in landfills. The half-life period (life span) for the different product groups were 50 years for the long life span products, 16 years for medium-long life span products, 4 years for medium-short life span products and 1 year for short life span products. These life spans are similar or slightly shorter that in Row and Phelps (1990), Karjalainen et al (1994) and Pingoud et al. (1996, 2000).

The wood product stocks for products in use have been initialised by running the model with harvesting data from 1960 to 1990.The data source on historic removals (roundwood production) and commodities (fuelwood, sawn timber, wood-based panels, and pulpwood) was FAOSTAT database on forestry (FAO, 1998). The United Nation Statistical Division (UNSTAT) COMTRADE trade statistics (UN, 1999) and one commodity producer supplied additional data. Detailed description of the calculation of wood product carbon stocks can be found from Eggers (2000).

5.2.1.6 Calculation of the carbon budget

Carbon stocks and stock changes in tree biomass, soil and products are calculated per region but are presented by country. In order to allow comparison with flux measurements and flux modelling, net primary production (NPP, net tree biomass carbon balance plus litter production and timber harvesting), net ecosystem exchange (NEE, = NPP plus net soil carbon balance), net biome production (NBP, = NEE minus timber harvesting), net product exchange (NPE, net product carbon balance), and net sector exchange (NSE, = NBP plus NPE) are calculated (Figure 4.1.4). Carbon budgets are presented as average values per hectare (average for the area) or for the whole area in consideration.

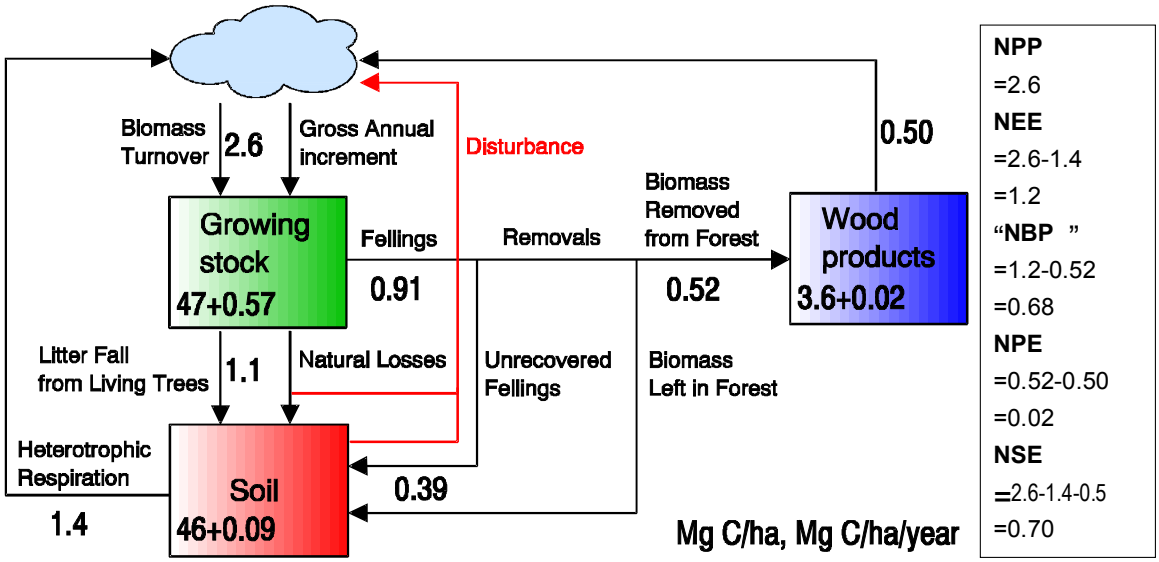

Figure 5.1.4. Example of the carbon stocks (boxes) and fluxes (arrows). Boxes include also net change in stock, i.e. 0.57 Mg C/ha/year for tree biomass. Calculation of NPP, NEE, NBP, NPE and NSE is shown on the right hand box.

5.2.1.7 References

Berg, B., Berg, M.P., Bottner, P., Box, E., Breymeyer, A., Calvo de Anta, R., Couteaux, M., Escuerdo, A., Gallardo, A., Kratz, W., Madeira, M., Mälkönen, E., McClaugherty, C., Meentemeyer, V., Munoz, F., Piussi, P., Remacle, J. & Virzo de

Santo, A. 1993. Litter mass loss rates in pine forests of Europe and Eastern United States: some relationships with climate and litter quality. *Biogeochemistry* **20**: 127-159.
Berg, B., Ekbohm, G. & McClaugherty, C. 1984. Lignin and holocellulose ralations during long-term decomposition of some forest litters. Long-term decompositiono in a Scots pine forest. IV. *Canadian Journal of Botany* **62**: 2540-2550.

Berg, B., Hannus, K., Popoff, T. & Theander O. 1982. Changes in organic chemical components of needle litter during decomposition. Long-term decomposition in a Scots pine forest. I. *Canadian Journal of Botany* **60**: 1310-1319.

Eggers, T. 2000. Implications of wood product manufacturing and utilization for the European carbon budget. Manuscript in preparation.

FAO, 1998. FAOSTAT Forestry Database on a) Roundwood, Sawnwood, Wood-Based Panels and b) Pulp, Paper & Paperboard, Food and Agricultural Organization of the United Nations, FAO, Rome, 1998. Internet database: http://apps.fao.org/page/collections?subset=forestry

Karjalainen T., Kellomäki S. & Pussinen A. 1994. Role of wood-based products in absorbing atmospheric carbon. *Silva Fennica* **28(2):**67-80.

Liski J., Ilvesniemi H., Mäkelä A. & Starr M. 1998. Model analysis of the effects of soil age, fires and harvesting on the carbon storage of boreal forest soils. *European Journal of Soil Science* **49(3):** 407-416.

Liski, J. & Westman, C. J. 1995. Density of organic carbon in soil at coniferous forest sites in southern Finland. *Biogeochemistry* **29**: 183-197.

Liski, J., Ilvesniemi, H., Mäkelä, A. & Westman, C.J. 1999. CO2 emissions from soil in response to climatic warming are overestimated - the decomposition of old soil organic matter is tolerant of temperature. *Ambio* **28(2):** 171-174.

Nabuurs, G.J.& Päivinen, R. 1996. Large scale forestry scenario model - a complication and review. EFI Working Paper 10. European Forest Institute. Joensuu, Finland. 174 p.

Nabuurs, G.J., Pajuoja, H., Kuusela, K. & Päivinen, R. 1998. Forest Resource Scenario Methodologies for Europe. EFI Discussion Paper 5. European Forest Institute. Joensuu, Finland. 30 p.

Nilsson, S., Sallnäs, O., Duinker, P. 1992. Future forest resources of Western and Eastern Europe. International Institute for Applied Systems Analysis. The Parthenon Publishing Group. England. 496 p.

Päivinen, R., Nabuurs, G.J., Lioubimow, A.V. & Kuusela, K. 1999. The state, utilisation and possible future developments of Leningrad region forests. EFI Working Paper 18, European Forest Institute. Joensuu, Finland. 59 p.

Pingoud, K., Perälä, A. & Pussinen A., 2000. Inventorying and modelling of carbon dynamics in wood products. In Robertson, K.A. & Schlamadinger, B. (eds.): Proceedings of the Workshop 'Bioenergy for mitigation of CO2 emissions: to power, transportation and industrial sectors', 27-30 September 1999, Gatlinburg, Tennessee, USA. pp. 125-140.

Pingoud, K., Savolainen, I. & Seppälä H., 1996. Greenhouse Impact of the Finnish Forest Sector Including Forest Products and Waste Management. Royal Swedish Academy of Sciences, *Ambio* **Vol 25., No. 5**. pp. 318 - 326.

Pussinen, A., Schelhaas, M.J., Verkaik, E., Heikkinen, E., Liski, J., Karjalainen, T., Päivinen, R. & Nabuurs, G.J. 2000. Manual for the European Forest Information Scenario Model (EFISCEN 2.0). Internal Report. European Forest Institute Joensuu, Finland.

Row, C. & Phelps, R.B., 1990. Tracing the flow of carbon through U.S. forest product sector. Presentation at the 19th World Congress, IUFRO, Montreal, Canada, August 5 - 11, 1990. 13 p.

Sallnäs, O. 1990. A matrix growth model of the Swedish forest. Studia Forestalia Suecica. No 183. Swedish University of Agricultural Sciences. Faculty of Forestry. Uppsala. 23 p.

Schelhaas, M.J., Varis, S., Schuck, A., Nabuurs, G.J., 1999. EFISCEN's European Forest Resource Database, European Forest Institute, Joensuu, Finland, http://www.efi.fi/projects/eefr/.

UN, United Nations, 1999. United Nation Statistical Division, UNSTAT. COMTRADE trade statistics. EFIDAS database of the European Forest Institute. Internet: http://www.efi.fi/efidas/restricted/tf_query.phtml

5.3 Remote Sensing Approach

Frank Veroustraete & Hendrik Sabbe

5.3.1 Introduction

Vegetation, whether natural or human influenced, plays an important role in the carbon cycle: the processes of photosynthesis, respiration and litter decomposition in terrestrial plant communities consume and/or produce large amounts of cxarbon dioxide, the predominant greenhouse gas in global warming. The monitoring of carbon dynamics at the ecosystem level thus is a crucial issue in studies of global change (Woodwell, 1984). Carbon fluxes can be measured in detail at selected test sites by means of eddy covariance techniques. This approach is for instance applied at several forest sites in Europe within the frame of the EUROFLUX network ("Long term carbon dioxide and water vapour fluxes of European forests and interactions with the climate system"). However, such point measurements are costly and difficult to extrapolate in space and time a process genuinly named up-scaling.

To obtain spatially explicit information on carbon exchange models simulating this process can be used. To validate model results with the full complexity of measurements from the physical environment simulated, these models may rapidly become complex and start gasping lots of input parameters. These are sometimes hardly available. The gap between both strategies, point measurements of biophysical quantities and the regional to continental up-scaling of these same quantities, can partially be bridged by the use of imagery captured by earth observing satellites.

The *C-Fix* model, presented in its embryonal form by Veroustraete et al. in 1994, quantifies carbon fluxes, by integrating satellite observations in a simplified carbon exchange model. The key element in this approach, is that the evolution –not of the "amount" - but of the "greenness state" of the vegetation are directly inferred from space observations, and hence do not have to be estimated by a model.

C-Fix was applied with reasonable success over the Belgian territory by means of NOAA-AVHRR images of 1990 (Veroustraete et al., 1996) and over Europe by means of NOAA-AVHRR images of 1992 - 1993 (Sabbe et al., 1999).

In the following chapters a description of the model charachteristics is given. In a first part a complete description of the *C-Fix* algorithms, definitions, formulas, constants, temperature dependencies and calculations of the different respiration processes is given. In a second part the up-scaling scheme for the biophysical input paramters is explained. In other words, an account is given how a "pixel model" like *C-Fix* is implemented in a raster/image environment to map the geographical distribution of carbon balance fluxes using remote sensing data.

In this project *C-Fix* is applied over the European continent by means of a one-year series of NOAA-AVHRR images and an extensive set of meteorological data of the World Meteorological Organisation (WMO) for the same year. A forest probability map also for the same year was used to extract forest ecosystems and to estimate their carbon fluxes.

In a third part, meteorological data are described that are used as input data for *C-Fix*, the available parameters needed for their estimation and the geographical and temporal distribution of the meteo stations. A spatial interpolation technique was developed in the frame of this project and relationships to estimate global radiation from meteorological data were applied for the European continent. Remote sensing data post processing is discussed as well, e.g. the cloud removal procedure and the relationship between *f*APAR and the NDVI (Normalised Difference Vegetation Index).

5.3.2 The C-Fix Model

5.3.2.1 Algorithm description

For a given point location, the model uses the following equations to estimate three types of fluxes (all in g C/m²/d) on a daily basis (subscript d):

$$GPP_d = p(T_{atm})\ CO_2 fert\ \varepsilon\ \ fAPAR\ c\ S_{g,d} \quad (5.2.1)$$

$$NPP_d = GPP_d(1 - A_d) \quad (5.2.2)$$

$$NEP_d = NPP_d - R_d \quad (5.2.3)$$

GPP_d represents gross uptake of carbon (expressed as C) by photosynthesis. NPP_d is GPP_d taking account of autrotroph respiratory losses flux [$GPP*A_d$]. A_d is an autotroph respiratory fraction. NEP_d includes soil respiratory losses (flux R_d), originating from heterotrophic decomposition of soil organic matter. Monthly (subscript m) and yearly (subscript y) average values are subsequently calculated by numerical integration of the flux functions over the number of days in the considered assessment period, mostly one year. In equation 5.2.1., the GPP-approach of Kumar and Monteith (1981) is represented. The product terms in 5.2.1. are presented in table 5.2.1.

Table 5.2.1.: Terms, their significance and units for equation 5.2.1.

c	Climatic efficiency equal to 0.48 (Mc Cree, 1972)	[-]
$p(T_{atm})$	Normalised temperature dependency factor (value between 0 and 1)	[-]
$CO_2 fert$	Normalised CO_2 fertilisation factor, formalised according to Veroustraete (1994). No fertilisation means value equal to 1. Fertilisation means values larger than 1.	[-]
$fAPAR$	Fraction of absorbed PAR (Photosynthetical Active Radiation)	[-]
ε	Radiation Use Efficiency (RUE) equal to 1.10 Wofsy et al (1993)	[gC/MJ(APAR)]
$S_{o,d}$	Daily incoming global solar radiation	[MJ/m²/d]

The temperature dependency factor, $p(T)$, takes the thermodynamic properties of the carboxylation/oxygenation reactions at the Rubisco level (photosynthesis) into account, of which the formal expression will be discussed in one of the following chapters. The normalised CO_2 fertilisation factor takes into account the CO_2 and O_2 dependency of the CO_2-fixation reaction at Rubisco level.

APAR (absorbed PAR [MJ/m²/d]), used in ε, gives a photosynthetic efficiency on a dry mater (DM) basis equal to 2.45 [gDM/MJ(APAR)]) with a ratio of carbon to dry mater of 0.45. This calculation of photosynthetic efficiency is a rough approach, e.g. the assumption is that ε is constant during the entire year and constant for all vegetation types in Europe and represensts a mximal value. Since we are working with 1 km² resolution, most if not all (European pixels) represent mixed vegetation types and these assumptions are not entirely inconvenient.

5.3.2.2 An algorithm for estimating *f*APAR

Gross carbon assimilation or phytomass production is the result of photosynthesis, which in its turn - according to equation 5.2.1. - is a function of radiation absorption efficiency at the vegetation level (*f*APAR). The spectral band of importance for

photosynthesis is the Photosynthetic Active Radiation band (PAR band) and is situated between 0.4 and 0.7 μm. It is assumed that the energy of PAR at the surface of the earth is about 50% of the total shortwave or global radiation, this ratio is defined as climatic efficiency (Mc Cree, 1972). Table 5.2.2. lists conversion rates for the calculation of PAR present in global direct (S_g) and global diffuse radiation (S_d) and in function of different solar angles (β) in clear sky cases.

Table 5.2.2: Conversion factors for the calculation of PAR present in global direct (S_g) and global diffuse radiation (S_d) for different solar angles (β) for clear sky conditions

	Solar elevation (β)							
	5°	10°	20°	30°	40°	50°	60°	70°
S_g	0.2	0.28	0.37	0.4	0.42	0.43	0.43	0.43
S_d	0.61	0.62	0.63	0.65	0.67	0.70	0.73	0.76

At first sight the conversion factors are a function of solar elevation, since the path of solar radiation through the atmosphere increases with lower solar heights. The effect of an increasing path express itself in two ways:

(i) the spectral composition of direct and diffuse global solar radiation changes, and;

(ii) the ratio of direct to diffuse changes as well. This is the result of increased scattering with a longer atmospheric path. Nevertheless, the fraction of PAR in global incoming radiation is practically independent of the atmospheric path and hence from solar elevation. This can be explained by the fact that with increasing solar heights, the increase of PAR in direct radiation is compensated by a decrease in diffuse radiation (and so a decrease in the PAR contribution). Thus, the 50% ratio is a reliable number. This rule of thumb however is not correct once radiation is interacting with canopies of forests or crops since then the spectral changes in the radiation field occur due to selective absorption by chlorophyll.

Only a fraction of total incoming PAR at the top of the canopy (TOC) is absorbed by vegetation. The denser the vegetation (the higher the Leaf Area Index, LAI[1]) the larger the absorption of PAR. The fraction of incoming PAR to absorbed PAR by the canopy is defined as the fraction of absorbed PAR or briefly *f*APAR. Other biophysical variables like projected leaf surface (LAI1), chlorophyll and water content of the leaves, leaf shape and orientation, gap fraction, tree clumping etc. play an important role in canopy absorption as well.

Photosynthetic pigments elicit different absorption characteristics in the blue, red and near-infrared wavelengths. As a consequence of these specific absorption differences, vegetation can be considered as a spectral filter. Hence the solar spectrum transmitted through grassland or forest is modfied as compared to incoming shortwave radiation. Figure 5.2.1. illustrates the reflectance spectra of water, soil and vegetation.

1 Leaf Area Index (LAI) or leaf surface is the ratio of a unilateral leaf surface (in m^2) projected vertically on the soil, and expressed per unit of soil surface covered by the leaf projection in m^2

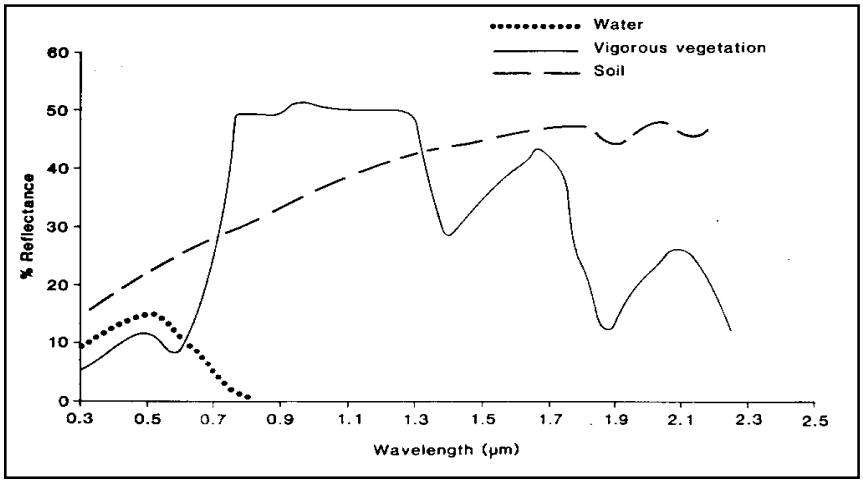

Fig.5.2.1: [%] reflectance of water, bare soil and vegetation in function of wavelength

These spectral changes are the more important when LAI or the radiative transfer path in the vegetation increases. Since the blue part of the spectrum is absorbed more significantly than the infra-red part, there is a so called "near-infrared enrichment" in vegetation. Well know inversion techniques are based on the spectral reflection characteristics of vegetation in the red (RED) (0.6 - 0.7 μm) and the near infra-red (NIR) (0.75 - 1.10 μm) wavelengths who are different from these of bare soils and water surfaces. The most common vegetation index used for a long time in remote sensing is the Normalized Difference Vegetation Index or NDVI which is defined by the following relationship:

$$NDVI = (\rho_{nir} - \rho_{red})/(\rho_{nir} + \rho_{red}) \quad (5.2.4)$$

Where ρ_{red} is the reflectance in the red band of the solar spectrum and ρ_{nir} the reflectance in the near-infrared band. The NDVI is a dimensionless index, with a value ranging between 0 and 1. The index is a normalised one because of the division by the sum ($\rho_{nir} + \rho_{red}$). Hence, the index is insensitive for variations in shortwave radiation and is mainly influenced by the reflective characteristics of the vegetation (leaves), leaf pigmentation, LAI, gap fraction and the BRDF or bidirectional reflectance distribution function.

The determination of the $NDVI_{toc}$ (NDVI on Top of the Canopy) is performed with satellite observations in this project. Various platforms can be used, such as the NOAA (US, National Oceanic and Atmospheric Administration) satellites equipped with the AVHRR sensor (Advanced Very High Resolution Radiometer). AVHRR images are available daily and have a spatial resolution at nadir of 1.1 at 1.1 kilometers. The French SPOT4 satellite (Système Probatoire d'Observation de la Terre) with the VEGETATION (VGT) sensor is available since beginning 1998 with the same spatial and temporal resolution. The SPOT4/HRVIR sensor by the way has a ground resolution of 20 by 20 meters at nadir and hence is more suitable for crop

monitoring. The disadvantage of this platform is its revisit time. 26 days are needed to process a complete image of the world. Table 5.2.3. illustrates the spectral characteristics of NOAA/AVHRR and SPOT4/VGT.

Table 5.2.3: Spectral characteristics in the RED and NIR bands in ηm for the NOAA/AVHRR and SPOT4/VGT instruments: λ is the central wavelength and $\Delta\lambda$ is the bandwidth at half height.

	RED band		NIR band	
Satellite platform	λ	$\Delta\lambda$	λ	$\Delta\lambda$
NOAA/AVHRR	630	100	910	375
SPOT4/VGT	645	70	835	110

Myneni and Williams (1994) invetsigated by means of a radiative transfer model the *f*APAR nadir $NDVI_{toc}$ relationship and came to a linear relationschip for a large set of different vegetation – soil - atmopshere – observation conditions. The relationship looks as follows:

$$fAPAR = a * NDVI_{toc} + b \tag{5.2.5}$$

a and b are empirical constants equal to 0.8642 and -0.0814 according to Myneni and Williams (1994). This relationship is independent of the cover heterogeneity of the pixel. It only depends on 'greenness' as indicated by the $NDVI_{toc}$. Myneni considered backgrounds of moderate brightness, hence background effects may also be ignored. However, the *f*APAR / $NDVI_{toc}$ relationship is very sensitive to soil reflection and the sun / sensor geometry (Roujean & Breon, 1995). Hence this simplified model of the relationship between *f*APAR and $NDVI_{toc}$ must be seen as a typical or average model, for it is derived to represent a large canopy problem parameter space (ground cover, LAI, leaf orientation and optical parameters).

The disadvantage of the Myneni relationship is that its parameters change from sensor to sensor. Hence another approach to estimate *f*APAR using the NDVI is based on the following relationship:

$$fAPAR = a\left(NDVI - NDVI_{\min}\right) \tag{5.2.6}$$

Where $NDVI_{min}$ is the lowest measurable NDVI value in a scene, and *a* is a regression constant defined as the ratio of the difference between the maximum and minimum NDVI and the highest possible *f*APAR in the same scene.

A last approach is the determination of *a* and *b* in equation (5.2.6.) based on the cumulative histogram of the $NDVI_{toc}$. In this case, the values of the intercept and slope are dependent on the distribution of the NDVI measurements.

5.3.2.3 The dependency of GPP on atmospheric temperature

The temperature dependency fatcor *p(T)* for equation 5.2.1. was described by Wang (1996) and parameterised according with data of Samson (1997) for deciduous forests and of Jach (2000) for a pine forest :

$$p(T) = \frac{e^{\left(C_1 - \frac{\Delta H_{a,P}}{R_g.T}\right)}}{1 + e^{\left(\frac{\Delta S.T - \Delta H_{d,P}}{R_g.T}\right)}} \qquad (5.2.7)$$

Table 5.2.4. lists the parameters of the temperature function.

Table 5.2.4: List of the parameters used in the temperature function p(T).

C_1	Constant	[-]
$\Delta H_{a,P}$	Activation energy	J.mol^{-1}
R_g	Gas constant	J.K^{-1}.mol^{-1}
T	Air temperature	K
ΔS	Entropy of the denaturation equilibrium of CO_2	J.K^{-1}.mol^{-1}
$\Delta H_{d,P}$	Deactivation energy	J.mol^{-1}

This function has a maximal value of 1 at a specific temperature depending on the parameterisation. Most parameters in the above equation are species specific. An overview of the parameters is given in table 5.2.5. The values are from Jach (2000) for Scots Pines (*Pinus sylvestris L.*) and from Samson (1997) for Beech (*Fagus sylvatica*), Oak (*Quercus robur*) and ash (*Fraxinus excelsior*). Since we are working with a 1.1 km² resolution, most if not all (European) pixels represent mixed vegetation types, and hence we assume a mean or constant value for all vegetation types in Europe. However, this relationship can be adjusted for specific tree species for a certain number of pixels if wanted or necessary.

Table 5.2.5: Overview of the parameters of equation 5.2.7. for three tree species describing the temperature dependency of GPP parametrised according to Jach (2000) and Samson (1997). The last column (C-Fix) are the mean values used in C-Fix

	Beech	Oak and ash	Scots pines	C-Fix
C_1	21.92	21.62	21.59	21.77
T_{opt} (P_{max}) [K]	293.13	298.13	298.13	295.13
ΔS	709.95	700.00	699.00	704.98
$\Delta H_{a,P}$	52750	52750	52750	52750
$\Delta H_{d,P}$	211000	211000	211000	211000
R_g	8.31	8.31	8.31	8.31

Figure 5.2.2. illustrates the temperature dependency of GPP.

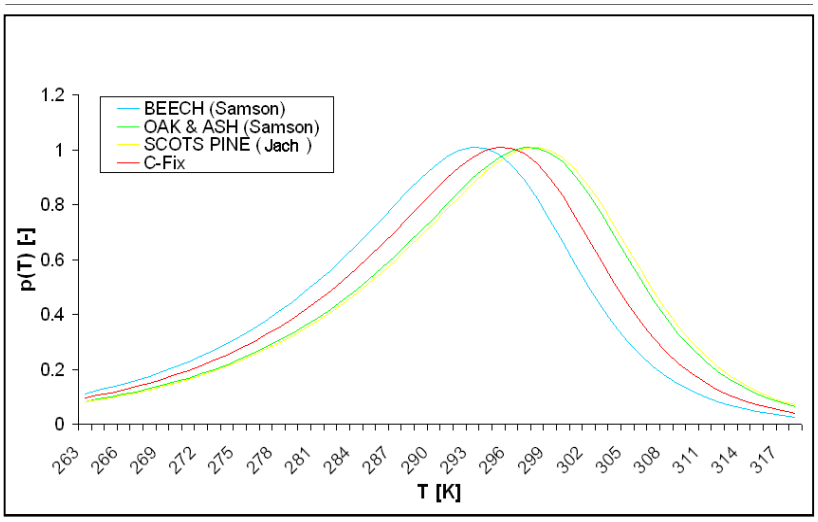

Fig. 5.2.2: The temperature functions of the GPP in function of air temperature describe by Wang (1996) and parametrised according to Jach and Samson (1997). A mean value of beach, oak, ash and scots pine is used in C-Fix.

5.3.2.4 Determination of the CO_2 fertilisation effect

Veroustraete (1994) defined CO_2 fertilisation as the increase in carbon assimilation due to CO_2 levels above the atmospheric background level (or reference level):

$$CO_2 effect = \frac{F_{CO_2}}{F_{CO_2}^{ref}} \tag{5.2.8}$$

Here F_{CO2} is the CO_2 assimilation rate and $[CO_2]^{ref}$ is the CO_2-concentration occuring in the reference year 1833 being equal to 281 ppmv. Photorespiration is taken into account by assuming the following relationship for F_{CO2} after Collatz et al. (1991) :

$$F_{CO_2} = \frac{V_{\max}\left([CO_2] - \frac{O_2}{2\tau}\right)}{K_m\left(1 + \frac{[O_2]}{K_0}\right) + [CO_2]} \tag{5.2.9}$$

Table 5.2.7: Parameter values at 20°C used in the CO_2 fertilistation effect equation 4.2.10.

Parameter	Value	Parameter	Value
τ	2550	$[O_2]$	20.9
K_m	948	$[CO_2]^{ref}$	281
K_0	30	CO_2effect	1.26

5.3.2.5 Global radiation and air temperature

An important parameter in equation (5.2.1.) is daily global radiation. This meteorological parameter can be measured (for example with a pyranometer) or derived from other meteorological parameters. In the case no observations for incoming global solar radiation are available, formulas postulated by Ångström (1924), Hargreaves (1985) and Supit (1998) can be used to estimate this parameter using sunshine duration and cloud cover observations.

The daily air temperature plays an important role in the carboxylisation and photosynthese rate. This parameter is measured in synoptic stations.

5.3.2.6 Description of the sub model for autotroph respiration and NPP

Plant respiration or autotroph respiratory fraction A_d is an important, sensitive component of the carbon balance. Our knowledge of respiratory processes is rather limited, in particular for trees and forests under field conditions. Respiration increases with temperature, because temperature increases the rate of the enzymatic reactions in respiration. The relative temperature dependency of autotroph respiration used in *C-Fix* is based on the parameterisation of Goward and Dye (1987). This parametric model for respiratory losses is assumed state (phytomass) independent and only determined by temperature according to equaiton 5.2.13:

$$A_d = (7.825 - 1.145T_{atm})/100 \qquad (5.2.13)$$

where A_d [-] is the fraction of assimilated photosynthates consumed by autotroph respiration and T_{atm} [°C] the atmospheric temperature. This equation is a simplification, since maintenance respiration is strongly dependent on canopy and living wood phyotomass.

Finally NPP is calculated from GPP, according to the following relation :

$$\text{NPP}=(1 - A_d)\text{GPP} \qquad (5.2.14)$$

It is obvious, that this approach is a simplification.

According to Wang (1996) the temperature-dependency of the respiration rate at the level of foliage is described by:

$$R_d(T) = e^{(C_r - \Delta H_{aR}/[R(T_a+273.2)])} \quad \text{during daytime} \qquad (5.2.15)$$

$$R_d(T) = 1.45e^{(C_r - \Delta H_{aR}/[R(T_a+273.2)])} \quad \text{during dark period} \qquad (5.2.16)$$

where ΔH_{aR} is the activation energy, C_r is a constant. The temperature-dependence of R_d during the night was assumed to have the same response pattern with the

respiration rate in light. However a correction coefficient (1.145) was used. As in equation (5.2.7.) these relations are rescaled between 0 and 1.

5.3.2.7 Derivation of soil respiration and NEP

In this chapter, the determination of heterotrophic respiration (soil organic matter and humus decomposition) and Net Ecosystem Productivity is discussed. The soil carbon flux due to heterotrophic respiration is a dependent on several parameters as temperature, soil carbon content, pH, humidity, he description of this soil carbon flux is a complex matter and at this moment there are no simple relationships available. Therefore simplifying assumptions were made to quantify heterotrophic respiration on a pixel basis. Daily heterotrophic respiration $R_{h,d}$ is estimated as follows:

$$R_{h,d} = k_s . Q_{10}^{T/10} \tag{5.2.17}$$

Wherein Q_{10} the relative increase is of the respiration flux for an 10° increase in temperature T (Q_{10} is 1.5 according to Maisongrande et al., 1995), k_s is a heterothropic respiration coefficient, which is estimated using the following boundary condition :

$$k_s = \frac{\sum_{d=1}^{365} \frac{GPP_d}{b}}{\sum_{d=1}^{365} p(T)_d} \tag{5.2.18}$$

The value of k_s is determined with (5.2.18.), so that $R_{h,d}$ and NEP_d can be computed on a daily basis. The parameter b is obtained from calibrations with EUROFLUX NEP yearly profiles. It is now possible to estimate heterotroph respiration on a daily basis according to equation (5.2.18.) and also NEP_d for each pixel.

5.3.3 Up-scaling of meteorological data to the continental scale

5.3.3.1 Data description

The data used in this porject were obtained from the WMO (World Meteorological Organisation) and contain 3 hourly measurements form several meteorological variables for a great number of European stations for the year 1997. Table 5.2.8. presents an overview of the available variables. Not less then 4125 measuring sites in Europe were processed to establish temperature and global radiation fields for Europe.

Table 5.2.8: Units and abbreviations for the different climatological and meteorological variables in the WMO data set.

Parameter	Units	WMO Abbrevation
LandID	[-]	LID
StationID	[-]	SID
Land/see Flag	[-]	L/S
Longitude	[°]	Lon
Latitude	[°]	Lat
Kartesische X-Richting	[-] n/a	X
Kartesische Y-Richting	[-] n/a	Y
Reduktion height	[m] n/a	H
Priority	[-] n/a	P
Border lower clouds	[CODE] WMO-classes	BLC
Visibility	[CODE] WMO-classes	Vi
Cloudiness	[1/8]	Cl
Winddirection	[°] Southwest	Wd
Windspeed	[Kn]	Ws
Air Temperature	[C/10]	Ta
Dew Temperature	[C/10]	Td
Red. Air Pressure	[hPa/10] Sea level	RAP
Nature Air Pressure change	[CODE] WMO-class (*)	NAPc
Value Air Pressure change	[hPa/10]	VAPc
Weather prediction	[CODE] WMO-class (**)	WP
Weather last 3 hours dominant	[CODE] WMO-class (***)	WP3
Weather last 6 hours dominant	[CODE] WMO-class (***)	WP6
Cover lowest clouds	[1/8]	CLC
Nature low clouds	[CODE] WMO-class	NLC
Nature middle clouds	[CODE] WMO-class	NMC
Nature height clouds	[CODE] WMO-class	NHC
Maximum wind speed	[Kn]	WsM
n/a	[-]	-
n/a	[-]	-
n/a	[-]	-
Precipitation amount	[mm/10]	P
Precipitation interval	[CODE] WMO-class (****)	Pi
Surface pressure	[hPa]	SP

Table legend:
(*): 0-3: falling, 4: equal, 5-8 : arising within 3 hours
(**): 0-19:forget, 20-29:prec.last hour, 40-49:fog, 50-59:dizzle, 60-69:rain, 70-79: snow, 80-89: showers ,90-99: thunder storm
(***): 0,1,2 cloud cover equal, growing, less, 4: fog, 5: dizzle, 6: rain, 7: snow, 8: shower, 9: thunder
(****) 0: 12 hours 1: 24 hours

The data do not contain any information on global radiation nor sunshine duration. Alternative formulas were needed to calculate these variables needed in the *C-Fix* model.

5.3.3.2 Meteo data processing

Not all 4125 European synoptic stations dispose of usefull data. First of all there are a great number of stations not represented in the data files and secondly there are a lot of gaps in the data. Therefore a quality checkup and gap screening was performed on the WMO data.

5.3.3.2.1. Selection of the stations

Only these stations with a number of missing data or gaps lower then a preset maximum number of gaps were retained. The preset value was made dependent on the quality and gap occurence of the WMO data set.

(i) a maximum number of gaps (independent of their occurence in time) may not be exceeded and

(ii) an uniform geographical distribution over the entire region is pursued. For all available stations the total number of measurements for each meteorological variable was counted for the period of interest (normally one year). Table 5.2.9. presents an overview of the number of selected stations available in function of different gap occurences.

Table 5.2.9: Number of available stations in function of the tolerated number of measuring gaps (%) (period : 1 January 1997 till 31 December 1997).

	Preset value of maximum alowable number of gaps			
Variable	100%	30%	20%	10%
Temperature	4125	1327	1210	1003
Cloudiness	4125	991	886	681

An example of the geographical distribution for the parameter cloudiness of the WMO-stations in function of the tolerated number of gaps is given in the following figure (Fig. 5.2.3.).

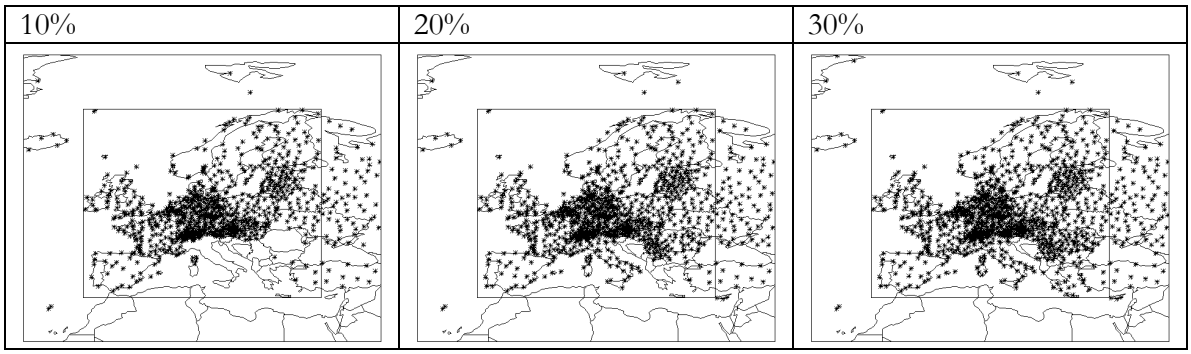

Fig. 5.2.3: Geographical distribution of the synoptic stations (for the parameter cloudiness Cl) in function of the preset maximum number of data gaps. Right : 30% gaps, middle: 20% gaps and left : 10% gaps for a year 1997 WMO data set.

Figure 5.2.3. shows that the geographical distribution in the case of a tolerance of 20% data gaps shows a more uniform geographical distribution than a toleraance of 10% data gaps. On the other hand, a value of 30% does not show a significant improvement compared to the 20 % case. Therefore in this project all stations with a presett maximum value of less then 20% missing data were retained.

5.3.3.2.2 Gap filling

Once the stations that qualify for the up-scaling of the meteorological data are identified, a gapfilling procedure can be applied. Three different methods can be used:

(i) linear interpolation;
(ii) spline techniques and;
(iii) fourier regression.

Despite that linear interpolation techniques may give biased results - when a long series of sequential values are missing - this method was applied. The two other techniques are far more time-consuming and do not always lead to a higher degree of accuracy.

5.3.3.2.3. Spatial interpolation

At this level the meteorological variables are now cmplete yearly series for all the selected stations. However spatial interpolation of the data is needed to calculate the value for each meteo grid point X, Y needed as input for *C-Fix*. A simple and fast interpolation algorithm is used. First of all, a selection of relevant stations for the location (or pixel) of interest is executed. It is obvious, that only the closest stations are important and that a cluster of stations, can be represented by a single station as well. Secondly, a distance weighted method is applied for the nearest neighbour stations.

Suppose we want to know the meteorological variable for an arbitrary point P in a certain region (Fig. 5.2.4.). For each available station, a "shadow zone" is determined in relation to P. This zone is a function of a "shadow angle" β, which is the half width of the angle and the connection line between the stations and the point P. Only these stations that are not in the "shade zone" of any other station are selected. The result of this algorithm, is that only the nearest stations around P are selected. Also, different stations lying close to each other are represented by a single station (Fig. 5.2.4.). The angle β is user defined, its value plays an important role in the number of rejected stations. The bigger β, the less stations are selected and vice versa.

For each selected station the distance to point P can be calculated. The importance or influence of a station is inversely proportional to the distance. A weighting factor w_i is defined as the inverse of the distance d:

$$w_i = \frac{1}{(d_i)^m} \qquad (5.2.19)$$

wherein d_i is the distance between the point P and the selected station. m is a power which is user defined and can increase or reduce the distance dependency of the stations.

The estimated value of the point p (V_p) is then calculated as :

$$V_p = \frac{\sum_{i=1}^{stations} w_i V_i}{\sum_{i=1}^{stations} w_i} \qquad (5.2.20)$$

where V_i is the value for station i.

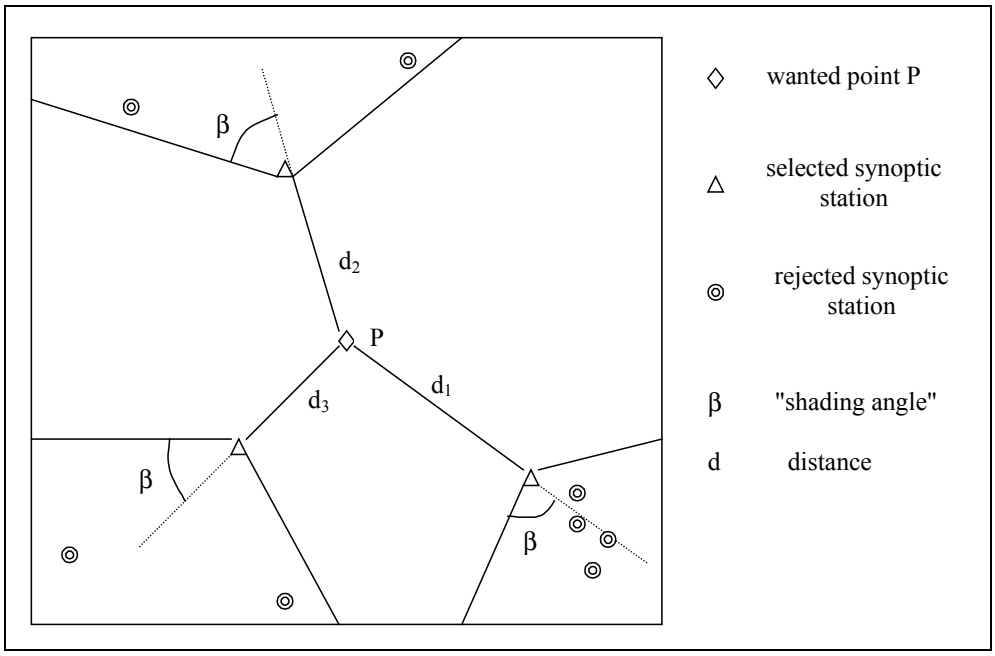

Fig. 5.2.4: Schematic representation of the spatial algorithm used in C-Fix for the up-scaling of meteorological data.

5.3.3.2.4 Global radiation

Since no direct measurements of global radiation are available for the European continent an empirical relationship was used to estimate this meteorological variable. The Supit or extended Hargreaves formula calculates incoming global radiation as a function of cloud cover and air temperature (Supit et al., 1994).

$$S_{g,d} = C_a S_{o,d} \sqrt{T_{\max} - T_{\min}} + C_b S_{o,d} \sqrt{1 - Cloud/8} + C_c \qquad (5.2.21)$$

Table 5.2.10. lists the parameter values used to calculate global radiation.

Table 5.2.10: Parameters used to calcualte global radiation using equation 5.2.21.

$S_{g,d}$:	Incoming daily global radiation	[MJ.m^{-2}.d^{-1}]
$S_{o,d}$:	Daily extra-terrestrial radiation	[MJ.m^{-2}.d^{-1}]
T_{min} :	Minimum temperature	[°C]
T_{max} :	Maximum temperature	[°C]
Cloud :	Mean total cloud cover during daytime	[octa's]
C_a :	Empirical constant	[-]
Cb :	Empirical constant	[octa's$^{-1/2}$]
Cc :	Empirical constant	[MJ.m^{-2}.d^{-1}]

Note that the empirical constants C_b and C_c are not dimensionless. For different regions in Europe the constants C_a, C_b and C_c have been established (Supit et al., 1994). Figure 5.2.5. illustrates the stations for which C_a, C_b and C_c have been estimated. There are certain regions with little or no stations, i.e. the eastern part of Europe, the middle part of France, Norway, and the southeastern part of Europe (Greece, Macedonia, Bulgaria, Bosnia-Herzegovina, Yugoslavia, …). It must be stated that for these regions the SUPIT-parameters are less accurate. For each location or pixel centre, the SUPIT-parameters are estimated with the above mentioned spatial interpolation technique.

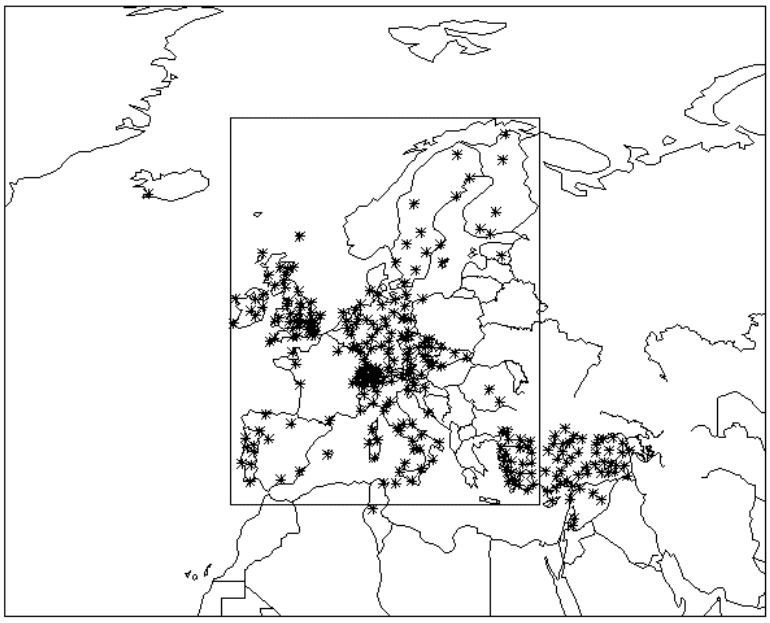

Fig.5.2.5: Stations for which the SUPIT parameters Ca, Cb and Cc have been estimated.

The daily extra-terrestrial radiation $S_{o,d}$ which is also known as the Angot radiation is estimated as:

$$S_{o,d} = S_{c,d} . \sin H \qquad (5.2.22)$$

where $S_{c,d}$, is the average solar constant at the top of the atmosphere for a certain day. The average solar radiation S_c at the top of the atmosphere is estimated 1370 [W.m^{-2}] (Supit et al., 1994). A daily solar radiation constant can than be calculated as a cosine times the average solar radiation at the top of the atmosphere multiplied by a

correction factor for the eccentricity of the earth's orbit. This correction factor is estimated 0.033 (Supit et al., 1994) :

$$S_{c,d} = S_c\left(1 + 0.033\cos\left(2\pi\frac{t_d}{365}\right)\right) \qquad (5.2.23)$$

In 5.2.23, t_d [-] is the number of days since January 1st. Note that during winter in Europe the solar radiation at the top of the atmosphere is at its maximum.
The sun eleveation sinH at any moment throughout the day and at any place and date is calculated as:

$$\sin H = \cos\vartheta = \sin\beta\sin\delta + \cos\beta\cos\delta\cos\psi \qquad (5.2.24)$$

where β is the latitude, δ the solar declination which is a function of the day, θ the zenith distance (H=90-θ) and ψ the solar hour angle.

(i) $\psi = 0$: maximum height of the sun (solar noon)

$$\sin H_{\max} = \cos\theta_{\min} = \sin\beta\sin\delta + \cos\beta\cos\delta \qquad (5.2.25)$$

(ii) $\psi = \pi$: minimum height of the sun (night time)

$$\sin H_{\min} = \cos\theta_{\max} = \sin\beta\sin\delta - \cos\delta\cos\beta \qquad (5.2.26)$$

(iii) $\psi = \pi/2$: sunset or sunrise

$$\sin H = \cos\theta = 0$$
$$\cos\psi^* = -\frac{\sin\beta\sin\delta}{\cos\beta\cos\delta} = -tg\beta g\delta \qquad (5.2.27)$$
$$\psi^* = bg\cos(-tg\beta tg\delta)$$

the astronomical daylenght D can be calculated as :

$$D = 2\psi^*$$
$$D^h = \frac{12}{\pi}D \qquad (5.2.28)$$

The integral of the solar height over the day can be obtained as the integral from sunrise ($-\psi^*$) to sunset (ψ^*):

$$\int_{-\psi^*}^{\psi^*}\sin H\,d\psi = \sin\beta\sin\delta\int_{-\psi^*}^{\psi^*}d\psi + \cos\delta\cos\beta\int_{-\psi^*}^{\psi^*}\cos\psi d\psi \qquad (5.2.29)$$

or

$$\int_{-\psi^*}^{\psi^*} \sin Hd\psi = \sin\beta \sin\delta(2\psi) + \cos\beta\cos\delta[\sin\psi - \sin(-\psi)] \qquad (5.2.30)$$

or

$$\int_{-\psi^*}^{\psi^*} \sin Hd\psi = D\sin\beta \sin\delta + \cos\beta\cos\delta[\sin\psi - \sin(-\psi)] \qquad (5.2.31)$$

where β is the latitude [rad], δ the solar declination [rad] calculated as:

$$\delta = -23.45\cos\left(2\pi\frac{t_d + 10}{365}\right) \qquad (5.2.32)$$

Mathematically the calculation of equation (5.2.31.) can be indeterminable if the latitude is greater then 66.5 degrees in the northern hemisphere (NH) or -66.5 in the southern hemisphere (SH). An extreme case are the polar caps where λ is 90° or $\pi/2$ radians in the NH. Equation (9.) can only be solved in the case where -tanδtan is greater then -1 and lower then 1 :

if $-tg\delta tg\beta > 1$ then $\psi^* = 0$ and D = 0
if $-tg\delta tg\beta < 1$ then $\psi^* = \pi$ and D = 2π or D = 24 hours

Two simplifications were introduced in equation (5.2.21.). First, the initial data have no information concerning the daily T_{max} and T_{min}. For this reason the daily maximum temperature difference was estimated by means of the difference between the highest and lowest temperature out of the 8 daily measured values. Secondly, the parameter *Cloud* defined as the mean total cloud cover from sunrise till sunset (daytime) is a function of time and geographical position. In this project this variable is estimated as the mean value of the four middle measurements for each day. This simplification is visualized in the following figure for three sites in Europe. The graphs illustrate that the assumption for reduced cloud calculation can be retained.

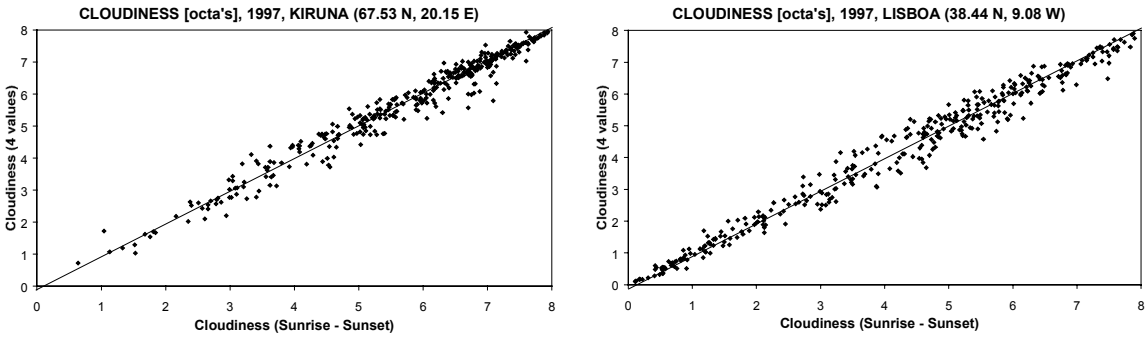

Fig. 5.2.6: Correlation between daily cloud cover estimated between sunrise and sunset and out of 4 measurements

Equation 5.2.21, with the two simplifications taken into account, was validated for different stations in Europe. A correction factor equal to 2 was applied for the temperature difference in the original equation or:

$$\left(T_{\max} - T_{\min}\right) = \left(T_{high} - T_{low}\right) * 2 \qquad (5.2.33)$$

wherein T_{high} and T_{low} are the highest and lowest temperature out of 8 measurements per day. T_{max} and T_{min} are the maximum and minimum air temperatures for the same day.

Figure 5.2.7. illustrates the result of this validation for some Euroflux station global radiation measurements.

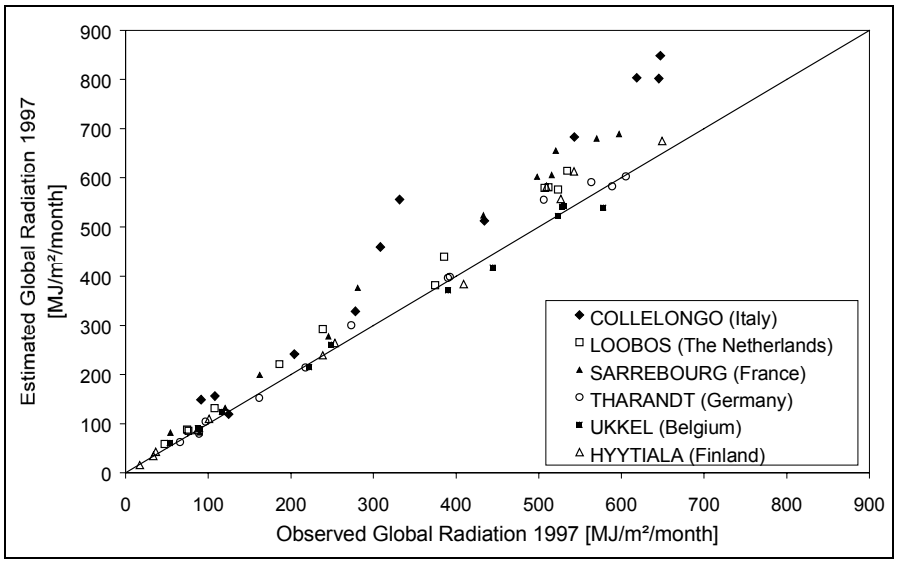

Fig. 5.2.7: Monthly total values of global radiation, estimated with the Supit method, plotted against observed values for various locations in Europe for 1997

5.3.3.4.5. Spatial resolution of the meteo grid

Once temperature and incoming global radiation are know for a certain number of stations, the required meteorological data for each grid centre can be derived by the distance-weighted interpolation technique. An important parameter in climatology is scale. In general, three types of scales are defined: regional climate (100 km), topological climate (10 km for a plain, 1 km in mountains) and microclimate (100 m for a plain, 10 m in mountains). In this project the size of the meteorological grid was held constant for the sake of simplicity. A grid size of 0.25 degrees was selected. An example of the obtained results is shown in the following figure.

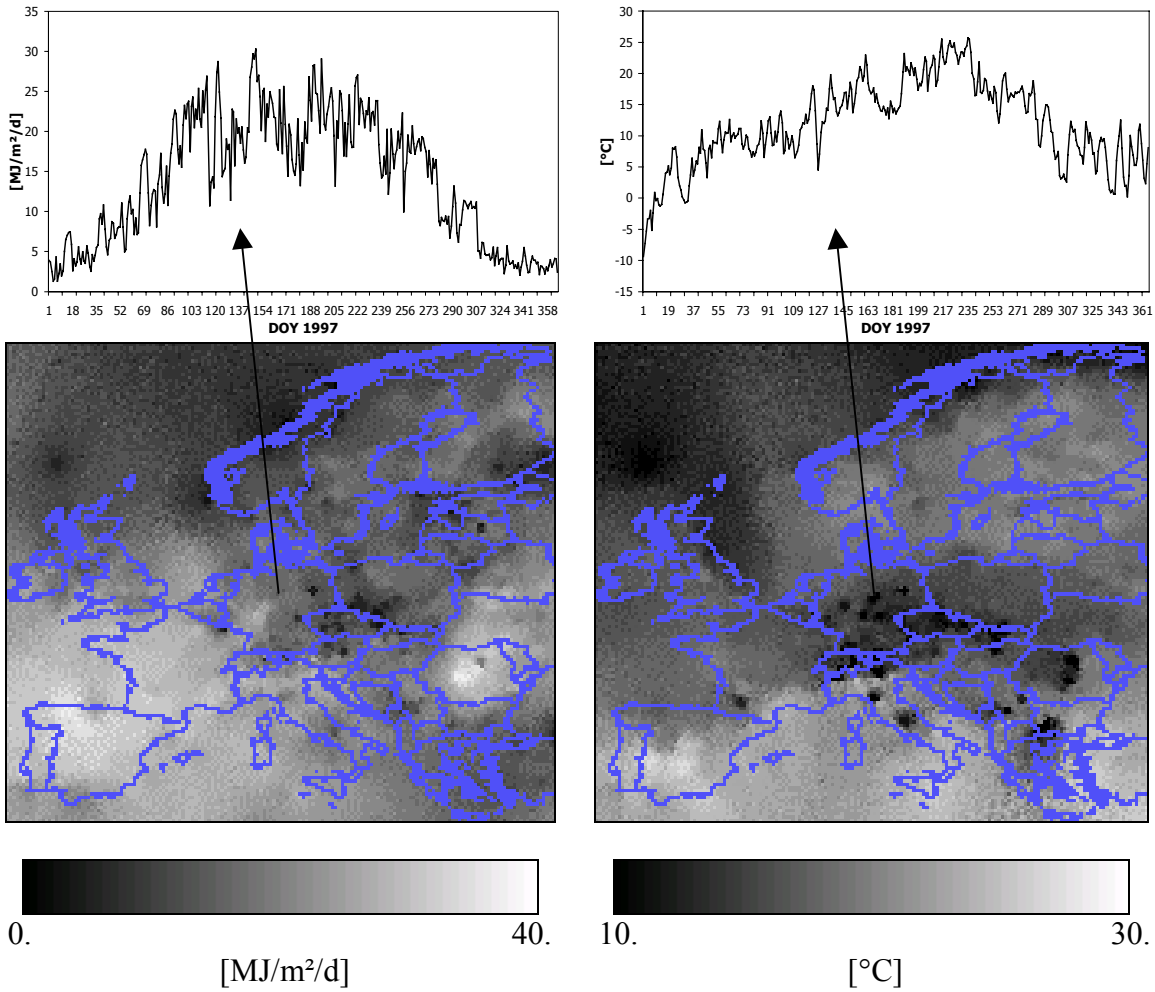

Fig. 5.2.8: Yearly time course and spatially interpolated daily incoming global radiation (left) and daily mean air temperature (right) for the first of May 1997. The spatial resolution is 0.25 x 0.25 degrees.

5.3.4 Remote Sensing data

5.3.4.1 NOAA-AVHRR imagery

The remote sensing imagery for this project was extracted from a rasw level1b NOAA-AVHRR Data Set. 36 NDVI (decadal or 10 daily) European NDVI-composites were calculated from daily European imagery by means of the Vito-VTT NOAA-chain. Multitemporal composites were calculated based on the min RED reflectance criterion.

Inspection of the yearly pixel profiles (36 subsequent NDVI-values) pointed out that the multitemporal 10 daily data were still cloud contaminated. Therefore the decadal NDVI-data were submitted to a diachronic cloud removal procedure (Canters et al., 1998 and Eerens et al, 2000) and subsequently more stable monthly mean NDVI-values were obtained and stored in 12 separate NDVI-images. The latter were then converted into 12 corresponding *f*APAR raster images by means of the linear *f*APAR - NDVI relationship discussed in chapter 5.2.2.2. The parameters of this equation were defined as previously described with histogram analysis.

All values of all pixels from the monthly mean NDVI images are plotted in a histogram (Fig. 5.2.9.). From this graph the cumulative histogram is calculated. This graph is then used to establish the relationship between NDVI and *f*APAR :

$$fAPAR = 1.4925 * NDVI - 0.2537 \qquad (5.2.34)$$

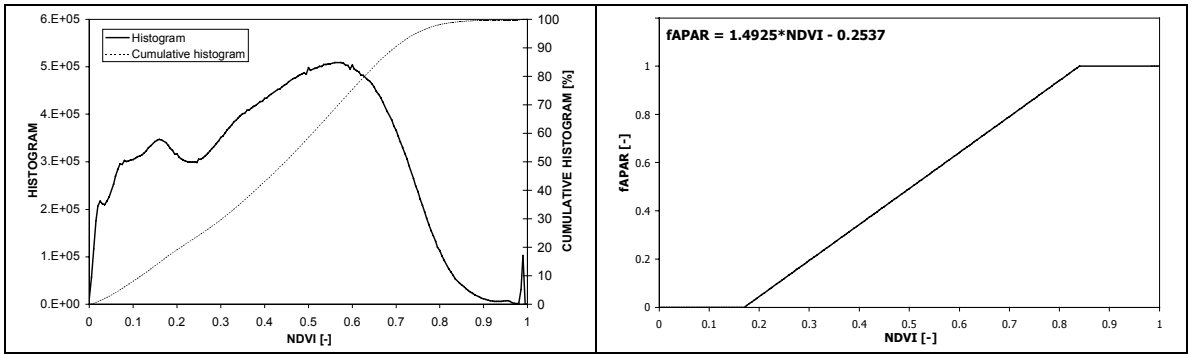

Fig. 5.2.9: Left: histogram and cumulative histogram of all monthly mean NDVI images for 1997; Right: linear relationship fAPAR – NDVI.

Finally, the 12 monthly *f*APAR-images are projected into the geographic Plate Carrée co-ordinate system with a resolution of 0.0125° (± 1km at 45°N). Daily *f*APAR-values are derived by linear interpolation from the monthly mean values. They are illusrated in figure 5.2.10.

January 1997

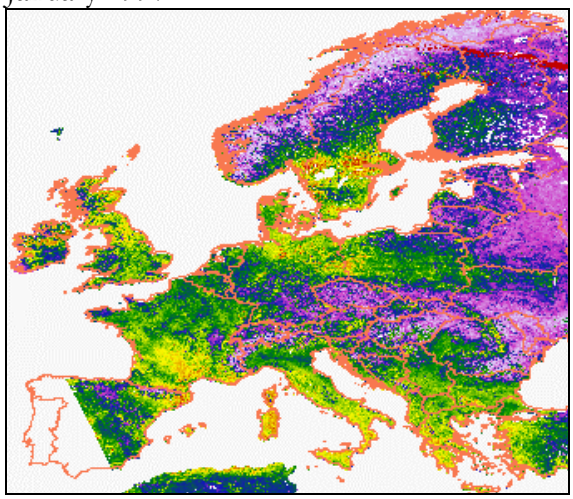

February 1997

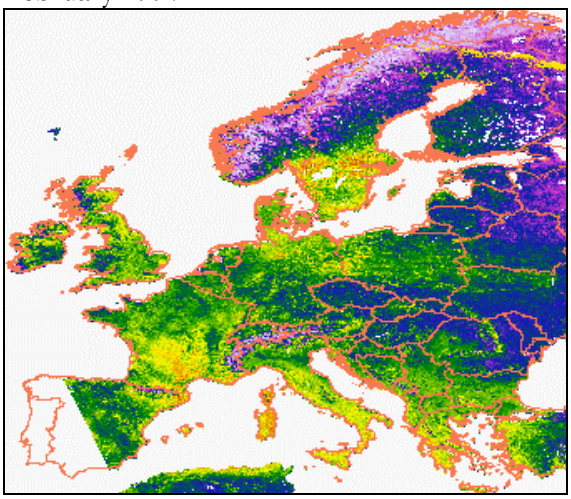

March 1997

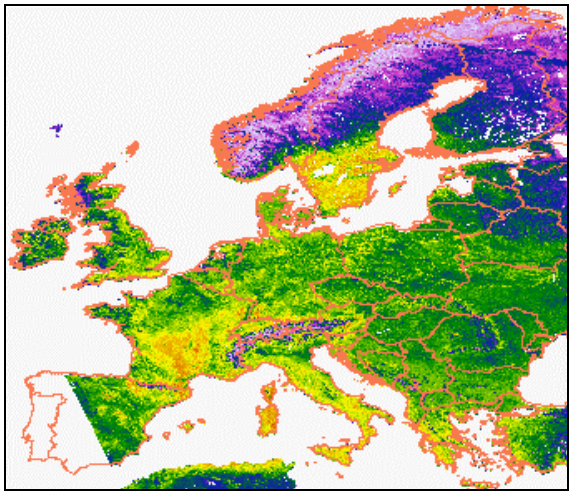

April 1997

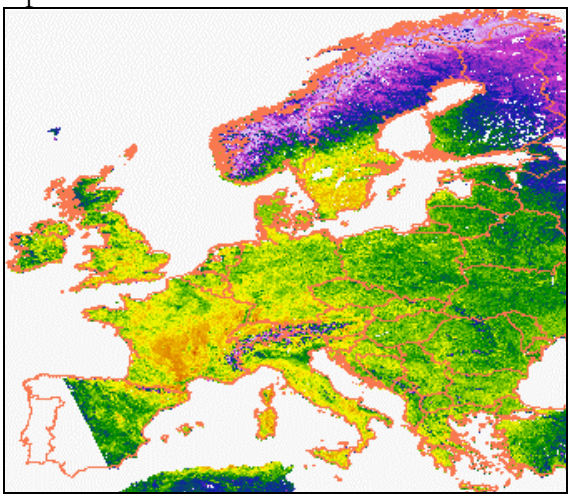

May 1997

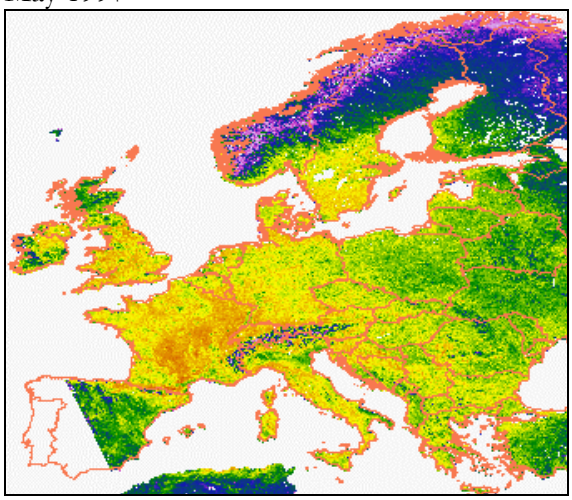

June 1997

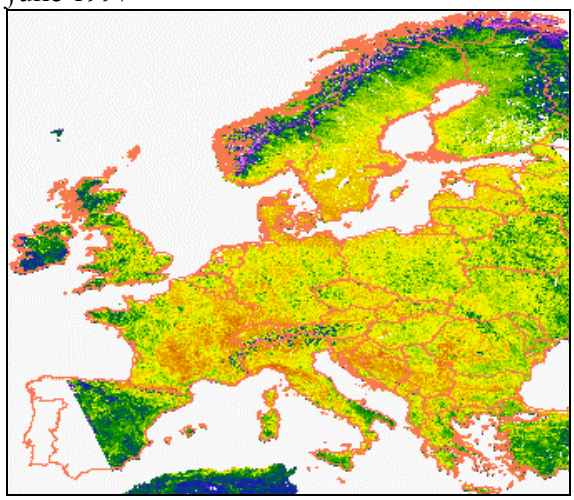

Fig. 5.2.10: Monthly fAPAR values for the year 1997.

July 1997

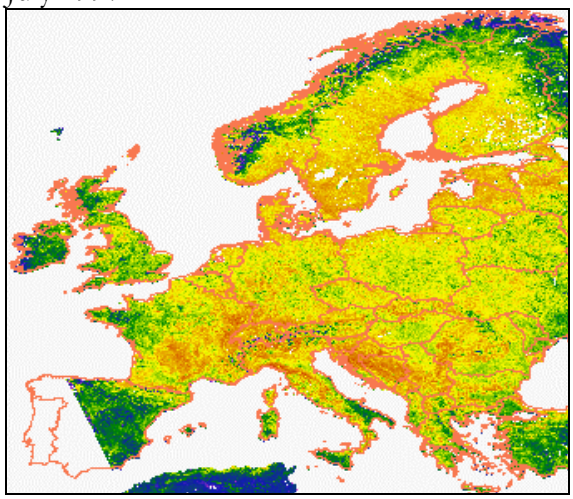

August 1997

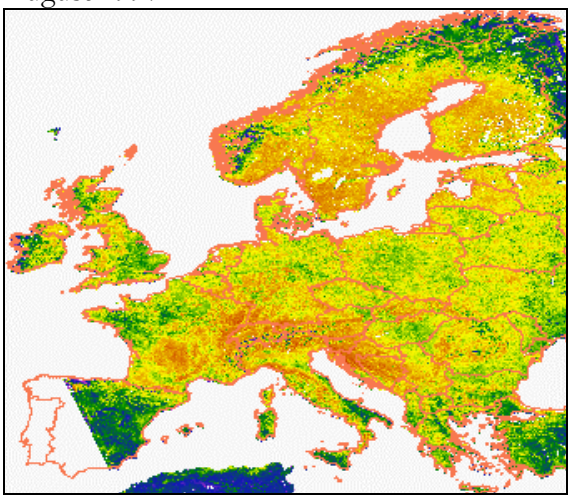

September 1997

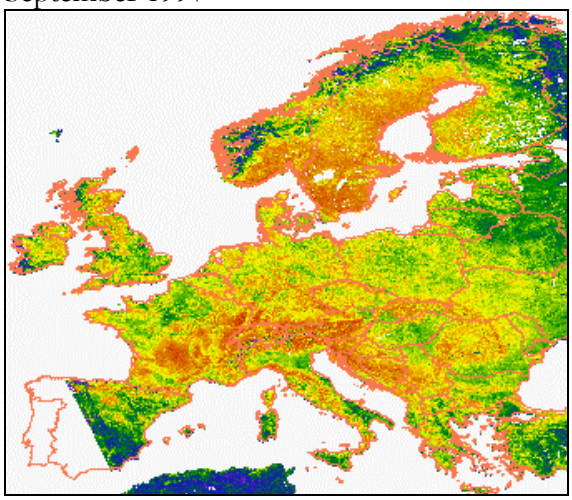

October 1997

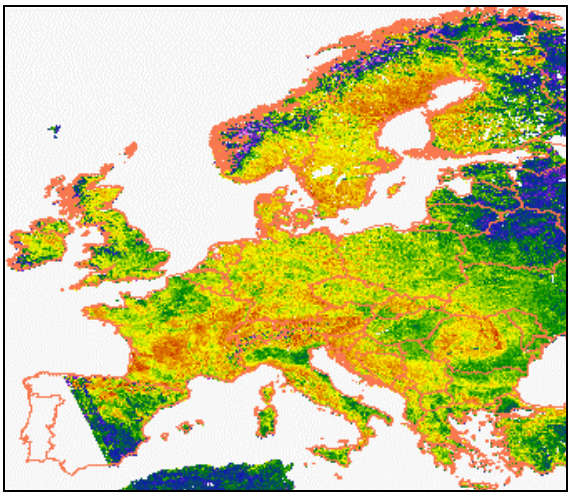

November 1997

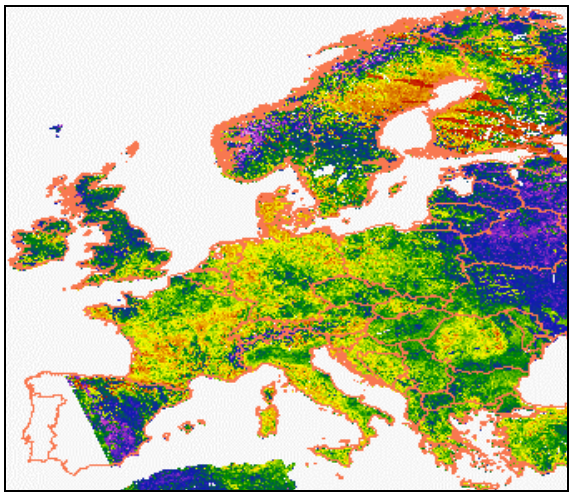

December 1997

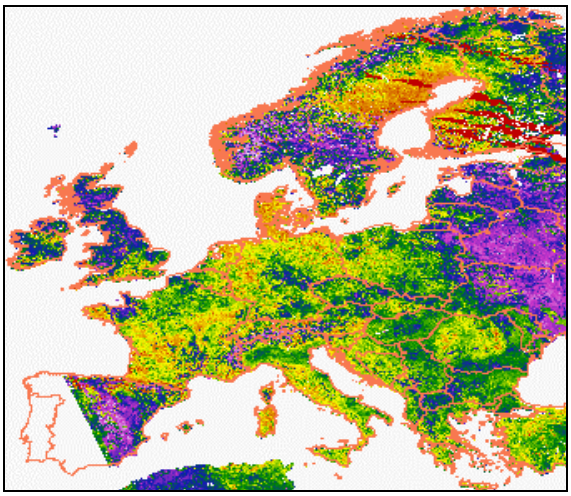

5.3.4.2 Forest Probability map

To be able to calculate Carbon fluxes for forest non-forest was masked out of the European maps using a forest probability map. This map was derived from NOAA-AVHRR data for 1997, indicating the fraction of a pixel covered by forest, was overlaid. Forest NEE was then calculated by multiplying the raster values of an NEE map with the probability of forest of the corresponding pixel in the forest probability map. expressed as a fraction.

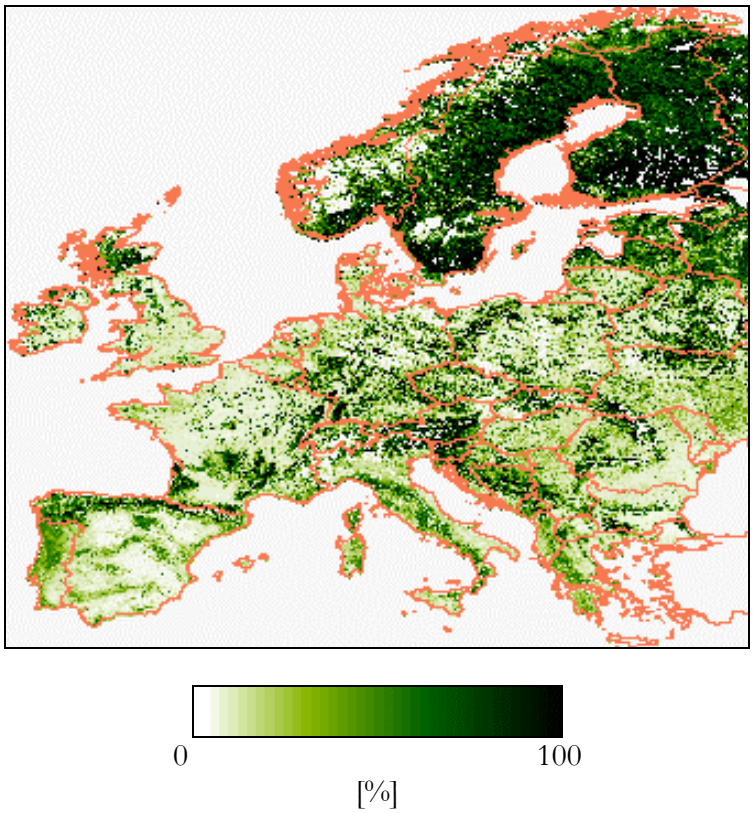

Fig. 5.2.11: AVHRR-based forest probability map of the pan-European area.

The map indicates the distribution and density of wooded area in the pan-European area. The 'forest' cover, depicted by percentage forest probability represents an estimate of woody vegetation present within a single AVHRR pixel. The EEA CORINE Land Cover data base (from southern and central Europe) was used as training data to establish the link between wooded area / non-wooded area and spectral response (Häme et al., 1999).

5.3.5 References

Badger, M.R. and Collatz, J.G. (1976). Studies on the kinetic mechanism of RudP-carboxylase and oxygenase, with particular reference to the effect of temperature on kinetic parameters. Garnegie Institution Annual Report, 1976 – 1997, Pittsburg, P.A.

Canters F., Eerens H. and Veroustraete F. (1998). Land cover classification and estimation of land cover proportions on a global scale. Final report contract T4/DD/002-3, Belgian Science Policy Office (in Dutch with summary in English).

Eerens H., Verheijen Y., Veroustraete F. and Wouters K. (2000). Opbrengstschatters afgeleid uit satellietbeelden met lage resolutie. In: Prévision des productions végétales a l'échelle nationale basée sur un système integré 'modele agrométéorologique-télédetection': analyse de sensibilité et domaine de validité en tant qu'outil d'aide a la décision en politique agricole, B-CGMS Project, eds. Tychon B. et al., Rapport Final, Juillet 2000, 77- 106.

Goward S.N. and Dye D.G. (1987). Evaluating North-American net primary productivity with satellite observations. *Advanced Space Research,* **7 (11),** 165-174.

Hame T., Stenberg P., Andersson K., Rauste Y., Kennnedy P., Folving S. & Sarkeala J. (1999). AVHRR-based forest probability map of the Pan-European area, JRC: 13911-1998-04 F1ED ISP FI.

Jach M.E. and Ceulemans R. (2000). Effects of season, needle age and elevated atmospheric CO2 on photosynthesis in Scots pine (Pinus sylvestris). *Tree physiology*, **20**, 145 – 157.

Kumar U M. and Monteith J.L. (1981). Remote sensing of crop growth. In: Plants and the Daylight Spectrum, eds. Smith, H., Academic Press, San Diego, California, 133-144.

Mc Cree, K.J. (1972). Test of current definitions of photosynthetically active radiation against leaf photosynthesis data. *Agricultural Meteorology*, **10**, 442-453.

Maisongrande P., Ruimy A., Dedieu G. and Saugier B. (1995). Monitoring seasonal and interannual variations of gross primary productivity, net primary productivity and ecosystem productivity using a diagnostic model and remotely sensed data, Tellus 47(B).

Myneni R.B. and Williams D.L. (1994). On the relationship between fAPAR and NDVI. *Remote Sensing of Environment*, **49**, 200-211.

Sabbe H., Eerens, H. & Veroustraete. (1999). Estimation of the carbon balance of European terrestrial ecosystems by means of the C-Fix model. In: Proceedings of 'The 1999 EUMETSAT Meteorological Satellite Data Users' Conference, Copenhagen, 6 –10 September 1999, 271- 278.

Samason, R., Follens S. and Lemeur R. (1997). Scalling leaf photosynthesis to canopy in a mixed deciduous forest. I. Model description. *Silva Gandavensis*, **62**, 1 – 21.

Angstrom, A., 1924. Solar and terrestrial radiation. *Quarterly Journal of the Royal Meteorological Society*, **50**, 121 – 125.

Hargreaves G.L., Hargreaves G.H. A Hargreaves and Rayley J.P. (1985). Irrigation water requirement for Senegal River Basin. Journal of Irrigation and Drainage Engineering, ASCE 111 **(3),** 265 – 275.

Roujean J.L. & Breon F.M. (1995). Estimating PAR absorbed by vegetation from bidirectional reflectance measurements. *Remote Sensing of Environement*, **51**, 375 –384.

Supit I., Hooijer and Van Diepen C.A. (1994). System description of the WOFOST 6.0 crop simulation model implemented in CGMS, Volume 1: Theory and Algorithms, JRC, EUR 15956 EN, 144 pp.

Supit I., and Van Kappel R.R. (1998). A simple method to estimate global radiation. *Solar Energy*, **63 (3),** 147-160.

Valentini R., Matteucci G., Dolman A.J., Schulze E.D., Rebmann C., Moors E.J., Granier A., Gross P., Jensen N.O., Pilegaard K., Lllindroth A., Grelle A., Bernhofer C., Grunwald T., Aubinet M., Ceulemans C., Kowalski A.S., Vesala T., Rannik U., Berbigier P., Loustau D., Guomundsson J., Tthorgeirsson H., Iibrom A., Mmorgenstern K, Clement R., Monqciff J., Montagnani L., Minerbi S. & Jarvid P.G. (2000). Respiration as the main determinant of carbon balance in European forests. Letters to nature, *Nature*, **404,** 861 – 865.

Veroustraete F., Patyn, B. (1994). Forcing of a simple ecosystem model with fAPAR and climatic data to estimate regional scale photosynthetic assimilation. In: Vegetation, Modelling and Climate Change Effects, eds. Veroustraete F. et al., Academic Publishing, The Hague, the Netherlands, 151-177.

Veroustraete F., Patyn F. J. & MYNENI R.B. (1996). Estimating net ecosystem exchange of carbon using the Normalised Difference Vegetation Index and an ecosystem model. *Remote Sensing of Environment*, **58**, 115-130.

Wang, F. K.Y. (1996). Canopy CO_2 exchange of Scots pine and its seasonal variation after four year exposure to elevated CO_2 and temperature. *Agricultural and Forest Meteorology*, **82**, 1-27.

Wofsy F. S.C., Goulden F. M.L., M Veroustraete F. J.W., Fan F. S.M., Bakwin P.S., Daube F. B.C., Bassow F. S.L. & Bazzazz F.A. (1993). Net exchange of CO_2 in midlatitude forests. *Science*, **260**, 1314 - 1317.

Woodwell F. G.M. (1984). The role of terrestrial vegetation in the global carbon cycle, Measurement by remote sensing. SCOPE/ICSU, Wiley & Sons, Chichester, 247 pp.

5.4 Large-scale vegetation modelling

R. Milne, D. Mobbs & J. Grace

5.4.1 The EUROBIOTA forest system model

5.4.1.1 Description of the model

The EuroBiota forest ecosystem model primarily describes the effect of changing temperature and atmospheric carbon dioxide concentration on productivity. The model is based on the work of Wang & Polglase (1995) who described these effects on 3 different biomes. Extensive modification of the original model has taken place to allow the influence of geographical variation in weather and the presence of evergreen and deciduous forest at different locations to be taken into account. The structure of EuroBiota model is presented in Figure 5.3.1. This shows which pools and fluxes have been taken into consideration to simulate the carbon dynamics of forest ecosystems.

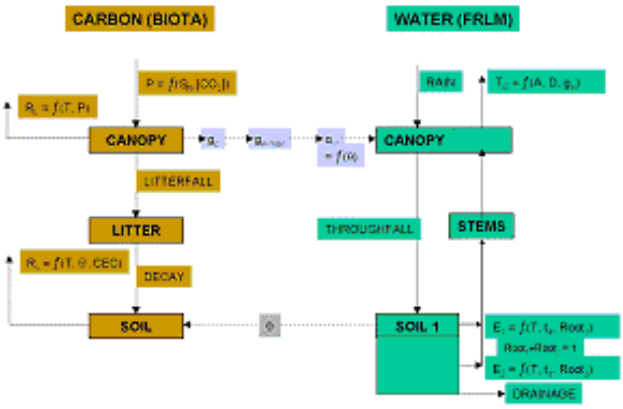

Figure 5.3.1. Structure of EuroBiota model showing links between carbon and water modules.

For application to European forests the input data for each cell or groups of cells were used as follows.

The basic scale of application for the model was for each 0.5^0 x 0.5^0 latitude by longitude grid cell covering land in Europe between 34 °N, 25 °W to about 72.5°N, 36 °E.

A baseline daily pattern of weather was developed from the mean monthly climatology of the Climate Research Unit for the period 1961 to 1990 and the daily weather generator of Friend et al (1997). This daily pattern has maximum and minimum air temperature, water vapour pressure deficit, solar radiation and precipitation and was assumed to apply for each year from 1860 to 2100.

The effect of changing air temperature was described using a version of the data of the analysis of HADCM2 GCM output (at decadal scale) and CRU 1901- 1995 climate data described in Chapter 6 but regridded to the 0.5^0 cell size required by

EuroBiota. This gave monthly temperature anomalies for each cell for each year from 1860 to 2100 with reference to the 1961 to 1990 baseline weather pattern.
Changes in carbon dioxide concentration throughout Europe follwed the IS92a emission scenario and are as estimated by University of Bern for the IPCC Second Assessment Report

The location and area of forests were estimated from the USGS/IGBP-DIS Global Land Cover Characteristics 1 km scale data projected to latitude/longitude and gridded into 0.5^{o} x 0.5^{o} cells. Conifer and deciduous forests are distinguished. Bio-Climatic zones (Boreal, Temperate and Mediterranean) were as defined in Chapter 6.

For each Bio-Climatic zone the physiological parameters relevant to European evergreen and deciduous forests were selected from the results from LTEEF II process-based models and from the ECOCRAFT Database (Medlyn & Jarvis 1999) Appropriate soil characteristics (clay content, rooting & overall depth) for each zone were chosen from the Global Environment Database (Webb et al. 1992). For each country the age structure of forests was taken from the EFISCEN database and model.

EuroBiota was run for European forests in 3 stages. 1: The carbon pools were initialised with effectively zero value and 1860 weather and cabon dioxide conditions assumed for each subsequent year and the model run to equilibrium carbon stocks. 2: Using these equilibrium tree and soil carbon stocks as new starting values the model was rerun with changing temperature and carbon dioxide for the years from 1860 to 2100 3: To assess the effect on productivity of the different age structure in different countries, and for times in the future, this transient run was recalculated, but in each country all forests had a simulated felling and replanting in the year indicated by the average age of forest for the year under consideration. The average of forest age for each country was calculated from the distribution of ages used in the EFISCEN model. For 1990 the EFISCEN base data was used and for later years the age distribution predicted by the Business As Usual Scenario was taken. This felling and replanting was modelled by removing in the appropriate year all stem carbon from the model and transferring leaf and root carbon to the litter pools. The forest was then forced to re-established. The result of this approach is that productivites will be different in different countries, not only due to local weather conditions, but due to the stage of recovery which the model forest has reached since the simulated felling/regrowth.

5.4.1.2 References

Friend, A.D. (1998) Parameterisation of a global daily weather generator for terrestrial ecosystem modelling. *Ecological Modelling* **109,** 121-40.

Webb, R.S., Rosenzweig, C.E. & Levine, E.R. (1992) A global data set of soils partocle size propoerties. Digital raster data on a 1 degree geographics 180x360 grid In; Global Ecosystems Database Ver 1.0. Noaa national Geophysical Data Center, Boulder, USA

Medlyn B.E. & Jarvis P.G. (1999). A parameter database for analysis of effects of elevated CO2 on European forest species. *Ecol. Model.* **124**: 69-83.

Wang, Y-P. & Polglase, P.J. (1995) Carbon balance in the tundra, boreal forest and humid tropical forest during climate change: scaling up from leaf physiology and soil carbon dynamics. *Plant, Cell and Environment*, **18**, 1226-1244.

5.4.2 The HYBRID ecosystem model

5.4.2.1 Description of the model

A dynamic, global vegetation model, Hybrid v4.1 (Friend *et al.* 1997), was driven by transient climate output from the UK Hadley Centre GCM (HadCM2) with the IS92a scenario of increasing atmospheric CO_2 equivalent, sulphate aerosols and predicted patterns of atmospheric N deposition. Changes in areas of vegetation types and carbon storage in biomass and soils were predicted for areas from 34 °N, 25 °W to about 72.5°N, 36 °E from 1860 to 2100. The basic spatial resolution of this application of the model is the 3.75° x 2.5° of the GCM and the outputs are the predicted changes in carbon per unit area in the potential vegetation types for each of these cells. Hybrid is a combined biogeochemical, biophysical and biogeographical model of natural, potential ecosystems. Hybrid represents plant physiological and soil processes regulating the carbon, water and N cycles and competition between individuals of parameterised generalised plant types. The latter were combined to represent 9 vegetation types of which temperate grassland, broadleaf forest, mixed forest and coniferous forest were the most important for the European area. The model simulated the current areas and estimated carbon stocks in the various vegetation types.

A complete description of the Hybrid model is given by Friend *et al.* (1997) and Friend and White (2000). The model has been evaluated for its ability to simulate current measured carbon fluxes at particular sites (Friend *et al.* 1997) and it has been shown to successfully predict the major global patterns of undisturbed pre-industrial vegetation, NPP, biomass and soil carbon (Friend and White, 2000). White *et al.* (2000) used it to predict changes in carbon fluxes and potential vegetation types for locations north of 50°N. Here we present results for productivity per unit area from those grid cells which include each country.

The model operates conceptually like a forest gap model, in which individuals of all potential plant types are seeded every year into 200 m^2 plots (with no dispersal constraint) grow, die and regenerate year by year, with all underlying processes calculated on a sub-daily timestep. Vegetation types are assigned different parameter values which determine their success in competing for light, water and N in any climatic regime and hence the resulting vegetation. Thus, the model describes the transient responses and properties of vegetation, which can be composed of different proportions of specified plant types at any time. However, unlike most gap models, plant growth is determined entirely by climatic variables operating through plant

physiological and soil processes. The carbon, water and nutrient cycles are coupled, including all the major interactions, feedbacks and exchanges between the soil, vegetation and atmosphere. The model contains no statistical relationships between vegetation properties and the current climate except for phenology. The model, as described by Friend *et al.* (1997) and Friend and White (2000), does not include land use change or disturbance due to fire.

5.4.2.2 References

Friend, A. D., A. K. Stevens, R. G. Knox, and M. G. R. Cannell, A process-based, terrestrial biosphere model of ecosystem dynamics (Hybrid v3.0), *Ecol. Modell.,* **95**, 249-287, 1997.

Friend, A.D. & White, A. 2000 Evaluation and analysis of a dynamic terrestrial ecosystem model under pre-industrial conditions at the global scale. *Global Biogeochemical Cycles*, In press.

White, A., M. G. R. Cannell, A. D. Friend, 2000 The high-latitude terrestrial carbon sink: a model analysis, *Global Change Biology,* **6**, 227-245.

6 Climate data

Markus Erhard, Marcus Lindner, Wolfgang Cramer

6.1 Introduction

Analyzing the sensitivity of forest growth to climate and climate changes requires long - term weather data of more than 100 years, corresponding to the average rotation period of European forests. For a detailed description of the processes of tree and stand growth and their response to changes in environmental conditions the data should be available in at least daily temporal resolution.

Due to the high needs of initialisation data and computing capacity simulating forest growth with very detailed process based models can only be executed at a very limited number of sites. In the context of upscaling the simulation results to European level, selected sites should represent the average growth conditions of the most common tree species. In our case the sites should also be related to the average values of the forest inventory data sets, which are based on countries and second order administrative units (see also Chapter 9).

In this chapter we describe the processing of long-term climate data for forest growth and large scale vegetation modelling and a method for selecting representative sites. Results of spatial and temporal down-scaling of large scale climate data to local conditions by using measured data, GCM (General Circulation Model) output and a weather generator will be demonstrated.

6.2 Methods

6.2.1 Climate data

For the years 1901 - 1989 climate data were provided by CRU (Climatic Research Unit, University of East Anglia, Norwich). It include monthly average values of mean temperature, temperature range, precipitation, vapour pressure and cloud cover derived from measured station data interpolated on a grid with 0.5 ^{o} x 0.5 ^{o} spatial resolution (New et al. 1998, Hulme et al. 1995).

For the simulation of climate change impacts on forest growth we used the GCM projection of the HadCM2 run (Hadley Center, University of East Anglia, Norwich; Mitchell et al. 1995). It is based on the business as usual emission scenario IS92a (Houghton et al. 1995). An exponential increase of atmospheric CO2 concentration between the years 1990 (350 μmol mol^{-1}) and 2100 (700 μmol mol^{-1}) is assumed in the scenario For the beginning of the simulation period (1831) the pre-industrial level of atmospheric CO2 concentration was estimated by the authors to be 280 μmol mol^{-1}.

GCM simulations were carried out in a transient mode including the cooling effects of sulphur aerosols on climate. The scenario data provide monthly values of minimum and maximum temperature, precipitation, relative humidity, sunshine and global radiation, for the time period 1831 until 2100 in 3.75° x 2.5° spatial resolution.

Two data sets were prepared. Daily weather data for a number of representative sites and the years 1831 - 2100 and long term climate data for Europe with average values per decade (1840ties - 2090ties) down-scaled on a 0.5° x 0.5° grid for the area 30°W - 60°E and 35°N - 82.5°N.

6.2.2 Selection of representative sites

To select representative sites for process based forest growth simulations a GIS-based analysis was performed. First a forest cover map was generated by extracting the forest classes of the CORINE land cover map (CORINE 1997). For areas without CORINE land cover information such as Norway and South-eastern Europe the ESA-ESTEC remote sensing based forest - non-forest map was used (ESA 1992). To take into account the major gradients in climate, Europe was separated in five different zones (northern, southern boreal, maritime, continental temperate and mediterranean). Because the European inventory data set is related to administrative units, this information was also included for upscaling purposes. For this reason administrative units (ESRI 1992) were also taken into account for the definition of the climate zones.

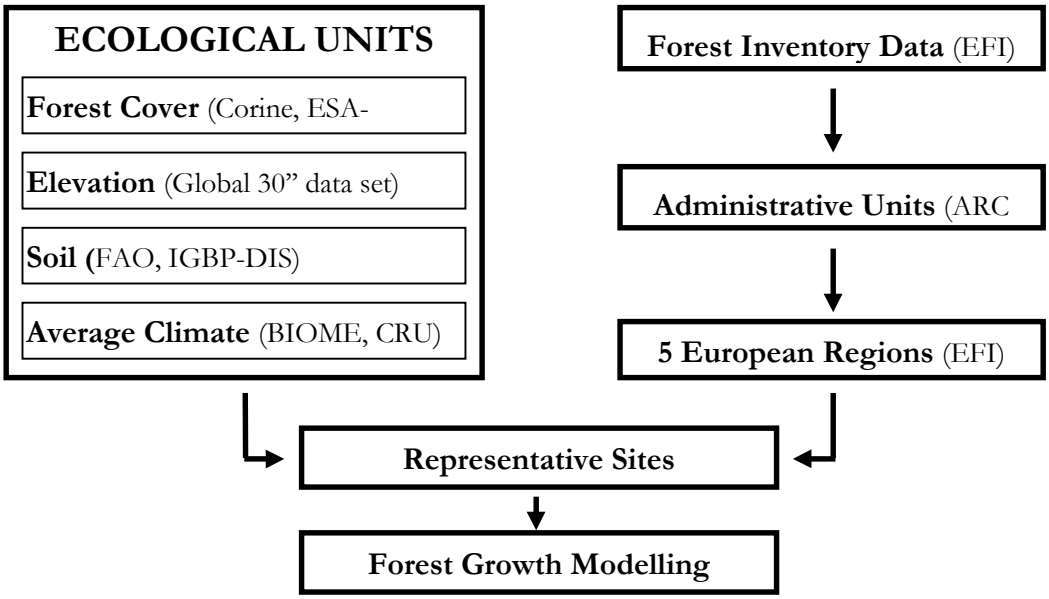

Figure 6.1: Information layers for selecting representative sites

The forest map was overlaid with digital elevation data (Hastings & Dunbar 1999), the FAO Soil Map (FAO 1994) and the climate zones as shown in Fig. 6.1. Average climate (temperature, precipitation, growing season and moisture index) was derived from the Cramer - Leemans data set by using the climate module of the BIOME Model (Prentice

et al 1992, Sykes et al. 1996). Temperature precipitation and sunshine data was interpolated on a 10' x 10' grid with a thin plate interpolator before (Hutchinson 1995). So the dependency of climate parameters on terrain is included. Especially for the mediterranean area simple rules were established (e.g. maximum or minimum elevation, latitude) for each tree species which describe its geographic distribution (Table 1, see also Jalas & Suominen 1987a, b, Walter & Breckle 1991). Then the area weighted mean of the climate parameters, the elevation and latitude was calculated per tree species and climate zone for the areas covered by forests. A site was then selected where long term CRU data with comparable average values was available. Because most of the models are highly sensitive to global radiation the sites were also located close to stations where measured global radiation data was available (Global Radiation Atlas, Palz & Greif 1995).

Further different levels of elevation were selected to estimate the impact of the length of growing seasons on forest growth, especially in mountainous regions.

To represent average soil conditions the most common soil type in forested areas of every climate zone was selected. If necessary calcareous and acid soil types were delivered for different tree species (e.g. Pinus pinaster on silicic soils, Pinus halepensis preferably on calcareous soils a.s.o.)

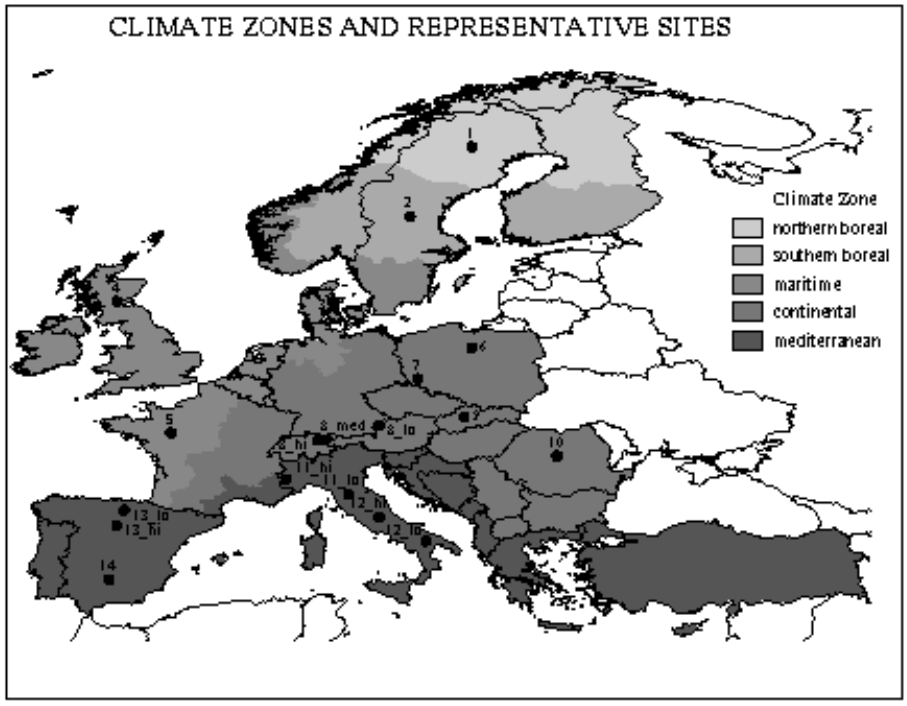

Figure 6.2. Climate zones and location of representative sites. Nineteen sites in five different climate zone were selected each representing typical growth conditions for the most important tree species in European forests under northern and southern boreal, maritime and continental temperate and mediterranean climate (see table 6.1).
Table 6.1: Tree species which are simulated at the different representative sites. In relation to the geographic distribution of the tree species and the forest inventory data the site conditions sometimes are not only linked to the forest covered areas but also to certain levels of elevation.

Climate zone	Site No.	COUNTRY	Altitude	Tree Species
1	1	SWEDEN		Pinus sylvestris, Picea abies, Betula spec.
2	2	SWEDEN		Pinus sylvestris, Picea abies, Betula spec.
3	3	DENMARK		Pinus sylvestris
	4	SCOTLAND		Picea sitchensis
	5	FRANCE		Pinus sylvestris, Quercus robur
4	6	Northern POLAND	<500 m	Picea abies
	7	South-West POLAND		Pinus sylvestris, Quercus robur
	8-lo	AUSTRIA	<650 m	Picea abies, Abies alba
	8-med	AUSTRIA	650 - 1150m	Picea abies, Abies alba
	8-hi	SWITZERLAND	1150 - 1700m	Picea abies, Abies alba
	9	SLOVAKIA	500 - 1000m	Picea abies, Fagus sylvatica
	10	ROMANIA		Pinus sylvestris, Quercus robur
5	11-lo	Northern ITALY	<1000m	Quercus pubescens
	11-hi	Northern ITALY	700 - 1600m	Pinus sylvestris, Fagus sylvatica
	12-lo	Southern ITALY	<800m	Quercus ilex, Pinus pinaster
	12-hi	Southern ITALY	1000 - 1800m	Fagus sylvatica [1)]
	13-lo	Northern SPAIN	<1400m	Quercus ilex, Quercus pubescens
	13-hi	Northern SPAIN	500 - 2000m	Pinus sylvestris
	14	Southern SPAIN	<1250 mm	Quercus ilex, Pinus halepensis, Pinus pinaster

[1)] Southern border of species distribution is limited to 38° northern latitude

6.2.3 Downscaling to site level

GCM results were downscaled to the sites calculating the difference of each parameter between the time period 1990 - 2100 and the average values of the period 1931 - 1960 on monthly time steps. The time series of these anomalies were then added to the average values of the CRU - data of the same reference period (Figure 6.3). Anomaly calculations were made by subtracting and adding the values of the different parameters except for rainfall were this was done by division and multiplication. GCM-model intern artefacts and systematic errors can be eliminated in this way. The historic period of climate data was extended with GCM data of the years 1831 - 1900 with the same method for forest model validation purposes.

To relate the GCM projections to the area for which the representative sites stand for, anomalies were averaged over the climate zones or regions before down-scaling to the values of the sites.

For the large scale vegetation modelling (see Chap. 10.2) an European data set was generated. Anomalies were interpolated on the 0.5 x 0.5° grid of the CRU data set with a combination of linear Delaunay triangulation and a bivariate linear interpolation of the triangulated data on the CRU grid (ESRI 1991).

The monthly climate data of the representative sites was disaggregated to daily values with the C2W weather generator (Bürger 1997), which had been fitted with climatological station data to the conditions at the modelling sites. A stochastic weather process derived from monthly or seasonal anomalies disaggregates long -

term climatological means. The advantage of this method is the preserving of the mean values of the input data. Therefore the aggregated values of the stochastic weather should reproduce the mean values of the input data exactly.

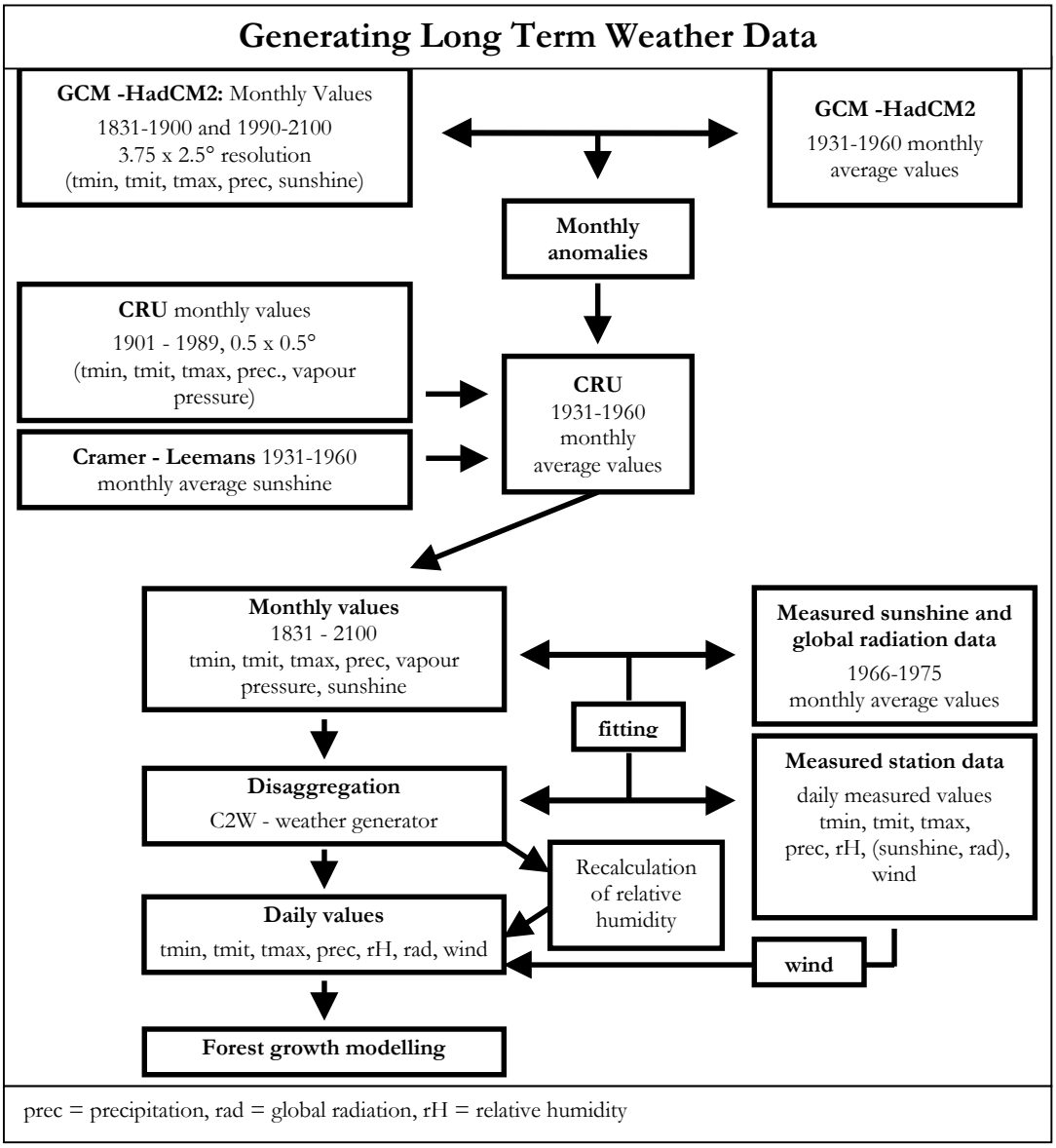

Figure 6.3: Temporal disaggregation of monthly climate data and GCM projections to daily weather data. Global radiation and humidity was recalculated out of sunshine data and minimum temperature, daily potential evapotranspiration and annual precipitation respectively

After disaggregation of the monthly values daily relative humidity was then recalculated with an empirical regression using minimum temperature, daily potential evapotranspiration and annual precipitation as described in Kimball et al. (1997). The global radiation was recalculated out of sunshine data after the approach of Angström (1924) and then corrected with the data of the European Radiation Atlas within the time period 1966-75. The consistency between global radiation and the other parameters is given by the statistical relationships implemented in the weather generator. GCM output was not used because errors in the global radiation data was

estimated to be 15-25%. Since no long term wind speed data was available, daily data of nearby climatological stations was joined to the output of the weather generator.

6.3 Results and discussion

Concerning the impact of present and future climate on forest growth, changes in average climate conditions as well as in the interannual variability are important for forest ecosystems growth. In this chapter special focus is on temperature and precipitation.

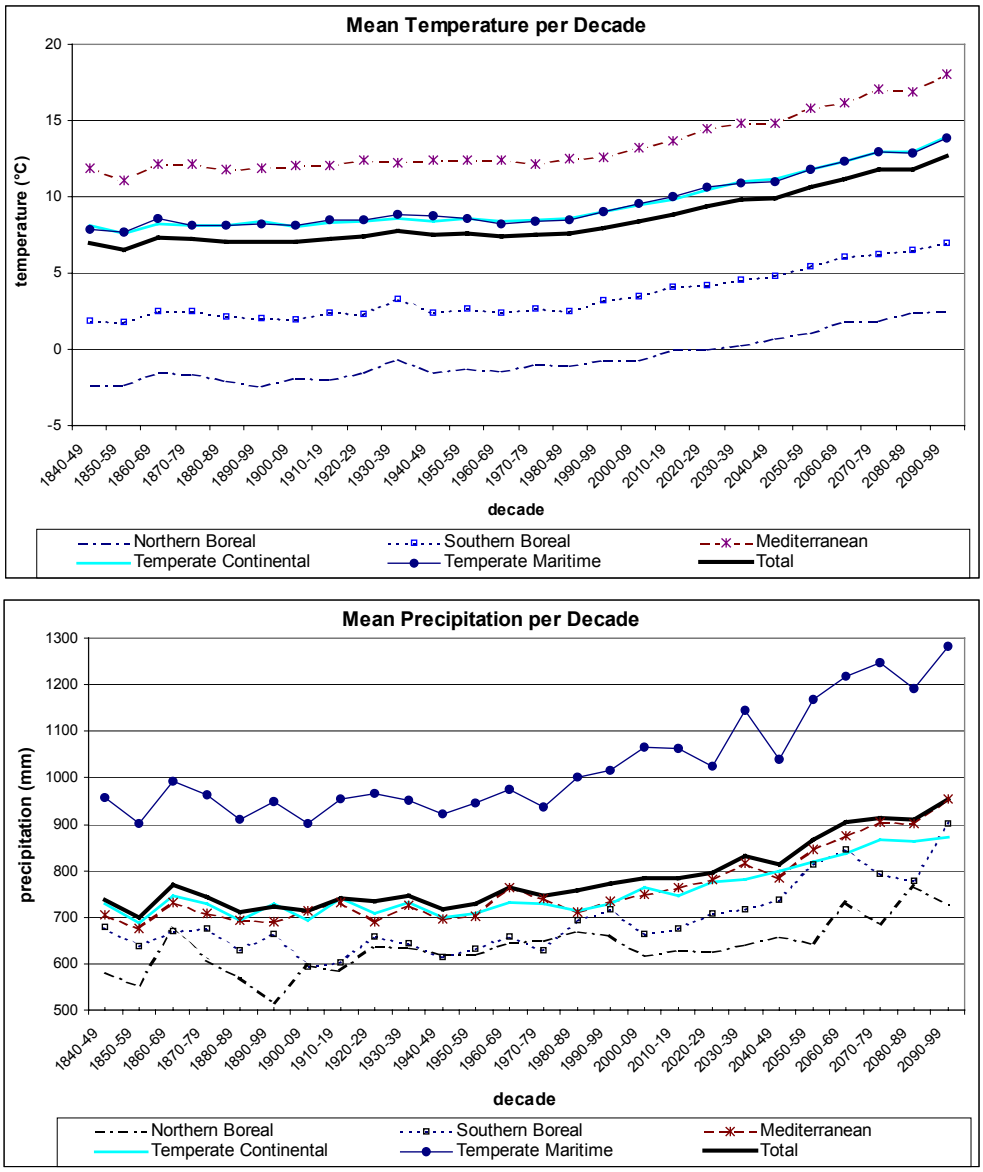

Figure 6.4: Mean temperature and precipitation per decade for the years1840 - 2099 as average value for Europe (climate zones 1 - 5) and per climate zone (see Fig. 6.2); The data set is a combination of CRU (1901-1989) and down-scaled HadCM2 data (1840-1900 and 1990-2099)

Future trends in mean temperature and precipitation are shown in Figure 6.4. Average increase in temperature between 1990ties and 2090ties is about 5.4 degrees with almost the same trend in all climate zones. For precipitation an increment of about 20% between 1990 and 2100 was calculated. Most of the increase can be found after the 2050ties. Even in the highly aggregated values variability in rainfall is much higher than in temperature. But because most of the variations are in the time series of the northern boreal and temperate maritime climate the impact on ecosystems can be expected to be very limited.

Projected climate changes calculated with anomalies are strongly influenced by the differences between the data sets of the reference periods and by the time slices which are compared. For temperatures good coincidences between CRU and HadCM2 data can be found in the reference period 1931-60. In the boreal region GCM tends to overestimate winter temperatures. GCM data shows a slight increase in temperature between 1931-60 and 1961-90, especially in winter time while the differences between the both data sets are decreasing from north to south.

In boreal and temperate continental climate summer precipitation is overestimated in the GCM data (Fig. 6.5). In the temperate maritime area GCM values are generally lower than CRU data. In most cases trends in precipitation between 1931-60 and 1961-90 show a slight increase in precipitation for this time period.

In the mediterranean area differences between the data sets and trends in the GCM data are varying monthly. So future trends in precipitation are strongly influenced by differences in the data sets of the reference periods and by the time slices which are compared. This also can lead to different trends in the anomalies and may therefore partly change the trend from precipitation decrease to increase in future projections.

Concerning the interannual variability of temperature and precipitation no systematic difference between CRU and GCM data can be seen (Table 6.2).

Except from the northern part of Europe standard deviation of temperatures show a higher interannual variability in GCM data than in the CRU values. In the northern continental part variability tends to increase with time. For precipitation no clear regional trend can be seen. Variability of GCM data is higher in the northern and alpine areas while variation tends to be lower in the mediterranean area as it is in the interpolated station data of the CRU data set.

Variation of present, historic and future climate within the year is demonstrated for the mediterranean area, because of the high sensitivity of mediterranean ecosystems to water supply and the saisonality of rainfall pattern (Figure 6.6).The data show a constant increase of precipitation with only low changes in interannual variability during winter. Changes in summer rainfall are very low. The combination of increasing temperatures and constant precipitation in summer may therefore increase future water stress.

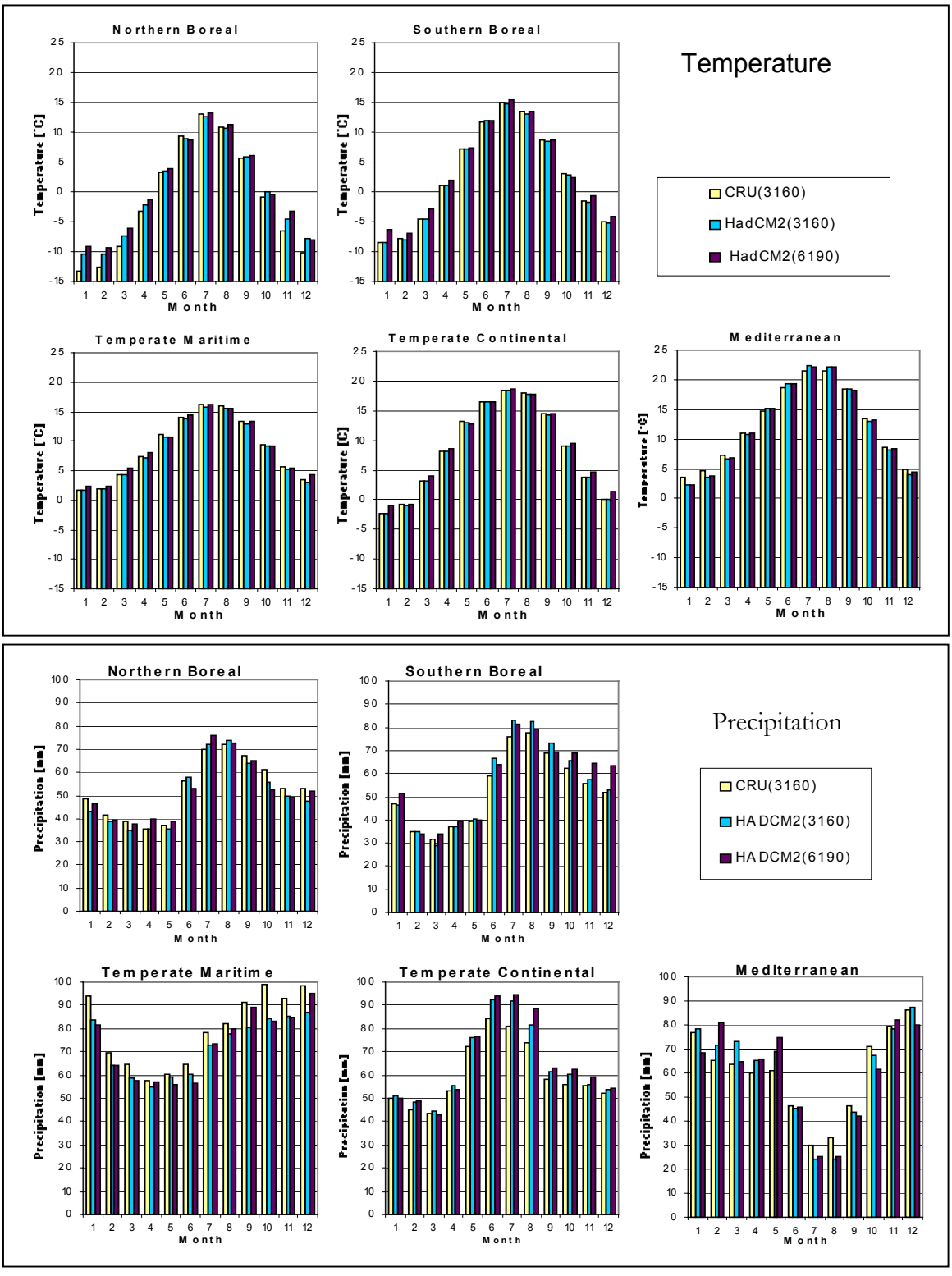

Figure 6.5: Differences in average monthly temperature and precipitation between CRU and GCM data in the reference period 1931-60 and trends in GCM data between 1931-60 and 1961-90

Table 6.2: Mean values and standard deviation of temperature and precipitation at the representative sites for three different time slices (CRU (1901-1989) and down-scaled HadCM2 data (1840-1900, 1990-2099). Standard deviation may be used as indicator for the interannual variability of the climate parameter.

Climate zone	Location	No.	Mean annual temperature (°C)						Mean annual precipitation (mm)					
			1831-1900		1901-1989		1990-2100		1831-1900		1901-1989		1990-2100	
			Mean	SD	Mean	SD	Mean	SD	Mean	SD	Mean	SD	Mean	SD
1	SWEDEN	1	-2.8	.94	-2.5	1.00	0.1	1.33	534.2	90.96	550.8	65.74	619.6	95.01
2	SWEDEN	2	1.8	.54	1.7	1.02	4.8	1.32	654.7	105.58	596.1	88.12	758.4	159.18
3	DENMARK	3	7.6	0.71	7.8	0.77	10.9	1.61	554.2	76.58	574.7	77.26	667.1	99.90
	SCOTLAND	4	7.2	1.07	7.6	0.48	10.9	1.94	1198.7	157.35	1264.9	114.53	1389.	191.46
	FRANCE	5	10.8	0.68	11.1	0.58	14.3	1.84	626.7	53.81	618.6	116.92	730.4	75.63
4	Northern POLAND	6	8.2	0.82	8.1	0.89	11.3	1.55	526.0	47.37	536.4	78.67	559.7	52.06
	South-West POLAND	7	8.3	0.87	8.6	0.78	11.7	1.79	655.8	75.24	655.4	89.50	750.0	94.55
	AUSTRIA	8-lo	8.2	1.03	8.4	0.68	11.8	1.93	1014.4	134.37	990.8	118.79	1120.2	142.05
	AUSTRIA	8-med	6.7	1.34	7.1	0.66	10.3	2.08	1501.0	259.03	1573.7	443.54	1632.4	276.44
	SWITZERLAND	8-hi	5.1	1.34	5.5	0.65	8.7	2.08	1481.2	257.98	1503.9	144.18	1614.9	278.72
	SLOVAKIA	9	6.2	0.96	6.4	0.69	9.8	1.83	883.3	100.17	887.9	80.85	1012.2	122.93
	ROMANIA	10	8.0	0.85	8.0	0.71	11.2	1.54	592.5	52.95	595.5	79.10	646.1	60.89
5	Northern ITALY	11-hi	8.8	0.86	8.5	0.68	11.3	1.33	1127.9	231.34	1185.9	146.72	1276.4	234.86
	Northern ITALY	11-lo	12.8	0.84	12.6	0.54	15.6	1.47	780.8	78.20	806.6	150.29	881.9	97.73
	Southern ITALY	12-hi	9.4	1.65	9.4	0.47	12.7	2.06	813.1	85.21	842.3	109.30	919.1	114.71
	Southern ITALY	12-lo	13.9	1.65	14.0	0.51	17.2	2.06	625.8	65.19	654.5	83.50	719.2	97.64
	Northern SPAIN	13-hi	9.6	1.56	9.5	0.63	12.8	1.97	802.3	82.20	804.3	84.86	881.5	102.14
	Northern SPAIN	13-lo	10.5	1.56	10.5	0.64	13.7	1.97	513.7	54.58	509.9	83.43	565.3	66.12
	Southern SPAIN	14	14.3	0.86	14.9	0.56	18.0	1.91	455.4	40.27	493.9	103.96	576.8	79.57

According to the future trends in temperature and precipitation water stress desribed as the ratio between actual and potential evapotranspiration is decreasing in winter time and slightly increasing during summer (Figure 6.7). In many cases values also indicating higher water stress in the 19th than in the 20th century (see also Figure 6.5 and Table 6.2). Higher temperatures in the 20th century seem to be overcompensated by higher precipitation in this time. But it is not clear if this results are climate trends or model artefacts.

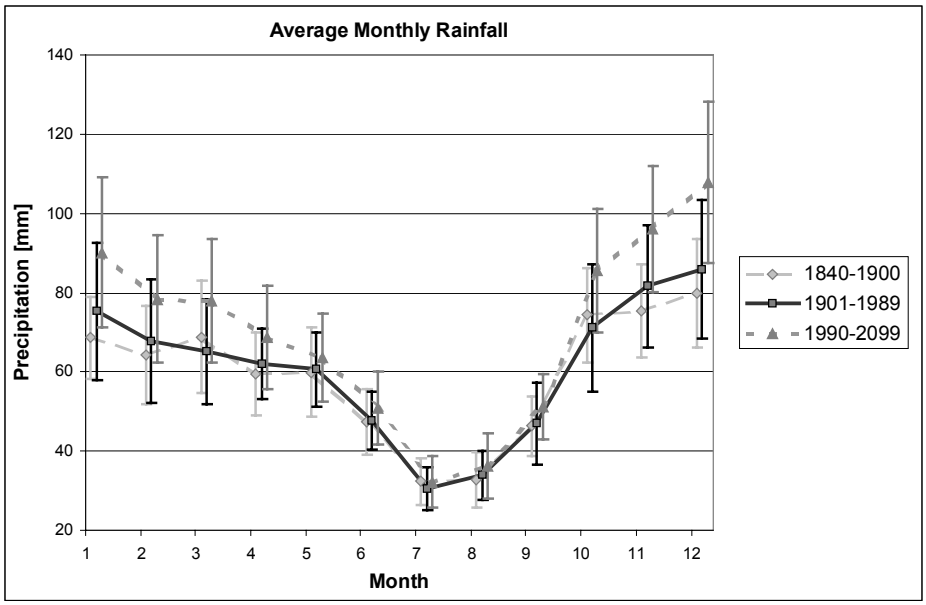

Figure 6.6: Average monthly rainfall for three different time slices (CRU 1901-1989, GCM 1840-1900 and 1990-2099) in the mediterranean area

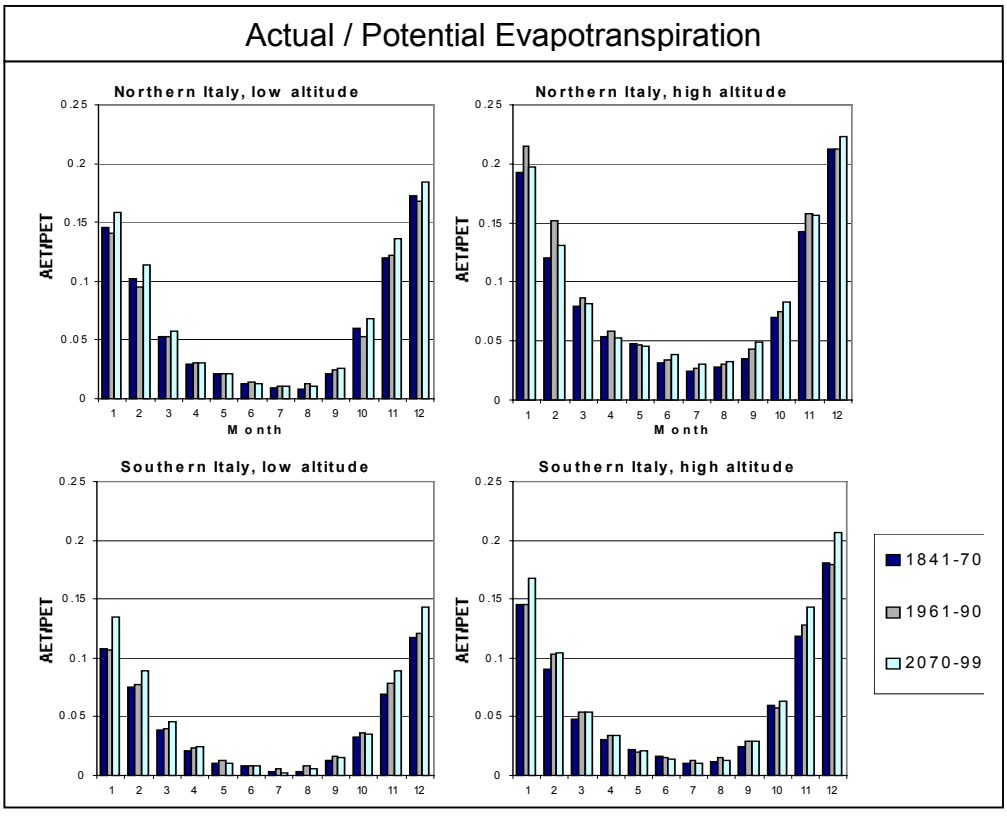

Figure 6.7: Relation of AET / PET (actual to potential evapotranspiration) at two representative sites (northern Italy, 11 and southern Italy, 12 with two different levels of elevation) and for three different time slices (CRU 1901-1989, GCM 1840-1900 and 1990-2099). Values are calculated with the bioclimatic module of the BIOME model (Sykes et al. 1996).

Disaggregation of monthly climate to daily weather data leads to some shifts in the time series (Table 6.3). Temperatures are slightly over estimated, precipitation and humidity are underestimated by the disaggregation scheme. Higher errors in mean temperature may be due to the lack of mean temperatures in the GCM data and the providing of daily temperature range instead of minimum and maximum temperatures in the CRU data set (see Figure 6.3). Therefore asymmetries between minimum, maximum and mean temperature are not included in the monthly climate data but are reproduced with the weather generator by the fitting procedure with measured station data.

Table 6.3: Mean error between monthly climate and disaggregated daily weather data at the representative sites for the years 1831-2100

	Mean Error (%)	Std. Dev.
Minimum Temperature	1.89	4.047
Mean Temperature	3.13	3.743
Maximum Temperature	1.82	2.448
Precipitation	-5.49	2.762

The missing of extreme rainfall events partly eliminated by temporal and spatial averaging to monthly data in half degree or less resolution and the reproduction of such events out of these data may lead to the systematic underestimation in disaggregated rainfall patterns.

6.4 Conclusions

A method is presented here which makes it possible to generate long-term time series of weather out of present and projected climate data in any spatial resolution. Thin plate interpolation of climate data including elevation as independent input variable allows the spatial disaggregation of the data even in complex terrain. Mean values of climate data are reproduced with the disaggregation scheme of the weather generator quite well but because of this conservative approach future potential changes in extreme events can not be described with this method. Another disadvantage is the lack of spatial consistency in the daily weather due to the statistically randomly disaggregation of monthly data to daily values.

Concerning the rotation period of forest ecosystems and the interrelation between forest inventory data and climate which include several decades the use of long term historical climate data and transient scenario outputs seems to be more feasible than time - slice experiments which in most cases cover single decades only. The output of regional climate models in higher spatial resolution may provide spatial consistent data but results are only available for decades and quite often do not cover large regions like Euope. Further there are still unsolved problems in simulating surface climate with regional models as described in Christensen et al. (1997).

Future climate of the HadCM2 run project a significant increase in temperature and precipitation. In relation to other GCM outputs the scenario output which was used

for this study is in the range of the average climate change signal for the "business as usual" scenario IS92a (IPCC/DDC, 2000). So the scenario seems to represent the main climate trend which is plausible for the emission scenario and the state of the art in climate modelling. In contrast to most of the other GCM outputs an increase in precipitation in the mediterranean area is projected with this approach. The signal of the four HadCM2 "ensembles" deliver different outputs for this region (IPCC/DDC, 2000). Especially in the western part of the Iberian peninsula and in northern Italy increases in precipitation are partly projected by the GCM. Because only GCM - land pixels were available for the calculations data from the northern part of the mediterranean region was relatively more represented than data from central and southern mediterranean areas. As already mentioned before different reference periods (1931-60 instead of 1961-90 in the most other studies) and differences between simulated GCM and station data can in some cases lead to different results of future climate trends.

Because of the sensitivity of forest ecosystems to precipitation patterns and the uncertainties in GCM precipitation projections (Houghton et al 1996) further investigation should be carried out to improve our knowledge about forest ecosystem dynamics especially in the mediterranean area.

Acknowledgement:
The authors like to thank Mike Hume and David Viner from the Climate Research Unit, University of East Anglia, Norwich for providing the climate and GCM data and Gerd Bürger, PIK for making the weather generator available.

References

Angström A, 1924. Solar and terrestrial radiation; Quart. J. of Roy. Met.Soc. London **50:** 121.

Bürger G, 1997. On the disaggregation of climatological means and anomalies; *Climate Research* **8(3):** 183-194.

Christensen JH, Machenhauer B, Jones RG, Schär C, Ruti PM, Castro M, Visconti G, 1997. Validation of present-day regional climate simulation over Europe: LAM simulations with observed boundary conditions; *Climate Dynamics* **13**: 489-506.

CORINE (Coordination de l'information sur l'Einvironment), 1997. Technical and Methodological Guide for Updating CORINE Land Cover, EEA/JRC; Brussels.

ESA (European Space Agency), 1992. RemoteSensing Forest Map of Europe; ESA/ISY project report; ESTEC - European Space Research and Technology Centre; Noordwijk, The Netherlands.

ESRI, 1992. Arcworld, a comprehensive GIS database for use with ARC/INFO® and ArcView™; Environmental Systems Research Institute Inc. Redlands, CA.

FAO, 1994. Digitized Soil Map of the World. CD-Rom Version 3.0. Food and Agriculture Organisation of the United Nations, Rome.

Hastings DA, Dunbar PK, 1999. Global Land One-kilomater Base Elevation (GLOBE) Digital Elevation Model, Documentation, Vol.1; National Oceanic and Atmospheric Administration, Report 34; Boulder, Colorado.

Houghton JT, Meira Filho LG, Bruce J, Hoesung L, Callander BA, Haites E, Harris N, Maskell K, 1995. Climate change 1994. Radiative forcing of climate change and an evaluation of the IPCC IS92 emission scenarios. Cambridge, UK: Cambridge University Press. 339 p.

Hulme M, Conway D, Jones P D, Jiang T, Barrow E M, Turney C, 1995. Construction of a 1961-1990 European climatology for climate change modelling and impact applications; *International Journal of Climatology* **15**: 1333-1363.

Hutchinson MF, 1995. Interpolating mean rainfall using thin plate smoothing splines. *International Journal for Geographical Information Systems* **9(4):** 385-403.

IPCC/DDC, 2000. Intergovernmental Panel of Climate Change, Data Distribution Centre; Scenario Gateway: http://ipcc-ddc.cru.uea.ac.uk/cru_data/cru_index.html.
Jalas J, Suominen J, 1987a. Atlas Florae Europaeae I Cambridge University Press; 43pp.

Jalas J, Suominen J, 1987b. Atlas Florae Europaeae II Cambridge University Press; 124 pp.

Kimball JS, Running SW, Nemani R, 1997. An improved method for estimating surface humidity from daily minimum temperature; *Agricultural and Forest Meteorology* **85**: 87-98.

Mitchell, JFB, Johns TC, Gregory JM, Tett SFB, 1995: Climate response to increasing levels of greenhouse gases and sulphate aerosols; *Nature* **376**: 501-504.

New M, Hulme M, Jones P, 1998. Representing twentieth century space-time climate variability; II. Development of 1901-1996 monthly grids of terrestrial surface climate; Report; Climate Research Unit, Norwich.

Palz W, Greif J (Commission of the European Communities, Eds.), 1995. European Solar Radiation Atlas; Solar Radiation on Horizontal and Inclined Surfaces, 3rd edition; Springer Verlag Berlin, Heidelberg, New York 333 pp.

Prentice IC, Cramer W, Harrison SP, Leemans R, Monserud RA, Solomon AM, 1992. A global biome model based on plant physiology and dominance, soil properties and climate; *Journal of Biogeography* **19(2):** 117-134.

Sykes MT, Prentice IC, Cramer W, 1996. A bioclimatic model for the potential distributions of North European tree species under present and future climates; *Journal of Biogeography* **23(2):** 203-233.

Walter H, Breckle S-W, 1991. Ökologie der Erde Band 4 Gemäßigte und arktische Zonen außerhalb Euro-Nordasiens UTB Gustav Fischer Verlag Stuttgart.

7 Process-based model applications to sites and scenarios of climate change. Analysis of impacts of climate change on biological processes and species

7.1 Introduction

The general objective of this chapter is to present different process-based model results after their applications to different sites and Climate Change scenarios, which have been presented in chapter 6. Different models represent processes from different perspectives, as well as most of them integrate such processes in a different manner (See chapter 2 and 3). Furthermore, models were checked and tested in chapter 4. Now we aim to show how the models were applied and the main outcomes produced by them in framework of LTEEF developments, i.e. analysing the long-term effects of Climate Change on European forests. Some of the exercises have been performed, by paying more attention to specific biological processes, but all of them with the final goal of checking how Climate Change may affect carbon budgets and its dynamics.

7.2 Hydrall applications. climate change, growth processes and the interaction with age: the case of European pine species

F. Magnani & M. Borghetti

7.2.1 Response to climate and acclimation processes: the case of *Pinus sylvestris*

In this study the Hydrall model is used to to explain the geographic variability of Scost pine growth across Europe. The results will highlight the sensitivity of the species to key environmental parameters, laying the ground for the prediction of its response to future Climate Change.

The model has been parameterized for *P. sylvestris* and tested against growth and functional data corresponding to different conditions across Europe, then applied to simulate Scots pine growth along two regional transects and to explain yield differences commonly observed in the species range. These correspond to conditions of good nutrient availability, so as to be able to analyze the effects of climate alone.

.

Temperature and water availability are among the main limiting factors for plant growth on a regional scale. The sensitivity of model predictions to a temperature change of $\pm$ 2 °C and to a $\pm$ 10 % shift in precipitation has been therefore analyzed in detail (Table 7.1), taking the climate of Southeast England as a reference, so as to be able to interpret any differences observed along the European transects. Both height and total volume are negatively affected by a temperature change in either direction, but for

different reasons: warming, on the one hand, would beneficially affect canopy photosynthesis, but because of the direct effect on respiration a slight reduction in net primary production would be expected. Moreover, allocation to fine roots is predicted to increase under warmer conditions, leading to an overall reduction in aboveground increments. Colder conditions, on the other hand, would mainly result in lower gross primary production, whilst only marginal changes in respiration and carbon allocation are predicted. Starting from the relatively mild British conditions, precipitation changes are predicted to have a relatively minor effect on growth, mainly the result of a shift in the allocation pattern.

Table 7.1. *Sensitivity of selected growth variables to key environmental factors. Percentage changes in stand height (H) and total volume at 100 years (V_{tot}), average gross (GPP) and net primary production (NPP) and fraction allocated to fine root production (λ_r) as a result of imposed changes in air temperature and precipitation. Sensitivity S is defined as: $S = (O_1-O_0)/O_0$, where O_0 and O_1 are model output under reference and changed conditions.*

		H	V_{tot}	*GPP*	*NPP*	λ_r
		%	*%*	*%*	*%*	*%*
Temperature	+ 2 °C	-5.2	-6.7	3.2	-1.5	7.6
	- 2 °C	- 8.6	- 21.4	- 22.7	- 19.0	- 0.4
Precipitation	+ 10 %	1.0	1.5	- 0.4	- 0.6	- 3.1
	- 10 %	- 2.4	- 2.4	0.6	1.1	4.6

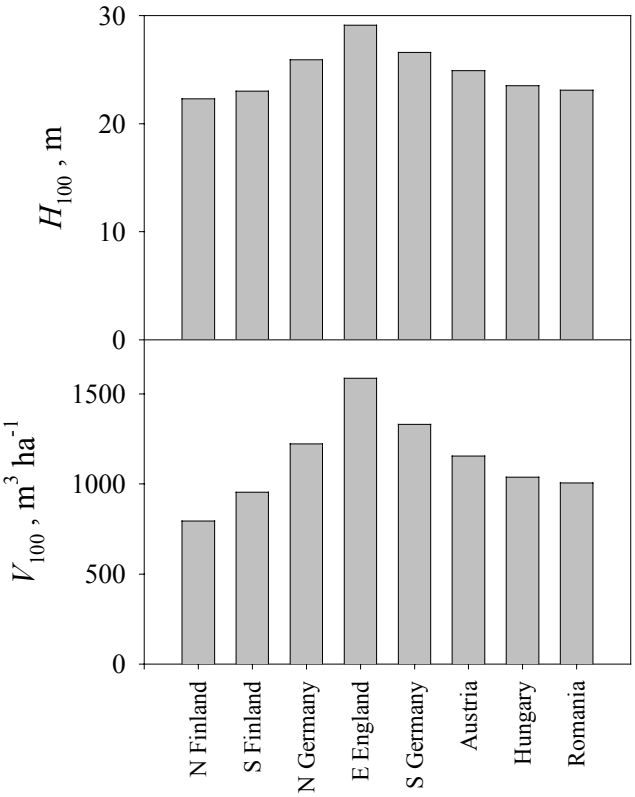

Fig. 7.1. Simulated height (H_{100}) and total volume at age 100 (V_{100}) for a range of sites along two latitudinal and longitudinal transects across Europe.

Moving from this general understanding, it is now possible to analyze the growth of Scots pine along two climatic gradients across Europe, spanning much of its natural range. Two regional transects have been identified, exploring a latitudinal gradient from Northern Finland to Southern Germany and a longitudinal one from the maritime climate of England to the more dry and continental climate of Rumania, at the south-eastern limit of the species range (Fig.7.1).

When values of stand height and total (standing plus self-thinned) volume after 100 years are compared, a rather clear picture emerges (Fig. 7.1), with a marked decline in final height and even more in total volume moving northwards and eastwards. The lowest volume increments are predicted at the northern limit of the range (50 % of the maximum, corresponding to Southeast England), while modelled values for Rumanian stands at the southeastern extreme are still 63 % of the maximum. Differences between sites are not limited to final values but involve the dynamics of height and volume growth (not shown).

The relationship between height and total volume increments is known to be rather constant at any particular site but quite variable at the regional scale, possibly as a result of climatic differences (Christie & Lines 1979). This variability is captured by the model: the slope of the relationship is highest at the most productive sites, since total volume production is more strongly reduced than height under limiting environmental conditions (Fig. 7.2).

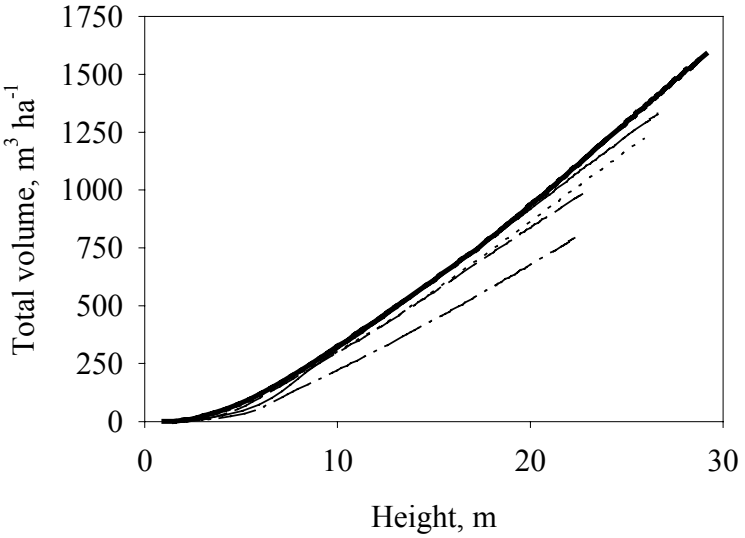

Fig. 7.2. Simulated total volume production-height curves for a range of sites across Europe. Results are reported for Southeast England (continuous thick), Northern Finland (dash-dot), Northern Germany (dotted), Southern Germany (continuous thin) and Rumania (dashed line).

Contrasting processes seem to be involved in the response of forest growth to limiting conditions under different climates, as shown in Fig. 7.3. When figures are normalized to optimum values, it can be seen that at the northern limit of the range the reduction in gross primary production (-53 %) exceeds the corresponding value for growth (-50 %; Fig. 7.2), as low temperatures also reduce the proportion of available carbon that is lost through respiration. The opposite is true at the dry limit of the range, where a 26% reduction in *GPP* translates in a 36 % decline in growth rates. In this case the discrepancy is the result not of respiration differences, but of greater belowground allocation (+ 13 %).

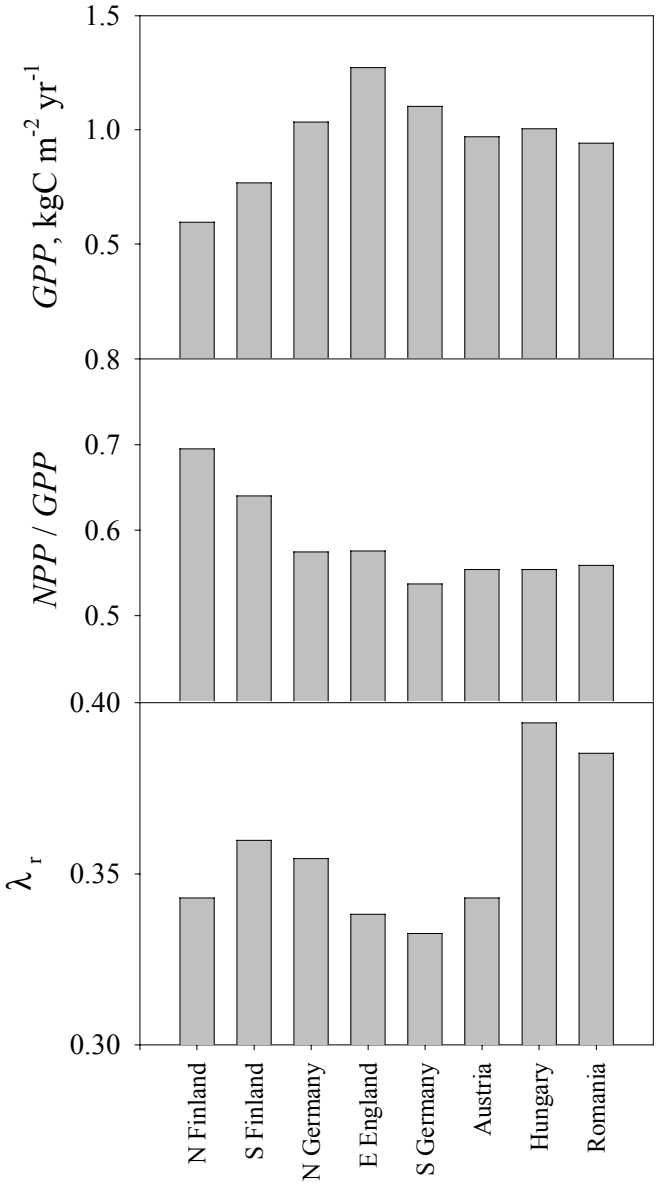

Fig. 7.3. Simulated determinants of stand growth for a range of sites along two latitudinal and longitudinal transects across Europe. Mean values over 100 years of stand gross primary production (GPP), the ratio between net- and gross primary production (NPP / GPP) and the fraction of growth allocated to fine root production (λ_r) are reported.

Scots pine seems to find near-optimal conditions in the English climate. It is therefore not surprising that, according to the sensitivity analysis reported in Table 7.1, growth would be reduced both by an increase and by a decrease in temperature, although by different mechanisms. Cold temperatures would mainly impair photosynthesis and net carbon exchange, whilst a climate warming would result in higher vapour pressure deficits, inducing higher transpiration rates and eventually resulting in a greater allocation belowground. This apparent sensitivity to water stress is confirmed by the response to changes in precipitation (Table 7.1) and is consistent with the conclusions by White (1982) that variations in *P. sylvestris* productivity in Great Britain are associated primarily with changes in solar radiation and soil water balance.

The predicted response to temperature, on the contrary, contradicts the suggestion by Cannell *et al.* (1989) that a 3 °C warming could result in a growth increase as high as 54% under British conditions. This prediction, however, was derived from an analysis of growth sensitivity to temperature under boreal conditions and the authors warned that the response to temperature could flatten off at a July temperature of 15 °C. Our results suggest that the relationship could be even reversed at higher temperatures.

A key role of low temperatures at the boreal (as well as at the altitudinal) limit (Grace 1988) and of water availability in the southern part of the range (Oberhuber, Stumböck & Kofler 1998) is confirmed by the site comparison across European transects. The sites considered encompass much of the natural range of the species in Western Europe (Boratynski 1991), covering a wide interval of latitude, temperature and water availability. Simulation results are in good agreement with the conclusions of Ineson *et al.* (1984), who studied the productivity of Scots pine across Europe. From a re-analysis of a data-set of 18 *P. sylvestris* stands throughout Europe (Cannell 1982) by principal component analysis (PCA), they found that almost 50% of the variability in productivity was explained by the first eigenvalue, related to temperature, whilst an additional 26% was associated to the second PCA axis, related to precipitation. Once referenced to the climate of Europe, their results show a good agreement with the pattern resulting from the present study.

The results are only partly confirmed, on the contrary, by the review of *P. sylvestris* growth and yield tables across Europe presented by Christie and Lines (1979): height increments are quite similar across most of the temperate zone, but markedly lower in the boreal zone. Even greater differences are observed when volume increments are considered. On the other hand, the growth decline at southern and eastern locations predicted by the model is not apparent in growth and yield tables. This probably stems from the fact that simulations always refer to lowland sites, whilst *P. sylvestris* in these regions is more commonly found (and generally planted) at higher elevations and under moister conditions. The delayed rise and subsequent fall of height and volume increments under more maritime conditions (Southeast England, Northern Germany) on the contrary, is confirmed by the results in Christie and Lines (1979). More simulations and experimental observations would be needed, however, to confirm this trend.

The use of a functional model makes it possible not only to predict, but also to understand the mechanisms behind such changes in forest productivity. Stand aboveground net primary production (and stand current annual increment, which is closely related to *ANPP*) is the result of three processes, acting in series: stand gross primary production (*GPP*) is reduced by respiration to net primary production (*NPP*) which is allocated above- and belowground. In mathematical terms:

$$ANPP = GPP \cdot \frac{NPP}{GPP} \cdot (1 - \lambda_r)$$

where λ_r represents the fraction of *NPP* allocated belowground. The three component factors in which productivity has so been partitioned are affected in different ways by climatic conditions across Europe, as visualized in Fig. 7.3. Gross primary production is reduced below its maximum value, corresponding to the British site, because of low temperatures and a short vegetative period, on the one hand, and of low air and soil humidity (as captured by the increasing *PET* / *P* values in Table 7.1) on the other. The ratio between net and gross net primary production, in turn, is quite constant across all of the temperate region and only increases in the boreal zone, reflecting the pattern of annual mean temperature. Under dry conditions, on the contrary, aboveground productivity is most seriously hampered by the need to allocate increasing amounts of resources to fine root production and maintenance.

The potential relevance of tree structural acclimation for forest growth under dry conditions has already been stressed by Berninger and Nikinmaa (1997), who considered in their simulations only potential changes in foliage-to-sapwood area ratio. In analogy with Hydrall predictions, they suggested that a strong reduction in volume increments at the southern limit can only be explained by climate-induced changes in tree functional structure. An additional increase in carbon allocation belowground, as predicted by the Hydrall model, could have even more important effects, because of the fast turnover rate of fine roots (Persson 1980; Schoettle & Fahey 1994).

Such changes in allocation, however, although of utmost importance under dry conditions, have only a minor and not so clear effect when other climates are considered. This explains why they have been generally neglected in forest growth models, traditionally applied to boreal or temperate moist conditions (Ågren *et al.*1991; Breymeyer *et al.* 1996). Explicit consideration of structural acclimation, on the other hand, appears to extend the generality of the Hydrall model to a wider range of environments.

How general is the model, anyhow? Two important questions remain unanswered. First of all, it remains to be ascertained whether an optimal functional structure is achieved through long-term adaptation or medium-term acclimation. In other words, have local provenances tuned their structure to long-term local climatic conditions, or has the species evolved a strategy of constant adjustment to a variable climate? In the first case, any provenance should be viewed as an ecotype, that would fail to accomodate to any future changes, and model generality would be limited to geographic comparisons, but would not extend in time (Berninger & Nikinmaa 1997). Much available experimental evidence (Mencuccini & Grace 1995; Axelsson & Axelsson 1986) suggests that

acclimation is at work, on the contrary, implying that evolution under ever-changing environmental conditions has resulted in an optimal strategy of structural adjustment. The results of Palmroth *et al.* (1999), on the other hand, seem to point in the opposite direction. Moreover, it is well known from provenance trials that a considerable proportion of the variability in productivity across the range of the species is the result of long-term genetic differentiation (Giertych 1991).

On the other end of the spectrum, it has to be seen to what extent the conclusions reached for *P. sylvestris* also apply to other species and functional types. In this view, it is interesting to note that the pattern of forest productivity predicted by the Hydrall model mirrors the results for Europe of the empirical model of Paterson (1956), who correlated maximum forest productivity for a large number of species with summary climatic statistics. This seems to suggest that, irrespective of the species considered, the same basic processes are at work in determining the response to climate of forest ecosystems.

7.2.2 The impact of climate change and the interaction with age: the case of pine species with a special look to the effect in the Mediterranean region

In this study the Hydrall model is used to simulate the potential effect of climate change on forest stands at a numer of representative sites in Europe under climate change scenarios; sites and scenarios were according to the LTEEF procedure described elsewhere. The effects are expressed considering the impact on current annual increment (CAI), which is one of the most important growth measurements to forestry, and on standing volume.

We first pay attention to the interaction of climate change with age. In Fig. 7.4 the synchronic pattern of current annual increment at two sites in Europe is presented, where by synchronous we mean a snapshot of the CAI of stands of different age at a given time.

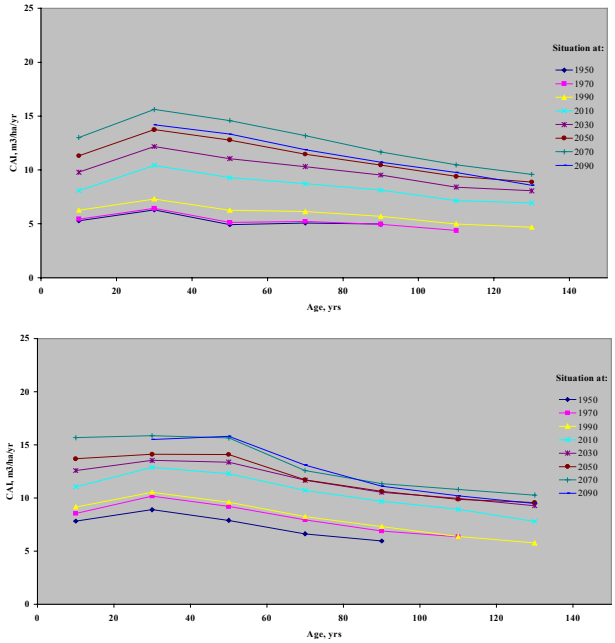

Fig.7.4. Synchronic pattern of current annual increment at two sites in Europe under Climate Change scenarios: above, the case of Pinus silvestris in Finland; below, the case of Pinus halepensis in Spain.

In Fig. 7.5, on the other hand, the development of CAI over time for individual stands is shown.

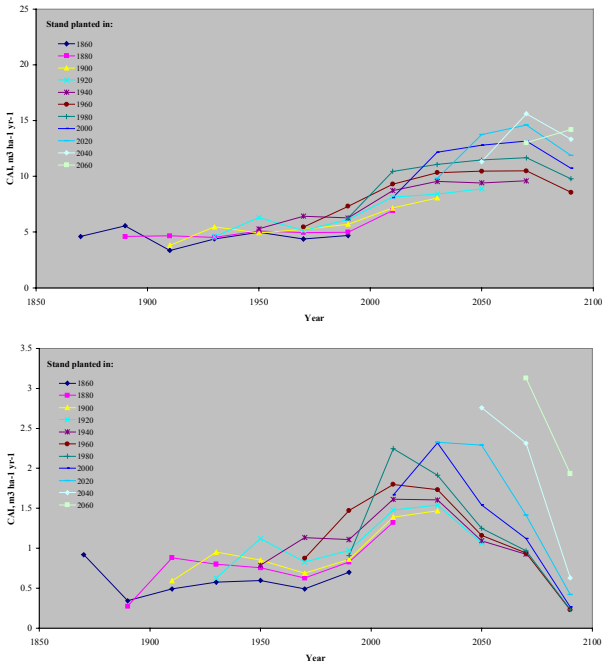

Fig.7.5. Temporal development of current annual increment at two sites in Europe under Climate Change scenarios: above, the case of Pinus silvestris in Finland; below, the case of Pinus halepensis in Spain.

Overall, these simulations show that the age-related decline is shifted but maintained in the synchronic picture under climate change, but that if we consider an individual stand the effect of climate change (possibly resulting in the improvement of growth conditions) can overcome the age effect and we may also expect a growth increase at an old age.

A look at the geographic pattern of growth and climate change effects is presented in Fig. 6, where simulated maximum standing volume at a number of sites for *P. sylvestris*, *P. pinaster* and *P. halepensis* show that (a) under any conditions, growth is maximum at intermediate latitudes and (b) the effect of climate change is positive everywhere and maximum at the extremes of the range.

Much variability seems to exists under Mediterranean conditions, depending on site and species. A more detailed look at the Mediterranean region, using additional climate change scenarios for 10 locations in Italy, ranging from the thermo-Mediterranean to the oro-Mediterranean zone (sensu Quezel 1985), details such a variability: the positive impact of climate change is expected to increase with altitude (and latitude), presumably because here (a) temperature is already a limiting factor and (b) precipitation is enough to sustain the greater potential evapotranspiration under warmer conditions. On the contrary, no effect (or a small negative effect) is predicted under thermo-Mediterranean conditions, possibly for the opposite reasons (Fig. 7.7).

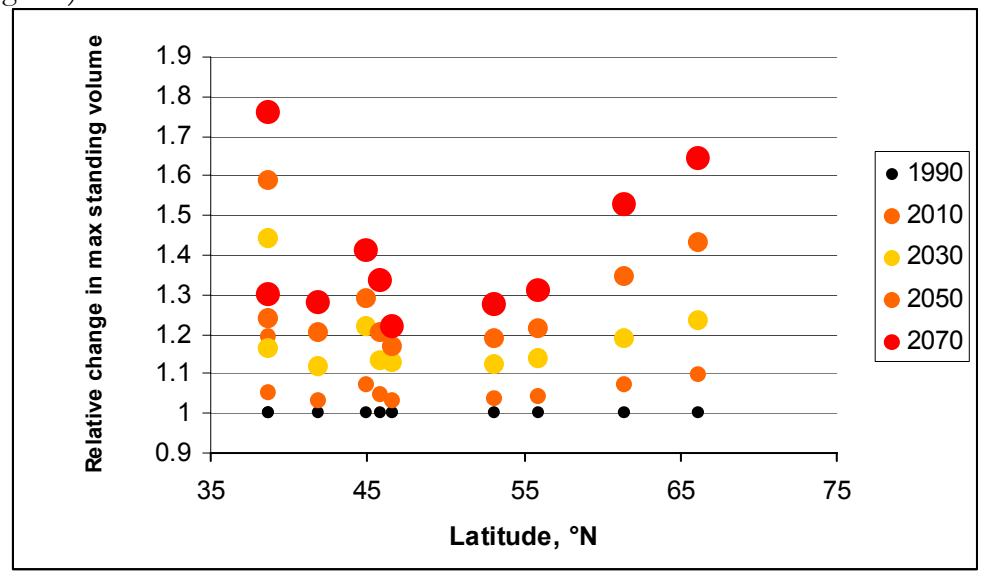

Fig.7.6. The effect of climate change on maximum standing volume (relative to 1990) varies with latitude.

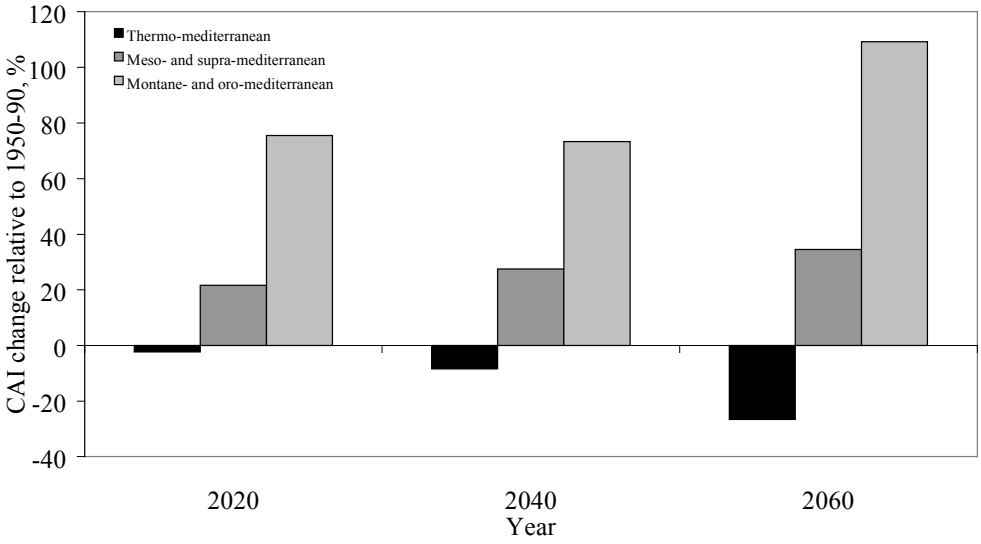

Fig. 7.7. The effect of Climate change on current annual increment of pine species in the different zones (sensu Quezel) of the Mediterranean region.

7.3 Forgro applications. An analysis of the importance of phenology and growing season length driven by climate change

K. Kramer & I. Leinonen

The aim of this study was to analyse the effects of climate change on growth of some European forest ecosystems of which either temperature regulates the phenology or water availability. The forest types represented include boreal Scots pine (*Pinus sylvestris* L.) and birch (*Betula pendula* Roth) forests in southern Sweden, and both monospecies and mixed-species temperate-zone deciduous forests of beech (*Fagus sylvatica* L.), oak (*Quercus robur, Q. petraea* L.), birch (*Betula pendula* Roth, *B. pubescens* Ehrh.) in The Netherlands and Germany.

The phenological models for boreal and temperate zone species were coupled to the process-based forest growth model FORGRO (Mohren 1987, 1994; Kramer 1995. See also Chapter 3). This approach allows evaluating the effects of climate change scenarios on growth of each of these forests. Here the results of this approach are outlined and the role of phenology discussed, whereas the validation of the models used is referenced.

7.3.1 Effects of increasing temperature on the length of the growing season in boreal trees

In the simulations for the boreal zone, climatic scenario data based on the output of HadCM2 climate model (Chapter 6), were used. The data covered the time period from year 1950 to 2100 and predicted the increase of annual average temperature by

approximately 2°C during this period. Two phenological models were utilized to predict the annual duration of the photosynthetically active period in deciduous trees and conifers. The effect of phenology on annual gross primary production (GPP) and net primary production (NPP) of a coniferous stand under the conditions of climatic warming was quantified with the aid of a process based forest growth model (FORGRO). Only the temperature effect was taken into account in the simulations, i.e. the direct effect of increased CO_2 concentration was excluded.

A model developed and parametrized to predict the timing of bud burst of birch (Häkkinen et al. 1998) was used to simulate the beginning of the photosynthetically active period in deciduous trees. In this model, the rate of spring bud development was dependent on air temperature according to a logistic function (Sarvas 1972). The model includes two parameters, namely the critical developmental stage when the bud burst occurs, and the calendar day when buds begin to respond to warm temperatures, both of which were estimated from long term phenological time series (Häkkinen et al. 1998).

The seasonal changes in the photosynthetic capacity of conifers were predicted by a temperature-based model, developed for Scots pine (Pelkonen and Hari 1980). The model predicts the alternation of the photosynthetic capacity between wintertime zero-level and maximum summertime level, and includes both the spring recovery and the autumn cessation.

In order to quantify the effects of annual variation in weather conditions and climatic warming in both deciduous trees and conifers, the amount of annual radiation available for photosynthetic production was calculated. The active photosynthetic period was determined in the case of deciduous trees to begin at the time of bud burst and end at a fixed calendar day, i.e. only the beginning of this period was affected by climatic conditions. In the case of conifers, the photosynthetic period included all days when the photosynthetic capacity was above the level of 50% from the maximum summertime level.

The annual amount of radiation available for photosynthetic production, as predicted by the two phenological models in the scenario climate, is presented in Figure 7.8. For comparison, the results are shown also in the case that a fixed calendar day is used for both the beginning and end of the photosynthetically active period. In cases where phenological models were applied, both strong annual variation and clear increasing long-term trend occurred in the amount of available radiation. The observed trend was solely determined by the effect of rising temperature, since no trend in the amount of total annual radiation is included in the scenario.

The results show also the relative difference in the temperature effect in two difference models. The pine model predicts stronger increase in the available radiation under the changing climatic conditions compared to the birch model. This is caused by the differences in the assumed environmental responses included in the models. In the case of pine, the spring photosynthetic recovery is assumed to be determined only by temperature, whereas in the bud burst model of birch, the

photoperiodic limitation in spring reduces the temperature effects. In addition, the active photosynthetic period in pine is prolonged also in autumn under warming climatic conditions, due to the delayed cessation of photosynthesis.

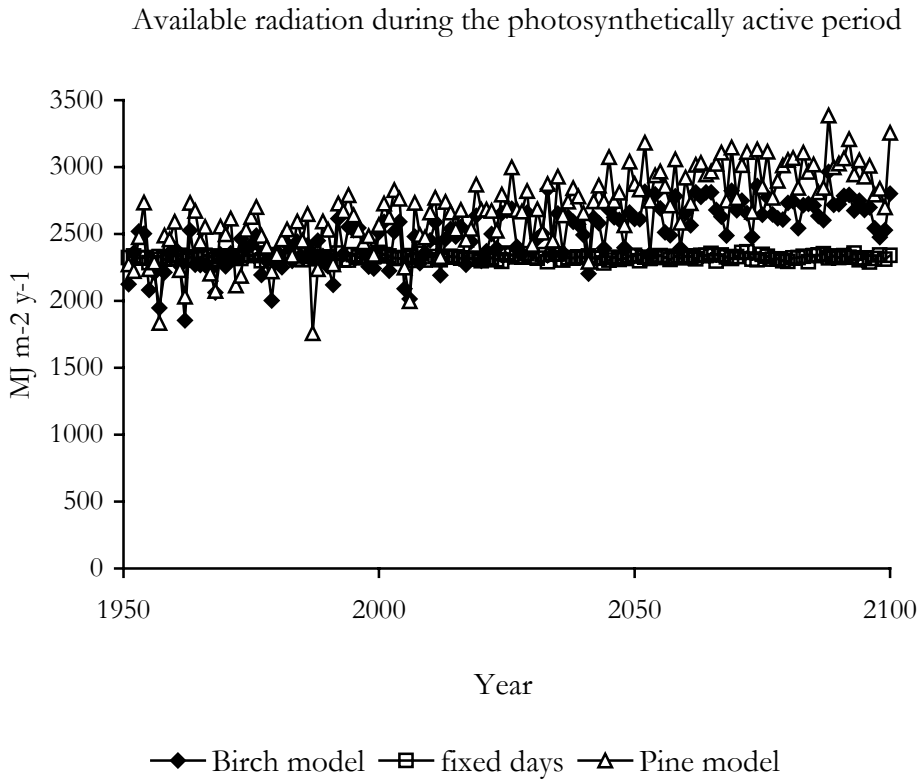

Figure 7.8 Model predicted annual available radiation for photosynthetic production under the scenario climate as affected by the timing of bud burst in deciduous trees (Birch model), beginning and cessation of the photosynthetically active period in conifers (Pine model) and constant duration of the photosynthetically active period (fixed days).

The FORGRO simulations consisted of three subsequent model runs, each covering a 50-year time period and applying same initial stand conditions. The seasonal changes in the photosynthetic capacity were included in the simulations by using the model of Pelkonen and Hari (1980) as a sub-model.

Figure 7.9 shows strong relationship between the duration of the photosynthetically active period and the GPP and NPP of a Scots pine stand, as predicted by the FORGRO model. This indicates that the temperature driven changes in the forest production under the conditions of climatic warming are mainly caused by phenological effects. In fact, according to the model predictions, the direct short-term temperature effects on the net photosynthesis during growing season are opposite, i.e. increased temperature usually causes decreased production due to the increased respiration.

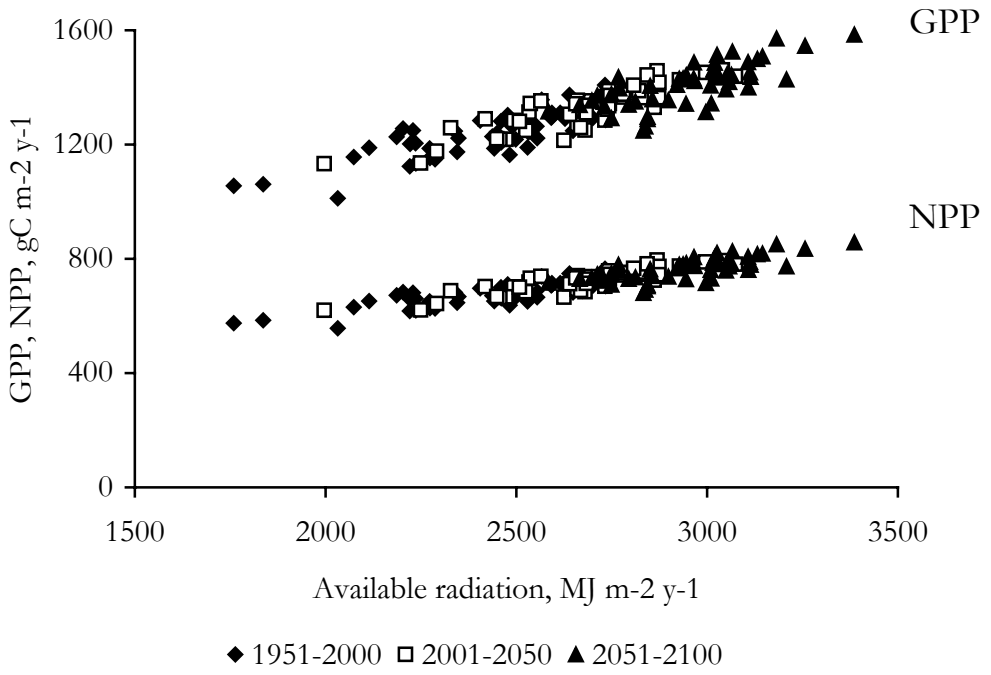

Figure 7.9 The relationship between the annual GPP and NPP, and the available radiation during the photosynthetically active period. Results from three simulation runs of the FORGRO model.

7.3.2 Temperate deciduous trees

For the simulations describing the phenology of temperate trees, a synthetic weather series was generated using the statistical model WGEN (Richardson and Wright 1984). 50 years of synthetic weather was generated with WGEN and taken as the current climate. Four transient scenarios were defined by superimposing on this series a linear increase in CO_2, temperature and precipitation, to occur in a time span of 50 years (Table 7.2).

Table 7.2 Climate change scenarios used in this study

No:	Linear increase over 50 years:	Range:
1	Reference	-
2	T	0 - 3°C
3	CO_2	350-500 μmol mol^{-1}
4	T + CO_2	
5	T + CO_2 + P	2) and 3) -15% precipitation

For deciduous trees in both the boreal and temperate zone include the timing of leaf unfolding and leaf fall. These moments determine the duration of the growing season and thereby the amount of radiation a tree may intercept for photosynthesis. Moreover, late spring frost may affect the duration of the growing season if leaf unfolding is too early to avoid these frosts. In the following the possible impacts of

increasing temperature of these characteristics will be analyses and their joint long-term effect on net primary production.

Table 7.3 presents the goodness of fit of the sequential model to 11 deciduous tree species in Europe. Generally, a good correspondence between observed and predicted response is found using the same phenological model.

Table 7.3. Variance of the timing of bud burst explained by the sequential model for The Netherlands (Nl) and Germany (G) (From Kramer 1994).

Species:	Country:	R^2:	Species:	Country:	R^2:
Larix decidua	G	0.73	*Quercus rubra*	Nl	0.87
Betula pubescens	Nl	0.86	*Quercus robur*	G	0.55
Betula pubescens	G	0.76	*Quercus robur*	Nl	0.82
Tilia platyphylla	G	0.78	*Fraxinus excelsior*	G	0.28
Fagus sylvatica	Nl	0.68	*Quercus petraea*	Nl	0.70
Fagus sylvatica	G	0.49	*Picea abies*	G	0.41
Tilia cordata	G	0.58	*Pinus sylvestris*	G	0.33

Based on a statistical analysis of the data set, there appeared to be three types of phenological response of the duration of the growing season to an increase in temperature: *(i)* unchanged, because the date of leaf unfolding advanced to a similar degree as the day of leaf fall; *(ii)* increased because the date of leaf unfolding advanced more than the date of leaf fall; and *(iii)* reduced, because the date of leaf fall advanced more than the date of leaf unfolding (Table 7.4). These three types of phenological response are represented by *Betula, Fagus,* and *Quercus*, respectively. In the following, these genus names will be used to represent the phenological response types for temperature driven phenology of temperate zone deciduous trees.

Table 7.4 Phenological characteristics of Betula, Fagus, and Quercus. U, average date of leaf unfolding based on a statistical analysis of the response of phenological events to temperature (Kramer 1994); U: date of leaf unfolding; F: date of leaf fall; P_0: probability of sub-zero temperature in a symmetric 11-day period around the date of leaf unfolding. U/T_w: change in date of leaf unfolding with mean winter temperature (d °C^{-1}. T_w: 1 November until leaf unfolding); F/T_s: change in date of leaf fall with mean summer temperature (d °C^{-1}. T_s: 1 May until leaf fall)

	Betula	*Fagus*	*Quercus*
U	22 April	1 May	6 May
F	4 October	16 October	20 October
P_0	0.58	0.37	0.18
U/T_w	-3	-2	-2
F/T_s	-3	0	-5

Consequently, both the probability of frost damage just before or after leaf unfolding Figure 7.10A and the amount of radiation available during the growing season (Figure 7.10B) of these phenological response types is affected differently by an increase in temperature. *Betula* has the highest probability of frost occurring around leaf unfolding as it has the earliest date of bud burst of the three phenological response types (Table 10.4). However, the available light during the growing season is not affected very much by temperature as leaf fall advances to a similar degree with an increase in temperature as leaf unfolding. *Quercus* has the lowest probability of

frost around bud burst (Table 10.4) but the available light during the growing season decreases with increasing temperature as leaf fall advances more with temperature than leaf unfolding. *Fagus* takes an intermediate position with the occurrence of frost around leaf unfolding, but takes much more advantage of the available light as leaf unfolding is advanced, but leaf fall is unaffected with increasing temperature.

Figure 7.11 presents the effects of a doubling of the atmospheric CO_2 concentration on the net primary production of the three phenological response types *Betula, Fagus* and *Quercus* as projected by the forest growth model FORGRO. These results show that for monospecies stands the effect of climatic warming and increased atmospheric CO_2 concentration does not lead to strong differences between the species. There is a general decline in NPP because the model predicts that respiration increases more strongly with temperature than photosynthesis. However, for mixed species stands the results indicate that global change will have a strong impact on the outcome of competition for light and thereby growth between the phenological response types. This is the consequence of differences in the probability of frost damage and amounts of radiation available during the growing season. In the long run this could have effects on the species composition of temperate-zone deciduous forests and the geographical distribution of species. These results were reproduced with another process-based model that includes forest dynamics. See for details of this study Kramer et al. (1996).

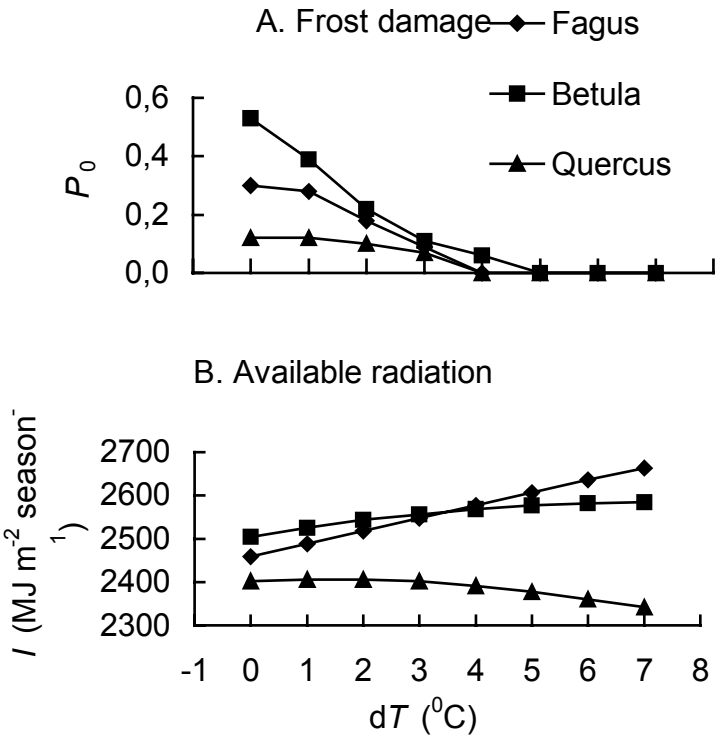

Figure 7.10 Effect of an increase of temperature on A. the probability of frost damage, and B. the available radiation during the growing season of three deciduous phenological response types.

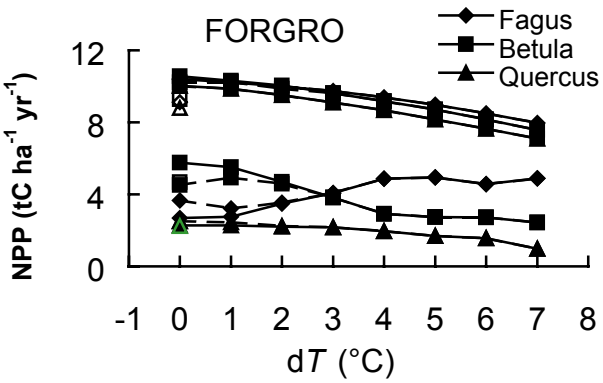

Figure 7.11 Effects of phenology on net primary production (NPP) in managed stands of three phenological types of temperate-zone deciduous forests, as predicted by the forest growth model FORGRO. *Upper lines: mono-species stand, lower lines: mixed-species stand. Open symbols: reference scenario (ambient CO_2 concentration of 350 ppm), closed symbols: doubled CO_2 concentration (700 ppm). Broken lines: including effects of frost damage, continuous lines: without the effects of frost damage.*

7.3.3 Discussion and conclusions

The functioning of trees is closely adapted to their local climate. Two modes of adaptation can be distinguished: *survival adaptation*, which consider the tree's features to survive unfavourable circumstances and *capacity adaptation*, which are the features enabling the tree to use available resources effectively (Hänninen 1990). Phenology is an important feature for both types of adaptation as is marks the shift from a dormant, resistant, stage to an active, but more vulnerable stage to adverse environmental conditions. If a rapid climate change would occur during the coming century, thus within the life of currently living trees, then these individuals may be less adapted to the prevailing climate. Furthermore, if tree species respond differently to a climate change, then the competitive relationships between species will alter, and thereby on the long run the species composition of forests, and possibly the geographical ranges of species.

The modelling of the mechanisms involved in the functioning of trees is the only method available to gain some insight in what might happen in the near future. The climatic factors driving seasonal aspects of trees are not identical for the different regions in Europe, and therefore considerable differences between regions can be expected in the effects of climate change on forest ecosystems. In the boreal zone, seasonality in temperature affects the photosynthetic machinery of coniferous trees, which appears to play the most significant effect on productivity. A mechanistic description of the seasonal development of frost hardiness and the seasonal changes of the photosynthetic capacity are thus essential to make a climate change impact assessment for this region. In the temperate zone of Europe, temperature is also the main driving factor of seasonality, whereas severe frosts and severe water stress does not occur in this region. The timing of leaf unfolding and leaf fall of deciduous tree species are the most important phenological events, and directly affect the period in which light can be intercepted for growth. Forest ecosystems are usually composed

of a mixture of tree species in the temperate zone. The results indicate that even relatively small differences phenological response types may significantly affect the competitive outcome when grown in mixed stands.

It can be concluded that there are significant differences between tree species in their response to climate change, and that even small differences in the phenology between species can lead to rather large changes in growth when grown in mixed forests. The implications for practical management of forests, and in particular for mixed forests are difficult to assess as the outcome of competition between tree species depend on many often-local conditions. What can be said is that a climate change will result in a significant change of selection pressure, and that phenology is a major aspect of tree functioning that needs adjustment for a future climate. Therefore, to maintain current forest functions a sufficiently large variability both in species and in genotypes is essential to allow the forest to respond to a changing climate.

7.4 GOTILWA applications. Effects of climate change on growth of *Quercus ilex*, *Pinus halepensis*, *Pinus pinaster*, *Pinus sylvestris* and *Fagus sylvatica* forests in the Mediterranean region

S. Sabate, C. Gracia & A. Sanchez

7.4.1 Introduction

Focusing on eco-physiological forest functioning, at present production of Mediterranean forest ecosystems is highly constrained by water, and to a lesser extent by nutrients (N in siliceous soils -Mayor and Rodà, 1992, 1994; Sabaté and Gracia, 1994- and P in calcareous soils –Sardans, 1997-). Growth is not limited by a lack of radiation. Furthermore, an excessive summer radiation combined with drought increase water stress and forest fire occurrences. In order to assess Climate change impact on ecosystem physiology, it would be good to know whether drought episodes will occur more often in the future, as well as whether the forest ecosystems may overcome such conditions, combined with other factors such as increased temperatures and atmospheric [CO_2]. Additionally, forest management should be considered because it clearly interacts with the effects of climatic conditions on forests. The impact of extreme drought events may be reduced by forest management, as found by thinning experiments applied on holm oak forests (Gracia et al., 1999a). Thus, forest management strategies may play an important role to overcome new climatic conditions (see Lindner, 2000).

In this section, the process based forest growth model GOTILWA (see chapter 3) has been applied to different species, growing in the Mediterranean area, and taking into consideration the future scenarios provided in Chapter 6. The tree species considered are *Quercus ilex, Pinus halepensis, Pinus pinaster, Pinus sylvestris* and *Fagus sylvatica.* The effects of Climate change on growth of these species are analysed. The effects on final wood yield at the end of the management cycle length at different soil depths and

climate scenarios are also evaluated. The analysed simulation period covers 140 years (1961-2100).

7.4.2 Climate change scenarios and sites

Table 7.5. Locations where Climate change scenarios have been simulated and species likely to be affected according to their current presence in the area.

Country (site name)	Longitude	Latitude	Altitude (m)	Tree species
Italy (S11-hi)	7.25	44.75	1160	*Fagus sylvatica*
Italy (S12-hi)	13.25	42.25	1133	*Fagus sylvatica*
Italy (S12-lo)	16.25	40.75	437	*Quercus ilex*
Italy (Ginosa)	16.87	40.42	2	*Pinus halepensis*
Spain (S13-hi)	-3.75	41.75	917	*Pinus sylvestris*
Spain (Prades)	0.92	41.21	500	*Quercus ilex*
Spain (S14)	-4.25	38.25	643	*P. halepensis, P. pinaster, Q. ilex*

The present analysis is based on climate data and scenarios from seven sites (four in Italy and three in Spain) that were presented in Chapter 6. These sites have different environmental conditions resulting from a wide range of altitude, latitude, rainfall and temperature values within the area (see Table 7.5). In addition to the increase of atmospheric [CO_2], the general pattern climate scenarios provided shows an increase in temperature and rainfall over the period (1961-2100). In Table 7.6 averaged values of these variables for three sub-periods of ten years are shown to illustrate the magnitude of change of these environmental variables in the seven sites. The general tendency of these projected climates over time is a similar amount of rainfall compared to the current one in the sub-period (2040-2049) and afterwards a clear increase. Nevertheless, despite the later increase, in the middle sub-period rainfall has decreased at S11-hi and S13-hi with respect to current values. In all cases, temperature values show a sustained increasing tendency. In addition to climate scenarios, management scenarios (with management cycle lengths of 20, 40 years, and no intervention until the end of the period, 140 years) have been simulated with two soil depth conditions (20 and 40 cm of soil depth). The thinning was defined by leaving a number of stems density at a certain stand age (see Table 7.7). This was chosen to allow easier comparisons through time.

Table 7.6. Mean annual values of Atmospheric CO_2, temperature and rainfall, obtained from three 10 year periods throughout the whole 1961-2100 simulated period in each site. Mean annual values ± Standard Deviation. In brackets the ratio with respect to the current values (1990-1999).

	Period				
	1990-1999	2040-2049		2090-2099	
			ratio		Ratio
Ambient CO_2 (ppm)	360.1 ± 6.9	493.5 ± 9.4	(1.4)	679.2 ± 12.9	(1.9)
Italy (S11-hi)					
T (º C)	10.5±1.1	12.1±0.7	(1.2)	14.3±0.6	(1.4)
Rainfall (mm yr^{-1})	1109±314	996±238	(0.9)	1456±354	(1.3)
Italy (S12-hi)					
T (º C)	10.8±1.1	13.5±2.0	(1.2)	16.9±1.1	(1.6)
Rainfall (mm yr^{-1})	804±176	806±137	(1.0)	1143±254	(1.4)
Italy (S12-lo)					
T (º C)	15.6±1.1	18.3±2.0	(1.2)	21.7±1.1	(1.4)
Rainfall (mm yr^{-1})	621±135	619±116	(1.0)	902±188	(1.5)
Italy (Ginosa)					
T (º C)	18.2±1.1	21.0±2.0	(1.1)	24.5±1.2	(1.3)
Rainfall (mm yr^{-1})	614±128	616±121	(1.0)	894±182	(1.5)
Spain (S13-hi)					
T (º C)	12.4±0.9	14.9±1.7	(1.2)	17.9±4.4	(1.4)
Rainfall (mm yr^{-1})	509±134	472± 99	(0.9)	660±125	(1.3)
Spain (Prades)					
T (º C)	16.3±0.9	18.8±1.8	(1.2)	21.9±0.9	(1.3)
Rainfall (mm yr^{-1})	489±130	471± 99	(1.0)	639±122	(1.3)
Spain (S14)					
T (º C)	16.8±1.0	19.5±0.5	(1.2)	23.1±1.0	(1.4)
Rainfall (mm yr^{-1})	459±78	475±104	(1.0)	724±136	(1.6)

Table 7.7.Management criteria by fixing the stand density (stems ha^{-1}) at different stand ages (years) with the interventions (I) according to the performed Management Cycle (MC). Initial stem densities were 3000 stems ha^{-1} in Pinus stands and 8000 stems ha^{-1} in Fagus and Quercus stands.

	Standing trees left after I (stems ha^{-1})			
			Q. ilex and *F. sylvatica*	
Stand age when I (years)	*Pinus* sp.			
	MC of 20 yrs	MC of 40 yrs	MC of 20 yrs	MC of 40 yrs
20			6500	6500
30	2750	2750		
40			5500	
50	2250			
60			4500	4500
70	1750	1750		
80			3500	
90	1225			
100			2500	2500
110	750	750		
120			1500	
130	750			
140			750	750

7.4.3 Output

The model outputs of different biological processes were integrated on a yearly time step since the aim of this analysis is to look at long-term effects of Climate change. We focused the results on the following model outputs: projected Leaf Area Index (LAI, m^2 m^{-2}), Mean Leaf Life (MLL, years and days for evergreen and deciduous respectively), Gross Primary Production (GPP, Mg DW biomass ha^{-1} yr^{-1}), Net Primary Production (NPP, Mg DW biomass ha^{-1} yr^{-1}) i.e. net carbon assimilation rate per unit ground area, Wood Production (Wood P, Mg DW wood biomass ha^{-1}) i.e. the net carbon assimilation rate per unit of ground area allocated into wood and Final Wood Yield (FWY, Mg DW wood biomass ha^{-1}), i.e. the amount of aboveground wood biomass that would be harvested at the end of the simulated period (140 years) in different soil conditions and management criteria.

7.4.4 Results

7.4.4.1 Leaf compartment

The effects of climate change scenarios on the leaf compartment are presented in Table 7.8. Results of GOTILWA show that LAI may tend to increase favoured by the increase of atmospheric CO_2 concentration, particularly in sites where rainfall is relatively high. This tendency vanishes by reaching steady values or even lower values in warmer sites as is shown by Aleppo pine in S14 and Ginosa, where the higher temperatures occur. The increase in temperature strongly influences MLL. This effect is opposite in deciduous trees, i.e. beech, as compared to evergreen trees, for both Holm oak and pines. MLL of beech increases with climate change, i.e. leaf life-span and thus the duration of the growing season. This increase represents a decrease of the resting period, due mainly to an earlier leaf unfolding but also a delay of leaf fall. In S11-hi, the average values of beech leaf unfolding is reduced from the Julian day 74 (1990-1999 period, current) to 36 and 40 in the periods 2040-49 and 2090-99, respectively. Leaf fall is predicted to move from the Julian day 324 until 338 and 340 (period 2040-49 and 2090-99 respectively). In S12-hi, these values showed even more differences. Beech leaf unfolding in this site goes from the Julian day 42 (current) to 27 and 7 (period 2040-49 and 2090-99 respectively) and leaf fall from the Julian day 328 (current) to 348 and 359 (period 2040-49 and 2090-99 respectively).

On the other hand the increase in temperature has an opposite effect on evergreen species according to the model results. MLL of Holm oak and pine species is reduced in accordance with the projected increase in temperature at each site provided by climate scenarios. The increase of leaf biomass combined with the decrease of MLL signify that leaf biomass turnover is accelerated and thus the carbon invested into this compartment.

Table 7.8. Mean annual values of simulated Leaf Area Index (LAI) and Mean Leaf Life (MLL) obtained from three 10 year periods throughout the whole 1961-2100 simulated period in each site and soil depth of 40 cm. No management was applied. Mean annual values ± Standard Deviation. Ratio is with respect to the current values (1990-1999).

		1990-1999	2040-2049	ratio	2090-2099	ratio
Fagus sylvatica (S11-hi)						
LAI	(m2 m^{-2})	4.7±1.1	7.0±1.5	(1.5)	8.6±1.3	(1.8)
MLL	(days)	251±40	303±45	(1.2)	301±41	(1.2)
Fagus sylvatica (S12-hi)						
LAI	(m2 m^{-2})	4.7±1.5	6.8±1.3	(1.4)	8.8±0.9	(1.9)
MLL	(days)	287±58	323±38	(1.1)	353±25	(1.2)
Quercus ilex (S12-lo)						
LAI	(m2 m^{-2})	3.7±0.4	4.2±0.1	(1.1)	4.8±0.2	(1.3)
MLL	(year)	2.0±0.2	1.7±0.2	(0.8)	1.4±0.1	(0.7)
Quercus ilex (Prades)						
LAI	(m2 m^{-2})	3.5±0.3	4.1±0.1	(1.2)	4.6±0.1	(1.3)
MLL	(year)	2.0±0.2	1.7±0.1	(0.9)	1.4±0.1	(0.7)
Quercus ilex (S14)						
LAI	(m2 m^{-2})	3.1±0.2	4.3±0.1	(1.4)	4.9±0.2	(1.5)
MLL	(year)	1.8±0.2	1.5±0.1	(0.9)	1.3±0.1	(0.7)
Pinus pinaster (S14)						
LAI	(m2 m^{-2})	2.0±0.1	3.3±0.1	(1.7)	4.4±0.1	(2.2)
MLL	(year)	2.0±0.1	1.8±0.1	(0.9)	1.4±0.1	(0.7)
Pinus halepensis (S14)						
LAI	(m2 m^{-2})	3.2±0.3	5.5±0.2	(1.7)	5.3±0.2	(1.7)
MLL	(year)	2.8±0.2	2.4±0.1	(0.8)	1.8±0.2	(0.6)
Pinus halepensis (Ginosa)						
LAI	(m2 m^{-2})	4.4±0.3	4.1±0.2	(0.9)	3.9±0.2	(0.9)
MLL	(year)	2.5±0.3	2.1±0.3	(0.8)	1.5±0.1	(0.6)
Pinus sylvestris (S13-hi)						
LAI	(m2 m^{-2})	2.5±0.2	3.2±0.2	(1.3)	4.1±0.3	(1.7)
MLL	(year)	1.9±0.1	1.6±0.2	(0.8)	1.2±0.1	(0.6)

7.4.4.2 Production

The effects of climate change scenarios on production are presented in Table 7.9. In all sites and climate scenarios, species show an increase of GPP, NPP as well as in most of the cases of Wood P. These increased values are promoted by the positive effect of increased atmospheric [CO_2] but also influenced by temperature and rainfall. Rainfall tends to increase in most of the cases (see ratios inTable 7.6) so it is also contributing to the positive effect on production. This is not the case for Scots pine Wood P at S.13hi in the middle of the simulated period due to the decrease in rainfall at this time. Temperature increase has different consequences for production. In beech, the longer growing period favours higher production, particularly when water is not limiting. On the other hand, as mentioned above, holm oak and pines spent more carbon maintaining and producing the leaf compartment, given its increased turnover. Another consequence of temperature increase is higher respiration values. Nevertheless, the final balance of production–respiration appears positive according to these simulations.

Table 7.9. Mean annual values of simulated Gross Primary Production (GPP), Net Primary Production (NPP), Wood Production (Wood P) obtained from three 10 year periods throughout the whole 1961-2100 simulated period in each site. Soil depth: 40 cm. No management applied. Mean annual values ± Standard Deviation. Ratio is with respect to the current values (1990-1999).

	1990-1999	2040-2049		2090-2099	
	Mg ha^{-1} yr^{-1}	Mg ha^{-1} yr^{-1}	ratio	Mg ha^{-1} yr^{-1}	ratio
Fagus sylvatica (S11-hi)					
GPP	39.2±3.5	44.8±3.1	(1.1)	48.9±3.2	(1.2)
NPP	13.9±2.0	17.1±2.0	(1.2)	18.8±1.7	(1.4)
Wood P	0.4±0.5	1.1±1.2	(2.8)	2.1±1.5	(5.5)
Fagus sylvatica (S12-hi)					
GPP	35.1±6.6	49.4±6.8	(1.4)	61.5±2.8	(1.8)
NPP	12.1±4.5	17.9±4.4	(1.5)	21.2±3.6	(1.7)
Wood P	1.3±1.1	2.3±0.9	(1.8)	5.0±1.8	(4.0)
Quercus ilex (S12-lo)					
GPP	37.6±6.2	50.5±5.4	(1.3)	68.1±5.3	(1.8)
NPP	8.0±5.1	10.5±4.0	(1.3)	11.9±5.9	(1.5)
Wood P	2.3±1.1	3.1±1.7	(1.3)	2.5±1.9	(1.1)
Quercus ilex (Prades)					
GPP	39.8±7.2	53.3±6.7	(1.3)	73.0±5.7	(1.8)
NPP	10.2±5.5	11.4±5.1	(1.1)	15.5±5.6	(1.4)
Wood P	3.1±1.4	3.2±1.3	(1.0)	4.3±2.1	(1.4)
Quercus ilex (S14)					
GPP	32.0±4.0	51.0±3.5	(1.6)	68.3±1.6	(2.1)
NPP	9.1±4.1	12.1±4.0	(1.3)	12.9±3.8	(1.4)
Wood P	2.7±0.9	2.8±1.0	(1.1)	3.2±1.3	(1.2)
Pinus pinaster (S14)					
GPP	18.2±2.5	32.8±3.5	(1.8)	60.0±3.4	(3.3)
NPP	9.3±2.0	16.3±2.3	(1.7)	29.5±2.2	(3.2)
Wood P	3.3±1.1	5.8±1.6	(1.8)	8.8±2.1	(2.7)
Pinus halepensis (S14)					
GPP	21.2±3.1	45.6±2.9	(2.1)	57.7±1.8	(2.7)
NPP	7.5±2.7	14.1±2.5	(1.9)	15.8±3.2	(2.1)
Wood P	2.6±1.0	3.5±1.3	(1.3)	4.2±1.9	(1.6)
Pinus halepensis (Ginosa)					
GPP	27.6±3.6	37.3±3.5	(1.4)	49.7±2.8	(1.8)
NPP	5.5±2.6	10.3±2.5	(1.9)	12.4±3.1	(2.3)
Wood P	0.9±0.9	3.1±1.5	(3.6)	2.7±1.8	(3.1)
Pinus sylvestris (S13-hi)					
GPP	21.9±5.1	32.4±4.7	(1.5)	54.5±5.6	(2.5)
NPP	8.6±3.5	12.2±3.0	(1.4)	20.2±3.9	(2.3)
Wood P	2.4±1.6	2.3±1.55	(0.9)	5.0±2.3	(2.1)

7.4.4.3 Aboveground biomass

Figure 7.12 shows the evolution of aboveground biomass over the simulated period for the different species, and site conditions when no management is applied. Beech simulation results show the higher standing biomass. The sustained increase of standing biomass is in agreement with results of production discussed above. Standing biomass in site 12-hi, is favoured by the increased [CO_2] and temperature, as well as rainfall at the end of the period. The simulation at site 11-hi is slightly

different. In this case decreased rainfall in the middle of the simulated period constrains the increase of standing biomass during the second half of the period. Standing biomass of holm oak is clearly smaller than that of beech one. Holm oak forests are located in sites where rainfall distribution and amounts are typically Mediterranean and thus their growth is now constrained by water already. During the first half of the simulation, the driest site, S-14, supports a smaller amount of biomass. It is worth noting that the climate scenarios used for this species (S-12lo, S-14, and Prades) presented an extreme drought throughout 1980-90 that is clearly reflected by standing biomass. In this decade standing biomass reaches a relative plateau or even slight decreasing values due to tree mortality. Later on, oak standing biomass continues to grow in all cases, but this is sometimes reduced by tree mortality events. Oak standing biomass in site S14 becomes more similar to the other two sites because of the relative increase in rainfall. Current conditions strongly constrain growth there.

Looking at simulations for pine species (lower panel Fig. 7.12), Aleppo pine growth appears very constrained by climate change scenario in Ginosa. This site has the higher temperature values compared to the other sites and is the only place where simulation results give a reduction of LAI in addition to MLL. Therefore, it is not surprising that Aleppo pine standing biomass shows the lower values after half of the simulated period. Its biomass increase over the simulated period is very slow. In S14, aboveground biomass of Aleppo pine and Maritime pine show a similar plateau as mentioned above for Holm oak, but later on the increased improved effect of rainfall is reflected by sustained growth until the end of the simulation. Simulation results for Scots pine in S-13hi show an increase in standing biomass favoured by relatively lower temperatures than at the other sites.

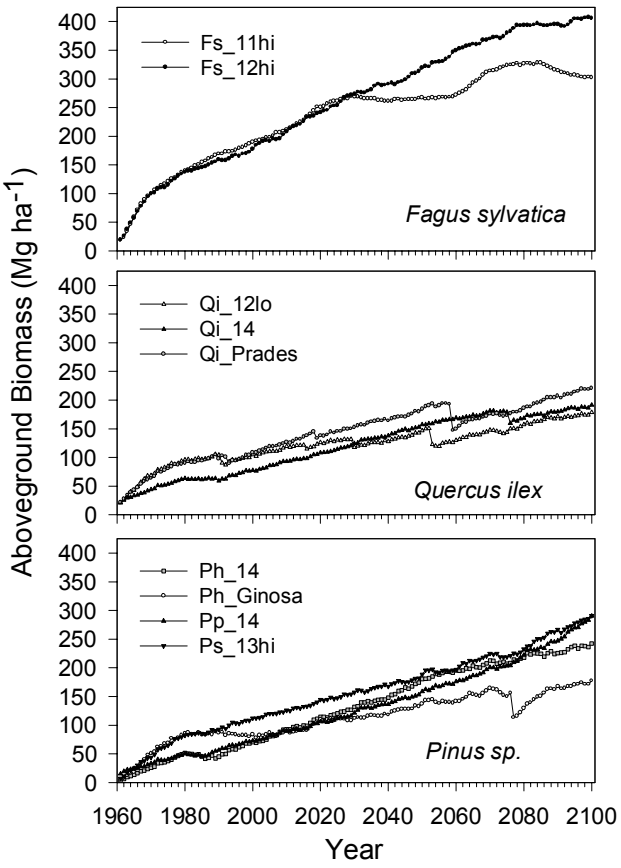

Figure 7.12 Standing aboveground biomass (Mg ha-1) over the simulated period 1961-2100 in different climates scenarios/sites and species (according to Tables 1 and 2). Soil depth 40 cm. No management applied. Upper panel shows Fagus sylvatica (Fs) in sites 11hi and 12hi, central panel shows Quercus ilex (Qi) in sites 12lo, 14 and Prades and lower panel shows Pinus sp. (Ph: Pinus halepensis, Pp: P. pinaster and Ps: P. sylvestris) in sites 13hi., 14 and Ginosa.

7.4.4.4 Management and soil depth analysis

The effect of management cycle length and soil depth on FWY is shown in Table 7.10. In general, as expected, increased soil depth results in increased FWY. An increase in soil depth represents in the present simulations an increase of soil water stored, and this larger amount of available water promotes higher transpiration and production rates. Nevertheless, sometimes deeper soils speed up growth and then competition. When this happens, a reduction of stored mobile carbon in larger trees may occur, and they may show slightly lower values of standing biomass in deeper soils at that moment. On the other hand, the shorter the management cycle length, the higher the FWY. By shortening the management cycle length, in the simulations most of the wood produced would be collected from the forest, otherwise part of this production may be decomposed on the site due to tree mortality. This mortality occurs after stressful periods, either because of high temperatures or drought.

Table 7.10. Simulated final wood yield (Mg ha^{-1}) after the 1961-2100 period, growing the forest at two soil depth (20 cm and 40 cm) and three management cycles (20 years, 40 years and no management until the end of the period: 140 years).

Site And tree species	Soil Depth (cm)	Management cycle (years) 20	40	140
		Final wood yield (Mg ha^{-1})		
Italy (S11-hi)	20	459	384	241
Fagus sylvatica	40	468	380	227
Italy (S12-hi)	20	503	426	290
Fagus sylvatica	40	600	449	305
Italy (S12-lo)	20	205	174	117
Quercus ilex	40	259	225	134
Spain (Prades)	20	249	238	161
Quercus ilex	40	298	270	166
Spain (S14)	20	224	197	134
Quercus ilex	40	243	212	143
Spain (S14)	20	236	155	197
Pinus pinaster	40	260	174	218
Spain (S14)	20	216	148	177
Pinus halepensis	40	245	170	182
Italy (Ginosa)	20	172	130	116
Pinus halepensis	40	202	143	133
Spain (S13-hi)	20	283	163	207
Pinus sylvestris	40	303	210	218

7.4.5 Discussion

The climate change scenarios analysed in these simulations have in general a positive effect on forest growth. It can be stated that this positive effect obtained by GOTILWA is explained by the increased atmospheric [CO_2] combined with the increase of rainfall amount in the area. Thus, according to the model results, both atmospheric [CO_2] and rainfall positive effects would be enough to compensate the increased respiration costs and the increased investment on leaves and fine roots turnover, driven by the projected rise of ambient temperature, providing that nutrients are available and do not limit tree growth. It is well known that temperature has a strong effect on plant respiration. Carey et al. (1997) did not find evidence of respiratory acclimation in arid zones. They suggested that the potential increases in aboveground carbon gain due to enhanced photosynthetic rates may be partially offset by increases in maintenance respiration in large trees growing in CO_2 enriched atmospheres but under predicted increases in temperature and aridity. Direct effects of rising atmospheric [CO_2] on down-regulating respiration rates are not included in this model analysis, but if they exist, they may be small (see Amthor, 2000).

The positive effects of increased atmospheric [CO_2] on growth has been found in experimental studies (e.g. Lin et al., 1999), and reported in some meta-analysis compilations (see Curtis and Wang, 1998; Medlyn et al., 1999). Curtis and Wang (1998) do not find consistent evidence of photosynthetic acclimation to CO_2 enrichment and no significant effect on stomatal conductance. Medlyn et al. (1999) found some evidence of down-regulation on photosynthesis, accounting for 10-20%

reduction, mainly explained by leaf nitrogen concentration decrease and its decreased use efficiency. Nevertheless the stimulatory effect of CO_2 enrichment was shown to be very important in any case. Looking at such long-term simulations, maybe nitrogen would play a more important role in the future by down-regulating the photosynthetic response of trees. Nevertheless, at present, nutrients do not limit growth (Mayor and Rodà, 1992) as water does in the Mediterranean region. Experimental work in controlled environment chambers have shown that positive effects on Holm oak growth promoted by increased [CO_2] tend to vanish when water stress is increased, or only it compensates the negative effects of increased water (López et al., 1997). Hence, rainfall regimes other than those obtained with the climate scenarios applied may alter the magnitude of the positive effects of climate change seen in the present exercise. It is important to note that no single climate change scenario for a site/area is likely to be definitive, and other situations may change completely the picture. Looking at our results, temperature and rainfall constrain growth within certain periods. If rainfall increases in the future, a positive effect on growth is very likely. Conversely, if rainfall amount decreases these positive effects of climate change on forest eco-physiological functioning may be offset or even become negative. Scots pine over a latitudinal gradient, which ranges from wet to dry climates, shows structural adaptations rather than water conservation strategies (Palmroth et al., 1999). This may mean that Scots pine trees currently living in the area, would simply acclimate their structure according to new climatic conditions, rather than promote more sparing water use. This result seems to mark a certain structural plasticity according to environmental conditions. On the other hand, the ability of plants to tolerate extremely high temperatures is remarkable, provided that adequate water is available (Kirschbaum, 2000). Thus, future rainfall patterns are crucial in assessing climate change induced stress and disturbance impact analyses. Furthermore, if temperature goes up, in the long-term its negative effects may not even be compensated by increases in rainfall and CO_2.

The increase in temperature promotes an increase in the duration of the growing season of beech forests and a decrease in leaf life-span for evergreen ones. The dramatic change in the duration of beech's growing season may be arguable, as there is no restriction applied to the plasticity of this species in the model. Previous analyses have shown that trees have certain amount of plasticity to accommodate such a change (Kramer, 1995). According to Kramer's analysis (Kramer, 1995, 1996) beech may advance its leaf unfolding, while leaf fall stays essentially the same. In S11-hi this advance accounts at the end of the simulation for slightly more than one month, and leaf fall is delayed around 15 days. S12-hi shows an even higher plasticity, that may need further checking with the model parameters and the genotypes living in this Southern European latitude. The pattern of these changes in leaf phenology of beech seems logical, but the absolute values themselves need further analysis. In relation to evergreen species, there is empirical evidence that Holm oak MLL lower values occur in warmer areas, as shown in the Iberic Peninsula (Gracia et al., unpublished data). If this reaction is accepted, it may lead to a larger investment of carbon allocation to the canopy with increasing temperatures, that would be more important when a larger amount of leaf biomass is sustained. Investment of primary production in leaf turnover represents an important proportion in Mediterranean

ecosystems. For instance, holm oak from Montseny (NE Spain) shows that litter fall accounts for about 57% of net primary production, and only 43% represents an increase in Biomass (Mayor and Rodà, 1994). Changes in a species' physiological behaviour may lead to a significant decline of some forests or of some particular species within forests (Kirschbaum, 2000).

Forest management strategies will play an important role in the future to achieve objectives such as maximising forest CO_2 uptake from the atmosphere. This is suggested by our results and other works (see Lindner, 2000). This author highlighted the influence of management strategies on forest growth, and the need to adapt management strategies to expected changes in climate. Furthermore, management may be very important to sustain Mediterranean forest ecosystems. It may reduce respiring biomass as well as it may increase the water available to each tree, so it is important to sustain forest ecosystems' functioning, especially to overcome severe periods of drought and high temperatures (Gracia et al., 1999b).

7.4.6 Conclusions

These simulations suggest that Mediterranean species may be positively affected by climate change if future conditions provide better conditions of rainfall than current ones. When this is not the case, the negative effect of the increase in temperature may be emphasised, and not compensated by the positive effects promoted by increasing atmospheric [CO_2]. Leaf phenology may be strongly modified by climate change (Kramer, 1995, see section above). Deciduous species may increase the duration of their growing season (beech in our analysis). Nevertheless, further analysis of the plasticity of such species is needed to evaluate the actual ability of living trees to modify their growth performance. It is also shown that evergreen trees will increase their turnover rate. Thus, it is important to pay closer attention to the effect of climate change on canopy functioning in terms of primary production invested in maintaining such a compartment, i.e. sustained leaf biomass and its turnover. New conditions may constrain the viability of some forest types if they need to invest too much carbon amounts in this compartment. Management would be a key tool to improve growth conditions, faced with unavoidable new climatic conditions.

7.5 References

Albrektson A. & Valinger E. (1985) Relations between tree height and diameter, productivity and allocation of growth in a Scots pine (Pinus sylvestris L.) sample tree material. In: *Crop Physiology of Forest Trees (eds. P.M.A. Tigerstedt, P. Puttonen & V. Koski),* pp. 95-105. University of Helsinki, Helsinki.

Amthor, J.S., 2000. Direct effect of elevated CO_2 on nocturnal *in situ* leaf respiration in nine temperate deciduous tree species is small. *Tree Physiology* **20**, 139-144.

Axelsson E. & Axelsson B. (1986) Changes in carbon allocation patterns in spruce and pine trees following irrigation and fertilization. *Tree Physiology* **2**, 189-204.

Berninger F. & Nikinmaa E. (1997) Implications of varying pipe model relationships on Scots pine growth in different climates. *Functional Ecology* **11**, 146-156.

Braekke F.H. (1995) Response of understorey vegetation and Scots pine root systems to fertilization at multiple deficiency stress. *Plant and Soil* 168-169, 179-185.

Cannell M.G.R. (1982) World Forest Biomass and Primary Production Data. Academic Press, New York.

Cannell M.G.R. & Dewar R.C. (1994) Carbon allocation in trees: a review of concepts for modelling. *Advances in Ecological Research* **25**, 50-104.

Cannell M.G.R., Grace J. & Booth A. (1989) Possible impacts of climate warming on trees and forests in the United Kingdom: a review. *Forestry* **62**, 337-364.

Carey, E.V., Callaway, R.M., DeLucia, E.H., 1997. Stem respiration of ponderosa pines grown in contrasting climates: implications for global change. *Oecologia* **111**, 19-25.

Christie J.M. & Lines R. (1979) A comparison of forest productivity in Britain and Europe in relation to climatic factors. *Forest Ecology and Management* **2**, 75-102.

Curtis, P.S., Wang, X., 1998. A meta-analysis of elevated CO_2 effects on woody plant mass, form, and physiology. *Oecologia* **113**, 299-313.

Edwards P.N. & Christie J.M. (1981) Yield Models for Forest Management. Forestry Commission Report No. 48

Gholz H.L., Linder S. & McMurtrie R.E. (1994) Environmental Constraints on the Structure and Productivity of Pine Forest Ecosystems: a Comparative Analysis. Vol. 43. *Ecological Bulletins*, Copenhagen.

Grace J. (1988) Temperature as a determinant of plant productivity. In Plants and Temperature (eds. S.P. Long & F.I. Woodward), pp. 91-107. *Society for Experimental Biology*, Great Britain.

Gracia, C.A., Sabaté, S., Martínez, J.M., Albeza, E., 1999. Functional Responses to thinning. In: Rodà, F., Retana, J., Gracia, C.A. and Bellot, J., (Eds.). Ecology of Mediterranean Evergreen Oak Forests. *Ecological Studies* **137**. Springer-Verlag, Berlin Heidelberg, pp 229-338.

Hänninen H (1990) Modelling bud dormancy release in trees from cool and temperate regions, *Acta Forestalia Fennica* **231**, 47 pp

Häkkinen R, Hari P (1988) The efficiency of time and temperature driven regulation principles in plants at the beginning of the active period. *Silva Fennica* **22**: 163-170

Häkkinen R, Linkosalo T, Hari P (1998) Effects of dormancy and environmental factors on timing of bud burst in Betula pendula. *Tree Physiol* **18**: 707-712

Helmisaari H.-S. & Siltala T. (1989) Variation in nutrient concentrations of Pinus sylvestris stems. *Scandinavian Journal of Forest Research* **4**, 443-451.

Ineson P., Jones H.F. & Heal O.W. (1984) Regional aspects of forests in Europe: a preliminary study of Pinus sylvestris. In *State and Change of Forest Ecosystems. Indicators in Current Research* (ed. G.I. Ågren), pp. 315-332. Swedish Univ. Agric. Sciences, Dept. Ecology & Environmental Research, Report No. 13.

Irvine J., Perks M.P., Magnani F. & Grace J. (1998) The response of Pinus sylvestris to drought: stomatal control of transpiration and hydraulic conductance. *Tree Physiology* **18**, 393-402.

Kirschbaum, M.U.F., 2000. Forest growth and species distribution in a changing climate. *Tree Physiology* **20**, 309-322.

Kramer K (1994a) Selecting a model to predict the onset of growth of Fagus sylvatica. *J Appl Ecol,* **31**: 172-181

Kramer K (1994b) 'A modelling analysis of the effects of climatic warming on the probability of spring frost damage to tree species in The Netherlands and Germany', Plant, *Cell and Environment,* **17**: 367-378

Kramer K (1995) Modelling comparison to evaluate the importance of phenology for the effects of climate change on growth of temperate-zone deciduous trees, *Clim Res,* **5**: 119-130

Kramer K, Friend AD and Leinonen I (1996) Modelling comparison to evaluate the importance of phenology for the effects of climate change in growth of mixed temperate-zone deciduous forests. *Clim Res,* **7**: 31-41

Kramer, K., 1995. Phenotypic plasticity of the phenology of seven European tree species in relation to climatic warming. *Plant Cell Environm.* **18**, 93-104.

Kramer, K., 1996. Phenology and growth of European trees in relation to climate change. Thesis, Wageningen Agricultural University, The Netherlands, 210 pp.

Lin, G., Adams, J., Farsnworth, B., Wei, Y., Marino, B.D.V., Berry, J.A., 1999. Ecosystem carbon exchange in two terrestrial ecosystem mesocosms under changing atmospheric CO_2 concentrations. *Oecologia* **119**, 97-108.

Lindner, M., 2000. Developing adaptive forest management strategies to cope with climate change. *Tree Physiology* **20**, 299-307.

López, B., Sabaté, S., Ruiz, I. and Gracia, C.A., 1997. Effects of elevated CO_2 and decreased water availability on holm-oak seedlings in controlled environment chambers. In: *Mohren, G.M.J., Kramer, K., Sabaté, S. (Eds.) Impacts of global change on tree physiology and forest ecosystems.* Kluwer Academic Publishers, Dordrecht The Netherlands. Forestry Sciences, 52, 125-133.

Magnani F., Borghetti M. & Grace J. (2000) Acclimation of coniferous tree structure to the environment under hydraulic constraints. In preparation.

Magnani F. & Grace J. (1999) On the causes of the age-related decline of forest growth. A meta-analysis of data from Pinus sylvestris L. Submitted to Trees.

Mayor, X., Rodà, F., 1992. Is primary production in holm oak forests nutrient limited?: A correlational approach. *Vegetatio* **99/100**, 209-217.

Mayor, X., Rodà, F., 1994. Effects of irrigation and fertilization on stem diameter growth in a Mediterranean holm oak forest. *For. Ecol. Manage.* **68**, 119-126.

Medlyn, B.E, Badeck, F.W., De Pury, D.G.G., Barton, C.V.M., Broadmeadow, M., Ceulemans, R, De Angelis, P., Forstreuter, M., Jach, M.E., Kellomaki, S., Laitat, E., Marek, M.,Philippot, S., Rey, A., Strassemeyer, J., Laitinen, K., Liozon, R., Portier, B., Roberntz, P., Wang, K., Jarvis, P., 1999. Effects of elevated $[CO_2]$ on photosynthesis in European forest species: a meta-analysis of model parameters. *Plant Cell Environm.* **22**, 1475-1495.

Mencuccini M. & Grace J. (1995) Climate influences the leaf area-sapwood area ratio in Scots pine. *Tree Physiology* **15**, 1-10.

Mencuccini M. & Grace J. (1996a) Developmental patterns of aboveground xylem conductance in a Scots pine (Pinus sylvestris L.) age sequence. *Plant Cell and Environment* **19**, 939-948.

Mencuccini M. & Grace J. (1996b) Hydraulic conductance, light interception and needle nutrient concentration in Scots pine stands and their relations with net primary productivity. *Tree Physiology* **16**, 459-468.

Mohren GMJ (1987) Simulation of forest growth, applied to Douglas fir stands in The Netherlands, Thesis, Agricultural University Wageningen, The Netherlands, 184 pp

Oberhuber W., Stumböck M. & Kofler W. (1998) Climate-tree-growth relationships of Scots pine stands (Pinus sylvestris L.) exposed to soil dryness. *Trees* **13**, 19-27.

Ovington J.D. (1957) Dry-matter production by Pinus sylvestris L. *Annals of Botany* **21**, 287-314.

Palmroth S., Berninger F., Nikinmaa E., Lloyd J., Pulkkinen P. & Hari P. (1999) No water conserving behaviour is observed in Scots pine from wet to dry climates. Oecologia, in press.

Palmroth, S., Berninger, F., Nikinmaa, E., Lloyd, J., Pulkkinen, P. and Hari, P., 1999. Structural adaptation rather than water conservation was observed in Scots pine over a range of wet to dry climates. *Oecologia* **121**, 302-309.

Pelkonen P and Hari P (1980) The dependence of the springtime recovery of CO2 uptake in Scots pine on temperature and internal factors. *Flora*, **169**: 398-404

Persson H. (1980) Death and replacement of fine roots in a mature Scots pine stand. *Ecological Bulletins* **32**, 251-260.

Quézel, P. (1985) Definition of the Mediterranean region and origin of its flora. In: *Gomez-Campo, C., (Ed.), Plant conservation in the Mediterranean Area.* W. Junk, Dordrecht, pp. 9-24.

Richardson CW and Wright DA (1984) WGEN: a model for generating daily weather variables, U.S. Department for Agriculture, Agricultural Research Service, ARS-8, pp 5-15

Sabaté, S., Gracia, C., 1994. Canopy nutrient content of a *Quercus ilex* L. forest: Fertilization and irrigation effects. *For Ecol Manage* **68**:31-37.

Sardans, J., 1997. Resposta de quatre espècies llenyoses mediterrànies a diferent disponibilitat d'aigua i nutrients. Ph D thesis, Autonomous University of Barcelona, Bellaterra.

Sarvas R (1972) Investigations on the annual cycle of development of forest trees. Active period. *Commun Inst For Fenn* **76(3):** 1-110

8 Regional impact assessment

Three regions have been characterised within LTEEF project framework: Boreal, Temperate and Mediterranean. The impacts of climate change are likely to differ between regions. Expected regional differences in climate change over Europe may come out because growth of the forest types occurring in these regions differ in their control by climatic factors (e.g. temperature in the North of Europe; water availability in the South). Thus, for each region a limited number of forest types have been characterised by the main tree species and the driving climatic factors on forest growth (corresponding to the main forest types as used in national forest inventories in the region). Process-based models for each region were calibrated and tested for these representative forest types (see Chapter 4), and subsequently used for the evaluation of forest growth and responses to climate change (see Chapter 7).

The aim of this chapter is to present a synthesis on the effects of environmental changes or climate scenarios (presented in Chapter 6), on physiological processes and on seasonal pattern of growth rates quantified, and integrated at the forest level over prolonged periods of time (years to decades). Here we also present and discuss which models at which sites and for what species were choosen for scaling up exercises over Europe.

8.1 Boreal forests

Michael Freeman and Sune Linder

This section summarises the modelling results for assessment of the impact of climate change on boreal forests. Modelling has been performed using six models: FEF (partner 08), FINNFOR (partner 07), FORGRO (partner 01), BIOMASS (partner 10), HYDRALL (partner 02) and TREEDYN (partner 09) for three tree species representing the Boreal region: *Pinus sylvestris*, *Picea abies* and *Betula spp*. Modelling was carried out for two sites: Site 1 (66.25° N) representing the Northern and Site 2 (61.75° N) representing the Southern part of the boreal region. Models were run with climate change scenarios provided by partner 03 (Chapter 6). We present and discuss climate change impact results in terms of maximum standing volume, annual stem wood production and annual carbon input to the soil.

8.2 Results - Model predictions for representative sites

The general result of the climate change scenario is that all models for all tree species, except in one case, predict an increase in maximum standing volume, i.e. simulated results for 2070 are higher than for 1990 (Table 8.1). However, there are differences in the magnitude of response among tree species and models. Boreal climatic

conditions with sub-zero air temperatures and soil freezing lead to winter damage of the photosynthetic system for coniferous species. This reduces photosynthesis in the spring due to a period of recovery of the damage and in the autumn due to early decline, which in turn leads to a shorter actual growing season. Difference among model results may reflect diversity in model parameterisation and model sensitivity to environmental changes concerning these circumstances special for the boreal region.

Maximum standing volume 1990 is for most models in the range of the prevailing inventory tables, except in some cases where FORGRO showed too high and FINNFOR too low volumes. The change in predicted maximum standing volume, i.e. volume 2070 compared to 1990, varied between +2 to +76 for *Pinus sylvestris*, -9 to +39 for *Picea abies* and +34 to +53 for *Betula spp.*

Table 8.1 Maximum standing volume (m^3/ha) in 1990 and 2070 for each site, tree species and model. Relative change 2070 to 1990 in [ ]. Model in ( ); FE: FEF, FI: FINNFOR, FO: FORGRO, BI: BIOMASS, HY: HYDRALL and TR: TREEDYN. Site 1 and 2 represent the Northern and Southern boreal region, respectively.

Site	*Pinus sylvestris* *1990 - 2070*	*Picea abies* *1990 - 2070*	*Betula spp.* *1990 - 2070*
1	170 - 300 [1.76] (FE) 209 - 213 [1.02] (FI) 783 - 841 [1.07] (FO) 333 - 547 [1.64] (HY) 290 - 378 [1.30] (TR)	416 - 524 [1.26] (BI) 224 - 203 [0.91] (FI) 454 - 480 [1.06] (FO) 267 - 371 [1.39] (TR)	144 - 193 [1.34] (FI)
2	600 - 1000 [1.67] (FE) 245 - 361 [1.47] (FI) 1267 - 1348 [1.06] (FO) 445 - 679 [1.53] (HY) 513 - 638 [1.24] (TR)	579 - 788 [1.36] (BI) 259 - 255 [0.98] (FI) 858 - 933 [1.09] (FO) 562 - 636 [1.13] (TR)	228 - 348 [1.53] (FI)

Annual stem wood production (m^3/ha/y) 1990 and 2070 at increasing stand age for each site and species, in general, showed an age related pattern of production corresponding to the prevailing production tables (Figure 8.1). HYDRALL showed a rather weak age related production and FINNFOR a significant peak at age class 21-40 followed by a steep decline. Differences among models were, as expected, more pronounced at the end of the scenario period 2070 due to the differences in sensitivity to the to the climate change scenario, where f. ex. FINNFOR and TREEDYN for *Pinus sylvestris* Site 2 responded with a considerable decline in production for age class 41-60 and onwards. Relative increase in annual stem wood production (m^3/ha/y) (relative to 1990) showed an increase throughout the whole period 1990-2070 (Figure 8.2). Except FINNFOR, that in some cases predicted a decline in relative increase for the older age class 81-100 after 2030 and 2050. In general, predictions varied with age class, most models predicting a larger relative increase in the younger age class 21-40 than in the older 81-100. Differences in relative increase between Site 1 and 2 were observed for all models, especially for TREEDYN with some extreme responses after certain years. FEF, HYDRALL and BIOMASS systematically predicted the highest relative increases in stem wood production, FORGRO systematically the lowest increases, whereas FINNFOR and TREEDYN showed no systematic.

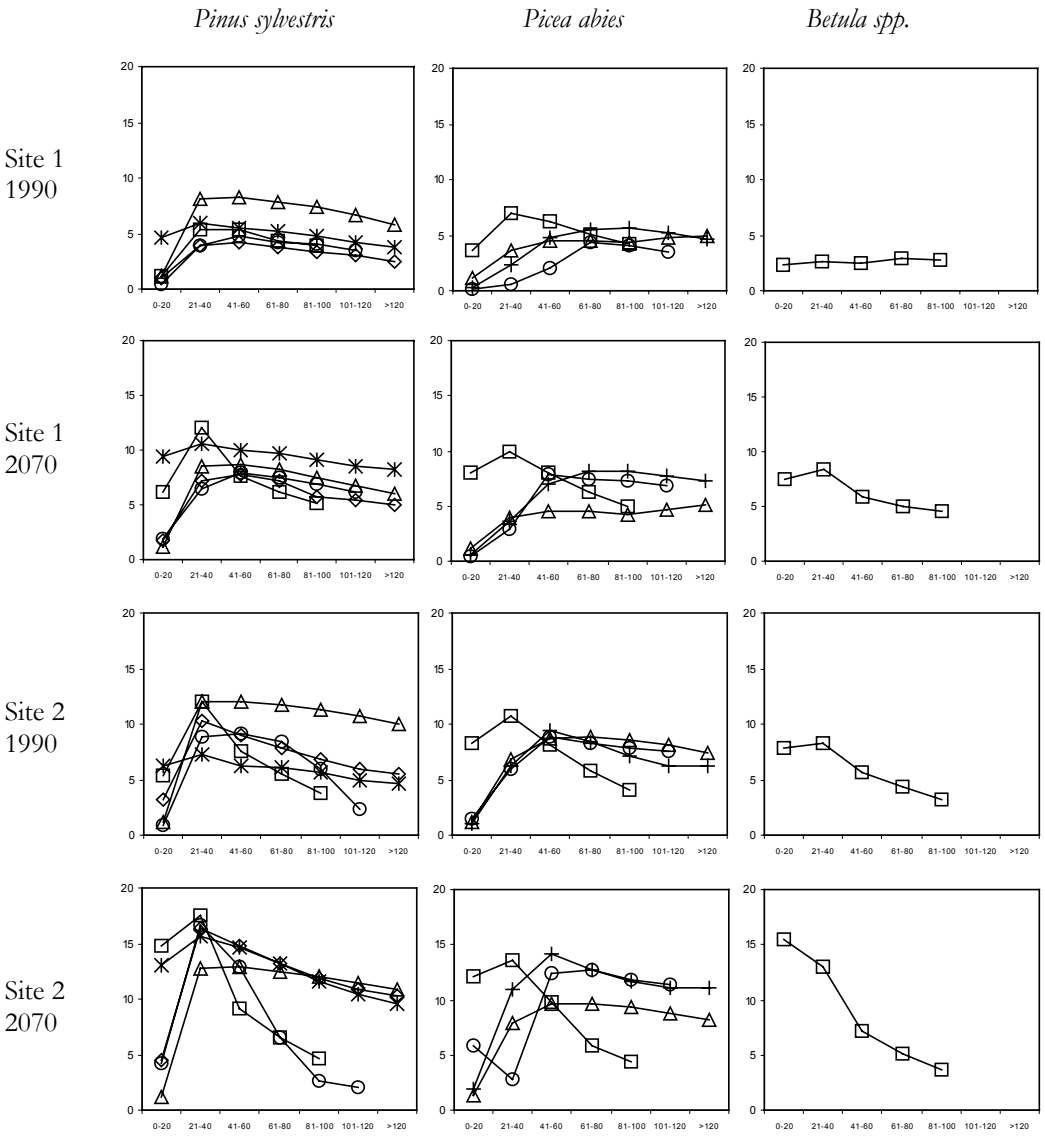

Figure 8.1 Stem wood production (m³/ha/y) of Pinus sylvestris, Picea abies and Betula spp. 1990 and 2070 at increasing stand age simulated for the Northern (Site 1) and the Southern (Site 2) boreal region. Model symbol: FEF (diamond), FINNFOR (square), FORGRO (triangle), BIOMASS (cross), HYDRALL (star), TREEDYN (circle).

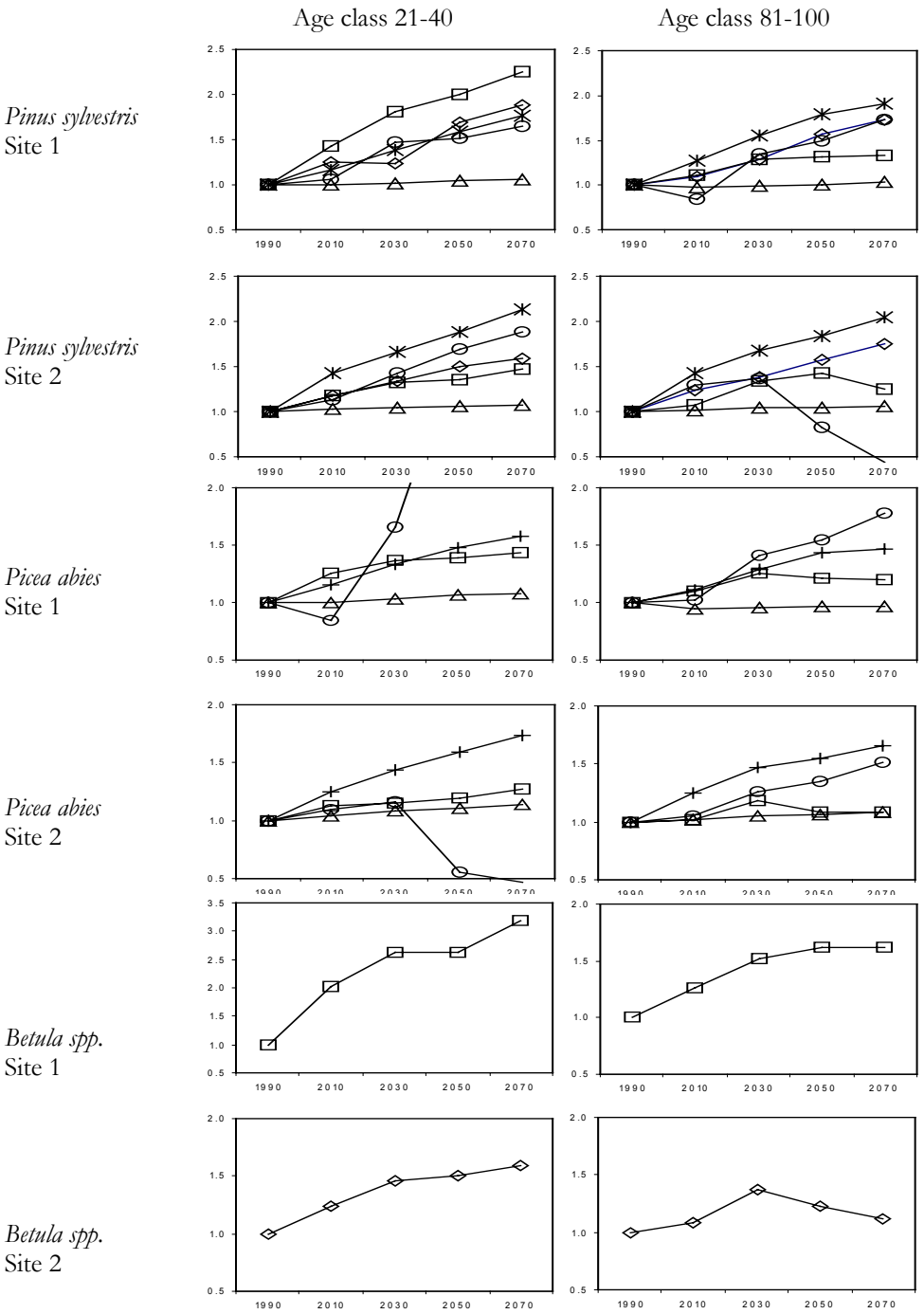

Figure 8.2 Relative increase (to 1990) in stem wood production of Pinus sylvestris, Picea abies and Betula spp. at increasing stand age simulated for the Northern (Site 1) and the Southern (Site 2) boreal region. Model symbol: FEF (diamond), FINNFOR (square), FORGRO (triangle), BIOMASS (cross), HYDRALL (star), TREEDYN (circle).

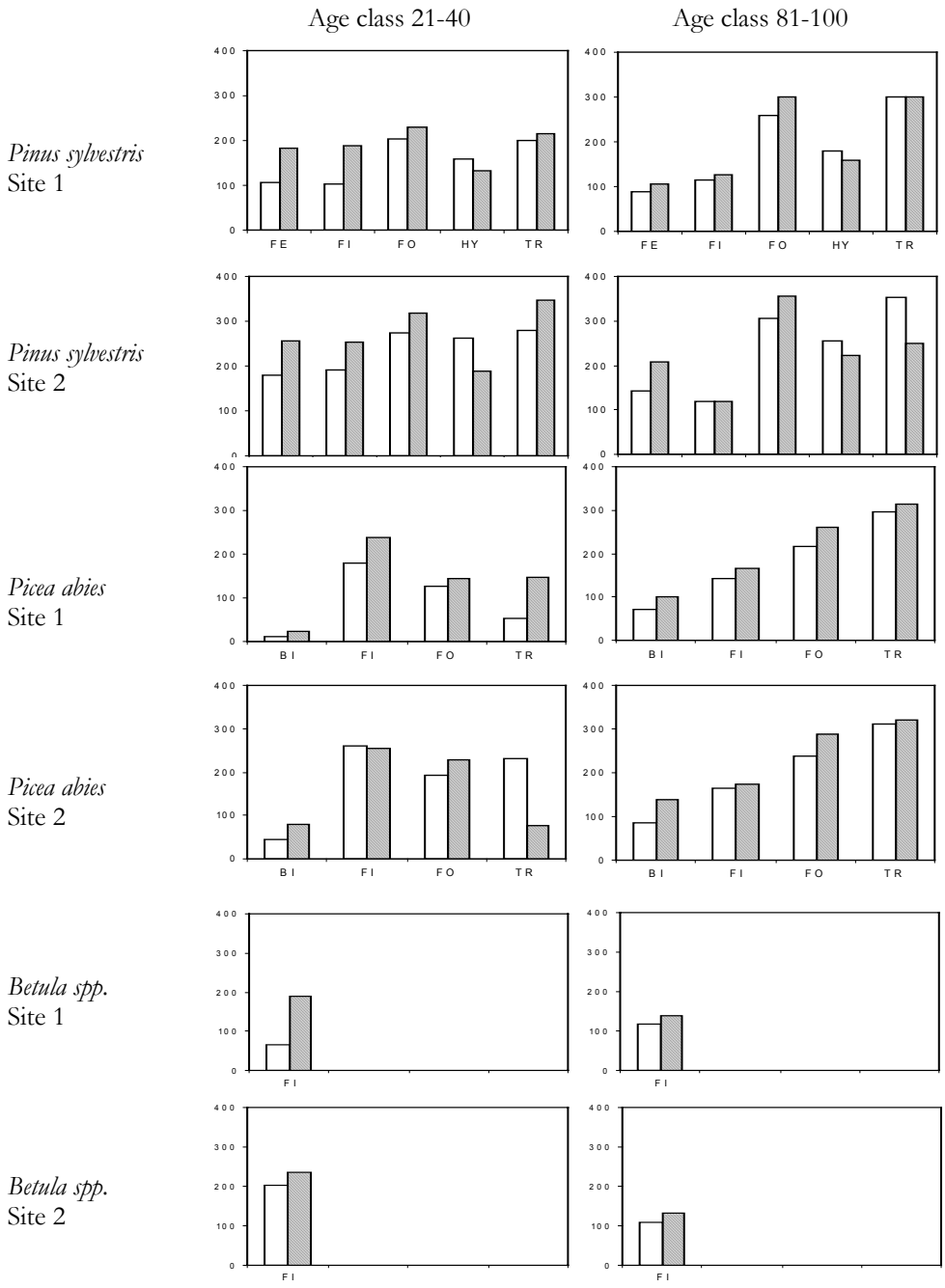

Figure 8.3 Total annual carbon input to soil (gC m²/y) at stand age 21-40 and 81-100 in 1990 (white bars) and in 2070 (hatched bars) simulated for the Northern (Site 1) and the Southern (Site 2) boreal region. Carbon input includes litter (turn-over) from foliage, branch, stem, coarse roots and fine roots. (FE: FEF, FI: FINNFOR, FO: FORGRO, BI: BIOMASS, HY: HYDRALL and TR: TREEDYN).

Total annual input of carbon to the soil differed significantly among models and there was a significant change in carbon input between age classes for most models 1990 (Figure 8.3). FOREGRO and TREEDYN showed the highest input, whereas BIOMASS and FINNFOR showed the lowest. The prediction of carbon input to the soil 2070 relative to 1990 increased in both age classes 21-40 and 81-100 for all models, expect HYDRALL and TREEDYN in some cases. In general, carbon input to the soil increased from Site 1 to Site 2.

8.2.1 Discussion

The results show that we can expect an increase in stem wood production in the boreal region in a future climate. The combined effect of elevated temperature on respiration of biomass and soil and the gain in assimilation from CO_2 fertilisation is positive. However, the magnitude of the increase in production is uncertain. The differences among model results may be attributed to the special conditions in the boreal region.

Tree growth is not limited only by temperature and CO_2 but also by light, water and nutrient availability. Temperature, however, is an important factor in the boreal region. Annual tree growth of boreal forests determined by the length of the period between the thaw in the spring and the freeze-up in the fall is mainly controlled through the effects of temperature on carbon dioxide uptake in the spring and on nutrient availability and uptake during the summer. Poor growth of trees in boreal forests are commonly seen as growth being constrained by temperature on physiological processes in the tree. But air temperature is not the major direct constraint on tree growth. However, temperature may possibly be influencing tree growth indirectly through the length of the growing season and effects on decomposition of soil organic matter and mineralisation of soil nutrients.

During growing season water in general is not a limiting factor of growth in boreal conifers but the availability of soil water in spring and early summer is a precondition for the recovery of photosynthetic capacity after winter damage. The effect of frozen soils on annual CO_2 uptake in boreal spruce around 64° N is particularly dramatic because, prior to the thaw, daily solar radiation is already substantial and effectively being wasted from the perspective of CO_2 capture.

Thus, modelling results are highly dependant on parameterisation of temperature dependant processes controlling the growth in the boreal region. Further, it should be kept in mind that soil and nutrient dynamics - relative to above ground processes - are still rather poorly formulated in several of the models.

The magnitude and inter annual distribution of the temperature increase generated by climate scenarios is of great importance in modelling the effects of climate change in boreal conifers. The effects on length of growing season and availability of nutrients will inevitably affect tree growth. The presented modelling results are based

on a single climate scenario and it should be observed that other scenarios would give other results.

8.3 Temperate forests

Denis Loustau

8.3.1 Introduction

In the European temperate zone, the growth of forests and their production are limited by a combination of trophic and climatic factors: water (excess or deficit) , nutrients, light, temperature, atmospheric CO_2. Besides, most of the temperate forests in Europe are distant by less than 200 km from a large urban or industrial zone and are therefore exposed to atmospheric pollution such as nitrogen and ozone deposition (Holland et al 1999). It was beyond the scope of this survey to encompass all the limitations of forest growth in the temperate zone. Rather, we aimed at describing, analysing and upscaling the impacts of the climate scenario described in chapter 6. However, it must be kept in mind that the predictions presented below are based a single climate scenario and do not take into account scenarios concerning e.g. nitrogen or ozone deposition or management options aiming at the improvement of site fertility and water balance such as fertilisation or drainage.

The models used in the temperate zone were FORGRO, HYDRALL, TREEDYN and GOTILWA. The table 8.2 summarises the limitations taken into account in each model. They differ in their ability to describe the trophic, climate and age limitations to forest production and tree growth but no model takes fully into account all the potential limitations to forest growth. In addition, it must be noticed that none of those models does include a full coupling between soil and canopy processes. Their predictions must consequently be regarded as valid only for forest stands growing in a steady state of nutrient availability.

Table 8.2 Climatic and trophic constraints taken into account by the LTEEF models applicable in the temperate zone.

	Climate Effects		Trophic constraints				Age	Species
MODELS	Phenology	Frost impact	N,P	Water	CO_2	Light		
FORGRO	x	x		x	x	x		all
HYDRALL		x		x	x	x	x	coniferous
TREEDYN	x		x		x	x	x	all
GOTILWA	x	x		x	x	x	x	all

Climate-induced limitations such as frost, soil water deficit, excessive heat, vapour pressure deficit, storms, show large and unpredictible inter-annual fluctuations. Among them, the soil water deficit has caused most of the forest productivity declines in the atlantic and continental temperate forests, such as most of the forest declines observed in the past decades, e.g. those attributed to acid rain in France during the early 80's (Becker 1989).

Soil water deficit is the result of the water budget of the forest stand. In temperate climate it is mainly caused by seasonal discrepancies between the water input by either rainfall or recharge from the subsoil and vegetation uptake driven by the net available radiation and atmospheric vapour saturation deficit. The likelihood of seasonal fluctuations in the driving variables predicted by the climate scenario used is therefore critical when considering the long term impacts of climate on forest growth. This point will be discussed in detail in a preliminary part. Model predictions in terms of stand growth and soil carbon inputs will then be presented for a range of site and species . These results will finally be discussed and compared with recent results from long term experiments and the likelihood of the scenario used will also be discussed and compared with some recent scenarios published in scientific literature.

8.3.2 Climate scenario used for predicting climate change impacts

The climate variables such as rainfall, temperature, radiation and air vapour pressure saturation deficit (VPD) determine the annual course of forest evapotranspiration and soil water recharge, the basic components of the soil water balance. Soil water deficit is due to the deficit between rainfall and evapotranspiration and occurs mainly in summer and autumn under a temperate climate. Since the climate change may affect potentially its determinant variables, it is important to examine the climate scenario used in terms of the seasonal course of climate variables for assessing the likelihood of the soil water regime predicted.

From that point of view, the climate scenario used predicts a warmer but not drier climate. Fig. 8.4 compares the seasonal course of rainfall, incident visible radiation relative humidity and temperature between 1990 and 2070 for representative sites of the temperate atlantic and continental zones. It is worth noting that first, the climate scenario does not show a difference in precipitation between summer and winter under the present climate; it does not either predict a shift between summer and winter precipitation, as it has been proposed by other scenario (Déqué et al.1998). Second, the relative humidity and irradiation are not affected by the scenario and last, the increase in temperature is relatively moderate as compared with recent simulations including vegetation feedback (Cox et al. 2000) and is higher in winter than summer.

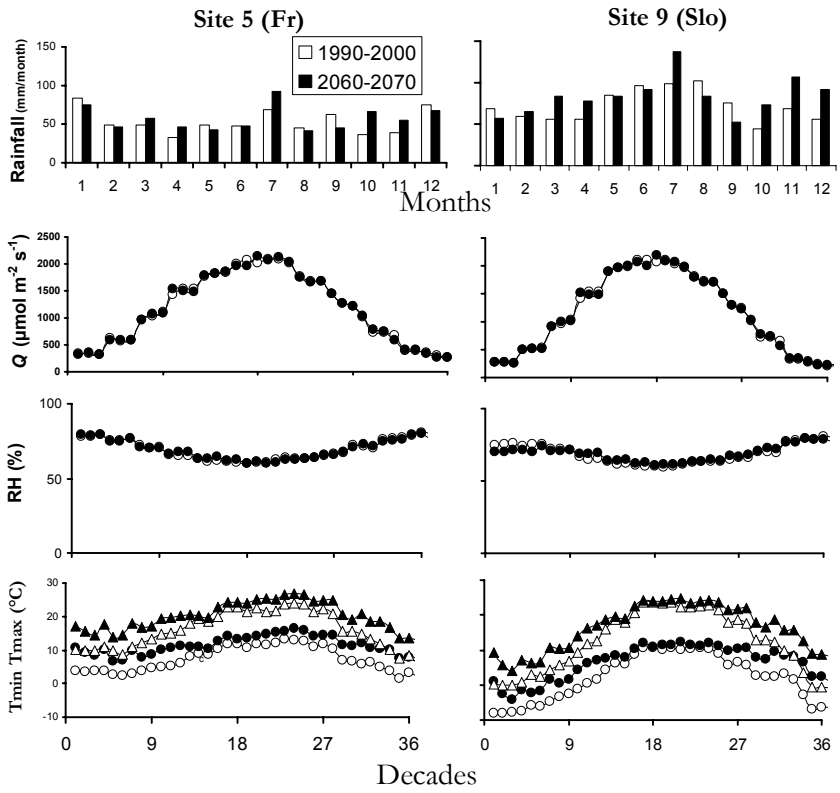

Figure 8.4 Average annual courses of precipitations, visible radiation (Q), relative humidity (RH) and maximum (triangles) and minimum (circles) temperatures for the periods 1990-2000 (open symbols) and 2060-2070 (closed symbols) at sites 5 (temperate atlantic) and 9 (temprate continental).

8.3.3 Results: Model predictions for representative sites.

The general trend predicted by all models is a net increase in maximum standing volume (Table 8.3). As compared with the 1990 standing volume, the change predicted in 2070 varies between -2 to + 33 % with an average of +11%. This change varies between models, FORGRO predicting the lowest increase and HYDRALL the highest. There is no systematic variation between the climate sub-zone, atlantic or continental, or species (*Picea abies*, *Pinus sylvestris* and *Fagus sylvatica*) under consideration.

Table 8.3. Values of Maximum Standing Volume (m³/ha) in 1990 and 2070 for each site, tree species and model (in parenthesis; F: FORGRO, G: GOTILWA, T TREEDYN and H: HYDRALL).

Site	*Fagus sylvatica* 1990 - 2070	*Pinus sylvestris* 1990 – 2070	*Picea abies* *1990-2070*
3		609 - 796 (H) 369 - 376 (F) 481 - 514 (T)	
5		700 - 852 (H) 369 - 374 (F) 717 - 862 (G) 497 - 485 (T)	
6		631 - 804 (H) 400 - 406 (F) 631 - 804 (G) 422 - 430 (T)	
7			790 - 803 (F) 700 - 675 (T)
8_lo	745 - 822 (T)		
8_hi			677 - 695 (F) 645 - 818 (T)
9	810 - 822 (F) 948 - 1051 (T)		790 - 810 (F) 1011 - 1100 (T)
10		567 - 756 (H) 402 - 408 (F) 534 - 547 (T)	

Fig. 8.5 shows the prediction in stem volume growth for *Pinus sylvestris* at three sites and for three age classes from 2010 onwards. Apart from FORGRO, the models predict an enhancement in stemwood growth which varies with age. For the young and mature stands , the growth enhancement is sustained or even increased over the whole period 2010-2070 for TRAGIC. HYDRALL predicts systematically the highest growth enhancement with little impact of the age-class. There is some discrepancy between models and sites for the oldest age class: FORGRO and HYDRALL predict a slight or no increase in volume growth for the oldest stands while in site 10, TREEDYN predicts a decrease in volume growth after 2030.

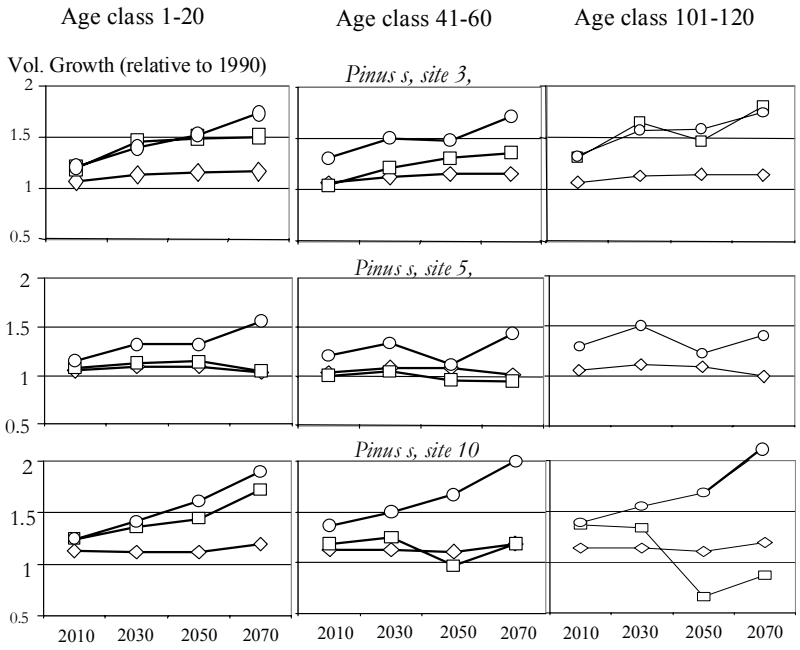

Figure 8.5 Relative changes in volume growth of Pinus sylvestris at three age classes in three representative sites of the temperate zone..

Surprisingly, no consistent change in the annual input of carbon into the soil is predicted for the managed stands, whatever the site and age class (Fig. 8.6). Significant changes are simulated only by HYDRALL, with a diminution in litter production for younger age classes and an increase in the oldest stands. FORGRO and TREEDYN do not predict any changes in soil carbon input.

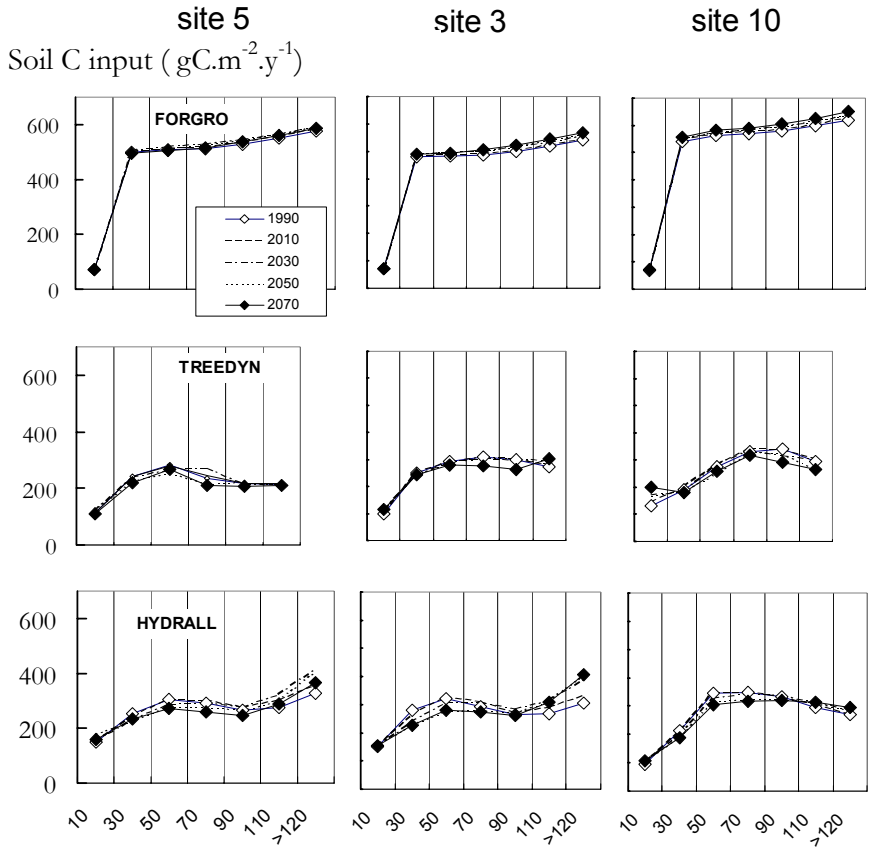

Figure 8.6 Total annual carbon input to the soil predicted by FORGRO, TREEDYN and HYDRALL at three temperate sites from 1990 to 2070 and for different age classes. Carbon input includes leaf litter, woody debris and coarse and fine roots turn-oover.

8.3.4 Discussion and conclusion

According to the scenario used, all models predict an increase in forest growth from 1990 to 2070. This is mainly explained by the scenario considered which does not predict an increase in climate limitations but conversely includes a sustained increase in atmospheric CO_2 concentration and a slight increase in annual rainfall. The potential impact of the temperature elevation on biomass and soil respiration are therefore limited and the CO_2-fertilisation effect is dominant The temperature elevation is relatively low in summer and induce a moderate increase in VPD. Temperature elevation predicted is stronger in winter which will essentially increase the growing season duration (see . The global increase in volume growth predicted by all models is consistent with the trend observed from forest inventories available for the last 30 years (Kauppi et al, 1992) and with most dendroecological surveys (Becker et al; 1994). The order of magnitude of the growth enhancement predicted is lower than those reported in the results available from long term FACE experiment carried out e.g. on *Pinus taeda* under temperate climate (DeLucia et al; 1999). In particular, models do not predict a significant acclimation over short or long terms. There is less

experimental support concerning the longer term acclimation but it may well be less important than previously expected (Medlyn et al. 1999)

Other long term scenarios may lead to opposite conclusions. The feed back impact of vegetation to climate was not included in the scenario considered. However, itsuch feed back may lead to much higher temperature elevation than predicted in the actual scenario (Cox et al. 2000, Betts 2000). In addition, a more detailed reconstruction of climate at the regional scale in Southern Europe , derived from the Hdcm2 model (Déqué et al. 1998) predict a higher temperature elevation, a winter shift in seasonal distribution of rainfall and a 20% increase in summer VPD. Altogether, these detrimental effects may offset the benefit of the CO_2 increase, especially in the low fertility sites, where most forest stands are established.

In the present exercise, it should additionally be remembered that the models have simulated stands corresponding to high fertility sites, where nutrient limitations are weakest. All models tend to overestimate the standing volume values issued from growth and yield tables available for the species and site considered. As mentioned already in the introduction, models do not include a full coupling with soil dynamics. Their present results must be considered as a steady state simulation not including possible changes in nutrient availability which was demonstrated to play a key role in long term trends behaviour of forest ecosystems (Medlyn et al. 2000). This may have led the models used to overestimate the change in yield and production of temperate forests

Acknowledgement:
The author likes to thank R Pujolle, F Pluviaud, A Bosc, V Pérarnaud A Porté and Michel Déqué for their collaboration during the LTEEF-2 project.

8.4 Mediterranean forests

Carlos A. Gracia, Santi Sabaté and Anabel Sánchez

This section summarises the results of modelling exercises developed to assess the impact of climate change on Mediterranean forests. Three models: FORGRO (partner 01), GOTILWA (partner 06) and HYDRALL (partner 02) have been run for tree species present in the Mediterranean region (*Pinus pinaster, Pinus sylvestris, Pinus halepensis, Fagus sylvatica* and *Quercus ilex*). This was done in representative sites of Mediterranean climatic zone (11_hi, 12_hi, 12_lo, 13_hi, 13_lo and 14) where climate change scenarios have been applied and provided by partner 03 (see Chapter 6). Here, to analyse the effects of these Climate change scenarios we discuss the results of two variables, maximum standing volume and stem wood production.

8.4.1 Maximum standing volume

According to models results, Climate change has a positive effect on maximum standing volume, i.e. results for 1990 show lower values than for 2070, (Table 8.4). This effect can be stated for all climates, tree species and models applied. Differences between model results may be explained by different model sensitivity to environmental conditions and different parameterisation. The different sensitivity to environmental conditions is mainly related to constraints on growth under water stress. Thus for all dates plotted infigure 8.7, GOTILWA (constrictive model under water stress) shows higher maximum standing volume in 11_hi (wet site) than in 13_hi (dry site) and, in both sites, a slight increase over time due to Climate change scenarios (dates 1990, 2010, 2030, 2050, 2070). Under the same conditions HYDRALL shows the same pattern than GOTILWA, but differences of maximum standing volume between dry (13_hi) and wet (11_hi) site conditions are smaller. Finally, FORGRO model shows a small effect of Climate change on maximum standing volume and very little differences between the dry and the wet site conditions are shown, being the less sensitive model to water stress.

Table 8.4 Values of Maximum Standing Volume (m³/ha) in 1990 and 2070 for each site, tree species and model (in parenthesis; F: FORGRO, G: GOTILWA and H: HYDRALL). Mean values of the main climatic variables of the climate files representing the sites in the Mediterranean climatic zone.

Site	*Mean P Mm/y*	*Mean PET mm/y*	*Mean Max T ºC*	*Fagus sylvatica* 1990 - 2070	*Pinus sylvestris* 1990 – 2070	*Quercus ilex* 1990 – 2070	*Pinus pinaster* 1990 – 2070	*Pinus halepensis* 1990 – 2070
11_hi	1155	698	13.5	616 - 794 (G) 795 - 804 (F)	676 - 952 (H) 771 - 786 (F) 946 -1067(G)			
12_hi	818	776	14.7	624 - 856 (G) 794 - 801 (F)				
13_lo	775	901	16.1			302 - 337 (G)		
12_lo	620	987	20.0			247 - 258 (G)		
13_hi	493	990	17.4		583 - 746 (H) 600 - 755 (G) 766 - 773 (F)			
14	466	1288	22.8				144 – 316 (G) 548 – 712 (H)	82 - 144 (H) 168 – 335 (G)

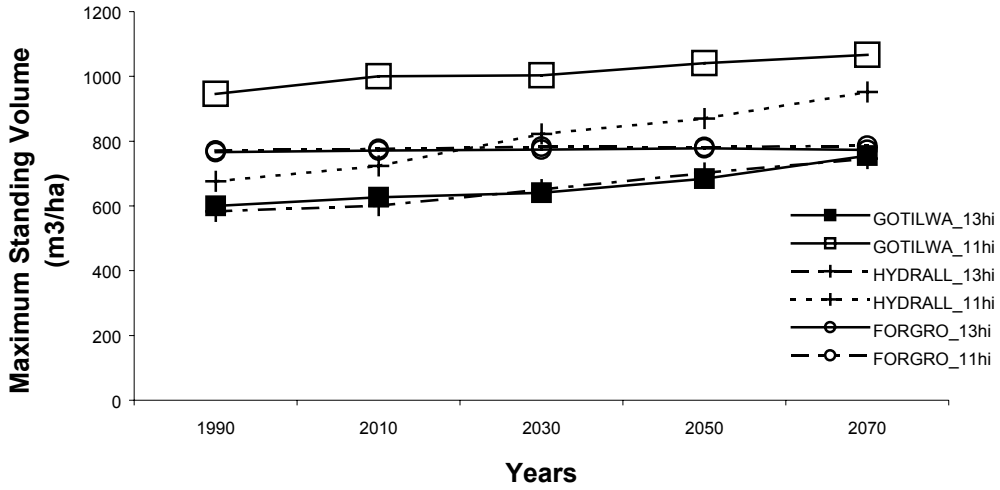

Figure 8.7 Maximum Standing Volume (m^3/ha) of Pinus sylvestris simulated by the models in two sites with contrasting climates: 11_hi (wet) and 13_hi (dry). Models are FORGRO, GOTILWA and HYDRALL.

8.4.2 Stem wood production

Stem wood production is shown in table 8.5, for both 1990 (8.5a) and 2070 (8.5b) and figures 8.8. In general, values are also higher for this variable in 2070. Thus a positive effect on wood production due to Climate change scenarios is also evidenced. Stand age affects these differences. *Pinus sylvestris,* and *Pinus pinaster* stem wood productions decrease with stand age as well as differences due to climate change (1990 vs. 2070), according to HYDRALL and GOTILWA models. On the other hand FORGRO model shows an initial increase of stem wood production in young stands and steady values onwards. The positive effect of Climate change on this variable shown by FORGRO rather small. *Quercus ilex* does not show as well as *Pinus halepensis* clear differences with stand age but Climate change seems to affect positively. Some differences between species are explained by different growth patterns shown by fast growing species (like *Pinus pinaster* and *P. sylvestris*) and slow growing species (like *Quercus ilex* and *Pinus halepensis*).

An important comment to be remarked about model results from GOTILWA is that some combinations of water availability, increased temperatures and management results in collapsing the forest. Although the positive effect on growth of increased CO_2 under Climate change scenarios, we should be aware of some meteorological events where high temperatures and low water availability that combined may produce very dramatic effects reducing the system sustainability. Management regimes applied within these simulations have been implemented according to present information from each area. Nevertheless, it is shown from model results that Climate change will require an adjustment of management to new future conditions.

Table 8.5 Values of Stem Wood Production (m³/ha/y) at stand age of 0-20 and >120 in 1990 and 2.b: The same in 2070, for each area , tree species and model (F): FORGRO, (G): GOTILWA and (H): HYDRALL.

a: 1990

Site	*Fagus sylvatica* 0-20 - >120	*Pinus sylvestris* 0-20 - >120	*Quercus Ilex* 0-20 - >120	*Pinus pinaster* 0-20 - >120	*Pinus halepensis* 0-20 - >120
11_hi	4.6 - 9.4 (F) 13.3 - 3.1(G)	5.5 - 10.6 (F) 15.3 - 4.8 (H) 17.6 - 11.8(G)			
12_hi	4.6 - 9.3 (F) 13.7 - 3.4(G)				
13_lo			6.2 - 3.7 (G)		
12_lo			7.6 - 5.2 (G)		
13_hi		5.5 – 9.9 (F) 12.4 – 5.2 (H) 15.8 – 8.6 (G)			
14				6.5 - 2.6 (G) 12.8 - 4.3 (H)	0.9 - 0.7 (H) 4.0 - 1.3 (G)

b: 2070

Site	*Fagus sylvatica* 0-20 - >120	*Pinus sylvestris* 0-20 - >120	*Quercus Ilex* 0-20 - >120	*Pinus pinaster* 0-20 - >120	*Pinus halepensis* 0-20 - >120
11_hi	5.4 - 11.1 (F) 16.7 -11.6(G)	6.7 - 12.8 (F) 24.6 – 10.6(H) 35.1 – 18.5(G)			
12_hi	5.3 - 10.6 (F) 17.6 -11.1(G)				
13_lo			10.7 -10.0(G)		
12_lo			8.8 - 7.8 (G)		
13_hi		5.7 - 10.3 (F) 21.4 - 8.6 (H) 24.2 – 13.8(G)			
14				17.7 - 8.3 (G) 18.8 - 5.8 (H)	3.1 - 0.9 (H) 11.8 - 6.0 (G)

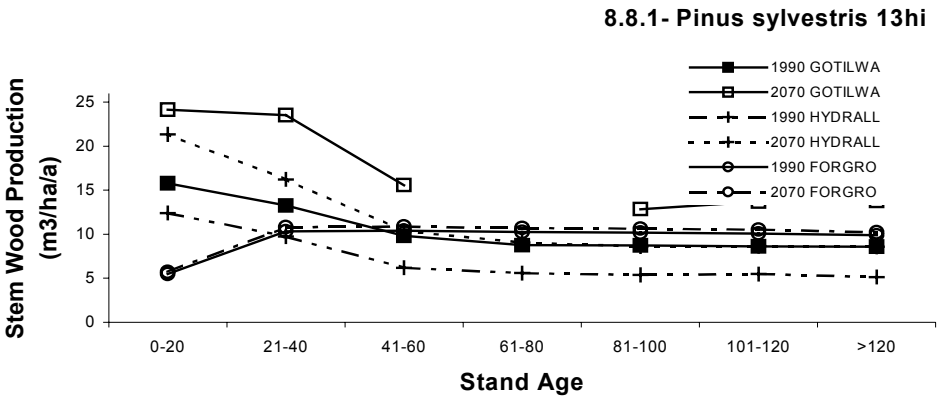
8.8.1- Pinus sylvestris 13hi
1990 GOTILWA
2070 GOTILWA
1990 HYDRALL
2070 HYDRALL
1990 FORGRO
2070 FORGRO
Stem Wood Production (m3/ha/a)
0
5
10
15
20
25
0-20
21-40
41-60
61-80
81-100
101-120
>120
Stand Age

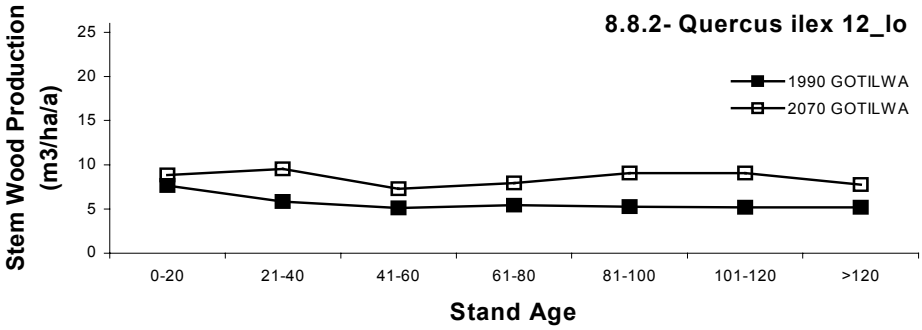
8.8.2- Quercus ilex 12_lo
1990 GOTILWA
2070 GOTILWA
Stem Wood Production (m3/ha/a)
0
5
10
15
20
25
0-20
21-40
41-60
61-80
81-100
101-120
>120
Stand Age

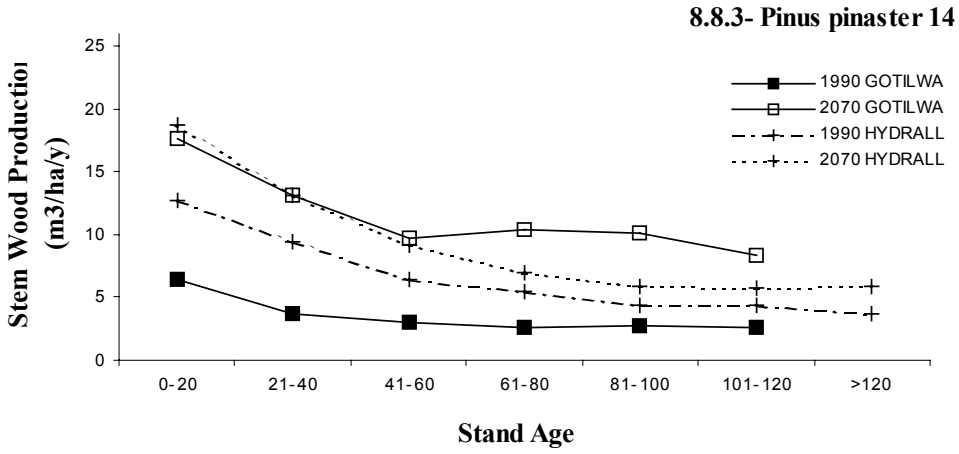
8.8.3- Pinus pinaster 14
1990 GOTILWA
2070 GOTILWA
1990 HYDRALL
2070 HYDRALL
Stem Wood Production (m3/ha/y)
0
5
10
15
20
25
0-20
21-40
41-60
61-80
81-100
101-120
>120
Stand Age

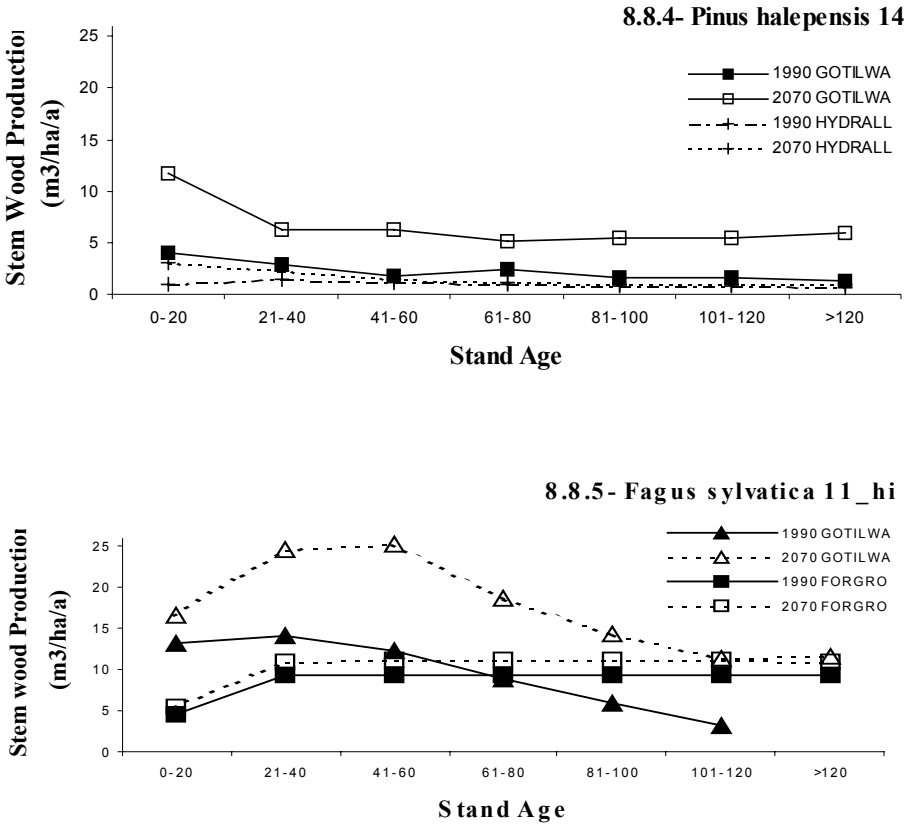

Figure 8.8 Stem wood production (m³/ha/a) at increased stand age for both 1990 and 2070 (Climate change scenario). Each panel shows results for different species at different sites in the Mediterranean area. Results for different models are plotted in the same panel when available (see legend on the panel). 9.2.1 Pinus sylvestris at 13_hi, 9.2.2 Quercus ilex at 12_lo, 9.2.3 Pinus pinaster at 14, 9.2.4 Pinus halepensis at 14 and 9.2.5 Fagus sylvatica at 11_hi.

8.4.3 Some considerations for the Mediterranean region

A combination of specific climate and site conditions for the Mediterranean have been analysed, looking at present conditions and applying future Climate change scenarios based on one GCM model (HadCM2). Some variables as litterfall do not show effects of Climate change with the provided scenarios and according to model results. When positive effect of this Climate change scenario is shown (see maximum standing volume and stem wood production), it may be explained by the fertilisation promoted by the increase of atmospheric CO_2 concentration, together with no limiting conditions imposed by water (lack of water) and/or temperature (increased values). Nevertheless, it is important to emphasise that other combinations of future climate scenarios and/or site conditions, which also may occur in the area, would provide different results. Special concerns are stated in the area with regard to the predicted increased values of temperature when they are combined with a rainfall decrease.

8.5 Quantifying the uncertainties in model predicted growth responses

Ilkka Leinonen

The criteria for selecting a model for a single site and species were i- the model was applied for this site and species, ii- the model was found to produce reliable results when compared to the flux measurements and growth and yield tables (Chapter 4), iii- the model properties where found to be most suitable to represent this site and species, and when several models were found to fulfil these three criteria, the chosen model was the one applied for a larger geographical range in Europe.

The long-term predictions of the large-scale carbon budgets of forests include uncertainties, the sources of which are, for example, the climatic scenarios used, the input data, and the assumptions of models used both for the predicting the responses of forest to climatic change and for the upscaling of these responses. The total model-related uncertainty consists of the uncertainties in model parameters and the model structure. In Chapter 4, the method for estimating the uncertainty caused by the parameter values is presented. In the following, the total uncertainty related to the outputs of process-based models is presented in terms of one variable, namely the change of the growth rate of forests as a result of the long-term climatic change.

In the large-scale predictions, the range of variation of the outputs of the process-based models can be considered to represent the uncertainty in input parameters of the large-scale forest scenario model. If all of these models are applied for the same site and tree species, the magnitude of the uncertainty for this site and species can be estimated directly from the range of variation of the model predictions. However, in the actual case, any of the site/species combinations was not represented by all models. Therefore, the expected range of variation of the model outputs was estimated according to the following procedure.

First, the systematic differences between the predictions of different models for the relative changes in the growth rate (average of all age classes) were estimated by the general linear model of the analysis of variance, where the model effect was separated from other factors causing variation in the model outputs (such as site effect). This was done separately for all three regions. Secondly, the region-specific model effect was subtracted from the prediction of each model, and the these values were used to calculate the corrected mean prediction for each site and species. Finally, the corrected range of variation around this mean value was determined by including the highest and lowest regional model effect.

The analysis showed that the main source of the variation in the predicted growth rate for different sites and species was the systematic difference between different models. The corrected mean predictions and variation ranges for the changes of stem wood growth from year 1990 to year 2070 for each site and species are presented in Table 8.6. For comparison, the mean values and ranges of the original model

predictions are also presented. In the same table, the models chosen for upscaling exercises by species and sites are also indicated.

As calculated on the basis of the site and species-specific corrected mean values, the models predicted for the boreal region on average 76% increase in stem growth. By including the highest and lowest model effects (+45 percent units, Treedyn and -65 percent units, Forgro, respectively), the average, model predicted range of variation in the increase of stem growth was found to be 10-121 % at the boreal region. At the temperate region, the average increase in stem growth was predicted to be 53%. The average range of variation was 20-87 %, where the highest model effect was found in Hydrall (+28 percent units) and lowest in Forgro (–34 percent units). At the Mediterranean region, the average increase in stem growth was 62%, with the range of 24-116 %. At this region, the highest model effect was found in Gotilwa (+55 percent units) and the lowest in Forgro (-37 percent units).

As a conclusion, all models predicted increasing growth trend of forests during the next decades at all regions of Europe, but the magnitude of this trend varied strongly in the predictions of different models. This variation is expected, due to the different long-term environmental sensitivities of the models (Chapter 4). The variation in predicted growth responses causes considerable uncertainties in the predictions of the future carbon budgets for different regions and countries. For such sites where most of these models are applied (for example site 2, Scots pine), the magnitude of this uncertainty can be directly estimated based on the actual predictions of all applied models. However, for some sites the prediction of only one model is available (for example site 12_lo, Quercus ilex). In these cases, especially if the applied model represents the upper or lower extreme in the range of systematic model effects, the estimated carbon budget, based on the response predicted by such model, can be strongly biased compared to the predictions for other sites. In these cases, the method to estimate the variation caused by the systematic model effect, as presented above, is the only way to make the predictions for different sites comparable with each other.

Table 8.6. Model predicted relative growth rate (average of all age classes), year 2070 (year 1990 = 1). Region: B= Boreal, T=Temperate, and M=Mediterranean.

Site	Species	Region	n of applied models	Model used for Upscaling	Original Mean Prediction	Original range of variation	Corrected mean prediction	Corrected range of variation
1	Pinus sylvestris	B	5	COCA/FEF	1.87	1.04 - 2.32	1.85	1.20 – 2.31
1	Picea abies	B	4	BIOMASS	1.85	1.48 – 2.58	1.86	1.21 – 2.31
1	Betula pendula	B	1	FINNFOR	2.21	-	2.28	1.63 – 2.73
2	Pinus sylvestris	B	6	COCA/FEF	1.62	1.07 – 2.13	1.61	0.96 – 2.06
2	Picea abies	B	4	BIOMASS	1.51	1.11 – 1.76	1.52	0.87 – 1.98
2	Betula pendula	B	1	FINNFOR	1.34	-	1.41	0.76 – 1.86
3	Pinus sylvestris	T	3	HYDRALL	1.41	1.14 – 1.70	1.52	1.19 – 1.86
5	Pinus sylvestris	T	4	HYDRALL	1.10	0.53 – 1.43	1.10	0.76 – 1.43
6	Pinus sylvestris	T	3	HYDRALL	1.33	1.10 – 1.63	1.44	1.10 – 1.78
7	Picea abies	T	2	FORGRO	1.05	0.91 – 1.19	1.36	1.02 – 1.69
8_hi	Picea abies	T	2	FORGRO	1.81	1.38 – 2.24	2.12	1.78 – 2.45
8_lo	Fagus sylvatica	T	1	FORGRO	1.31	-	1.59	1.25 – 1.93
9	Picea abies	T	2	FORGRO	1.25	1.18 – 1.31	1.55	1.21 – 1.89
9	Fagus sylvatica	T	2	FORGRO	1.25	1.18 – 1.33	1.56	1.22 – 1.90
10	Pinus sylvestris	T	3	HYDRALL, TREEDYN	1.45	1.17 – 2.00	1.56	1.23 – 1.90
11_hi	Pinus sylvestris	M	3	HYDRALL	1.53	1.22 – 1.73	1.53	1.15 – 2.07
11_hi	Fagus sylvatica	M	2	FORGRO	1.70	1.18 – 2.22	1.61	1.24 – 2.16
12_hi	Fagus sylvatica	M	2	FORGRO	1.60	1.15 – 2.06	1.52	1.14 – 2.06
12_lo	Quercus ilex	M	1	GOTILWA	1.53	-	0.98	0.61 – 1.53
13_hi	Pinus sylvestris	M	3	HYDRALL	1.43	1.04 – 1.65	1.43	1.05 – 1.97
13_lo	Quercus ilex	M	1	GOTILWA	2.29	-	1.74	1.36 – 2.29
14	Pinus halepensis	M	2	GOTILWA	2.37	1.57 – 3.16	2.18	1.80 – 2.72
14	Pinus pinaster	M	2	GOTILWA	2.12	1.41 – 2.82	1.93	1.56 – 2.48

8.6 References

Becker M., (1989). The role of climate on present and past vitality of silver fir forests in the Vosges mountains of northeastern France. *Canadian Journal of Forest Research,* **19:** 1110-1117.

Becker M., Nieminen T.M., Geremia F., (1994). Short-term variations and long-term changes in oak productivity in northeastern France. The role of climate and atmospheric CO2. *Annales des Sciences Forestieres* , **51**: 477-492.

Betts RA (2000) Offset of the potential carbon sink from boreal forestation by decreases in surface albedo. *Nature* **408**: 187-190.

Cox PM, Betts RA, Jones CD, Spall SA, Totterdell IJ (2000) Acceleration of global warming due to carbon-cycle feedbacks in a coupled climate model. *Nature* **408**: 184-187.

DeLucia E. H., Hamilton J. G., Naidu S. L., Thomas R. B., Andrews J. A., Finzi A. Lavine M., Matamala R., Mohan J. E., Hendrey G. R., Schlesinger W. H. (1999) Net primary production of a forest ecosystem with experimental CO2 enrichment. *Science.* **284**: 5417, 1177-1179.

Déqué M, Marquet P, Jones RG (1998) Simulation of climate change over Europe using a global variable resolution general circulation model. *Climate Dynamics* **14**: 173-189.

Holland E. A. Dentener F. J. Braswell B. H. Sulzman J. M (1999*)* Contemporary and pre-industrial global reactive nitrogen budgets. *Biogeochemistry.* **46**: 1-3, 7-43.

Kauppi P. E., Mielikainen, D. Kuusela K., (1992) Biomass and carbon budget of European forests, 1971 to 1990. *Science*, **256**: 70-74.

Medlyn, B. E. Badeck, F. W. Pury, D. G. G. de. Barton, C. V. M. Broadmeadow, M. Ceulemans, R. Angelis, P. de. Forstreuter, M. Jach, M. E. Kellomaki, S. Laitat, E. Marek, M. Philippot, S. Rey, A. Strassemeyer, J. Laitinen, K. Liozon, R. Portier, B. Roberntz, P. Wang, K. Jarvis, P. G (1999*)* Effects of elevated CO2 on photosynthesis in European forest species: a meta-analysis of model parameters. *Plant, Cell & Environment.*. **22**: 1475-1495.

Medlyn B, McMurtrie RE, Dewar R, Jeffreys MP (2000) Soil processes dominate the long term response of forest net primary productivity to increased temperature and atmospheric CO2 concentration. *Canadian Journal of Forest Research* **30**: 1-16

9 Upscaling of impacts to European forests

9.1 Introduction

Over the past two decades many methods have been developed and applied to quantify terrestrial carbon sources and sinks. Each of these methods has its strengths and weaknesses. These methods include inversions based on atmospheric chemistry (Bousquet et al. 1999, 2000), biogeochemical models (Schimel et al., 2000), land-use bookkeeping models (Houghton et al., 1999), flux towers (Martin et al. 1998, Valentini et al. 1999) and forest inventories (Dixon et al. 1994; UN-ECE/FAO 2000, Nabuurs et al. 1997). While atmospheric inversions constrain the magnitude of terrestrial carbon sinks, they have limited ability to discern the responsible mechanisms or exact location of the observed sink. Global biogeochemical models can explore the importance of ecosystem physiological responses to climate variability or increasing CO_2, but they do not yet consider natural or human-induced disturbances. In contrast, methods that focus on the effects of human land-use changes are insensitive to changes in ecosystem physiology (Houghton et al. 1999). Measurements from eddy flux towers reflect one signal from all of the mechanisms affecting net ecosystem production, but these local measurements at a few sites do not capture the variability of carbon flux across the landscape or nation. Neither do they capture the human influence as harvesting, because measurements are carried out over a short time period only (Valentini et al. 1999).

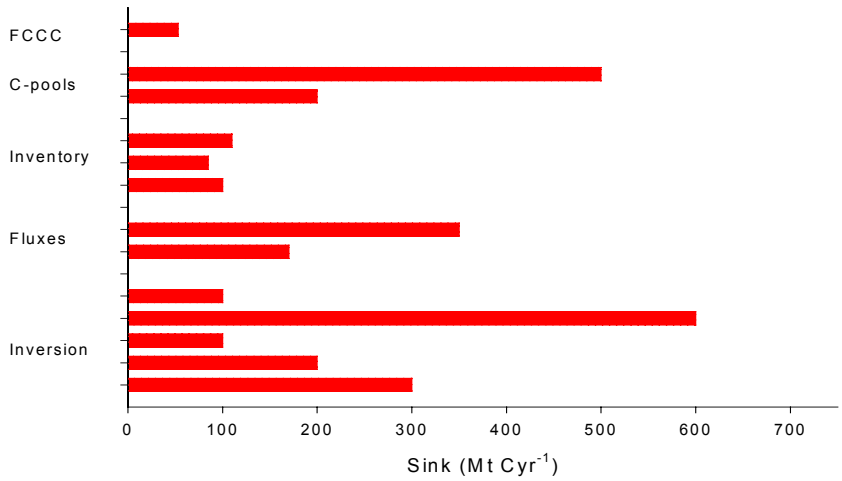

Figure 9.1 Estimates of the carbon sink in European forests (based on national submissions, and Ciais et al. 1995, Martin et al. 1998, Bousquet et al. 1999, Nabuurs et al. 1997, Valentini et al. 1999, UN-ECE/FAO 2000, Liski et al. 2000).

All of these different methods have thus produced a variety of estimates on the location and timing of the terrestrial carbon sink. Figure 9.1 displays this variety -

grouped by method- for the sink estimates for the European land base that were available in literature.

This chapter presents the results of three upscaling approaches that have been applied and developed in the LTEEF-II project (see Chapter 4). These are: upscaling based on forest inventory (section 10.2), upscaling based on a biome scale model (section 10.3), and upscaling based on remote sensing (section 10.4). The aim was to provide insight in the long term and large scale consequences of climate change on European forest, its implications on the carbon budgets, and the degree to which forest management could be adapted to elongate or enhance the carbon sink. In the overall discussion (section 10.5) the advantages and disadvantages of each method to reach that goal is discussed. Furthermore differences in outcome between each method are explained in the discussion as well.

9.2 Upscaling based on forest inventory data and EFISCEN

G-J. Nabuurs, A. Pussinen, J. Liski & T. Karjalainen

9.2.1 Initial situation

Altogether 27 countries and 128.5 million hectares of forest land (Table 9.1) are included in the upscaling based on forest inventory data and large scale forestry model EFISCEN as described in Chapter 4.1. Conventional forestry variables, like standing stem wood volume, net annual increment and total felling for the initial conditions in 1990 are reported in Table 9.1. In 1990, average standing volume was 140 m^3/ha, ranging between 43 m^3/ha in Spain and 393 m^3/ha in Switzerland. Growing stock is highest in Central European countries and lowest in Northern and Southern Europe. Growing stock in 1990 is as the initial values in the forest inventory database, numbers for consecutive years are based on modelling with EFISCEN. Average net annual increment was 5.1 m^3/ha/yr, highest in Central European countries and lower in Northern and Southern Europe. Felling levels varied between countries from 0.5 m^3/ha/yr in Albania to 6.3 m^3/ha/yr in Belgium. In 1990, average stock of carbon in tree biomass varied from 19 to 105 Mg C/ha, average for all countries was 47 Mg C/ha. Total carbon stock in the 128.5 million ha area was 6079 Tg and sink in the tree biomass 82 Tg C/year.

Table 9.1 Area of forest, average growing stem wood stock, net annual increment, fellings, and carbon stock in tree biomass for the 27 countries included in the assessment based on forest inventory data and EFISCEN.

Country	Area of forest, 1000 ha	Growing stock 1990, m^3/ha	Net Annual Increment, m^3/ha/yr (90-95)	Fellings, m^3/ha/yr (90-95)	Carbon stock in trees 1990, Mg C/ha	Carbon stock in trees 1995, Mg C/ha	Total carbon stock in trees in 1990, Tg C	Carbon sink, Tg C/yr
Albania	899	68	2.0	0.5	21.4	24.4	19	0.55
Austria	2942	310	9.8	5.3	82.1	88.7	242	3.84
Belgium	531	220	9.0	5.9	65.1	68.0	35	0.31
Bulgaria	3202	117	3.2	1.4	36.3	39.2	116	1.84
Croatia	1443	117	3.1	1.3	37.2	39.8	54	0.76
Czech Republic	2446	265	6.7	5.7	68.3	69.7	167	0.68
Denmark	442	144	9.6	4.9	41.1	45.3	18	0.37
Finland	19919	93	3.8	2.7	29.7	31.7	592	8.00
France	13300	143	5.8	3.9	55.2	57.6	734	6.56
Germany	9905	266	9.0	4.1	71.9	78.4	712	12.85
Hungary	1609	192	6.9	3.3	61.8	67.4	99	1.80
Ireland	344	108	12.2	4.3	29.1	36.7	10	0.52
Italy	5757	141	4.2	2.3	53.9	56.5	310	2.96
Luxembourg	71	321	11.2	5.1	92.0	100.9	7	0.13
Macedonia	805	56	1.9	2.2	18.6	18.0	15	-0.10
Netherlands	304	172	7.8	4.1	49.5	54.7	15	0.31
Norway	7070	86	3.2	2.1	28.5	30.4	202	2.67
Poland	6309	201	6.5	3.3	54.1	58.1	341	5.03
Portugal	1508	76	7.3	5.2	20.8	25.3	31	1.35
Romania	6211	203	7.2	2.6	64.4	72.1	400	9.55
Slovak Republic	1823	228	6.2	3.2	64.6	69.2	118	1.69
Slovenia	1072	262	5.4	2.7	73.3	76.2	79	0.63
Spain	13980	43	2.2	2.2	45.2	45.4	632	0.63
Sweden	22219	120	4.5	2.8	40.7	44.0	904	14.61
Switzerland	1043	393	10.3	4.8	105.1	112.5	110	1.54
United Kingdom	1898	139	8.4	3.6	39.9	46.4	76	2.47
Yugoslavia	1512	85	2.9	2.1	28.2	29.3	43	0.35
Total/average	**128564**	**140**	**5.1**	**3.0**	**47.3**	**50.5**	**6079**	**81.87**

We have compared the initial situation in terms of forest area, standing stemwood stock, increment and fellings to a recent UN-ECE/FAO forest resources report (UN-ECE/FAO 2000) which is later called TBFRA 2000 (Temperate and Boreal Forest Resources Assessment). In TBFRA, forest is defined as land with tree crown cover (or equivalent stocking level) of more than 10%, while in the database used in this study crown cover was 20%, explaining why the area in the current study was approximately 25 million hectares smaller (Figure 9.2). Differences were largest in southern Europe. Estimates for standing stemwood stock and increment were usually higher in the current study than in TBFRA, and this is partly due to same reason as the difference in the area, i.e. TBFRA covers also less dense forests than what was covered in the database used in this study. Also these two data sources do not cover exactly the same time periods, i.e. TBFRA covers data from early and mid

1990s, while database used in this study covers data from late 1980s and early 1990s. In felling levels there were less discrepancies in these two estimates.

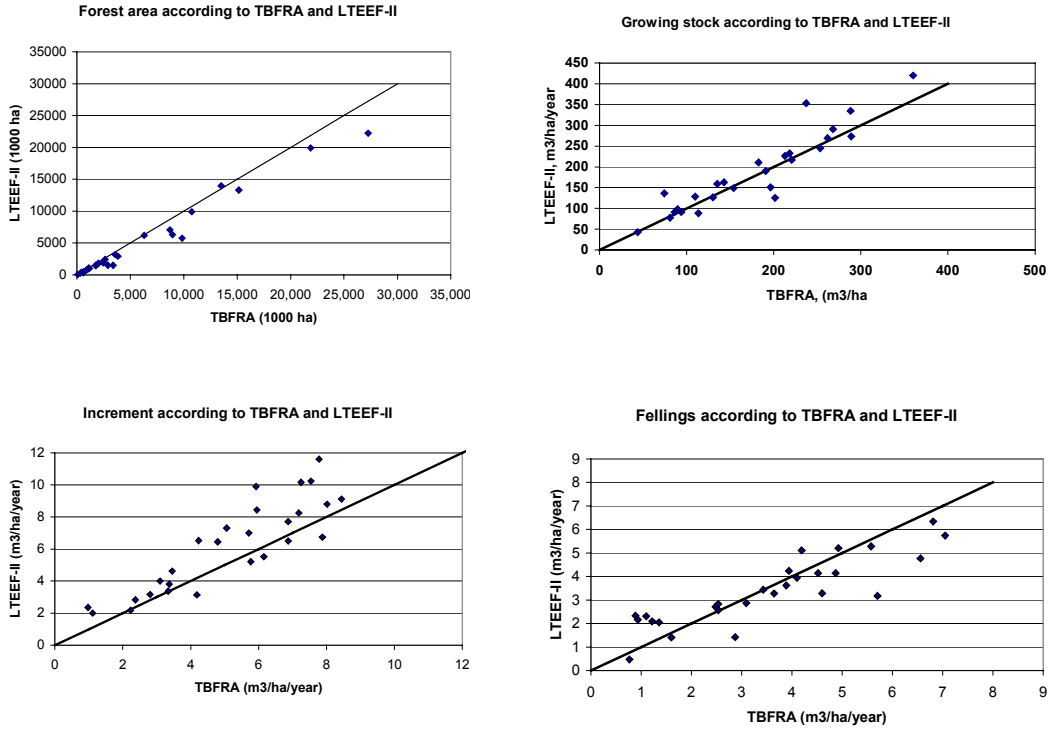

Figure 9.2 Comparison in forest area, growing stemwood stock, net annual increment and fellings in the current study (estimates based on the EFISCEN and the European Forest Resource Database, Schelhaas et al. 1999) and TBFRA 2000 (UN-ECE/FAO 2000) for the 27 countries included in this study. Data in the TBFRA study represents the situation in the early and mid 1990s, while our estimates are for 1990-1995

TBFRA provides also average and total carbon stock estimates for the tree biomass. For the TBFRA report countries were asked to report tree biomass. Biomass was then converted to carbon assuming that half of the dry mass is carbon. This estimate is independent of the estimate provided in this study and shows the differences in conversion factors from stem wood to total biomass (Figure 9.3). In most of the cases averege carbon densities in these two studies are in good agreement when taking into account that the two estimates are not exactly for the same time period in each country as explained earlier. In a few cases carbon densities differ substantially. For Ireland, TBFRA provides 15 Mg C/ha while our estimate is 37 Mg C/ha. Difference is due to much higher initial standing stemwood stock in this study compared to TBFRA which included larger area of newly established plantations which have lower standing stemwood stock. For Austria TBFRA provides 150 Mg C/ha while our estimate is 89 Mg C/ha. Difference is due to higher conversion factor from stemwood volume to total tree biomass in TBFRA (0.519 Mg C/m^3) than in this study (0.264 Mg C/m^3). For Spain TBFRA provides 14 Mg C/ha while our estimate is 45 Mg C/ha. Difference is due to much higher conversion factor

from stemwood volume to total tree biomass in this study (1.057 Mg C/m^3) than in TBFRA (0.314 Mg C/m^3).

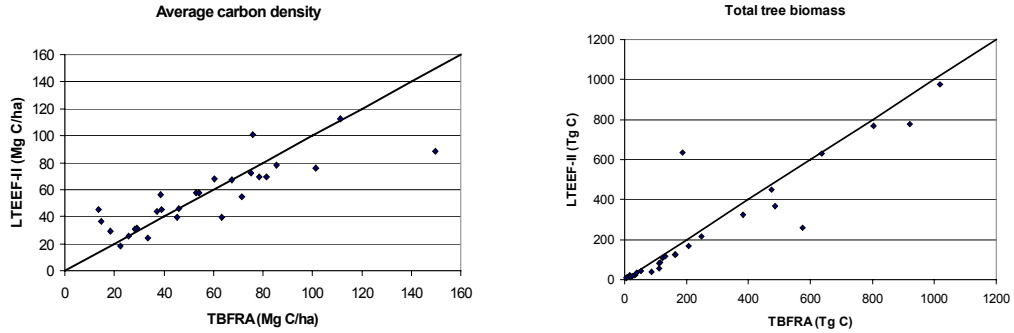

Figure 9.3 Comparison in the average carbon densities and total carbon content of tree biomass in TBFRA (UN-ECE/FAO 2000) and in the current study in 1995.

Average carbon density for the 27 countries is 46 Mg C/ha in TBFRA and 47 Mg C/ha in our study. Total carbon stock in tree biomass in TBFRA is 7246 Tg C, while our estimate is 6488 Tg C in 1995. TBFRA estimate would have been 6096 Tg C if same area (128.5 Mha) had been used as in this study, and therefore the actual difference would have been only 392 Tg C or 6% smaller than the estimate in this study as a result of differences in conversion of stemwood volume to total tree biomass and in the initial stemwood volume noting that these two estimates are not exactly for same time periods.

Carbon stocks in the soil and in wood products were initialised as described in Chapter 4.1. It should be noted that our estimates for soil carbon include carbon that originates from trees only, and therefore underestimates total carbon in the soil. Moreover it is worth noting that soil carbon stock (all compartments) was set to steady state with the input of the first studied year. This was due to fact that there is lack of empirical data to estimate the carbon stock in the soil and in particular the age of carbon in the soil. Situation was very similar for the wood products stock, too, since it was initialised by running the model with harvesting data from 1961 until 1990 in the wood product model. In order to have long enough time series for initialising the wood product stock, input of 1961 was used also for years 1931-1960. Average carbon stock in the soil for 1990 was 47 Mg C/ha and for wood products 6 Mg C/ha (Table 9.2). If the initial stock estimates are too low, they will increase substantially with the current input and if too high, they would decrease substantially with the current input.

Table 9.2 Carbon stock in tree biomass, soil and wood products in 1990.

	Trees, Mg C/ha	Soil, Mg C/ha	Products, Mg C/ha	Total, Mg C/ha
Albania	21.4	17.0	7.1	45.5
Austria	82.1	112.9	13.5	208.6
Belgium	65.1	59.5	8.144	132.8
Bulgaria	36.3	33.0	3.0	72.3
Croatia	37.2	21.0	9.4	67.5
Czech Republic	68.3	50.7	11.8	130.7
Denmark	41.1	44.5	16.2	101.8
Finland	29.7	37.5	2.9	70.0
France	55.2	45.6	7.9	108.7
Germany	71.9	59.3	12.6	143.7
Hungary	61.8	49.7	7.2	118.7
Ireland	29.1	47.6	4.4	81.1
Italy	53.9	41.6	3.7	99.2
Luxembourg	92.0	62.9	11.2	166.0
Macedonia	18.6	21.8	3.6	44.0
Netherlands	49.5	58.5	9.3	117.4
Norway	28.5	29.3	3.1	61.0
Poland	54.1	47.2	9.8	111.0
Portugal	20.8	42.1	11.0	74.0
Romania	64.4	45.5	12.1	122.1
Slovak Republic	64.6	42.5	4.7	111.8
Slovenia	73.3	40.1	8.8	122.2
Spain	45.2	61.3	2.7	109.2
Sweden	40.7	46.0	3.4	90.1
Switzerland	105.1	68.8	11.9	185.9
United Kingdom	39.9	35.6	5.9	81.3
Yugoslavia	28.2	28.1	11.7	68.0
Europe	**47.3**	**46.7**	**6.1**	**100.1**

Above estimates can be compared in some cases to other estimates but direct comparisons are difficult, since the estimates may cover different time periods, but most importantly are based on different methods and assumptions. Burschel et al. (1993) have estimated that trees in Germany contain 89 Mg C/ha, soil 157 Mg C/ha and products 6.3 Mg C/ha. Their estimates for trees and soil are higher than in this study due to different conversion factors but estimate for products is lower. Körner et al. (1992) have reported for Austria 93 Mg C/ha in trees, 123 Mg C/ha in soil and 4 Mg C/ha in products. Nabuurs and Mohren (1993) have estimated the Dutch forests to contain 82 Mg C/ha in trees and 112 Mg C/ha in the soil. Again those estimates are higher for trees and soil than in this study, but for products lower.

Cannell and Milne (1995) have estimated average carbon content of 37 Mg C/ha in tree biomass in British woodlands. Führer et al. (1993) have estimated that the growing stock of Hungarian forests (1.6 Mha) contains 66 Mg C/ha in tree biomass. Estimates of this study are in good agreement with those.

Murillo (1994) have estimated Spanish forests to contain 16-34 Mg C/ha in tree biomass and 13-97 Mg C/ha in the soil. Our estimate for the tree biomass is higher, and has been explained when comparing against the TBFRA estimate. Our estimate

for soil is within the range, but higher than the medium estimate of Murillo, 50 Mg C/ha.

In Finland, Karjalainen and Kellomäki (1993) have estimated tree biomass to contain as an average 32 Mg C/ha, and mineral forest soils 62 Mg C/ha, Kauppi et al. (1997) have estimated tree biomass to contain 27-34 Mg C/ha, mineral forest soils 72 Mg C/ha. Liski and Westman (1997) have estimated average C density of 56-62 Mg C/ha in mineral forest soils. Regarding tree biomass, our estimates are in good agreement with those, our estimates for soil are lower due to fact explained earlier, i.e. that our estimates include carbon originating from trees only.

Total amount of carbon in 1990 in those 27 countries was 12869 Tg, of which 6079 Tg C in tree biomass, 6005 Tg in the soil and 786 Tg in wood products in use. Approximately 88% of the carbon stock in wood products was in long and medium long lifespan products, such as buildings and furniture, and 12% in short lifespan products, such as paper and packing materials. During the period 1990-1995, carbon stock of tree biomass was increasing by a rate of 82 Tg C/year, that of soil was assumed to be in equilibrium (soil was initialised with that assumption), i.e. not increasing or decreasing, and carbon stock of wood products was increasing by a rate of 4.1 Tg C/year. Kauppi et al. (1992) have estimated an annual buildup of 50 Tg C/year in tree biomass in Europe between 1971 and 1990. Dixon et al. (1994) have estimated carbon pools and fluxes in global forest ecosystems, and suggest that average carbon density in Europe would have been 32 Mg C/ha in trees and 90 Mg C/ha in soils, and that forests would have been a sink of 90-120 Tg C/year in late 1980s. Recent estimate by Liski and Kauppi (2000) in the TBFRA report for Euroe suggest that the carbon stock in trees had been increasing by 110 Tg C/yr. Liski et al. (2000) haves estimated carbon sink in the EU forests to 63 Tg C/yr. All these estimates are in rather good or in good agreement with the estimates in this study. By comparison, carbon emissions from fossil fuel combustion were for 23 of the 27 countries included in this study 1163 Tg C in 1990 (data for Albania, Croatia, Macedonia and Yugoslavia not available) (FCCC/SBI/2000/11).

9.2.2 Forest management scenarios and production of wood products

Two scenarios for forest management were run, both under current climatic conditions and under changing climatic conditions. The scenarios were called 'Business as Usual' (*BaU*) and ' Multi functional' (*MultiF*) management. In the *BaU* scenario we assumed that the total national felling levels will stay at the 1990 level throughout the simulation period. Felling levels are specified for coniferous and deciduous tree species groups per country, separately for thinning and final cut. Management regimes are applied as they are today and no changes in the tree species composition nor in the total forest area are assumed. This scenario addresses the question what will happen to the European forest carbon budget if current management continues also in the future.

In the *MultiF* scenario we assumed that the fellings will increase with 0.3% per year during the first 30 years (based on e.g. the trend in Figure 9.4) and stabilises then. This assumption of a gradual increase in fellings reflects a combination of developments that influence demand for wood: firstly a reduced interest of forest owners in wood production because many do not depend on the forest for their income anymore; secondly a higher interest of forest owners in nature values of the forest; thirdly large imports of roundwood from Russia; fourthly continuous increase in demand for wood products, especially paper (Trømborg et al. 2000); and fiftly a higher demand for wood because of large-scale application for bioenergy. All together it was assumed that this leads to increased demand as mentioned above. Furthermore, new management regimes were adopted in this scenario in order to pay more attention to current trends in forest management towards more nature oriented management, i.e. all forests of usually more than 150 years old (depending on the country) are taken out of production. This would mean initially an area of 4 million ha, but during the simulated period, this area may increase because the forest will get older. Also the rotation length of all species is elongated by 20 years and the proportion of thinnings out of total fellings is increased from current 30% to 45 %. Tree species distribution is kept as it was in 1990. Moreover, a forest area expansion of 4 million ha in the period 1990 – 2020 was incorporated in this scenario because of marginal agricultural land being available. This scenario relates to possible forest management regimes based on the changed perception of forestry in general.

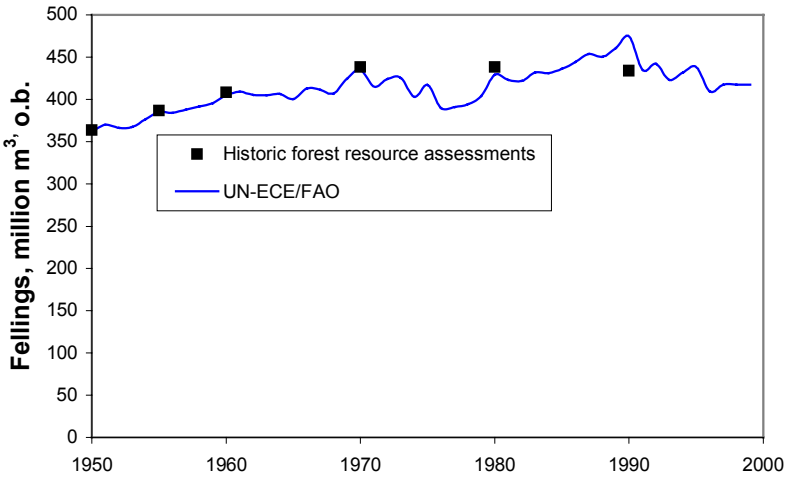

Figure 9.4 Historic fellings in European forests 1950 –1999.

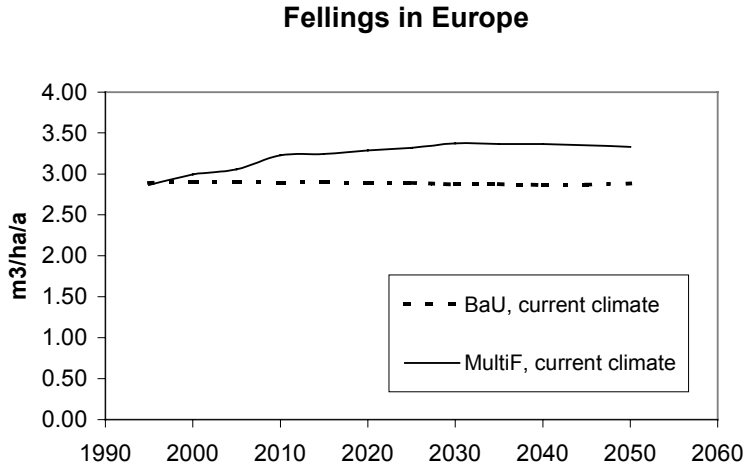

Figure 9.5 Simulated fellings (m^3 ha^{-1} a^{-1}) in the two scenarios. BaU is Business as Usual scenario assuming fellings to stay at level of 1990. MultiF is Multifunctional forest management scenario assuming fellings to increase 0.5 –1% per year till 2020, and forest management pays more attention to biodiversity value.

MultiF scenario provided 3223 million m^3 more fellings during the 60 year period, or as an average 54 million m3/year.

Total felling in 1990 was 372 million m^3, of which the main part, equal to 77.9 Tg C, went to forest industries. In addition, forest industries is using recycled material, and total amount of carbon in the used raw material was 104 Tg. Approximately 20% of the carbon in the raw material, or 20.7 Tg, was released when processed into final products. Approximately 83.2 Tg went into final products in 1990. At the same time, approximately 80.4 Tg C was removed from use (recycled, burned to generate energy, disposed to landfills). All in all, carbon stock of wood products was estimated to increase by 2.8 Tg in 1990. It should be noted that carbon in products exported outside these 27 countries were not included in these numbers, only the carbon that was bound in the harvested timber in these 27 countries was considered.

9.2.3 Impact of forest management and climate change on net annual increment and growing stock in Europe

The summation of net annual increment for the 27 European country's forests is presented in Figure 9.6. All scenarios present a stable or increasing increment till approximately 2020. The increase continues the longest in the MultiF scenario under climate change. Net annual increment peaks in that scenario at 5.9 m^3 ha^{-1} a^{-1} in 2025. In the BaU scenario the increment stays at best stable at 4.9 m^3 ha^{-1} a^{-1} till 2015. In all scenarios the increments then show a gradual decline varying between 4.1 and 5.1 m^3 ha^{-1} a^{-1} in 2050.

The trends in all scenarios are approximately the same. There is no major difference that either climate or management determines. It is the absolute values that differ, but the differences between the lines stay approximately the same. The larger felling amounts in the MultiF scenario result in the stimulation of net annual increment with

some 0.2 to 0.3 m^3 ha^{-1} a^{-1}. In the BaU scenario the build up of growing stock occurs at a faster rate, and EFISCEN indirectly simulates an increasing natural mortality in such cases by increasing areas of forest that have reached a high growing stock, showing no net annual increment anymore. All growth is assumed to be compensated by the same volume in natural mortality.

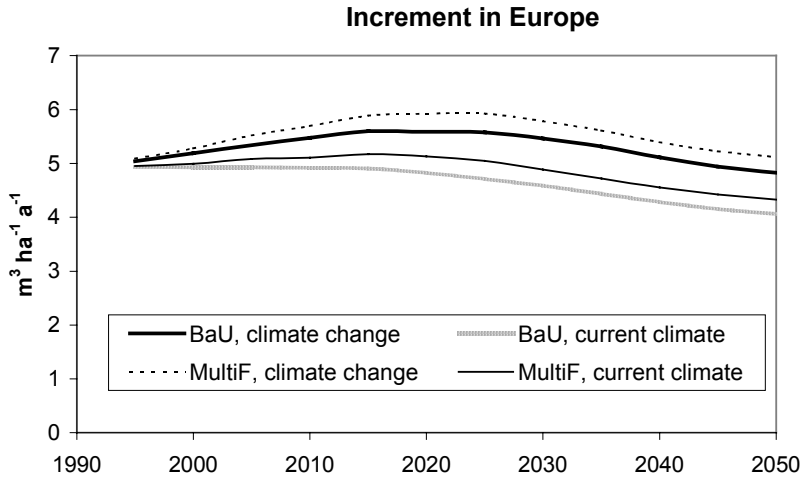

Figure 9.6 Net annual increment of the total European forests from 1990 to 2050 under current climate and climate change. BaU: Business as Usual: fellings stay at level of 1990; MultiF: Multifunctional forest management: fellings increase 0.5 –1% per year till 2020, and forest management pays more attention to biodiversity value.

The increment development and assumed felling levels lead to a continuous build up of the growing stock in all scenarios (Figure 9.7). Average growing stock starts from an amount of 137 m^3 ha^{-1} in 1990 in all scenarios. Climate change will lead in Europe to an enhanced build up of the average growing stock, i.e. in 2050 in the BaU scenario 245 m^3 ha^{-1} under current climatic conditions and 282 m^3 ha^{-1} under changing climatic conditions. This build up is only partially compensated by an increased felling level under the MultiF scenario. Under the latter management regime, the volume reached 270 m^3 ha^{-1} by 2050.

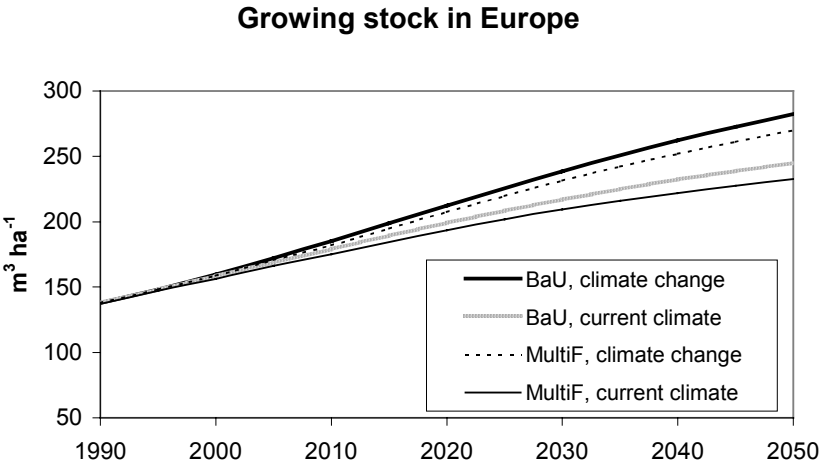

Figure 9.7 Average growing stock in the 27 countries from 1990 to 2050 under current climate and climate change. BaU: Business as Usual: fellings stay at level of 1990; MultiF: Multifunctional forest management: fellings increase 0.5 –1% per year till 2020, and forest management pays more attention to biodiversity value.

9.2.4 Impact of forest management and climate change on carbon stocks in Europe

This chapter provides how applied management scenarios (BaU and MultiF) and climate scenarios (current climatic conditions and changing climatic conditions) influence carbon stocks.

During the 60 year simulation period average carbon stock in the tree biomass in the studied 27 countries increased by 63% when BaU scenario was applied (Figure 9.8). When MultiF scenario was applied, average carbon stock of the tree biomass was slightly smaller, and at the end 3% smaller than in the BaU scenario. Climate change increased average carbon stocks of the tree biomass in both scenarios and the difference between BaU and MultiF scenario remained approximately the same as under current climate, i.e. 3%. Average carbon stocks of the tree biomass were approximately 10% higher under changing climate than under current climate by 2050.

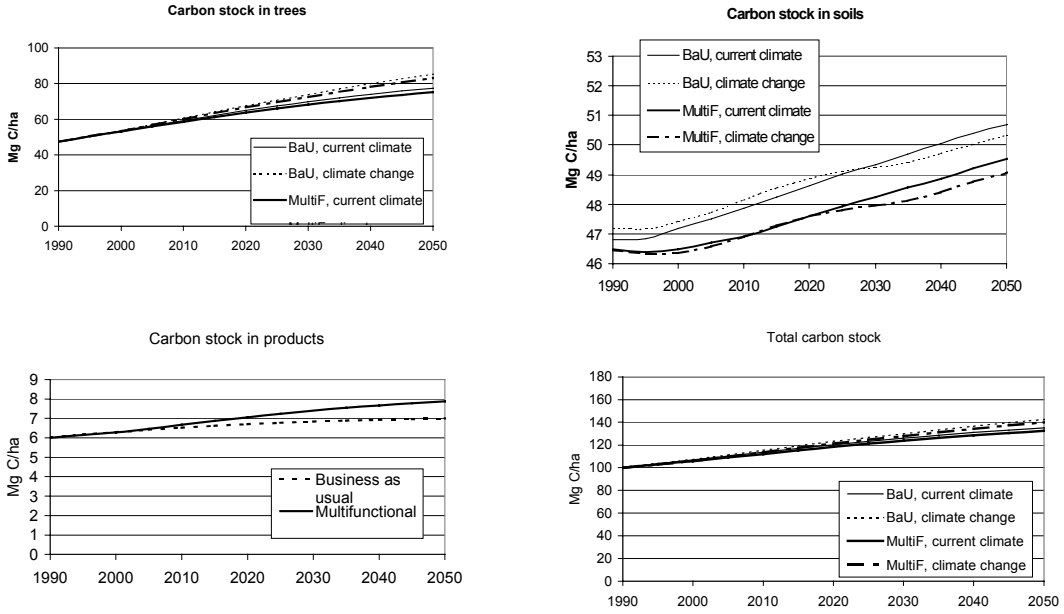

Figure 9.8 Development of carbon stocks in trees, soil, products and total carbon stock when different scenarios were applied. BaU is business as usual scenario, and MultiF is multifunctional scenario.

Average carbon stock of the soil increased by 8% during the 60 years simulation period when BaU scenario was applied under current climate. MultiF scenario had very small impact on the average carbon stocks of the soil. Under changing climatic conditions average carbon stock of the soil was slightly smaller than under current climatic conditions.

Average carbon stock of the products increased by 16% during the 60 years simulation period when Bau was applied. Since more timber was harvested in MultiF scenario during the 60 year period (3 223 million m^3 more than in BaU), also carbon stock of the products was higher in the MultiF scenario, 12% higher than in the BaU scenario at the end of the simulation period.

Average total carbon stock was 35% higher after 60 years simulation in the BaU scenario. In the MultiF scenario, average total carbon stock was slightly smaller (2%) than in BaU scenario. Average total carbon stocks were approximately 5% higher under changing climatic conditions than under current climatic conditions.

Forest area was approximately 4 million hectares larger in the MultiF scenario by 2050 than in the Bau. Under current climatic conditions total carbon stock was larger in the MultiF scenario than in the BaU scenario by 2050, only carbon stock of trees was smaller (Table 9.3). Under changing climatic conditions all the stocks were larger in the MultiF scenario by 2050.

Table 9.3 Total carbon stocks in trees, soil and products in 1990 and 2050.

	Forest area Mha	C stock in trees Tg C	C stock in soil Tg C	C stock in products Tg C	Total C stock Tg C
1990	128.5	6087	6013	774	12874
2050, BaU, Current climate	128.5	9955	6517	900	17372
2050, MultiF, Current climate	132.4	9949	6558	1042	17549
2050, BaU, Changing climate	128.5	10946	6473	902	18321
2050, MultiF, Changing climate	132.4	10989	6497	1050	18536

9.2.5 Impact of climate change on the carbon budget

Carbon budget of the forests and wood products for the period 1995-2000 when Bau under current climatic conditions was applied can be seen in Figure 9.9. Estimated net primary production (NPP) was 409 Tg C/year. Approximately 18% of the NPP was bound in the tree biomass, 20% was removed from the forest and 62% transferred into the soil as litter, natural losses, unrecovered fellings and felling residues. Net ecosystem production (NEP) was 164 Tg C/year, as the difference between NPP and heterotrophic respiration (245 Tg C/year). When biomass removed from forest is taken into account, we get net biome production (NBP), which was 84.5 Tg C/year, which was 21% of the NPP. Total net sequestration of the system, net sector exchange (NSE), requires that also the amount that is sequestered in wood products is taken into account (net product exchange, NPE), which was 2.8 Tg C/year higher than NBP, i.e. 87.4 Tg C/year. NBP shows the net amount of carbon that is sequestered in the system. Approximately 87% of the net sequestration was into the tree biomass, 10% into the soil and 3% into the products. This demonstrates that if only part of the system (e.g. NPP or NEP or tree biomass) is considered, we get biased estimates for carbon sequestration.

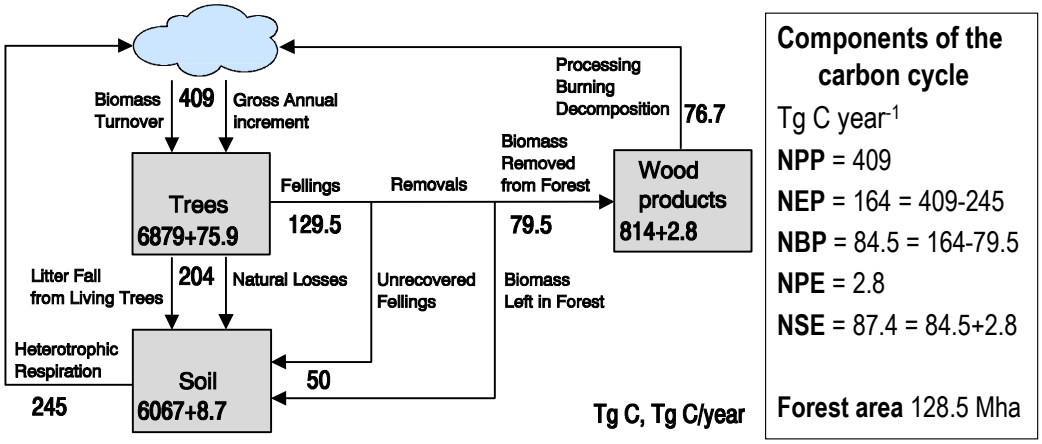

Figure 9.. Carbon budget of the included 27 countries, covering forest area of 128.5 million hectares, for the period 1995-2000 when BaU scenario was applied under current climatic conditions. Size of the carbon stock in tree biomass was 6879 Tg, in the soil 6067 Tg and in wood products in use 814 Tg. Other numbers in the graph represent carbon fluxes, Tg C/year.

When divided for the covered area, NPP was 3.18 Mg C/ha/year, NEP 1.29 Mg C/ha/year, NPE 0.02 Mg C/ha/year, NBP, 0.66 Mg C/ha/year and NSE 0.69 Mg C/ha/year (Table 9.4). NPP values per unit of forest area were highest in central Europe, smaller in southern and northern Europe. Net product exchange was negative in some countries, implying that more products are removed from use than manufactured. Net sector exchange was negative in one country, implying that forest and wood product sector is loosing carbon into the atmosphere and thereby enhancing greenhouse effect, while in other countries it was the contrary.

Table 9.4 Area average NPP, NEP, NPE, NBP and NSE values (Mg C/ha/year) for the 27 countries included in the study for the period 1995-2000 when BaU scenario was applied under current climatic conditions.

Country	NPP	NEP	NPE	NBP	NSE
Albania	1.40	0.60	-0.12	0.49	0.37
Austria	8.00	2.27	0.11	1.27	1.38
Belgium	5.25	1.87	0.16	0.66	0.82
Bulgaria	2.39	0.83	0.00	0.54	0.53
Croatia	1.87	0.85	-0.09	0.56	0.47
Czech Republic	4.00	1.38	0.08	0.23	0.31
Denmark	4.31	2.36	0.04	1.19	1.24
Finland	2.05	0.93	0.02	0.43	0.45
France	3.22	1.25	0.06	0.43	0.50
Germany	5.04	2.20	-0.01	1.34	1.32
Hungary	4.44	1.93	0.00	1.11	1.12
Ireland	5.30	2.74	0.11	1.92	2.04
Italy	3.10	1.39	0.03	0.67	0.69
Luxembourg	5.98	3.04	0.08	1.88	1.96
Macedonia	1.24	0.35	-0.03	-0.16	-0.19
Netherlands	4.53	1.90	0.03	1.11	1.14
Norway	1.70	0.78	0.04	0.40	0.44
Poland	3.80	1.60	0.03	0.87	0.91
Portugal	3.72	1.78	-0.05	0.92	0.87
Romania	4.60	2.28	-0.03	1.66	1.63
Slovak Republic	3.79	1.61	0.04	0.91	0.95
Slovenia	3.04	1.25	-0.02	0.65	0.63
Spain	2.85	0.53	0.05	0.00	0.05
Sweden	2.58	1.20	0.02	0.68	0.70
Switzerland	7.51	2.61	0.08	1.63	1.71
United Kingdom	4.48	2.31	0.06	1.65	1.71
Yugoslavia	1.95	0.69	-0.06	0.23	0.16
Europe	**3.18**	**1.29**	**0.02**	**0.66**	**0.69**

Net primary production increased slightly under current climatic conditions until 2030 when it started to decline slightly due to larger proportion of higher age classes (Figure 9.10). Under changing climatic conditions NPP continued to increase until 2050, when it was approximately 20% higher than at the beginning. NPP was slightly higher in the MultiF scenario than in the BaU scenario. Net ecosystem production decreased under current climatic conditions over time. This was due to fact that heterotrophic respiration increased more than NPP over time. Under changing climatic conditions NEP increased until 2010-2015, then it started to decline slightly. Also NEP was slightly higher in the MultiF scenario than in the BaU scenario. Net

biome production (NBP) also decreased under current climatic conditions, while under changing climatic conditions it increased until 2010. NBP was higher in the BaU scenario than in the MultiF scenario, since in the MultiF scenario more biomass was removed from the forest than in the BaU scenario. Also net sector exchange (NSE) decreased over time under current climatic conditions. Under changing climatic conditions NSE increased until 2015 and started to decline then. NSE was slightly higher in the BaU scenario than in the MultiF scenario.

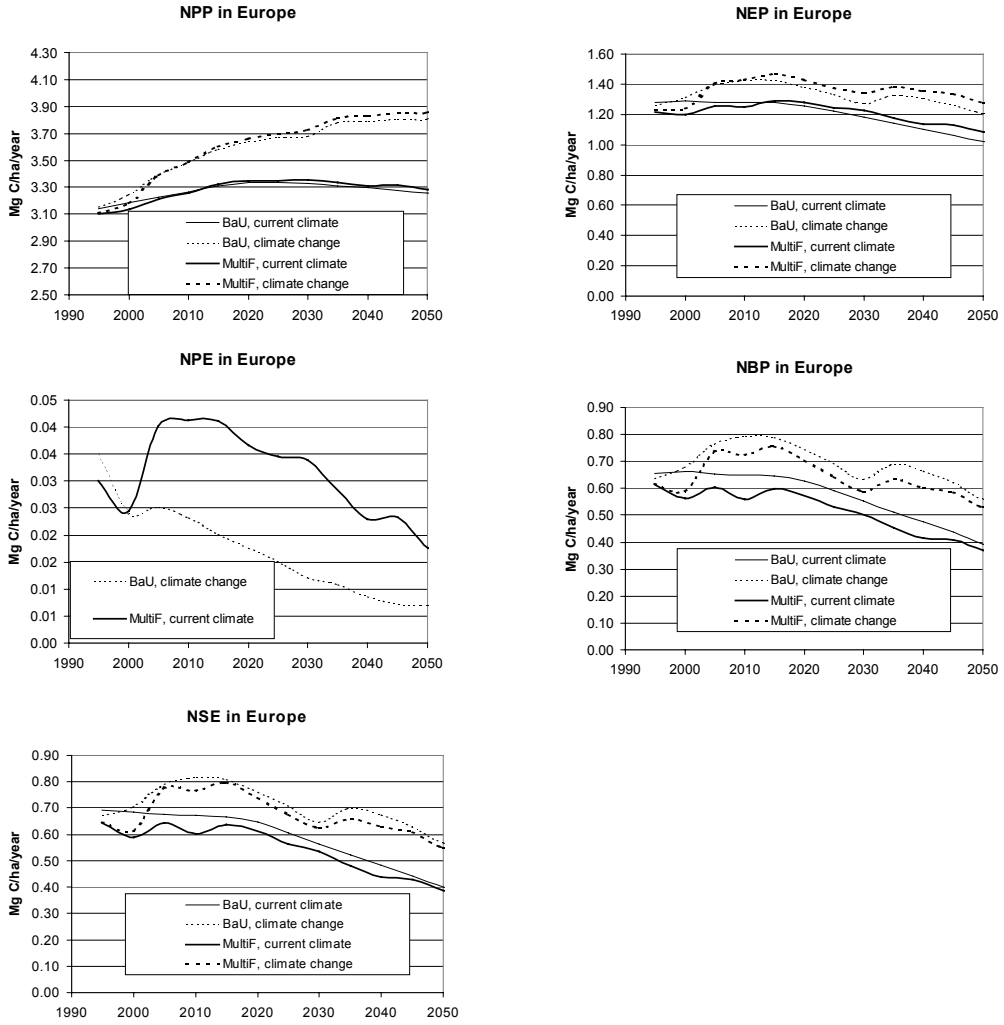

Figure 9.10 Development of the area average NPP, NEP, NPE, NBP and NSE values (Mg C/ha/year) of the 27 countries included in the study until 2050 under current and changing climatic conditions when BaU and MultiF scenarios were applied.

As a conclusion, carbon stocks in tree, soil and wood products will continue to increase next 50-60 years. Differences in carbon sequestration were very small between applied management scenarios, implying that on European level management should be changed more if aim is to influence carbon sequestration. Applied climate change scenario increased carbon stocks compared to current climatic conditions. Results also

demonstrate that the whole system should be considered when assessing carbon sequestration in forestry.

9.3 Map-based upscaling using GISMO's

R. Milne, D. Mobbs & J. Grace

Biome scale vegetation models

9.3.1 The EuroBiota forest ecosystem model.

9.3.1.1 Introduction

The EuroBiota ecosystem model describes the effect of changing temperature and atmospheric carbon dioxide concentration on productivity of European forests. The structure of the model was detailed in Chapter 4. Here we describe results from this model when driven by rising atmospheric CO_2 values and the pattern of change from 1830 to 2099 in mean monthly temperature for each 0.5° x 0.5° cell in Europe. Carbon stocks in trees and soils are discussed as well as net primary productivity (NPP), soil respiration (Rs) and net ecosystem productivity (NEP) for individual countries, boreal, temperate and Mediterranean eco-climatic zones and Europe as a whole.

9.3.1.2 Results and Discussion

The productivity of the forests of each eco-climatic zone zones (boreal, temperate, Mediterranean) of Europe as estimated by the EuroBiota model are presented in Figure 9.11 for Net Primary Productivity (NPP) and Soil Respiration (Rs) and Figure 9.12 for Net Ecosystem Productivity (NEP). The weighted averages for all of Europe are also shown.

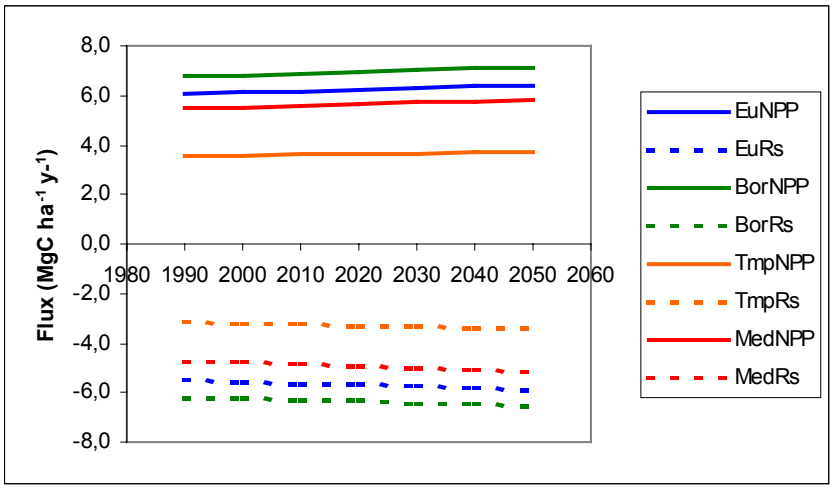

Figure 9.11 Productivity of European forest ecosystems from EuroBiota model for decades from the 1990s to the 2050s. Legend text refers to 'Eu' –Europe, 'Med' – Mediterranean zone, 'Tmp' - Temperate zone, 'Bor' – Boreal zone. 'NPP' – Net Primary Productivity, 'Rs' – soil respiration.

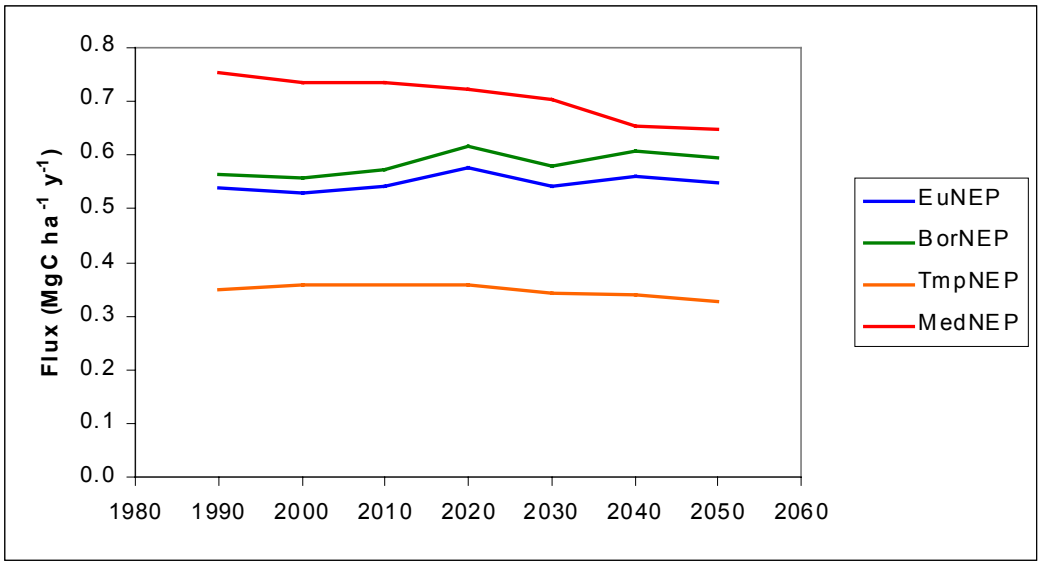

Figure 9.12 Net Ecosystem Productivity from EuroBiota model for European eco-climatic zones. (Legend text as in Figure 9.11 except 'NEP' – Net Ecosystem Productivity.)

The carbon dioxide concentrations and the average annual temperature anomaly for Europe, implied by the GCM data used to drive EuroBiota, are shown in Figure 9.13. Temperature anomalies are actually applied in EuroBiota to the mean 1960 to 1989 daily climatology for each month in each separate 0.5^0 cell separately. An illustration of the climatology is given in Figure 9.14 for a representative cell for each of the boreal, temperate and Mediterranean eco-climatic zones.

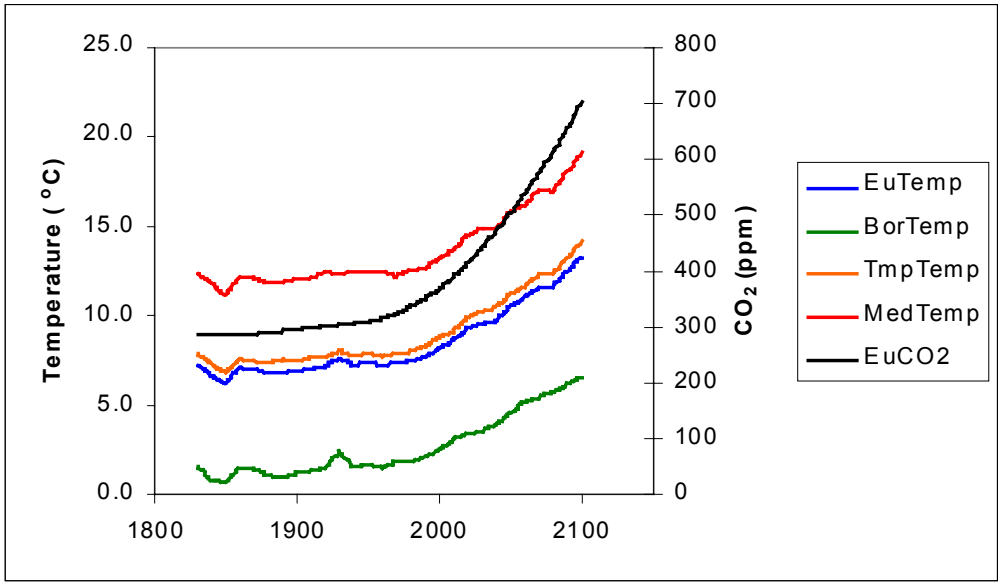

Figure 9.13 Mean European, boreal, temperate and Mediterranean average annual temperature anomaly (relative to 1960 to 1989 average) and variation in atmospheric CO_2 concentration from EuroBiota input climate data. (Legend text as in Figure 9.11)

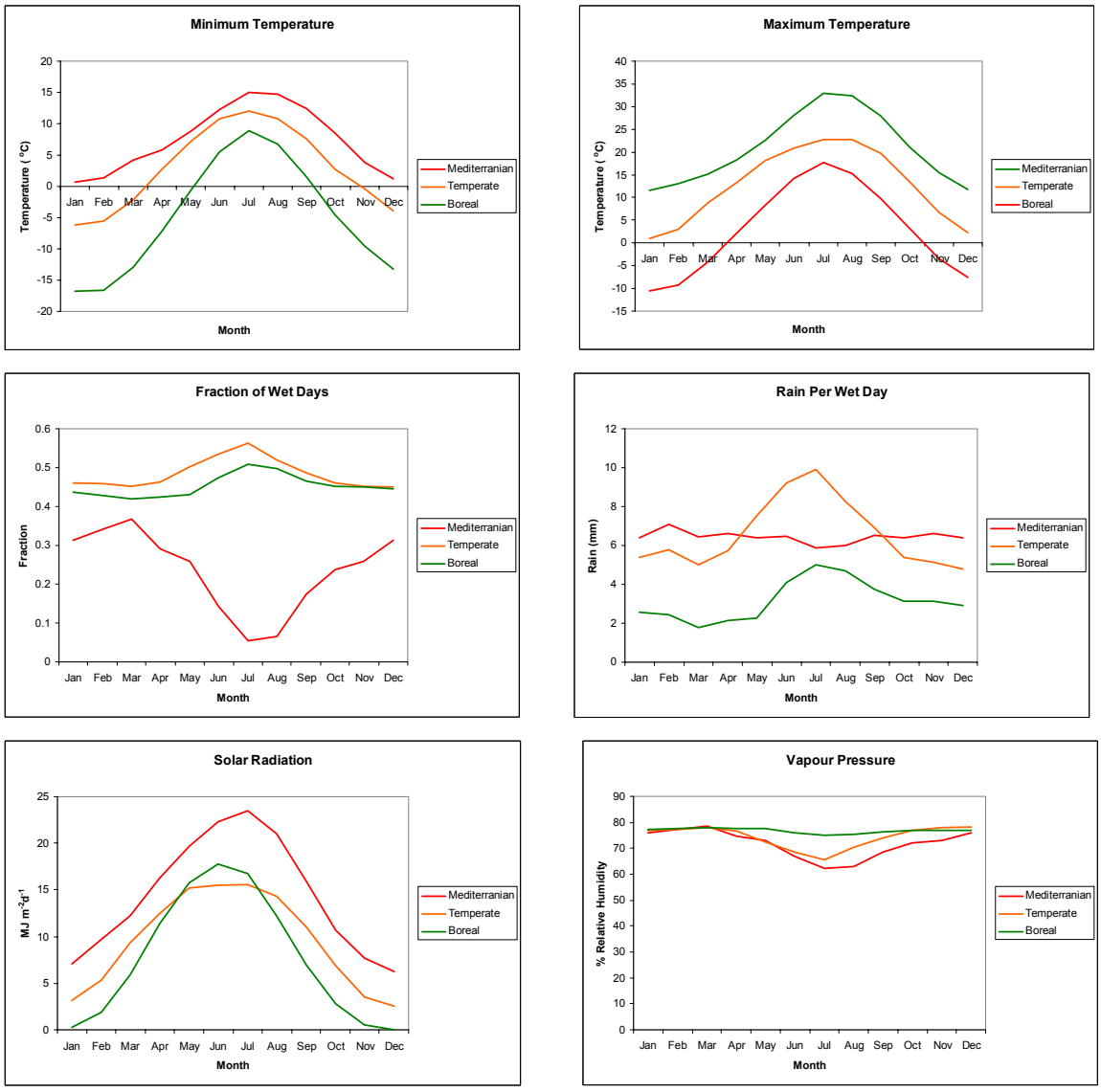

Figure 9.14 Mean 1960 to 1989 climatology of cells representative of boreal (Lat 66.0, Long. 19.0), Temperate (Lat. 48.0, Long. 13.0), Mediterranean (Lat. 38.0, Long. -4.0)

The estimates of NEP (Figure 9.12) show an overall increase in carbon uptake rate per unit area by European forest in the period from 1990 to 2050. This overall increase is however predominantly due to increases in the boreal zone whilst forests in both the temperate and Mediterranean zones have been estimated to have a reducing uptake rate per area of carbon. The contribution of changes in NPP and Rs in the different zones to the NEP changes is better shown in Table 9.5. We can see that in the boreal zone NPP increases more than Rs which results in the increase in NEP of Figure 9.12, in the temperate zone an increase in NPP is offset by a larger increase in Rs and in the Mediterranean zone a fairly large increase in NPP is heavily offset by the increase in Rs producing the large reduction in NEP.

Table 9.5 Changes predicted by EuroBiota in forest NPP, Rs and NEP between 1990 and 2050 in each of the three European eco-climatic zones compared to the European average

MgC/ha/y		EuNPP	EuRs	BorNPP	BorRs	TmpNPP	TmpRs	MedNPP	MedRs
	1990	6.06	-5.52	6.76	-6.19	3.53	-3.18	5.50	-4.75
	2050	6.41	-5.86	7.14	-6.55	3.74	-3.41	5.84	-5.19
Change		0.35	-0.33	0.38	-0.35	0.21	-0.23	0.34	-0.44
Change in NEP			0.01		0.03		-0.02		-0.10

These changes are likely to be due to the relative response to differing changes of temperature in the trees and soils of the three zones. In the Mediterranean zone the increase in temperature has caused a relatively greater increase in turnover of soil carbon compared to other zones and to the increase in productivity. It should be noted here that the soil carbon turnover model in EuroBiota has 4 separate compartments each with individual rate constants (ranging from days to many decades) which depend on temperature. It is therefore not influenced by problems associated with assumption in some other studies where a single soil carbon component has the effect of temperature on the rate for carbon turnover determined by short term experiments.

The overall change in the stock of tree and soil carbon per unit area in the period 1990 to 2050 as predicted by EuroBiota is shown in Figure 9.15 and as a total carbon stock in Table 9.6, assuming a fixed forest area intermediate between the European total forest area used in the EFISCEN model and in the Forest Probability map (Chapter 9.5).

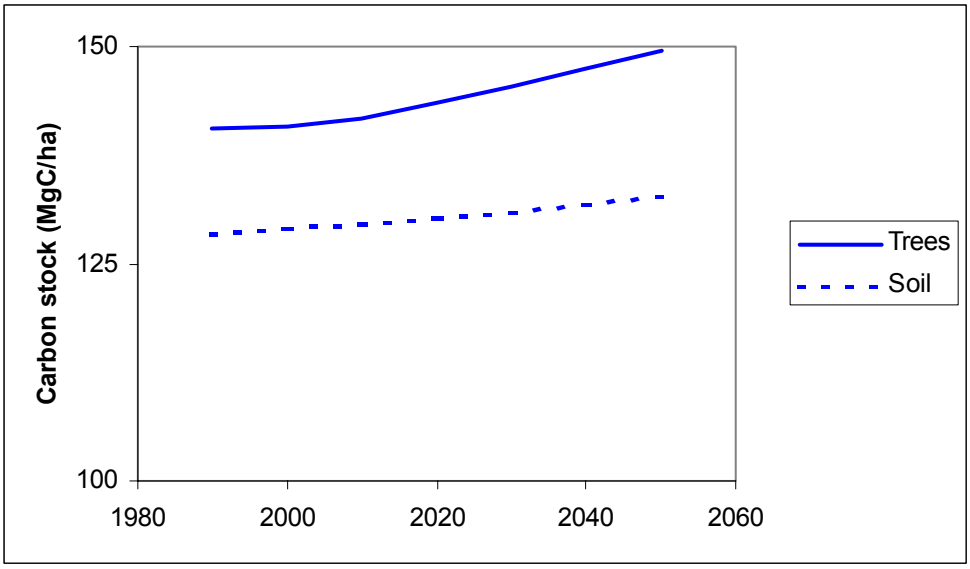

Figure 9.15 Changes between 1990 and 2050 in tree and soils carbon stock per unit area as estimated by EuroBiota model.

Table 9.6 Future changes in total carbon stock in European ecosystems as predicted by EuroBiota.

		1990	2050
Forest area	km²	1,250,000	1,250,000
Tree carbon stock	TgC	17.6	18.7
Soil carbon stock	TgC	16.0	16.6
NPP	TgC y^1	0.76	0.80
NEP	TgC y^1	0.07	0.07
Rs	TgC y^1	-0.69	-0.73

As the grid cell size (0.5°) is sufficiently small it was possibly to summarise the outputs of EuroBiota in terms of most European countries (except for a few cases where the country was too small or the model had computational problems). These data are presented in Table 9.7 and mapped in Figure 9.16.

Table 9.7 Future change in NEP of forest ecosystems in European countries as estimated by EuroBiota. These estimates are of MgC ha^{-1} y^{-1} and hence to don include effects of expansion in forest area but do include the effect of changing age structure as predicted in the EFISCEN 'Business as Usual' scenario.

Flux MgC ha^{-1} y^{-1}	**NEP 1990**	**NEP 2050**	**Change**
ALBANIA	1.39	0.81	-0.58
AUSTRIA	0.08	0.14	0.07
BELGIUM	0.74	0.82	0.08
BOSNIA AND HERZEGOVINA	0.14	0.20	0.06
BULGARIA	0.12	0.17	0.05
BELARUS	0.04	0.12	0.08
CROATIA	1.12	0.81	-0.31
CZECH REPUBLIC	0.66	0.50	-0.16
DENMARK	0.70	0.45	-0.25
ESTONIA	0.21	0.27	0.06
FINLAND	1.05	1.13	0.08
FRANCE	0.80	0.90	0.10
GERMANY	0.55	0.47	-0.08
GREECE	0.17	0.20	0.04
HUNGARY	1.05	0.74	-0.32
ICELAND	0.17	0.24	0.08
IRELAND	0.49	0.30	-0.19
ITALY	1.27	0.95	-0.32
LATVIA	0.13	0.21	0.08
LITHUANIA	0.10	0.15	0.06
MACEDONIA	1.35	1.05	-0.30
NETHERLANDS	0.10	0.16	0.07
NORWAY	0.93	0.92	-0.01
POLAND	0.61	0.51	-0.10
ROMANIA	0.86	0.61	-0.25
RUSSIA	0.24	0.24	0.01
SLOVAKIA	0.83	0.67	-0.16
SLOVENIA	0.73	0.71	-0.03
SPAIN	0.14	0.25	0.11
SWEDEN	0.21	0.23	0.02
SWITZERLAND	0.33	0.27	-0.07
TURKEY	0.17	0.24	0.08
UKRAINE	0.03	0.14	0.12
UNITED KINGDOM	0.72	0.50	-0.22

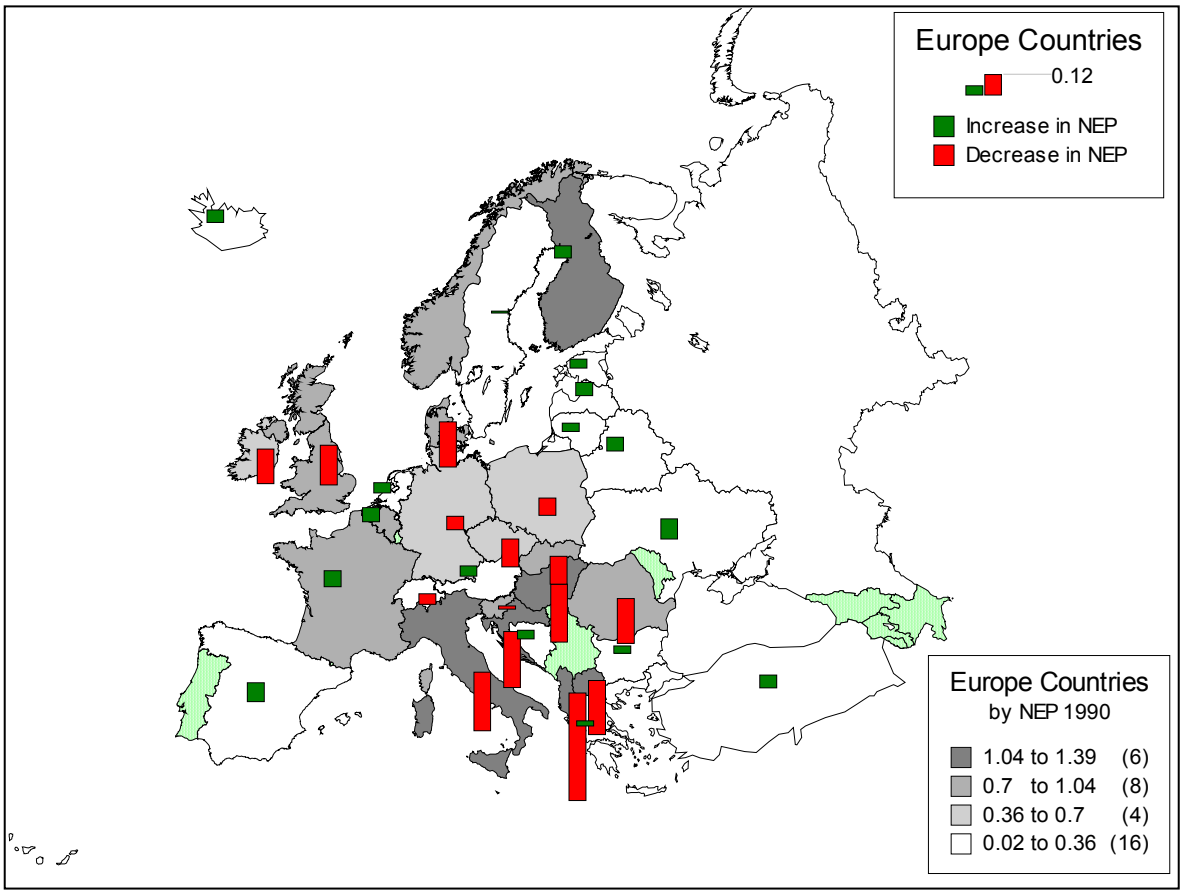

Figure 9.16 Net Ecosystem Productivity (MgC $ha^{-1}y^{-1}$) in 1990 and change predicted by 2050 by EuroBiota model of ecosystem productivity and EFISCEN 'Business as Usual' production scenario. (Countries shaded green have no data or the forest area data caused computational difficulties)

9.3.2 The HYBRID ecosystem model

9.3.2.1 Introduction

As described in Chapter 4, Hybrid (Friend *et al.* 1997), is a dynamic, global vegetation model. driven by transient climate output from the UK Hadley Centre GCM (HadCM2) with the IS92a scenario of increasing atmospheric CO_2 equivalent, sulphate aerosols and predicted patterns of atmospheric N deposition Changes in areas of vegetation types and carbon storage in biomass and soils were predicted for areas from 34 °N, 25 °W to about 72.5°N, 36 °E from 1860 to 2100. The basic spatial resolution of this application of the model is the 3.75° x 2.5° of the GCM and the outputs are the predicted changes in carbon per unit area in the potential vegetation types for each of these cells.

9.3.2.2 Results and Discussion

The productivity of all ecosystems in the three eco-climatic zones (boreal, temperate, Mediterranean) of Europe are shown in Figure 9.17 for Net Primary productivity (NPP) and Soil Respiration (Rs) and Figure 9.18 for Net Ecosystem productivity. The weighted averages for all of Europe are also shown. These productivities and respiration are for all plant types together, although the greatest contribution will be from forests.

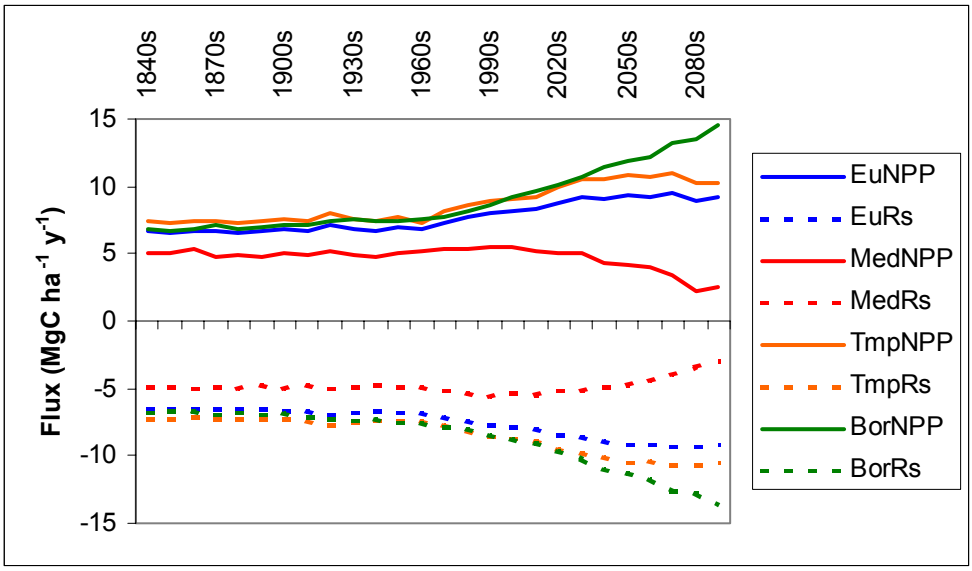

Figure 9.17 Productivity of European ecosystems (primarily forests) from Hybrid model for decades from the 1830s to the 2090s. Legend text refers to 'Eu' –Europe, 'Med' – Mediterranean zone, 'Tmp' - Temperate zone, 'Bor' – Boreal zone. 'NPP' – Net Primary Productivity, 'Rs' – soil respiration.

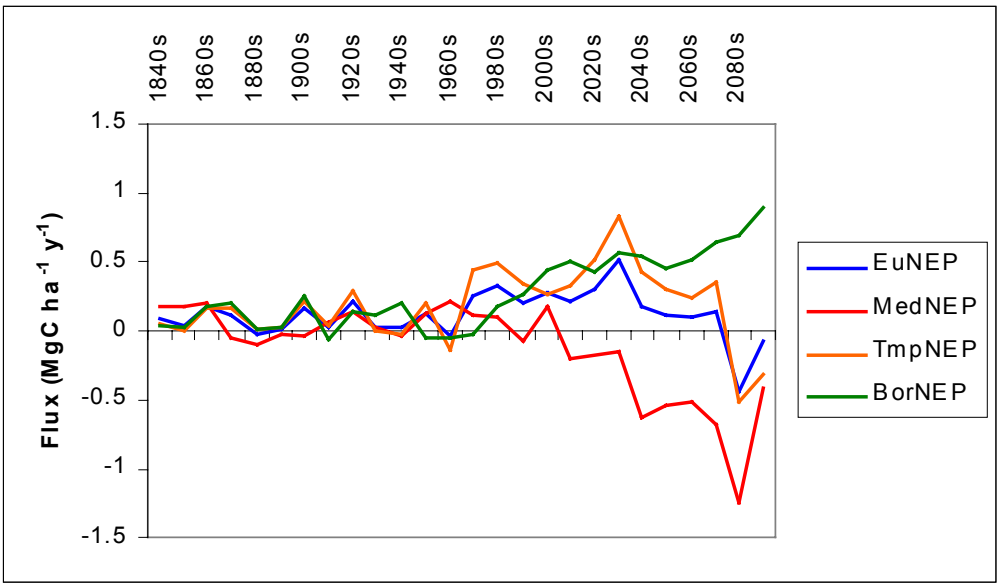

Figure 9.18 Net Ecosystem Productivity from Hybrid model for European eco-climatic zones. (Legend text as in Figure 9.17 except 'NEP' – Net Ecosystem Productivity.)

The equivalent climatic data is shown in Figure 9.19 (rainfall) and Figure 9.20 (temperature) and the assumed carbon dioxide variation in Figure 9.21.

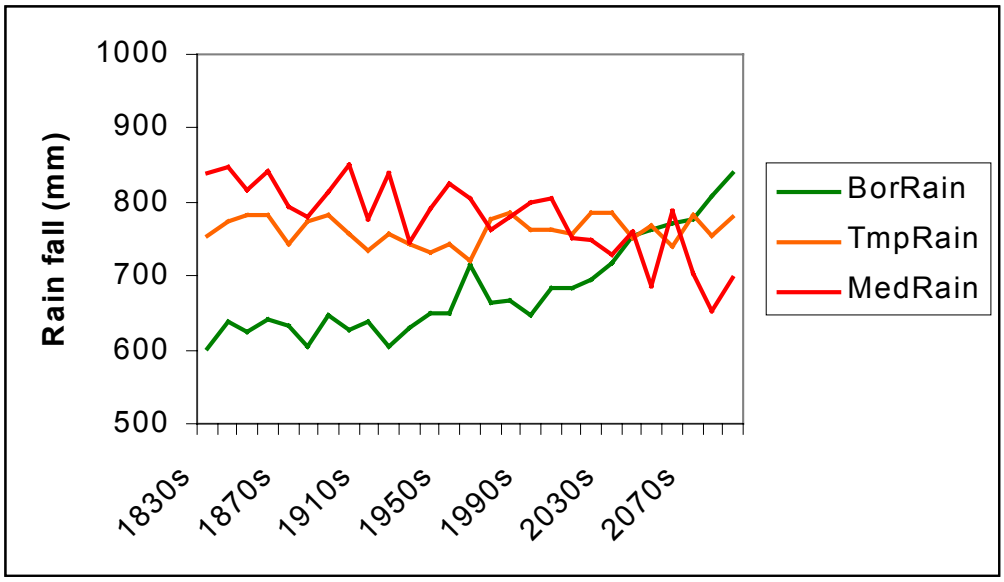

Figure 9.19 Rainfall derived from HadCM2 model used to drive Hybrid model. Average for all GCM cells in each eco-climatic zone shown. (Legend text as Figure 9.17 except 'Rain' – rainfall)

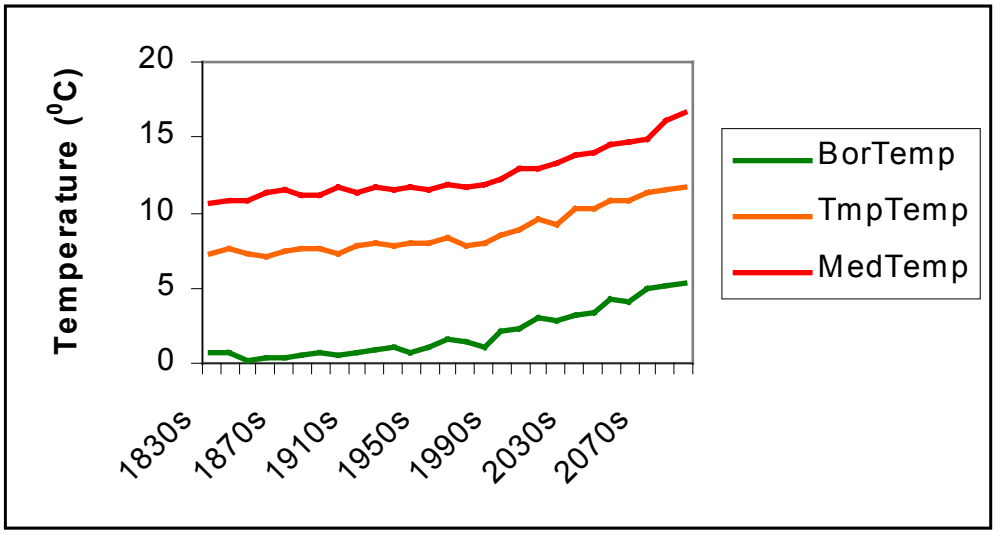

Figure 9.20 Temperature derived from HadCM2 model used to drive Hybrid model. Average for all GCM cells in each eco-climatic zone shown. (Legend text as Figure 9.17 except 'Temp' – Temperature)

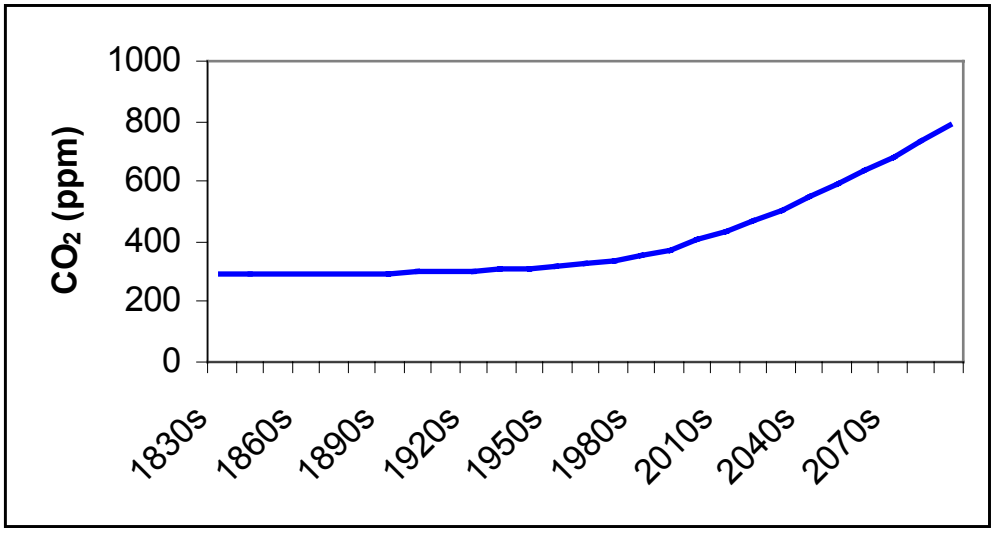

Figure 9.21 Change in atmospheric CO_2 concentration used to drive Hybrid.

The most distinct feature of these results is that although productivity in Europe as a whole increases from the 1930s onwards this increase masks different responses in the different zones. In particular increases in NPP in the Mediterranean zone are offset by increases in Rs which causes NEP to fall significantly and become negative (i.e. emission of carbon dioxide) from about the 1990s. A similar but less pronounced pattern can be seen for the temperate zone. Ecosystems in the boreal zone are predicted to increase their NEP up until the 2090s. Much of this increase will be driven by the increasing CO_2 concentration. Temperature will have a positive effect on NPP but will also increases turnover of carbon in soils (soil respiration, Rs). The overall effect of these effects is different in the 3 zones. In the boreal zone NPP increases faster than Rs resulting in increasing NEP. In the temperate zone, although NPP does increase under the influence of CO_2 and temperature, the offsetting effect

of temperature on Rs increases more quickly and hence NEP initially rises (up to about the 2030s) but then falls to become negative (implying emission of CO_2) after the 2070s. In the Mediterranean zone a similar pattern is estimated but NPP actually falls after about 2000 hence NEP never becomes much greater than zero before falling steeply into negative values after the 1990s. The predicted decrease in NPP in the Mediterranean is probably caused, in the Hybrid model, by the effect of changes in the composition of the ecosystem. Although most productivity (and stock) of carbon in Europe is related to forests within Hybrid, grassland can become more common if the climate is unsuitable for trees. The GCM prediction for rainfall in the Mediterranean zone shows reductions from about 840 mm per year in the 1930s to about 700 mm in the 2090s (Figure 9.20). The temperate zone shows little change (750 to 780 mm) whilst the boreal zone shows an increase from 600 to 840 mm. The reduction in Mediterranean rainfall will, in the Hybrid model, tend to shift the mix of plant types toward grasses, which have smaller NPP, and hence cause the reduction shown in Figure 9.21. Similar effects, but much more pronounced, have also been predicted by Hybrid for Amazonian forests late in the next century (White et al 2000). These predictions must however be treated with caution as they depend strongly on the HadCM2 prediction of reducing rainfall in these areas and on the sensitivity of the mechanisms in the Hybrid model which show preference for trees in drier conditions.

Thus although stock of carbon in trees is predicted by Hybrid to increase across Europe as a whole soil stock will eventually fall. This is show Figure 9.22 as stock density and as total stock in Table 9.8 for fixed European forest area, assumed to be intermediate between the total forest area used in the EFISCEN model and in the Forest Probability map (Chapter 9.5).

Table 9.8 Future changes in total carbon stock in European ecosystems as predicted by Hybrid.

		1990s	2050s
Forest area	km^2	1250000	1250000
Tree carbon stock	TgC	8.24	10.35
Soil carbon stock	TgC	18.25	18.18
NPP	TgC/year	1.00	1.17
NEP	TgC/year	0.03	0.01
Rs	TgC/year	-0.97	-1.15

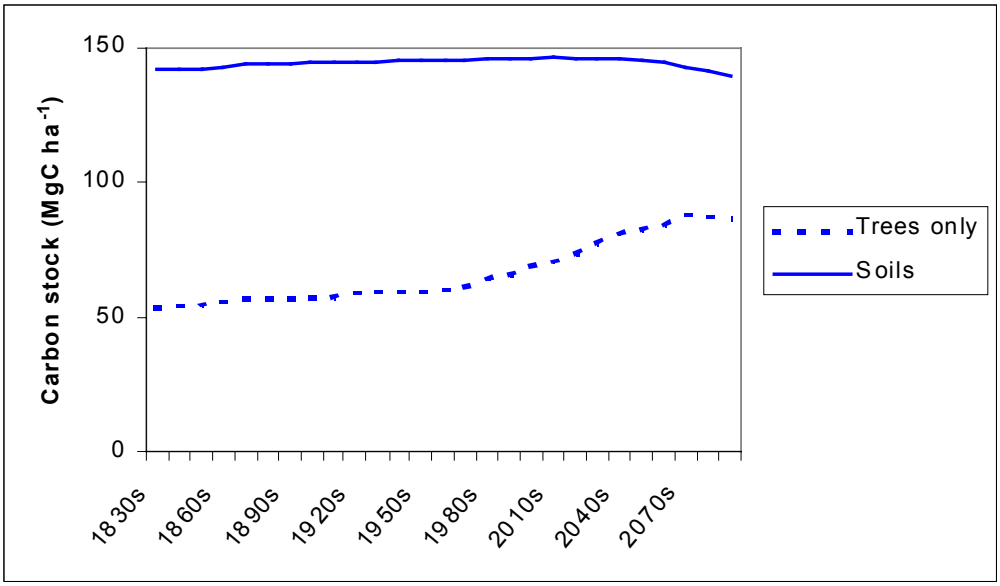

Figure 9.22 Changes in carbon stock in European forests as predicted by Hybrid model.

9.3.2.3 References

White, A., M. G. R. Cannell, A. D. Friend, CO_2 stabilization, climate change and the terrestrial carbon sink, *Global Change Biology,* ***6,*** 817-833, 2000.

9.4 Upscaling using remote sensing

Frank Veroustraete & Hendrik Sabbe

The C-Fix procedure was applied over the European continent with the data sets described in chapter 4.2. for the year January 1997 till December 1997

In a first step, in-depth quantitative validations were performed. C-Fix estimates were compared with eddy covariance flux measurements performed in the course of the year 1997 for a number of European forest sites within the framework of the EUROFLUX-project. Subsequently the European geographical and temporal distribution of C-Fix estimates of Net Ecosystem Production (NEP) is demonstrated.

To obtain information on the forest NEP for Europe, a forest probability map as described in chapter 4.2. was incorporated in C-Fix. In LTEEF-II, different simulation models were developed. Hence, an account is given of the comparison of their results with C-Fix estimates. Finally, a comparison of C-Fix results using SPOT-VEGETATION imagery as opposed to NOAA/AVHRR imagery is made.

9.4.1 Comparison with flux measurements

Carbon fluxes can be measured in detail at test sites by means of eddy covariance techniques. This approach is for instance applied for several forest sites in Europe, which are investigated within the framework of the EUROFLUX network ("Long term carbon dioxide and water vapour fluxes of European forests and interactions with the climate system"). These measurements are compared with C-Fix estimates at the NOAA pixel level (≈1.1 km²). Table 9.9 illustrated the main characteristics of the selected forest sites.

Table 9.9 Main characteristics of the selected EUROFLUX sites

Site	LAT [° N]	LON [° E]	Elevation [m]	Species ¥	Ecosystem Φ
Finland	61.51	24.17	170	C	PNM
Italy	41.52	13.38	1560	BD	NM
Netherlands	52.10	5.45	25	C	PNM
Germany	50.58	13.38	780	C	NM
France	48.40	7.05	300	BD	NM
France	44.05	0.05	60	C	PNM
Belgium	50.18	6.00	450	M, BD + C	PNM

¥ M. mixed, BD. broad-leaved deciduous, C. coniferous
Φ PNM. planted stand with traditional forest management, NM. Natural origin and managed

Figure 9.23 illustrates the evolution during 1997 of NEP measured as well as estimated with C-Fix, for the different forest sites as defined in table 9.9. The left pane shows the decadal (10 daily mean) values and the right pane a regression graph of the Euroflux measurements versus C-Fix estimates for the available daily measurements.

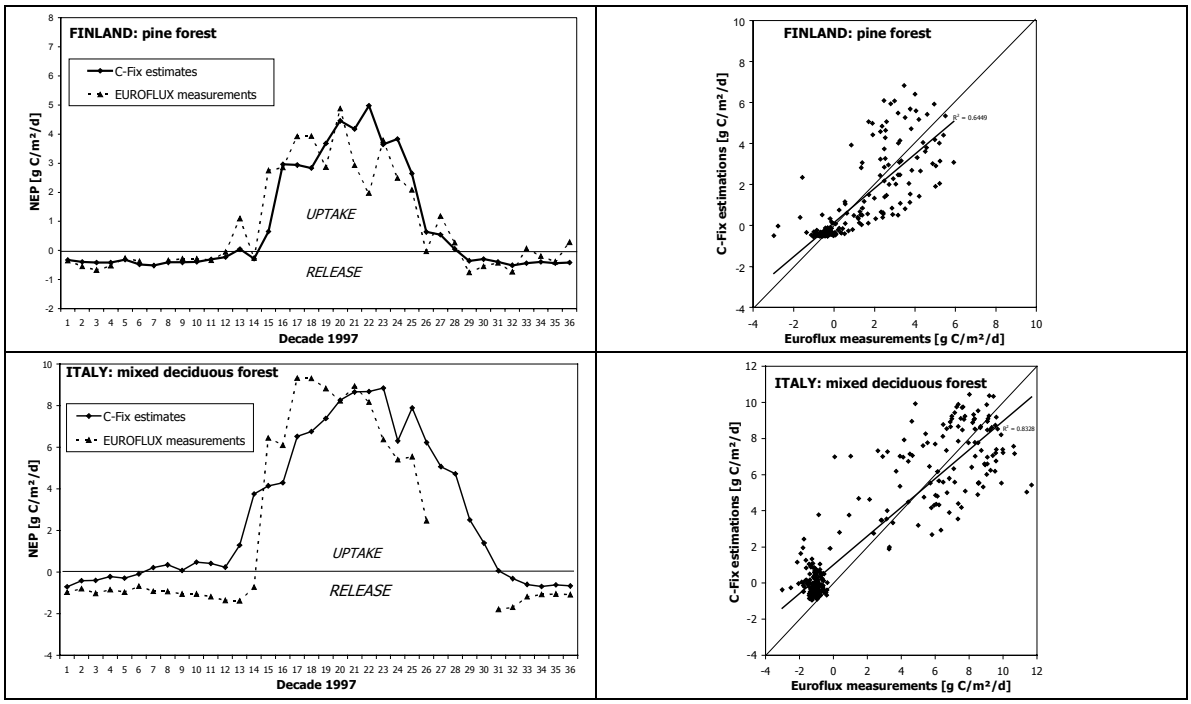

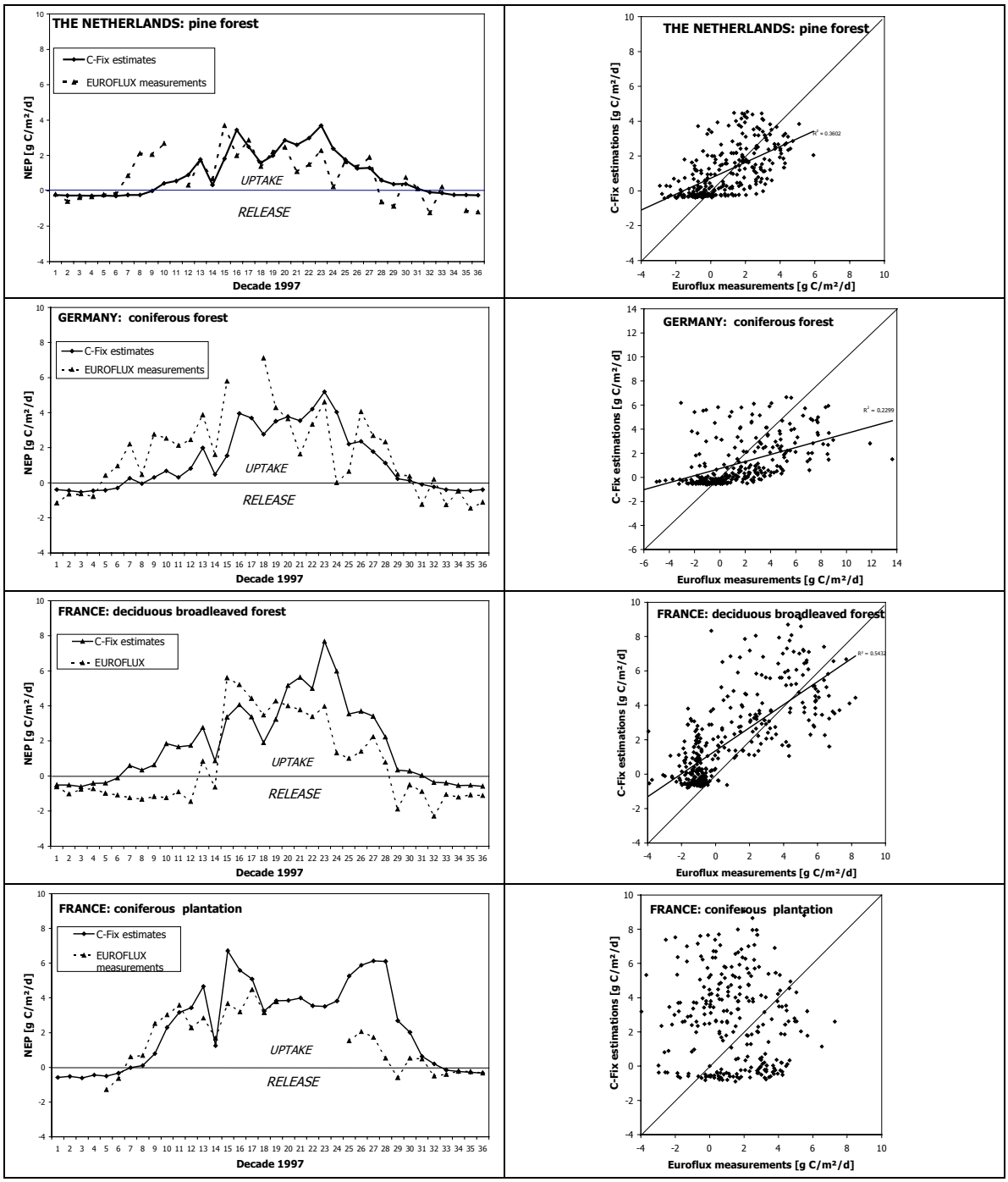
THE NETHERLANDS: pine forest
C-Fix estimates
EUROFLUX measurements
NEP [g C/m²/d]
UPTAKE
RELEASE
Decade 1997
THE NETHERLANDS: pine forest
C-Fix estimations [g C/m²/d]
Euroflux measurements [g C/m²/d]
GERMANY: coniferous forest
C-Fix estimates
EUROFLUX measurements
NEP [g C/m²/d]
UPTAKE
RELEASE
Decade 1997
GERMANY: coniferous forest
C-Fix estimations [g C/m²/d]
Euroflux measurements [g C/m²/d]
FRANCE: deciduous broadleaved forest
C-Fix estimates
EUROFLUX
NEP [g C/m²/d]
UPTAKE
RELEASE
Decade 1997
FRANCE: deciduous broadleaved forest
C-Fix estimations [g C/m²/d]
Euroflux measurements [g C/m²/d]
FRANCE: coniferous plantation
C-Fix estimates
EUROFLUX measurements
NEP [g C/m²/d]
UPTAKE
RELEASE
Decade 1997
FRANCE: coniferous plantation
C-Fix estimations [g C/m²/d]
Euroflux measurements [g C/m²/d]

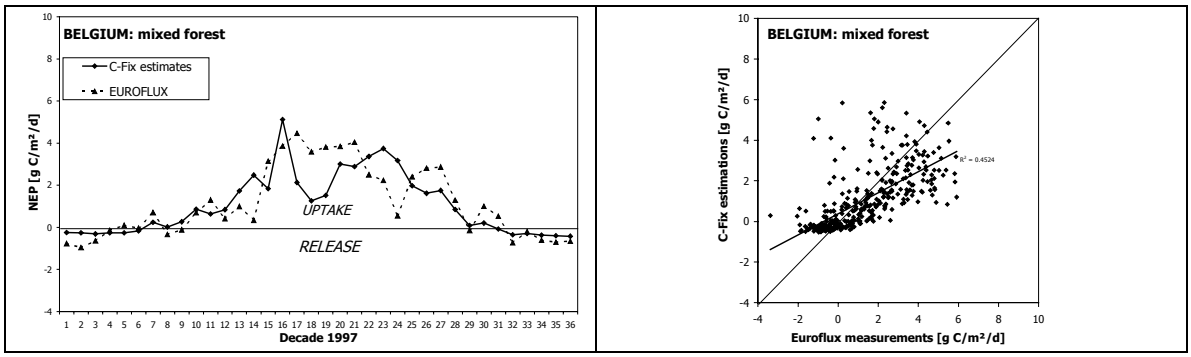

Figure 9.23 Evolution (decadal means - left) and regression (daily values - right) of Net Ecosystem Production (NEP) for seven forests sites of the Euroflux-network: Results of eddy covariance field measurements (January 1997-December 1997, data partly missing) versus C-Fix estimates (January 1997 – December 1997).

The correlation and 1 to 1 relationship observed for the C-Fix estimates and covariance measurements of the forests located in Finland and Italy agree fairly well. However, for the other sites these observations are less straightforward. Larger spreading of the observed points and a larger deviation form the 1:1 line is observed. The difference between sites is also strikingly elicited. For example, in summer, the Italian deciduous forest shows a much higher carbon uptake than the pine stand in the Netherlands. In winter, both forests act as carbon sources due to lower temperatures and incoming radiation. However, this source function is less pronounced for evergreen pinewood, which seems to maintain a smaller productivity in the cold season.

The next figure (Fig. 9.24) shows the regression between the yearly total carbon fixation estimated with C-Fix and covariance measurements from Euroflux sites. C-Fix NEP simulations can be observed to be systematically higher than covariance observations from the Euroflux network except for the Griffin site. An obvious reason for this can be that we are in this case taking the value for all vegetation in our calculation and it is well known that the Euroflux sites are typically forest sites. Any piece of a NOAA pixel that is non-forest hence would increase our estimate and lead to an overestimate with respect to a covariance measurements of a 1by 1 km plot, which is not fully forested.

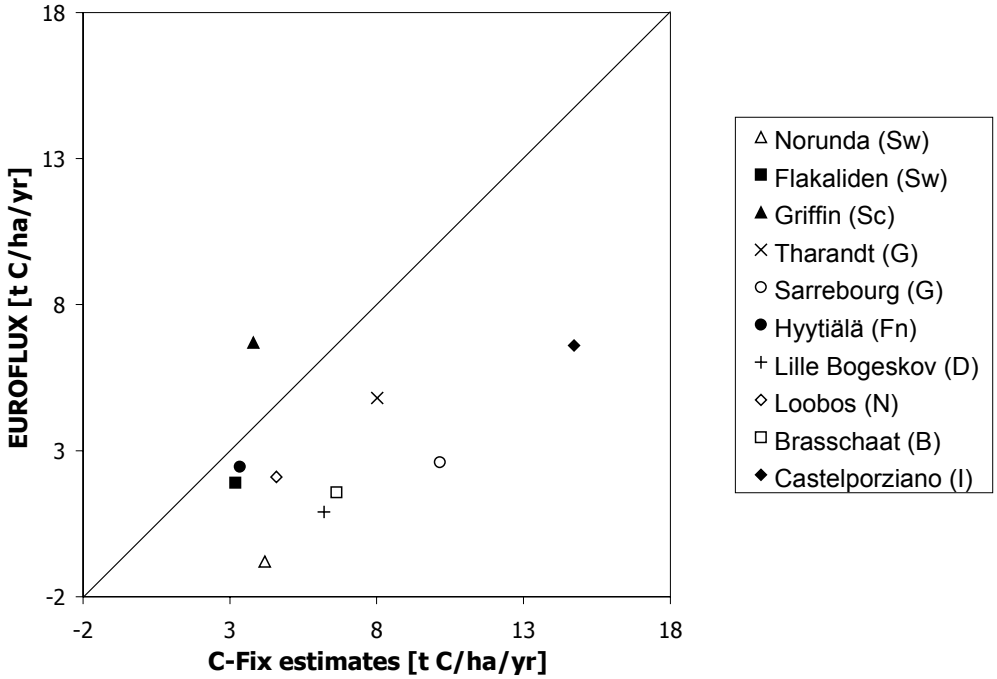

Figure 9.2: Regression of then Net Ecosystem Production (NEP - yearly total) for 10 Euroflux sites: results of the eddy covariance field measurements (January 1997 - December 1997, Courtesy: Valentini R. et al. (2000)) versus the C-Fix estimations.

9.4.2 European scale

As an example of the results obtained for the European continent, figure 9.25 illustrates the seasonality of mean Net Ecosystem Production (NEP) estimated with C-Fix.

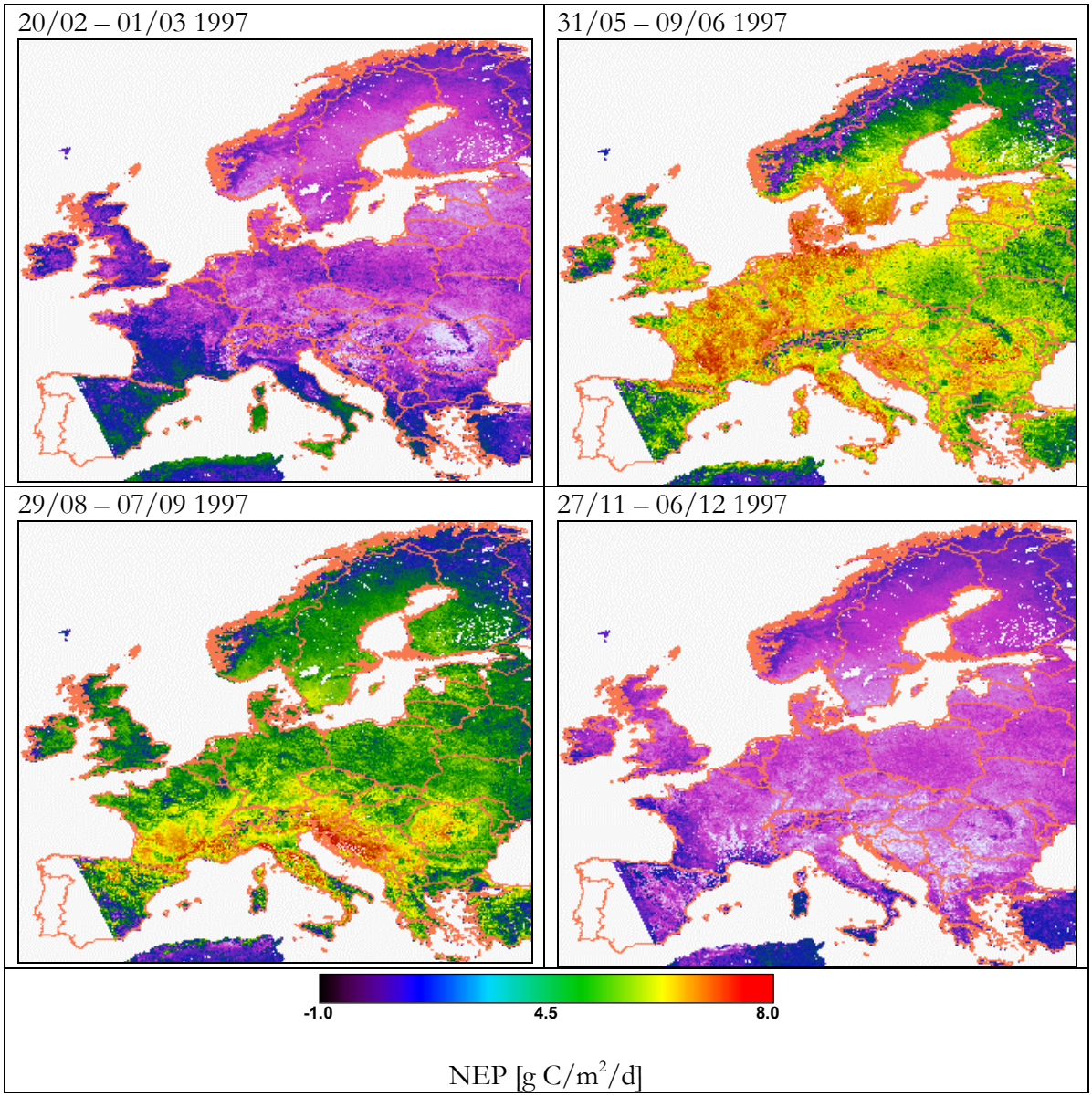

Figure 9.25 Seasonality observed with decadal mean values of Net Ecosystem Production estimates with C-Fix for the four seasons.

The temporal evolution, regional distribution and absolute NEP levels, illustrated in the figure above, all agree with intuitive expectations on NEP geographical distributions. Throughout Europe, NEP culminates (logically) in spring and summer, and productivity significantly decreases towards Northern latitudes. In autumn and winter, NEP is only significant in the Mediterranean belt with its winter regime of rains and temperatures higher relative to the North and centre of Europe. Persistently low NEP values can be observed in mountainous, boreal and semi-desert (North Africa) areas. Unfortunately, parts of Spain and Portugal are missing due to angular observation constraints in the NOAA image-processing step.

Figure 9.26 illustrates the mean NEP for the year 1997. High values are found in the southern part of Europe, low values in the northern part. The European carbon fixation for 1997 for the territory of the European continent as calculated with C-Fix is equal to 2.84 P (= 10^{15}) g C (Portugal and part of Spain not included). This value takes into account all vegetation (forests, crops, grasslands, …).

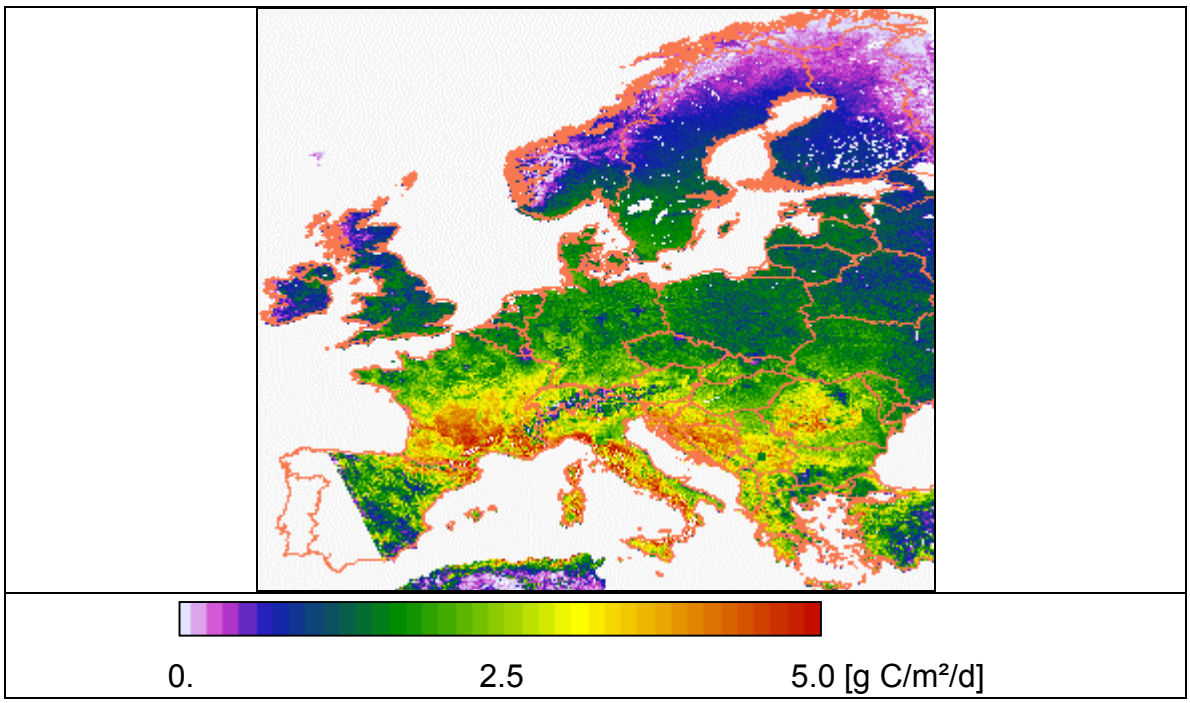

Figure 9.26 Yearly mean Net Ecosystem Production (NEP) for the year 1997 and for Europe (excluding some parts of Spain and Portugal).

Table 9.10 for each country of Europe gives the total area in km², the mean carbon fixation expressed as Mg C/ha/year and the total carbon fixation (NEP) in T (= 10^{12}) g C/country/year as well as the percentage contribution of each country to the European carbon fixation total.

Table 9.10 Net Ecosystem Production (NEP) for the year 1997 expressed in Mg C/ha and Tg C per country area for all European countries and percentage contribution of carbon fixation for each country to total European carbon fixation (NEP).

Country	Area [km²]	[Mg C/ha/yr]	[Tg C/country/yr]	[%]
Albania	28442	25.02	18.77	0.73
Austria	83741	8.42	51.12	2.0
Belgium	30589	25.67	14.81	0.58
Bosnia	51542	21.03	48.89	1.91
Belarus	201927	10.31	78.29	3.06
Bulgaria	110982	33.36	65.53	2.56
Denmark	41575	12.20	21.51	0.84
Ireland	68747	60.3	17.31	0.68
Estonia	43660	7.35	20.39	0.8
Czech	78633	8.99	38.79	1.52
Finland	313685	3.29	80.35	3.14
France	547210	31.22	427.63	16.73
Germany	293929	10.69	201.19	7.87
Greece	87725	12.06	70.92	2.77
Croatia	41053	19.50	49.28	1.93
Hungary	70603	25.42	55.56	2.17
Italy	211845	16.49	238.33	9.32
Latvia	60889	9.70	30.21	1.18
Lithuania	58925	17.99	26.78	1.05
Slovakia	38275	8.3	26.49	1.04
Luxembourg	2061	9.89	0.60	0.02
Moldova	25599	51.07	17.34	0.68
Macedonia	17618	30.03	16.03	0.63
Montenegro	9711	18.51	10.22	0.4
Netherlands	30116	21.68	17.03	0.67
Norway	384664	2.16	69.83	2.74
Poland	261840	9.96	137.20	5.37
Romania	175987	25.53	166.64	6.52
Russia	232401	4.39	55.10	2.16
Slovenia	15209	15.70	18.58	0.73
Serbia	63331	32.66	67.25	2.63
Sweden	503221	4.81	154.31	6.04
Switzerland	31313	6.64	22.80	0.89
United Kingdom	215618	9.58	87.77	3.43
Ukraine	228698	13.19	132.52	5.186
TOTAL	4661374		**2555.35**	

The total carbon fixation for 1997 for Europe is 2.55 P (=10^{15}) g C. High carbon mean values [Mg C/ha/yr] are found in the south and eastern part of Europe. We must notify that some countries are not completely in the region of interest, for example Russia and that some countries are not completely covered Spain and Portugal.

France has the highest carbon fixation expressed as percentage of the total carbon fixation. The highest mean carbon fixation is found in Ireland with a value of 60 Mg C/ha/year. This number is twice the value of other countries which have a sometimes higher forested and/or agricultural area. Northern areas like Scandinavia, have a low mean carbon fixation value due to the short growing season.

The following figure shows GPP, NPP and NEP in function of latitude along a transect traced at 13°E (see fig. 9.27). Despite the wide variation in land cover types, a consistent trend in GPP, NPP and NEP is found. Latitude is not a phenomenological driving variable per se, however it is a good proxy for the actions of a multiplicity of factors, for example radiation balance, length of growing season, frost events, temperature, … Moreover, the Monteith approach used in C-Fix to estimate GPP has a linear relationship with incoming radiation, NPP and NEP are also linear related to GPP and thus radiation. According to Valentini et al. (2000), GPP in EUROFLUX sites is rather conservative across sites and latitude.

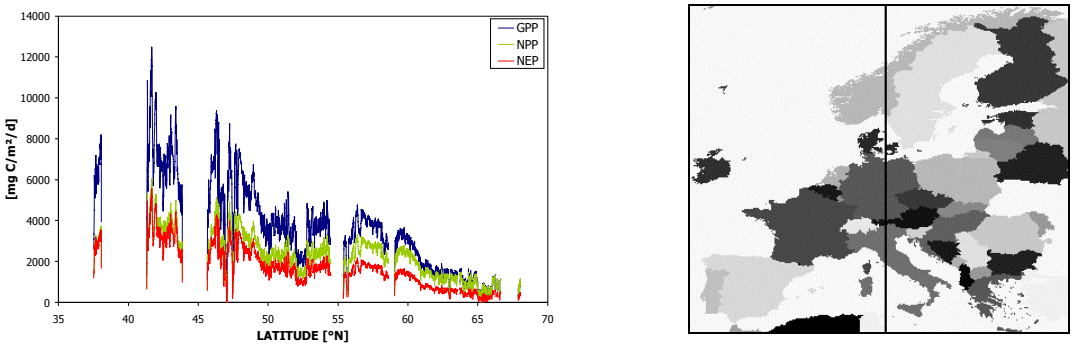

Figure 9.27 Gross Primary Production (GPP), Net Primary Production (NPP) and Net Ecosystem Production (NEP) estimated with C-Fix plotted against latitude. Transect is made at 13° E

9.4.3 Incorporation of a forest probability map

At this level, we discussed the total vegetation carbon fixation for the European area. However, to describe the forest carbon fixation, the amount of the forest area for each pixel is needed. For this objective a forest probability map is used (paragraph 4.3.). The map indicates the distribution and density of wooded area in the pan-European area. The 'forest' cover, depicted by percentage forest probability represents an estimate of woody vegetation present within a single AVHRR pixel (1.1 km by 1.1 km) (JRC, 1999).
For each pixel, the total carbon fixation is multiplied with the value of the probability map; a linear relationship is assumed between the carbon fixation and the forest surface.
The following figure shows the forest probability for Europe and the corresponding European forest yearly mean Net Ecosystem Production.

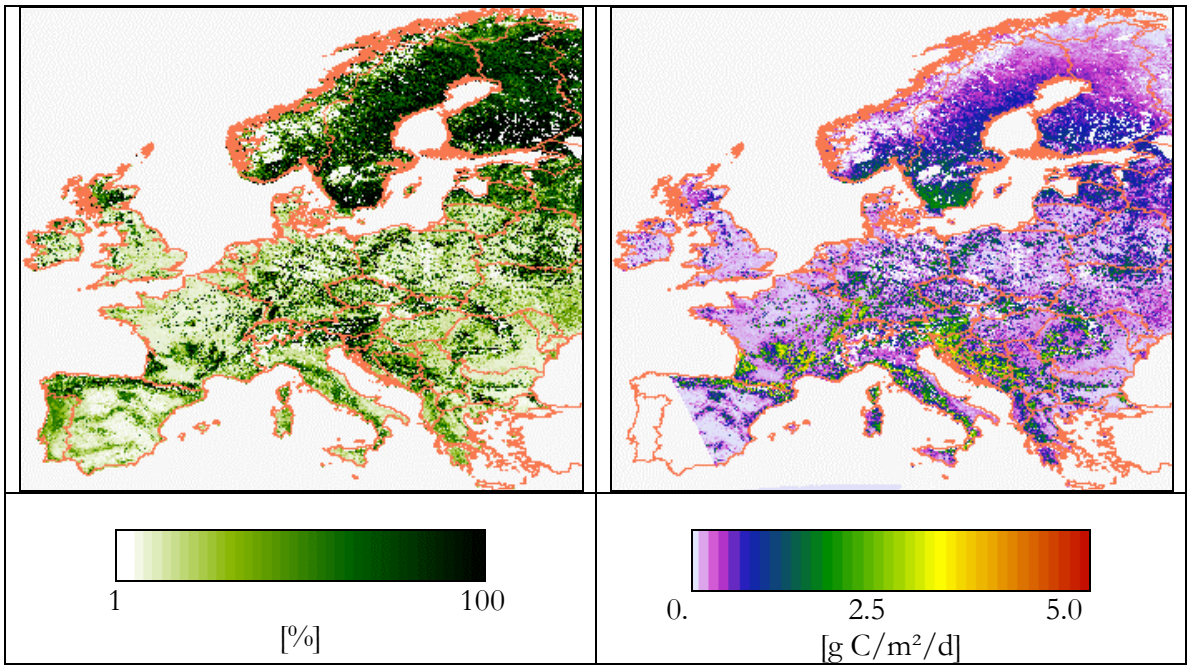

Figure 9.28 Left: AVHRR-based forest probability map of pan-European area. Right: yearly mean European forest Net Ecosystem Production (NEP)

Table 9.11 gives an overview of the carbon fixation for the forests in each country. As in Table 5.2 high values are found in the southern and eastern part of Europe.

Table 9.11 Overview of the forest area, mean forest carbon fixation, total forest carbon fixation and percentage for each country in Europe

Country	Forest Area [km²]	[Mg C/ha/yr]	[Tg C/country/yr]	[%]
Albania	5625	6.99	3.93	0.53
Austria	35071	6.53	22.91	3.12
Belgium	5486	4.86	2.67	0.36
Bosnia	21714	9.84	21.36	2.91
Belarus	62382	3.91	24.41	3.32
Bulgaria	18263	6.06	11.06	1.50
Denmark	5147	5.21	2.68	0.37
Ireland	13150	2.19	2.88	0.39
Estonia	18968	4.73	8.97	1.22
Czech	24197	5.10	12.35	1.68
Finland	200594	2.58	51.73	7.04
France	104526	8.94	93.40	12.70
Germany	90228	5.98	53.99	7.34
Greece	20928	6.29	13.17	1.79
Croatia	17368	9.49	16.78	2.28
Hungary	16044	6.37	10.22	1.39
Italy	62208	8.79	54.67	7.44
Latvia	28159	4.79	13.49	1.83
Lithuania	14251	4.15	5.92	0.81
Slovakia	12970	5.53	7.18	0.98
Luxembourg	609	2.36	0.14	0.02
Moldova	3312	5.28	1.75	0.24
Macedonia	5115	7.30	3.74	0.51
Montenegro	5059	7.60	3.84	0.52
Netherlands	4779	4.93	2.36	0.32
Norway	112004	2.78	31.09	4.23
Poland	66987	4.64	31.07	4.23
Romania	43429	7.49	32.55	4.43
Russia	103420	2.55	26.36	3.59
Slovenia	10289	9.46	9.74	1.32
Serbia	20456	7.94	16.24	2.21
Sweden	249654	3.71	92.73	12.61
Switzerland	9529	6.48	6.17	0.84
United Kingdom	43495	3.21	13.98	1.90
Ukraine	63653	4.67	29.75	4.05
TOTAL	1519387		735.25	

The total forest carbon fixation is estimated at 0.735 P(=10^{15}) g C for 1997 for the region of interest or almost 30 percent of the total European NEP. The highest mean forest carbon fixations are found in Croatia, Slovenia, Serbia or the countries near the Adriatic Sea.

The next figure (Fig. 9.29) illustrates the regression between yearly total forest carbon fixation estimated with C-Fix and eddy covariance measurements from the Euroflux sites. A better correlation can be observed between C-Fix forest NEP simulations and eddy covariance forest carbon exchange measurements for the Euroflux sites than the correlations observed in Fig. 9.24.

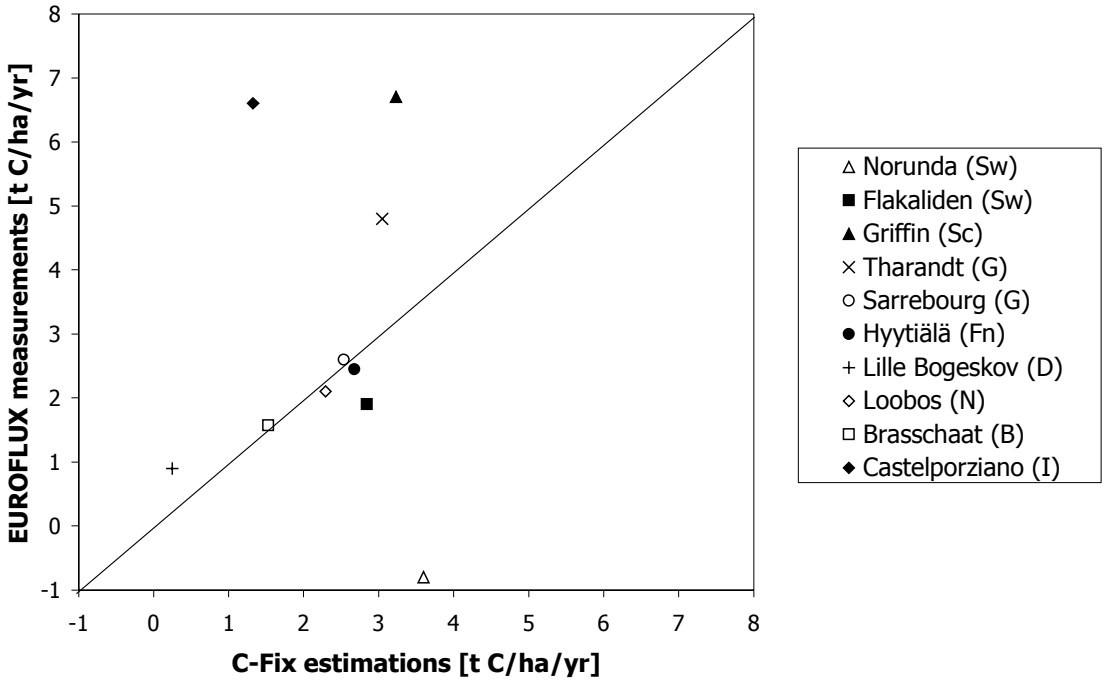

Figure. 9.29 Regression of then Net Ecosystem Production (NEP - yearly total) for 10 Euroflux sites: results of the eddy covariance field measurements (January 1997 - December 1997, Courtesy: Valentini R. et al. (2000)) versus the C-Fix NEP estimations multiplied with forest probability data.

An underestimation of the C-Fix model is found for the sites Griffin (Scotland), Tharandt (Germany) and Castelporziano (Italy). The rest of the sites are quite close to the 1:1 line. Te deviation of the thre beformentioned sites can be due to errors in the meteorological data and/or forest probability map.

9.4.4 Comparison with other LTEEF models

9.4.4.1 Comparison with point models

Within the LTEEF network, other ecosystem models are applied for the different forest sites in Europe. Comparisons between these models and C-Fix are made at different productivity levels. The first table (Table 9.12) gives an overview of GPP, NPP, NEP, autotroph and heterotroph respiration for the forest site in Hyytiala (Finland) estimated with six different models and C-Fix based on the forest probability map. We can conclude that the simulations of C-Fix are in the same range as those of the other models applied in LTEEF.

Table 9.12 Comparison of the Gross Primary Production (GPP), Net Primary Production (NPP), Net Ecosystem Production (NEP), autotroph respiration (Auto) and heterotroph respiration (Hetero) between different models and the C-Fix model for the forest site in Hyytiala, all in [g C/m²/yr] for 1997

	COCA-FEF	FINNFOR	FORGO	GOTILWA	HYDRALL	TREEDYN	C-Fix
GPP	1011	703	988	1138	1005	667	630
Auto	470	218	354	577	135	75	165
NPP	541	485	634	561	870	592	465
Hetero	266	101	297	378	635	826	197
NEP	275	384	337	183	235	234	268

Table 9.13 gives on overview of measured NEP values for different forest sites in Europe compared with models and the C-Fix model. Again, the C-Fix values are comparable with the other results and measurements. However, the results for the site in Bray (France) show a noticeable higher value then the measurements and the estimation for site in Tharandt (Germany) has a lower value.

Table 9.13 Comparison of the Net Ecosystem Production [g C/m²/yr] for 1997 between the measurements, different ecosystem models and C-Fix

	Measured	COCA-FEF	FINNFOR	FORGO	GOTILWA	HYDRALL	TREE DYN	C-Fix
Bray	430			1142	439	526	526	894
Collelongo	663			646	637			416
Hesse	257			302	304		225	
Hyytiala	245	275	384	337	183	325	243	268
Loobos	209			148	271	369	245	229
Tharandt	627			789				305

9.4.4.2 Comparison with EFISCEN model

The EFISCEN model, developed by the European Forest Institute (EFI), estimates the total carbon fixation for each country based on a forest inventory approach. Table 9.14 compares the C-Fix and the EFISCEN results for Germany. GPP shows a good agreement between both approaches. However, C-Fix estimations of NPP show about a 30 percent difference between C-Fix and EFISCEN. This difference is even more expressed at the NEP level.

Table 9.14 Gross Primary Production, Net Primairy Production and Net Ecosystem Production for Germany: calculated with C-Fix and the EFISCEN model (EFI)

	Mean carbon fixation [Mg C/ha/yr]		Total carbon fixation [Tg C/yr]	
	EFISCEN	C-Fix	EFISCEN	C-Fix
GPP	12.7	13.07	125.8	117.9
NPP	6.0	9.71	59.1	87.6
NEP	2.5	6.0	24.9	54.0

Figure 9.30 shows a detailed German forest NEP distribution. The highest values are found in the southwestern part of the country.

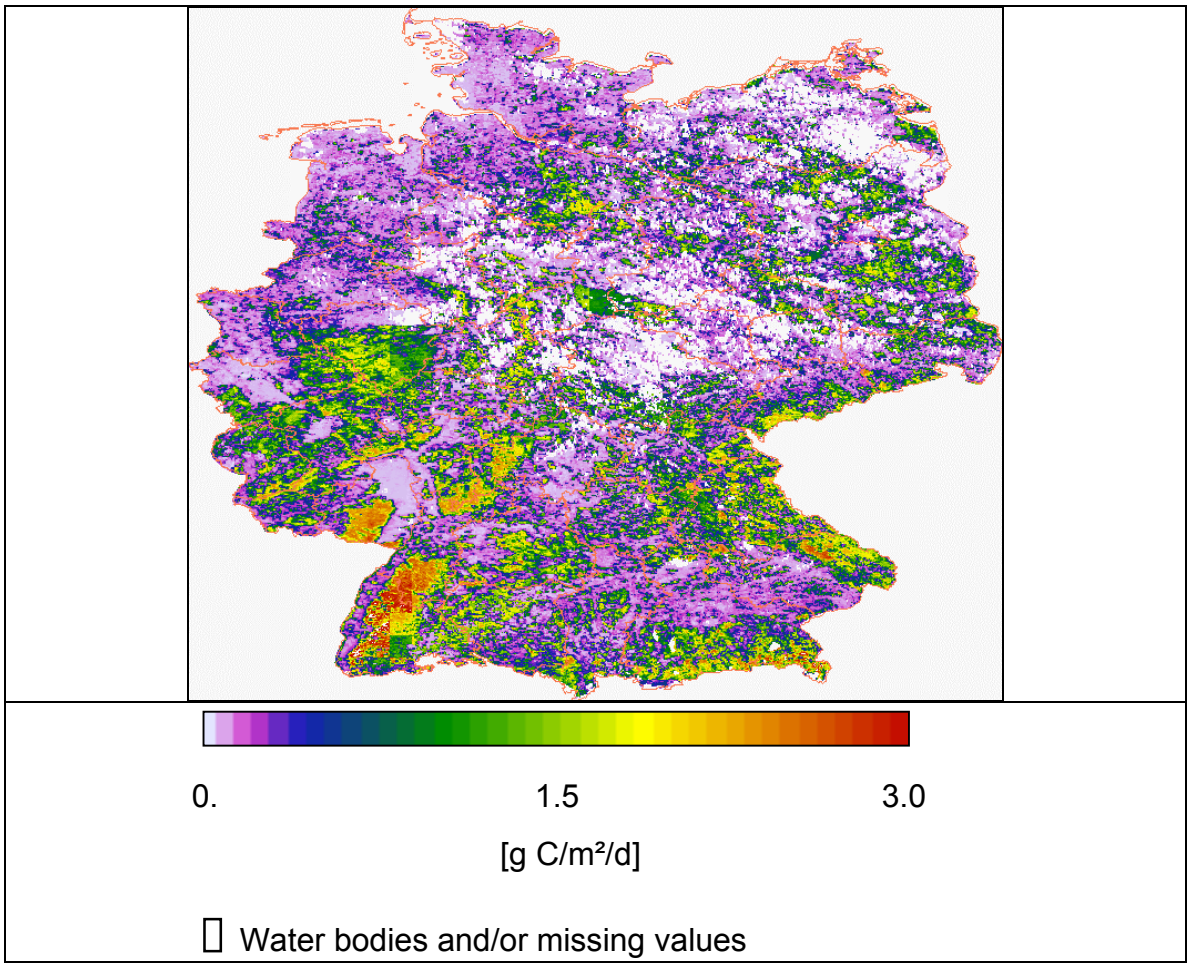

Figure 9.30 Yearly mean German forest Net Ecosystem Productivi y map for the year 1997.

9.4.5 Comparison with SPOT4/VEGETATION data

The C-Fix model was also applied with SPOT4-VEGETATION imagery for the period April 1998 until March 1999. The meteorological data used for this application are in this case obtained from the METEO FRANCE Arpège model. Daily mean air temperature and daily global incoming radiation are estimated with the Arpège model as stated before using a grid size of 1.5 by 1.5 degrees. As a result the following figure shows a comparison between C-Fix NEP simulations obtained with NOAA/AVHRR imagery and alternatively SPOT4/VEGETATION imagery.

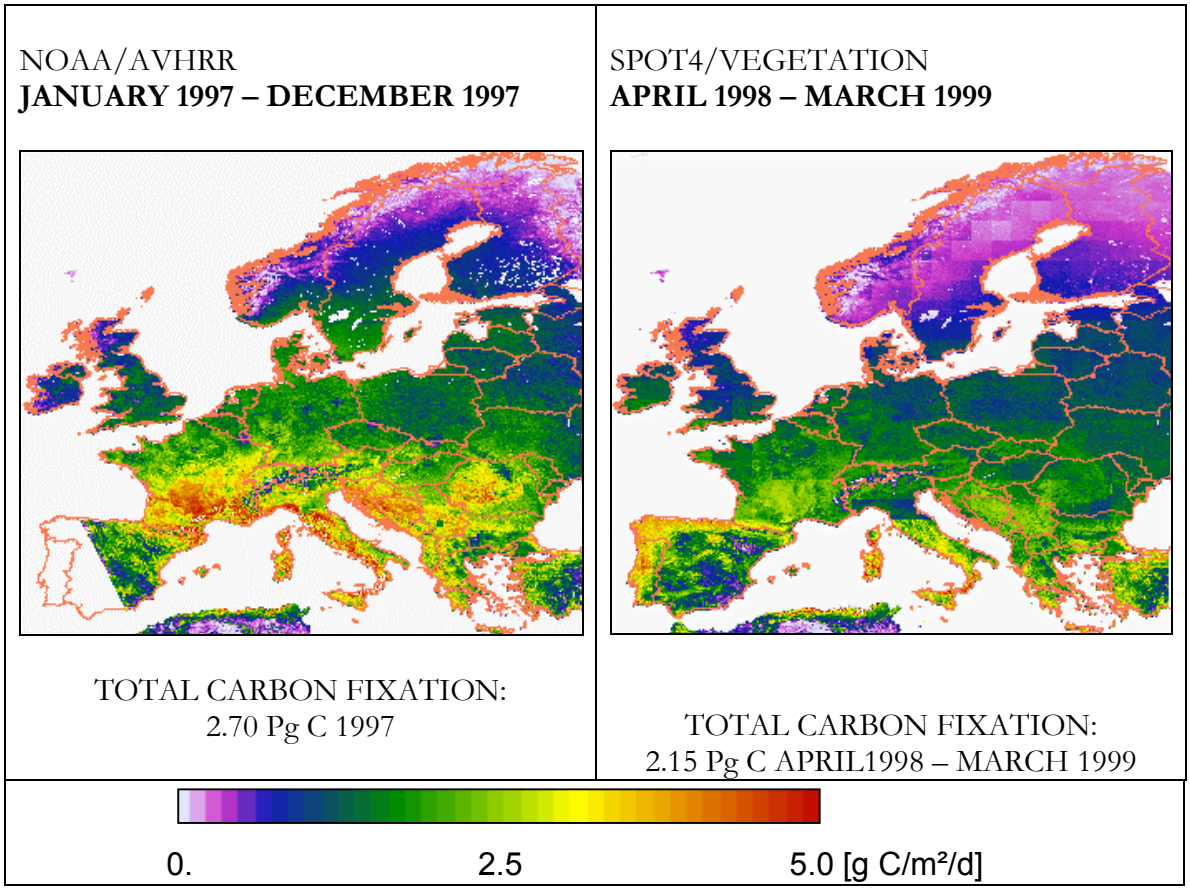

Figure 9.31 Yearly mean European carbon fixation estimated with C-Fix. Left pane: NOAA/AVHRR imagery (1997). Right pane: SPOT4/VEGETATION imagery (April 1998 – March 1999)

The left pane (NOAA/AVHRR based data) shows higher NEP values over the entire continent. As mentioned before the total carbon fixation for 1997 was estimated at 2.70 Pg C. For the period April 1998 – March 1999 a value of 2.15 is found which includes also Portugal and Spain.

Figure 9.32 shows a comparative table of the total carbon fixation (NEP) estimated with C-Fix for the year 1997 and the SPOT4/VEGETATION data for the period April 1998 – March 1999 for all European countries.

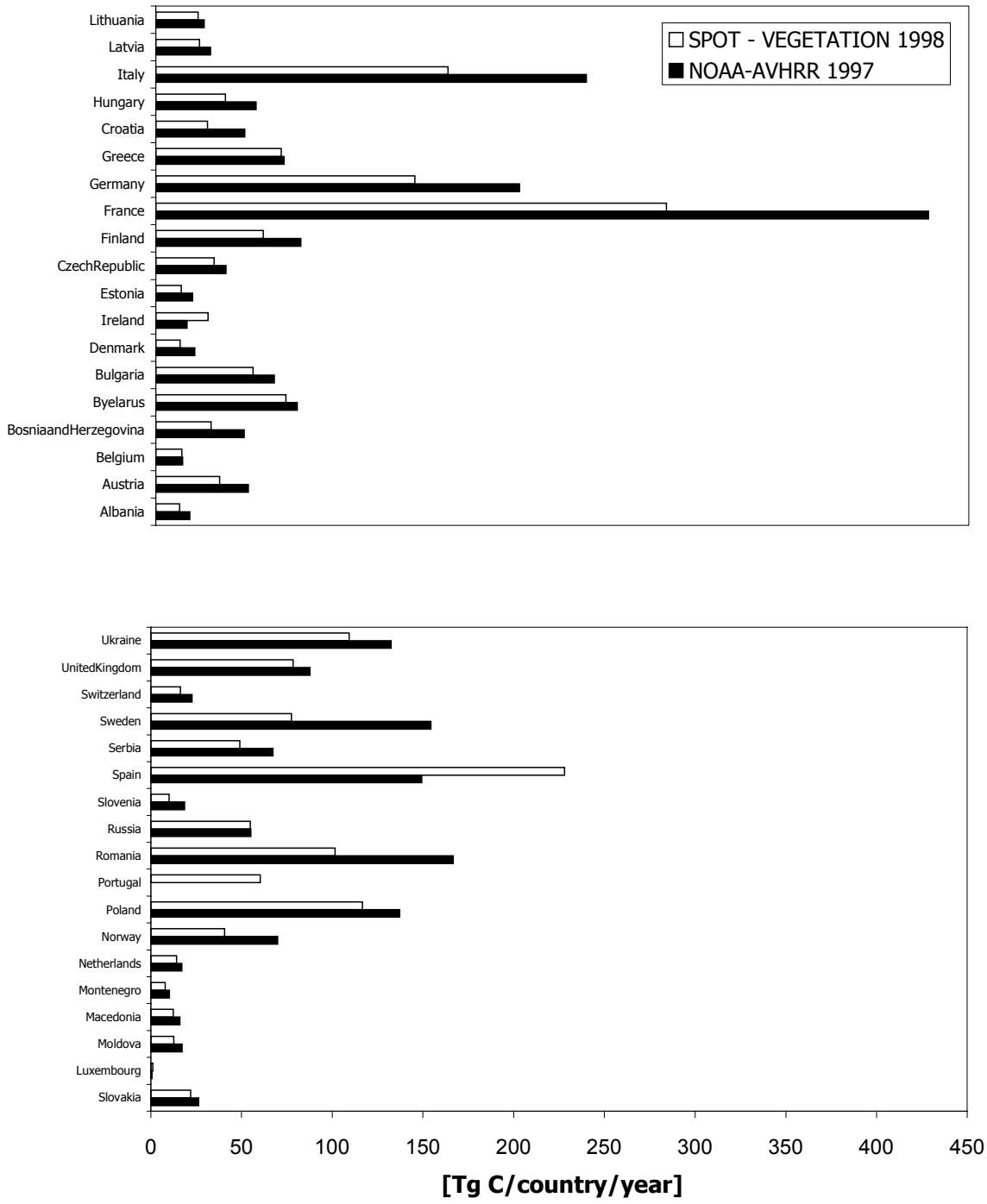

Figure 9.32 Comparison between NEP for all European countries, NOAA- AVHRR imagery (1997) and SPOT – VEGETATION imagery (April 1998 – March 1999).

The overall conclusion of this figure is that the estimated NEP values based on NOAA-AVHRR data are higher for each country then SPOT - VEGETATION data except in Ireland. Differences up to 50% and more are not an exception. Slovenia for example has a value of 18 Tg C in 1997, for the period April 1998 till 1999 the carbon fixation was estimated at 9 Tg C. Notice that the NOAA/AVHRR data contains only a part of Spain

and Portugal while the VEGETATION data cover the entire continent, which explains the large differences in the figure for Portugal and Spain.

Despite the differences it has to be considered that for both datasets there is a difference in the period of interest, that another type of meteorological data and data processing are used and finally that two different sets of satellite data are used which implies some (rather minor) differences in pre processing techniques to obtain the monthly NDVI-values. Taken this into account we are rather pleased with the correspondence between both datasets and see this as a confirmation of the robustness of our NEP estimation approach.

9.4.6 Conclusion

The C-Fix model provides a means to assess the evolution and geographical distribution of the main constituents of the carbon budget of terrestrial ecosystems. In this application monthly mean NDVI imagery, derived from NOAA-AVHRR data, was pre-processed and used in combination with meteorological data provided by the WMO to estimate the European carbon fixation for the year 1997.

Estimated decadal C-Fix NEP results were then compared with eddy covariance flux measurements carried out in several forest sites in Europe within the framework of the Euroflux project. For some sites high correlations were found between modelled and measured NEP and the values were close to the 1:1 line. Other sites showed larger deviations form the 1:1 line and a lower correlation.

The European NEP showed a clear-cut seasonal trend, as can be expected with the highest NEP values in spring and summer. The total European carbon fixation for 1997 was estimated at 2.55 P(=10^{15}) g C. Southern countries showed higher NEP-values than Northern countries in Europe. This latitude dependency was also found in GPP and NPP fluxes.

To extract European forest carbon fixation, a forest probability map was used (FIRS project). For each land pixel the corresponding forest coverage was multiplied with the yearly total NEP. The total European forest NEP for 1997 was then estimated to be 0.735 Pg C or 29% of the European terrestrial vegetation NEP. The yearly total forest NEP at the different Euroflux forest sites correspond well with the simulated values form C-Fix.

Regional modelling was used to estimate NEP at different forest sites as well. A special Chapter discussed on the comparison between C-Fix estimates and the different site models used in LTEEF. These models were applied on the different Euroflux forest sites and the NEP results compared with the C-Fix results. A good correlation was found.

Furthermore the EFISCEN model is an inventory-based method to estimate yearly total NPP and NEP at regional levels. GPP is derived from NPP with a rule of thumb

method. A comparison between C-Fix and EFISCEN was performed for Germany. GPP results agreed between both models, however NPP and NEP were deviating significantly C-Fix. Finally, C-Fix results obtained with SPOT4/VEGETATION satellite data, ranging from April 1998 until March 1998, were compared with 1997 NOAA/AVHRR data pre-processed by Vito. The VEGETATION NEP simulations were lower than the NOAA-AVHRR based results. This application illustrates that NEP calculated with C-Fix is in the same range as the Euroflux NEP values and that C-Fix produces realistic estimates of NEP.

Disregarding the simplified approach to describe the carbon balance of the forests of a continent, as incorporated in C-Fix, we suggest that remote sensing is a valuable tool for estimating radiation absorption at the forest canopy level. Hence it is a valuable tool for estimating the carbon fixation capacity of the European vegetation and for forests as well.

The role of soil respiration and hence Net Ecosystem Productivity (NPP) is a complex issue, which we tackled by parameterisation of yearly NEP from Euroflux data. To be able to quantify the heterotrophic respiration on a yearly or daily basis, an independent soil flux rate constant for each pixel or model grid was performed. In addition, autotrophic respiration was given due attention with a parametric relationship avoiding the use of standing biomass data. Methodologically it is improbable that biomass retrieval from remote sensing imagery is feasible. Despite these boundary conditions, NEP estimated with C-Fix shows a good agreement with Euroflux site flux measurements based on the application of eddy covariance methods. Respiration fluxes, as well as hydrological considerations are a field for further research and modelling efforts.

Finally our impression is, that especially for the European continent, there is a lack of projects providing basis geophysical data (incoming radiation for example) needed for a more accurate evaluation and validation of the inputs of carbon balance models applied at the continental scale. Nevertheless we think that this work presented here represents a first European model which has been validated with micrometeorological data as well as cross correlated with the results from as suite of different other models, which has given us a lot of confidence in the robustness of the approach and the accuracy of its estimates.

9.5 Discussion of large scale approach model results

9.5.1 Introduction

Suppose that terrestrial ecosystems would take up more carbon than they do now, a slow down of the growing greenhouse effect could be the effect. If on the other hand, terrestrial systems would elicit an increased release of carbon, an enhanced contribution to global warming would be the consequence. It is the carbon cycle, which interconnects terrestrial ecosystems with the atmospheric system and both

(together with oceanic systems) are intrinsic parameters in climate change phenomena.

Gross primary production (GPP), a carbon mass flux originating from terrestrial uptake by vegetation, amounts globally to approximately 120 Gigatons (Gt) C per year. Of that quantity, approximately half is returned to the atmosphere by respiratory processes of vegetation itself as well above as underground, i.e. by short-term carbon release processes. NPP (net primary production) amounts to approximately 60 Gt C globally and per year (IGBP 2000). When soil organic matter (SOM) decomposition processes are taken into account as well, hence taking uptake processes operating at mid-term into account, one obtains net ecosystem production (NEP), amounting approximately to 10 Gt C per year. This is less than 10% of the original 120 Gt of GPP. This clearly pinpoints the challenge that large-scale modelling approaches are faced with, e.g. how to plausibly estimate at the regional, continental and even global scales, the different carbon mass flux vectors just cited.

Given the significance of the effects of scale on carbon balance evaluation, scaling issues, in both space and time are of considerable interest. The development of scaling theories and the spin-off of accompanying models from local to global scales generates testable scientific hypothesis. With ecological research restricted to relatively small scales, inspired by practical as well as 'cultural' habits in ecological research, much of our knowledge and understanding of the environment relates only to relatively local scales. In this project, an important effort is made to estimate carbon balance fluxes at the continental scale, in casu the European continent. Since the effects of changing scales are complex and non-linear in nature, this is not an easy task, and essentially requires data at a range of different spatial scales. In part this requirement is met in the LTEEF II project where modelling has taken place from the local to the continental scales, and cross correlation studies have investigated the relationships between both scales. In addition, remote sensing (RS) biophysical data extraction and integration techniques are applied providing model independent radiation absorption efficiency estimates at the continental scale, which integrated with empirical modelling result in a completely alternative approach to estimate carbon balance components. It should be stated that the large-scale is likely to contain some characteristics that cannot be predicted from the knowledge – no matter how complete – of the small scale processes. In that respect RS offers an added value to conventional modelling by the synoptic and consistent nature of its observations.

The objective of the large-scale approaches as elaborated and applied in the LTEEFII project is to estimate the capacity of European forests to fix (or release) carbon e.g. to quantify NPP, NEP and soil respiration simulated with four different approaches and this at the European continental scale. These approaches include the conversion of traditional forest inventory data into whole tree biomass and soil carbon with the EFISCEN model, including forecasting results generated with the LTEEFII stand models and this for representative sites in Europe (coinciding with Euroflux sites). Flux estimates in EFISCEN are calculated at the country level, which was therefore adopted as the basic spatial unit against which the other large-scale

model results were compared, even though some of them offer finer spatial scales (1-km²).

A second model applied makes use of remote sensing to derive the fraction of absorbed photosynthetic active radiation (*f*APAR) e.g. the absorption efficiency of vegetation in the PAR band and the conversion of absorbed PAR into forest net primary and net ecosystem production. For this application the C-Fix model and climate data - essentially temperature and global radiation - are applied to result into NPP and NEP estimates at a 1-km² spatial scale for Europe and for 1997. Since use is made of remote sensing pre-processing techniques, no extrapolations into the future (forecasting) can be made. This does not exclude back-casting, which is a possibility enabled by available RS data archives, which can be utilised for trend analysis using existing image archives of global observing satellite sensor systems.

A third model applied is the EuroBiota forest ecosystem model, which primarily describes the effect of changing temperature and atmospheric carbon dioxide concentration on ecosystem productivity. The model allows the influence of spatial variations in weather and the presence of evergreen and deciduous forests at different locations to be taken into account.

A fourth model applied is Hybrid as described in chapter 4. Hybrid is a dynamic, global vegetation model driven by a transient climate output of a GCM. Changes in areas of vegetation types and carbon storage in biomass and soils are predicted for areas from 34 ° N, 25 ° W to about 72.5 ° N, 36 ° E for a time frame from the year 1860 to 2100. The outputs are the predicted changes in carbon per unit area in the potential vegetation types for each of the models' cells.

The methodological aspects of the four different large-scale approaches just cited are described in chapter 4 and the results obtained for each of the models are described respectively in chapters 9.1 to 9.4. This chapter discusses the comparisons of the forest cover data sets used, the model outputs of NPP, NEP and calculated soil respiration at the country level for twenty-six European countries, the spatial patterns observed and the uncertainties intrinsic to each of the approaches and of the overall result. It should be stressed that the results of the four models presented in the next Chapters provide fully independent estimates of NPP, NEP and soil respiration.

9.5.2 Comparison of model results at the country level for Europe

9.5.2.1 Forest cover comparison at country level

For the large-scale models, the basis for estimates of NPP, NEP and soil respiration for European forests, whether per 1-km² pixel as with C-Fix and EuroBiota or with coarser grid cells as with Hybrid, or per country as with EFISCEN, is the forest cover per surface unit. In this case we are dealing with forest cover per square km. The mere fact that different data sources of forest cover area are used in the LTEEFII large-scale models, represents a source of additional uncertainty for the estimates of NPP, NEP and soil respiration on top of the uncertainty introduced by differences in model design, its basic theoretical concepts and the input data quality. To get to grips with the degree of uncertainty introduced by using different sources of forest cover data, a comparison is made between them. Table 9.5.1, concisely summarises forest cover data for 26 European countries for which the forest NPP, NEP and soil respiration values were estimated with the four large scale models EFISCEN, C-Fix, EuroBiota and Hybrid. The forest cover data source (TBFRA 2000) used in the selection of the representative sites was added as well for reasons of completeness and as a refererence.

Table 9.5.1: Forest cover area expressed in cover area per km² for forests of 26 European countries. Different data sources are used to estimate the forest cover per country or per model grid cell. The Corine land cover is complemented with ESA/ESTEC forest non-forest data for the EFISCEN model. The FIRS Forest probability map is used in the C-Fix model and the IGBP/DIS data set is used in the EuroBiota and Hybrid models.. Sources: EFISCEN (Schelhaas et al. 1999), FIRS Forest Probability Map of Europe (Häme et al. 1999), IGBP/DIS global land cover data set (Loveland et al. 2000), Corine land cover (CORINE 1997), WCMC (Iremonger et al. 1997), TBFRA-2000 (UN-ECE/FAO 2000)

	Reference	EFISCEN database	C-Fix Forest prob 1997	EuroBiota/Hybrid 1990s		
	Area [1000 ha]	Area [1000 ha]	Area [1000 ha]	Area [1000 ha]		
	TBFRA-2000	Corine/ESA-ESTEC	FIRS	IGPB/DIS	Mean	%Stdev
Albania	1030	899	563	152	661	59
Austria	3840	2942	3507	2704	3248	16
Belgium	646	531	549	11	434	66
Bulgaria	3590	3202	1826	906	2381	52
Croatia	1775	1443	1768	1322	1577	15
Czech Republic	2630	2446	2420	216	1928	59
Denmark	445	442	515	41	361	60
Finland	21883	19919	20059	32755	23654	26
France	15156	13300	10453	2926	10458	51
Germany	10740	9905	9023	1679	7837	53
Hungary	1811	1609	1604	436	1365	46
Ireland	591	344	1315	12	566	98
Italy	9857	5757	6221	3244	6270	43
Luxembourg	86	71	61	73	73	14
Macedonia	906	805	512	410	658	36
Netherlands	339	304	478	18	285	68
Norway	8710	7070	11200	12684	9916	25
Poland	8942	6309	6699	333	5571	66
Portugal	3383	1508	1632	6	1632	85
Romania	6301	6211	4343	2794	4912	34
Slovak Republic	2016	1823	1297	973	1527	31
Slovenia	1099	1072	1029	643	961	22
Spain	13509	13980	4395	963	8212	80
Sweden	27264	22219	24965	37983	28108	25
Switzerland	1173	1043	953	795	991	16
United Kingdom	2469	1898	4350	367	2271	72
Yugoslavia	2894	1512	2552	1687	2161	31
Total	153085	128564	124288	106129	Mean	46

Values in table 9.5.1. represented in red are extrapolations.

A comparison of the different forest cover datasets elicits significant differences in forested area for several European countries. Looking at the percentage standard deviation on the mean for all the datasets illustrates this quite prominently. Values range from a minimum of 14 % for Luxemburg to a maximum of 98 % for Ireland. This suggests that flux differences between the models at the country level can be expected to be quite large only by the large differences observed for the forest surface estimates. At least a mean uncertainty of 46 % on the forest surface area of Europe is to be taken into account when interpreting NPP, NEP and soil respiration flux results of the large-scale models. Apparently, quite some methodological work with respect to forest cover estimation is still to be performed to get the observed uncertainty of 46 % to an acceptable level for the European continent.

It must be remarked, that already when starting with the definition of forested versus non-forested land cover types, the method(s) used for performing forest area surveys, lead to forest area estimates which elicit a strong numerical divergence. Many of the forest cover maps and basic data for Europe are based on remote sensing data. Hence, not only the land cover classification algorithms applied, but also the quality standards adopted in the satellite sensor pre-processing algorithms and pre-processing chains, as well as the spatial and multi-temporal resolutions selected by using different satellite sensors (NOAA/AVHRR, Landsat, SPOT/HRV) in short, all these factors play a crucial role in the final forest cover estimate accuracy. It is quite clear that a realm of improvement is possible in this field of research.

Taking the recently updated database, TBFRA-2000, as a reference, the observed differences between the forest cover data can partly be explained by the differences in time-period during which the forest cover area surveys were executed. Moreover the EFISCEN database mostly focuses on forests suitable for logging. This can explain why the EFISCEN forest cover values are systematically lower than the TBFRA-2000 data, though an absolute reference for forest cover does not exist yet. Since acreage data are primarily based on remote sensing observations, the tendency for over- or underestimation of forest cover is most prominent in areas with small-scale cover type patches in the landscape (e.g. in Southern, Central and Western Europe) or in regions with continuous transition gradients between forest and open land as in the Northern boreal and Mediterranean areas. Moreover, one would expect the uncertainty on forest surface area per country to decrease with increasing forest cover area per country. Figure 95.1 states this case convincingly. A significant decrease in the % standard deviation on the mean forest surface area per country with increasing % forest cover area per country can be observed for the countries taken up in table 9.5.1.

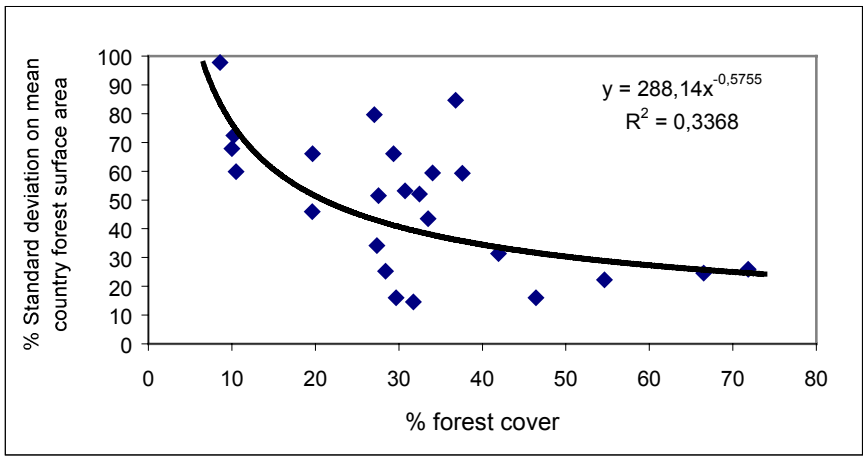

Figure 9.5.1: Percentage standard deviation on the mean country surface area in function of the percentage forest cover per country taken up in table 9.5.1. A power law function fits the data with the highest coefficient of determination.

9.5.2.2 Forest NPP, NEP and R_s comparison at country level

Table 9.5.2: Net Primary Productivity of forests for 26 European countries calculated with four different large spatial scale models. The forest area sources used to estimate forest cover per country are listed in table 9.5.1. In the lowest rows, mean values for 26 countries per model are listed with the percentage standard deviation indicating European mean NPP and its uncertainty including a grand mean value of 5.4 Mg C/ha/y with a 25% uncertainty. Mean values and standard deviations per country for all models are listed in the middle columns indicating a mean NPP per country for all models as well as uncertainties per country. The right part of the table lists the absolute deviations from the country mean value including, in the lower two rows, the total deviation and its absolute standard deviation. Values represented in red are extrapolations.

	Forests 1995-2001	Forests 1998-1999	Forests 1990s	All ecosystems 1990s				Forests 1995-2001	Forests 1998-1999	Forests 1990s	All ecosystems 1990s
	NPP	NPP	NPP	NPP	Mean	StDev		NPP-mean	NPP-mean	NPP-mean	NPP-mean
	[Mg C/ha/y]	[Mg C/ha/y]	[Mg C/ha/y]	[Mg C/ha/y]	[Mg C/ha/y]	[Mg C/ha/y]		[Mg C/ha/y]	[Mg C/ha/y]	[Mg C/ha/y]	[Mg C/ha/y]
	EFISCEN	C-Fix	EuroBiota	HYBRID				EFISCEN	C-Fix	EuroBiota	HYBRID
Albania	6.4	11.3	6,3	1,6	**6,4**	*4,0*		0,00	4,90	-0,06	-4,84
Austria	8.0	10.6	3,3	7,2	**7,3**	*3,0*		0,74	3,33	-4,01	-0,05
Belgium	5.3	7.8	4,1	2,2	**4,8**	*2,3*		0,42	2,96	-0,72	-2,65
Bulgaria	2.4	10.0	4,3	***5,6***	**5,6**	*3,2*		-3,20	4,45	-1,25	0,00
Croatia	1.9	15.3	5,4	4,6	**6,8**	*5,8*		-4,92	8,46	-1,35	-2,20
Czech Republic	4.0	8.4	3,7	1,9	**4,5**	*2,7*		-0,51	3,88	-0,77	-2,59
Denmark	4.3	8.5	3,2	3,1	**4,8**	*2,6*		-0,47	3,74	-1,57	-1,69
Finland	2.1	4.5	7,0	0,5	**3,5**	*2,8*		-1,48	1,01	3,46	-2,99
France	3.2	14.1	4,4	2,4	**6,0**	*5,4*		-2,79	8,06	-1,65	-3,63
Germany	5.0	9.7	3,8	1,9	**5,1**	*3,3*		-0,06	4,60	-1,30	-3,23
Hungary	4.4	10.4	4,5	7,5	**6,7**	*2,8*		-2,26	3,67	-2,21	0,81
Ireland	5.3	3.4	3,4	3,4	**3,9**	*0,9*		1,42	-0,47	-0,44	-0,51
Italy	3.1	14.1	5,1	4,5	**6,7**	*5,0*		-3,60	7,38	-1,58	-2,20
Luxembourg	6.0	3.8	***4,9***	***4,9***	**4,9**	*0,9*		1,09	-1,09	0,00	0,00
Macedonia	1.2	12.0	4,6	2,1	**5,0**	*4,9*		-3,75	6,97	-0,35	-2,88
Netherlands	4.5	7.9	3,6	3,2	**4,8**	*2,1*		-0,28	3,10	-1,23	-1,58
Norway	1.7	4.7	6,3	0,3	**3,2**	*2,8*		-1,54	1,46	3,06	-2,99
Poland	3.8	7.6	3,8	1,5	**4,2**	*2,5*		-0,37	3,44	-0,38	-2,69
Portugal	3.7	4.0	5,5	3,1	**4,1**	*1,0*		-0,36	0,00	1,37	-1,02
Romania	4.6	12.2	4,5	3,9	**6,3**	*4,0*		-1,72	5,92	-1,83	-2,37
Slovak Republic	3.8	9.1	4,4	6,1	**5,8**	*2,4*		-2,06	3,28	-1,43	0,20
Slovenia	3.0	15.2	5,1	5,2	**7,1**	*5,5*		-4,08	8,05	-2,03	-1,94
Spain	2.9	9.9	6,2	1,8	**5,2**	*3,6*		-2,35	4,67	1,03	-3,35
Sweden	2.6	6.3	6,1	0,4	**3,9**	*2,9*		-1,28	2,48	2,26	-3,46
Switzerland	7.5	10.5	2,9	3,3	**6,0**	*3,6*		1,47	4,43	-3,16	-2,73
United Kingdom	4.5	5.1	3,7	1,8	**3,8**	*1,4*		0,70	1,32	-0,04	-1,97
Yugoslavia	2.0	25.4	4,5	2,2	**8,5**	*11,3*		-6,57	16,84	-3,97	-6,29
Mean	**4.0**	**9.7**	**4,6**	**3,2**	**5,4**	**2,9**	Total	**-37,8**	**116,8**	**-20,2**	**-58,8**
%StDev	43	48	24	61	25		StDev	5,4	3,1	9,0	2,7

Typically in processes that are spatially scaled, a power law relationship between the magnitude and spatial scale of variability can be observed. The underlying power law structure is reflected in the scaling behaviour of the volume (mass), surface area (of forest in this specific case) or length of the structure.

The most explicit differences in country forest area estimates are found when comparing the IGBP/DIS set with the other data sets. In that case, the coarse spatial resolution (4-km² NOAA/AVHRR Global Area Coverage (GAC) data) of the global IGBP/DIS data set leads to losses in information by spatial aggregation of land cover types. Hence, an increased confusion of forest with other land-use classes is observed, resulting in an increased variability on the forest area estimate. With the coarse spatial resolution cited above, forest cover is strongly underestimated in areas where non-forest classes dominate the landscape (e.g. Central and Southern Europe) whereas in areas with a high proportion of forest, the forest cover area is overestimated (e.g. the Scandinavian countries).

The above discussion indicates that for Europe and at the country level, rather large differences in NPP, NEP and soil respiration can be expected to occur due to the still large uncertainty on the forest cover area estimates. When taking the European continent as a unit however, the total continental flux estimate uncertainty is bound to be lower due to a 'levelling out' effect between the country spatial units. Hence, European level NPP, NEP and soil respiration estimates can be expected to be more comparable between the large-scale models and are bound to offer a more quantitative stronghold tan those at the country level.

Table 9.5.2 summarises the NPP estimates generated with the four large-scale models, including a comparative analysis with respect to the country mean values of the four models. Though this does not give indications on the absolute accuracy of the NPP estimates, it certainly indicates the divergences between models per country as well as for Europe. Figures 9.5.2 and 9.5.3 essentially offer the same information as table 9.5.2, but give a more direct visual impression of the estimations and their divergences. Some of the key features drawn from table 9.5.2 and the figures just mentioned are the following. The mean NPP estimates for all countries for each of the models are 4.0 [Mg C/ha/y] for EFISCEN, 9.7 [Mg C/ha/y] for C-Fix 4.6 [Mg C/ha/y] for EuroBiota and 3.2 [Mg C/ha/y] for Hybrid. The results demonstrate that C-Fix elicits systematically higher NPP estimates as opposed to the other models. This is demonstrated on the right hand side of the table where C-Fix produces NPP estimates that are significantly above the model mean value for Europe. This is illustrated as well in figures 9.5.1 and 9.5.2 The overall mean NPP value for Europe is 5.4 [Mg C/ha/y] with an uncertainty of 25 %.

Another prominent feature from table 9.5.2 is that the uncertainty calculated for each model for all country estimates, is the highest for Hybrid (61%), the lowest for EuroBiota (24%) and intermediate for EFISCEN and C-Fix (respectively 43 % and 48 %). Especially the estimates for Yugoslavia seem to represent an extreme outlier for C-Fix, distorting the overall uncertainties quite significantly. This is illustrated by leaving out the results for that country. We obtain mean NPP estimates for all countries for each of the models of 4.0 [Mg C/ha/y] for EFISCEN, 9.1 [Mg C/ha/y] for C-Fix, 4.6 [Mg C/ha/y] for EuroBiota and 3.2 [Mg C/ha/y] for Hybrid with uncertainties which are much lower, respectively 41 %, 38 %, 24% and 61%. The uncertainty for the European NPP estimate is 23 %. These values are significantly lower than when the Yugoslavian results are taken into account. Hybrid remains the model with the highest uncertainty on NPP.

Another conspicuous result is that judging by the mean NPP value over all models, Norway has a minimal country NPP value of 3.2 [Mg C/ha/y] with a standard deviation of 2.8 [Mg C/ha/y], and Austria a maximal NPP of 7.3 [Mg C/ha/y] with a standard deviation of 3.0 [Mg C/ha/y]. All the other countries have values in between these two (I left out Yugoslavia in this comparison).

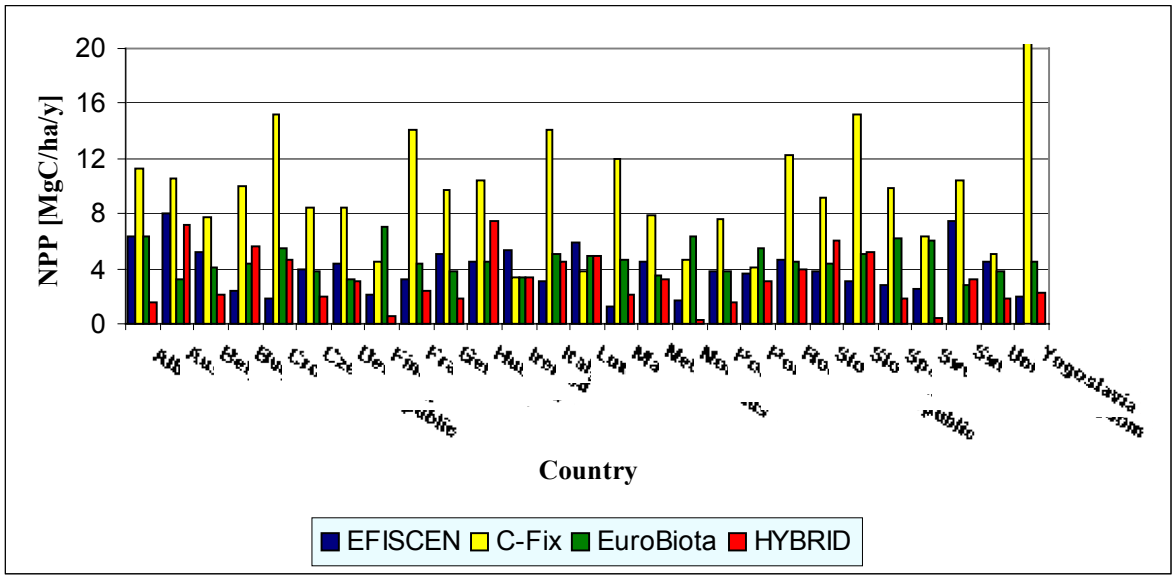

Figure 9.5.2: NPP comparison between the four large-scale models for 26 European countries taken up in the analysis of the large-scale results.

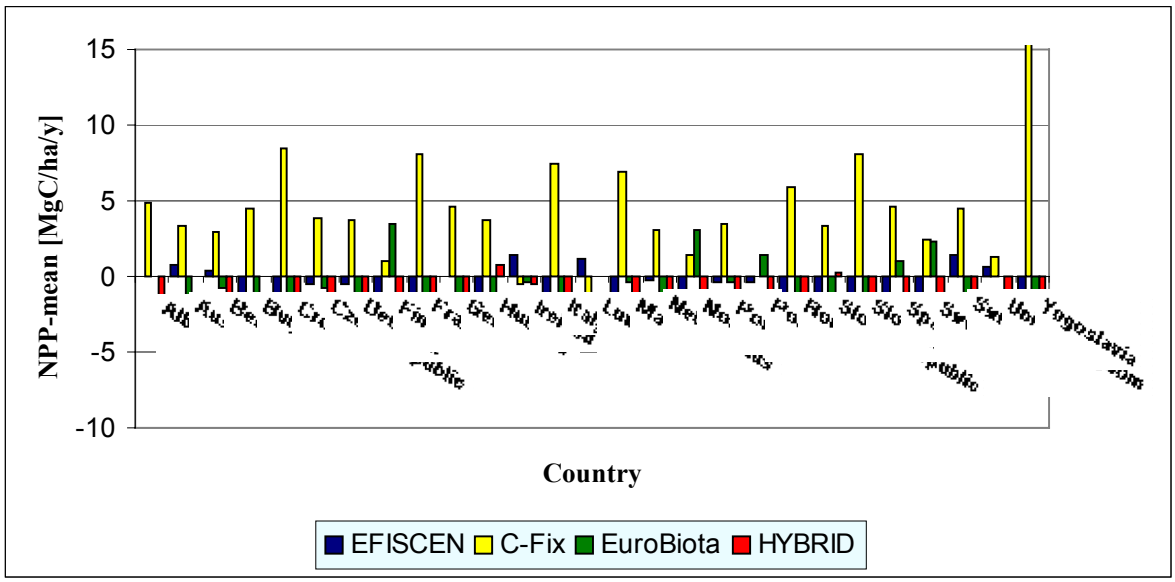

Figure 9.5.3: Analysis of the variation around the mean value of NPP for the four large scale models for each of the 26 European countries taken up in the analysis of the large-scale results.

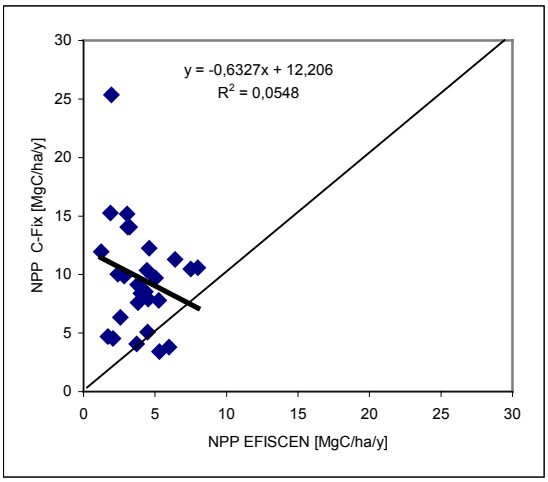

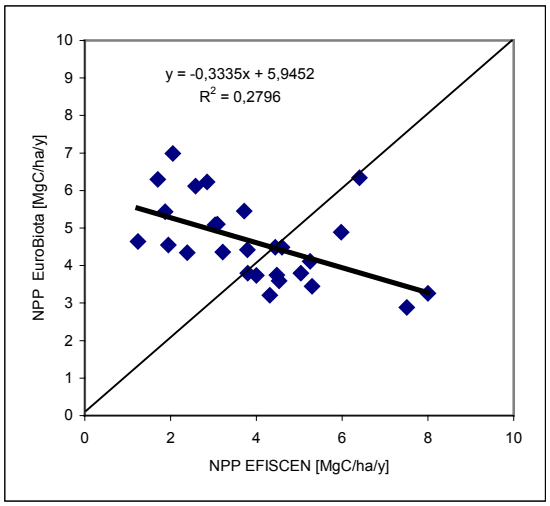

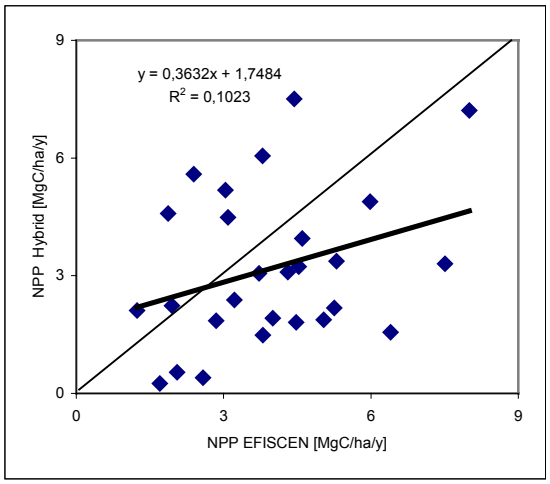

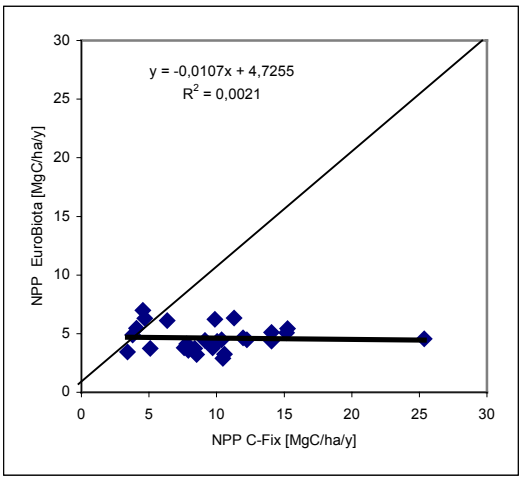

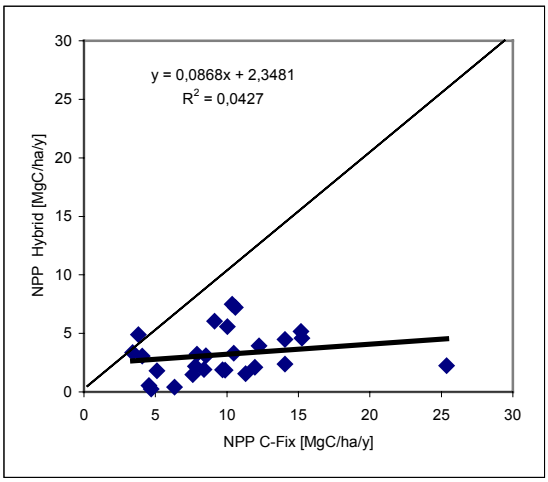

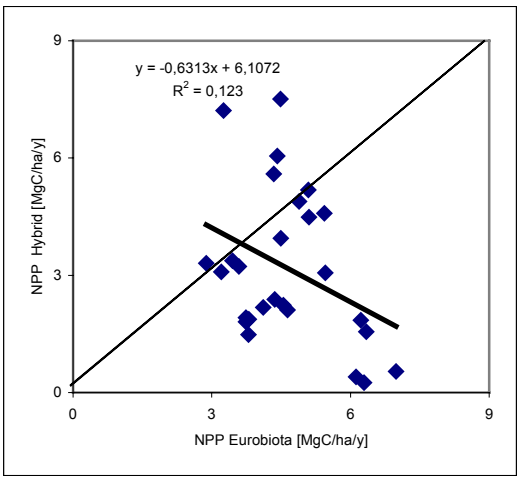

Figure 9.5.4: Cross correlation analysis between the four large-scale models for NPP. 1:1 lines are indicated as a reference along with R².

Figure 9.5.4 summarizes a cross correlation analysis between the four models. The highest correlation is obtained between EFISCEN and EuroBiota with a R^2 of 0.28. Nevertheless the correlation is negative, hence when the EFISCEN NPP estimate increases, the EuroBiota NPP estimate decreases. This indicates a basic difference in behaviour of both models, under conditions where NPP changes. To a lesser extent, Eurobiota and Hybrid are correlated with a R^2 of 0.123. Again the correlation is negative. EFISCEN does not correlate well with C-Fix but does so more significantly with Hybrid (R^2 of 0.1 and positive slope).

Another aspect is the relation to the 1:1 line for the model estimates. Apparently, most if not all of the trendlines drawn through the correlograms deviate quite strongly from the 1:1 line. This phenomenon was already emphasised in the previous results description (of table 9.5.2), where it is stated that the variation around the mean value for all models is high. Hence, deviations from the 1:1 line are more probable. In conclusion, with respect to the 1:1 line EFISCEN and Hybrid generate results of country estimates that match most closely the 1:1 line. With respect to mutual correlation, EFISCEN and EuroBiota show the highest coefficient of determination. C-Fix and Hybrid are very weakly positively correlated.

A general remark with respect to the results described here. It is not because good correlations are obtained between two models that these are bound to generate the best estimate for NPP. The same is true with respect to the match of the trendline with the 1:1 line. These results only indicate that some models generate results with are comparable at the process description level (high R^2) or at the NPP value (relative to the 4 model mean value) level (1:1 line). A true test of the plausibility of the absolute NPP values generated by the models is a comparison with NPP fluxes derived from covariance measurements. Since these do not exist at the country level, some if not all of the modellers actually compare simulated NPP at the patch level with NPP derived from eddy covariance measurements and soil respiration measurements. Even then, no certainty exists that this comparison is representative for the country level NPP fluxes.

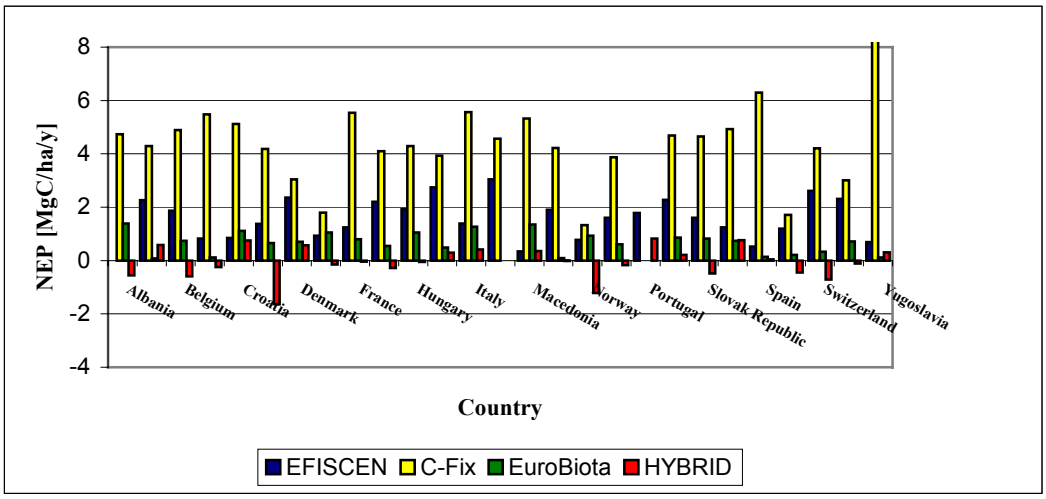

Figure 9.5.5: NEP comparison between the four large-scale models for 26 European countries taken up in the analysis of the large-scale results.

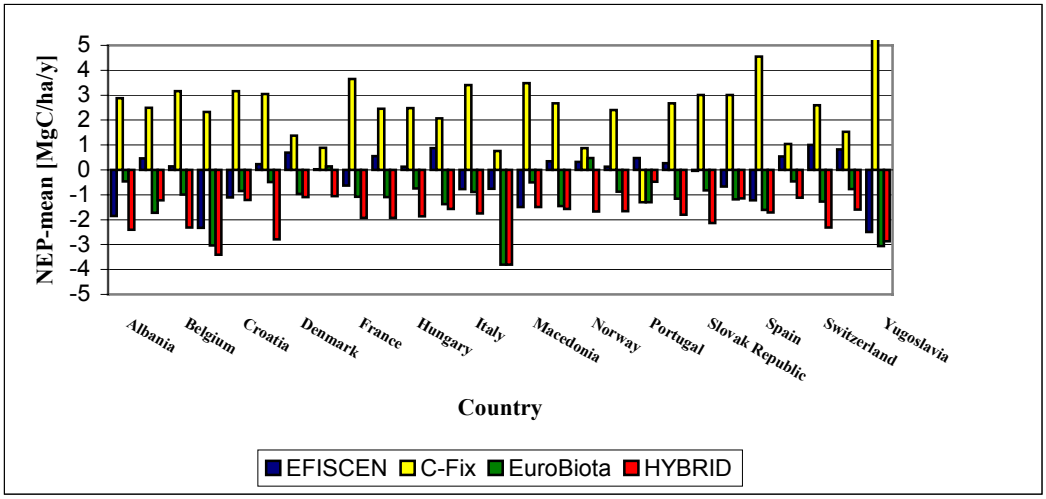

Figure 9.5.6: Analysis of the variation around the mean value of NEP for the four large scale models for each of the 26 European countries taken up in the analysis of the large scale results.

Table 9.5.3: Net Ecosystem Productivity of forests for 26 European countries calculated with four different large spatial scale models. The forest area sources used to estimate forest cover per country are listed in table 9.5.1. In the lowest rows, mean values for 26 countries per model are listed with the percentage standard deviation indicating European mean NEP and its uncertainty including a grand mean value of 1.7 Mg C/ha/y with a 42% uncertainty. Mean values and standard deviations per country for all models are listed in the middle columns indicating model mean NEP per country and uncertainties per country. The right part of the table lists the absolute deviations from the country mean value including, in the lower two rows, the total deviation and its absolute standard deviation.

	Forests 1995-2001	Forests 1998-1999	Forests 1990s	All ecosystems 1990s				Forests 1995-2001	Forests 1998-1999	Forests 1990s	All ecosystems 1990s
	NEP	NEP	NEP	NEP	Mean	StDev		NEP-mean	NEP-mean	NEP-mean	NEP-mean
	[Mg C/ha/y]	[Mg C/ha/y]	[Mg C/ha/y]	[Mg C/ha/y]	[Mg C/ha/y]	[Mg C/ha/y]		[Mg C/ha/y]	[Mg C/ha/y]	[Mg C/ha/y]	[Mg C/ha/y]
	EFISCEN	C-Fix	EuroBiota	HYBRID				EFISCEN	C-Fix	EuroBiota	HYBRID
Albania		4,7	1,39	-0,55	**1,9**	*2,7*		-1,86	2,87	-0,47	-2,41
Austria	2.3	4,3	0,08	0,58	**1,8**	*1,9*		0,47	2,49	-1,73	-1,23
Belgium	1.9	4,9	0,74	-0,59	**1,7**	*2,3*		0,14	3,16	-0,99	-2,32
Bulgaria	0.8	5,5	0,12	-0,25	**3,2**	*2,7*		-2,33	2,33	-3,04	-3,40
Croatia	0.9	5,1	1,12	0,75	**2,0**	*2,1*		-1,11	3,17	-0,84	-1,21
Czech Republic	1.4	4,2	0,66	-1,64	**1,1**	*2,4*		0,23	3,04	-0,49	-2,78
Denmark	2.4	3,0	0,70	0,57	**1,7**	*1,2*		0,69	1,37	-0,97	-1,10
Finland	0.9	1,8	1,05	-0,15	**0,9**	*0,8*		0,02	0,89	0,15	-1,06
France	1.3	5,5	0,80	-0,05	**1,9**	*2,5*		-0,64	3,65	-1,08	-1,93
Germany	2.2	4,1	0,55	-0,28	**1,6**	*1,9*		0,56	2,46	-1,09	-1,92
Hungary	1.9	4,3	1,05	-0,06	**1,8**	*1,8*		0,13	2,49	-0,75	-1,86
Ireland	2.7	3,9	0,49	0,30	**1,9**	*1,8*		0,87	2,07	-1,38	-1,57
Italy	1.4	5,6	1,27	0,42	**2,2**	*2,3*		-0,77	3,41	-0,89	-1,74
Luxembourg	3.0	4,6		0,00	**3,8**	*2,3*		-0,76	0,76	-3,80	-3,80
Macedonia	0.4	5,3	1,35	0,36	**1,8**	*2,4*		-1,50	3,48	-0,50	-1,49
Netherlands	1.9	4,2	0,10	-0,02	**1,5**	*2,0*		0,35	2,67	-1,45	-1,57
Norway	0.8	1,3	0,93	-1,22	**0,5**	*1,1*		0,32	0,88	0,47	-1,67
Poland	1.6	3,9	0,61	-0,18	**1,5**	*1,8*		0,12	2,40	-0,87	-1,65
Portugal	1.8		0,00	0,83	**1,3**	*0,9*		0,48	-1,30	-1,30	-0,48
Romania	2.3	4,7	0,86	0,22	**2,0**	*2,0*		0,27	2,68	-1,16	-1,79
Slovak Republic	1.6	4,7	0,83	-0,48	**1,7**	*2,2*		-0,04	3,00	-0,82	-2,14
Slovenia	1.3	4,9	0,73	0,77	**1,9**	*2,0*		-0,67	3,01	-1,19	-1,15
Spain	0.5	6,3	0,14	0,04	**1,8**	*3,0*		-1,22	4,55	-1,61	-1,71
Sweden	1.2	1,7	0,21	-0,45	**0,7**	*1,0*		0,53	1,04	-0,46	-1,12
Switzerland	2.6	4,2	0,33	-0,71	**1,6**	*2,2*		1,00	2,60	-1,28	-2,32
United Kingdom	2.3	3,0	0,72	-0,11	**1,5**	*1,4*		0,83	1,53	-0,77	-1,59
Yugoslavia	0.7	11,6	0,11	0,31	**3,2**	*5,6*		-2,49	8,42	-3,06	-2,87
Mean	**1.6**	**4,5**	**0,65**	**-0,06**	**1,7**	**2,0**	**Total**	**-6,4**	**69,1**	**-31,4**	**-49,9**
%StDev	45	42	64	-1042	42		StDev	15,4	2,4	2,9	-1,5

Table 9.5.3 summarises the NEP estimates generated with the four large-scale models, including a comparative analysis with respect to the country mean values for the four models. Though this does not give indications on the absolute accuracy of the NEP estimates, it certainly indicates the divergences between models per country as well as for Europe. Figures 9.5.5 and 9.5.6 essentially offer the same information as table 9.5.3, but give a more direct visual impression of the estimations and their divergences. Some of the key features drawn from table 9.5.3 and the figures just mentioned are the following. The mean NEP estimates for all countries for each of the models are 1.6 [Mg C/ha/y] for EFISCEN, 4.5 [Mg C/ha/y] for C-Fix 0.65 [Mg C/ha/y] for EuroBiota and -0.06 [Mg C/ha/y] for Hybrid. The results demonstrate that C-Fix elicits systematically higher NEP estimates as opposed to the other models. Hybrid is the only model which predicts Europe to be a source instead of a sink, but with a very large uncertainty as opposed to the other models. The right hand side of table 9.5.3 also demonstrates that C-Fix produces NEP estimates, which are significantly above the four model mean value for Europe. The same result is illustrated by figures 9.5.5 and 9.5.6. The overall mean value for Europe is 1.7 [Mg C/ha/y] with an uncertainty of 42%. This uncertainty has doubled when compared with that of the NPP estimate for Europe.

Another prominent feature in table 9.5.3 is that the uncertainty calculated for each model for all country estimates, is the highest for Hybrid (-1042%), the lowest for C-Fix (42%) and intermediate for Eurobiota and EFISCEN (respectively 64% and 45%).

Especially the estimates for Yugoslavia seem to represent an extreme outlier for C-Fix, distorting the overall uncertainty quite significantly. This can be illustrated by leaving out the results for that country. We then obtain mean NEP estimates for all countries for each of the models of 1.6 [Mg C/ha/y] for EFISCEN, 4.2 [Mg C/ha/y] for C-Fix 0.67 [Mg C/ha/y] for EuroBiota and -0.07 [Mg C/ha/y] for Hybrid with uncertainties which are much lower, respectively 44 %, 29 %, 61% and -851%. The uncertainty for the European NEP estimate is now 41 %. The uncertainty value for C-Fix now drops to a significantly lower value than when results of Yugoslavia are taken into account. Hybrid remains the model with the highest uncertainty on NEP estimations.

Another conspicuous result is that judging by the mean NEP values for all models, Norway again has a minimal country NEP value of 0.6 [Mg C/ha/y] with a standard deviation of 1.1 [Mg C/ha/y], and Luxemburg a maximal NEP of 3.8 [Mg C/ha/y] with a standard deviation of 2.3 [Mg C/ha/y]. All the other countries have values in between these two (I left out Yugoslavia in this comparison).

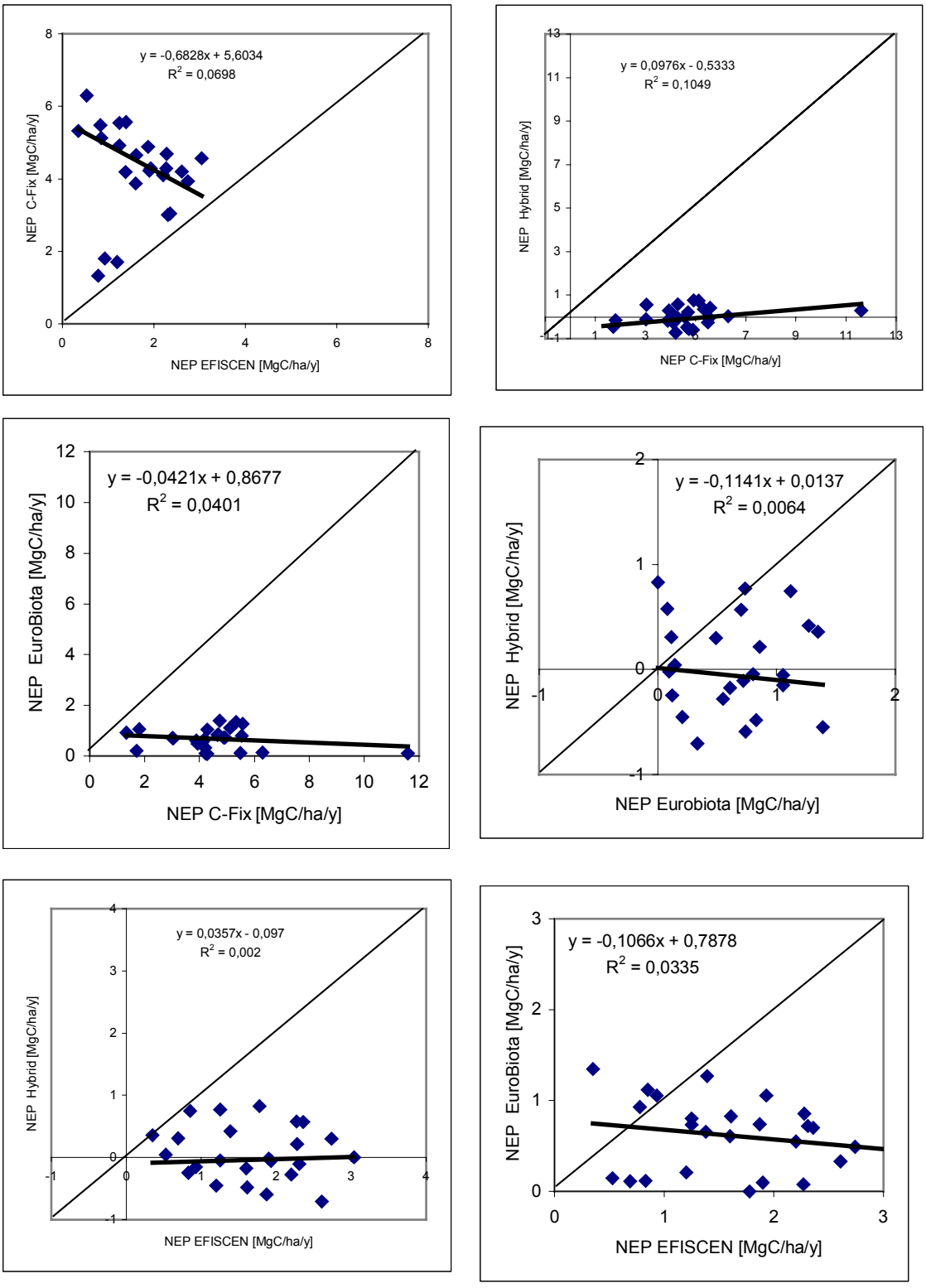

Figure 9.5.7: Cross correlation analysis between the four large-scale models for NEP. 1:1 lines are indicated as a reference along with R².

Figure 9.5.10 summarises a cross correlation analysis between the four models. Highest correlations for R_s are obtained between EFISCEN and EuroBiota with a R^2 of 0.28 (but the correlation is negative though) and to a lesser extent between EFISCEN and Hybrid with a R^2 of 0.1. EFISCEN correlates negatively with C-Fix and EuroBiota but a positive trend function with a weak correlation is observed between EFISCEN and Hybrid. EuroBiota and Hybrid correlate poorly and negatively.

Another aspect is the relation to the 1:1 line for the model R_s estimate comparisons. Most of the model trendlines in the correlograms deviate quite significantly from the 1:1 line except for the EFISCEN Hybrid relationship, which gets closest to the 1:1 line. This phenomenon is also emphasised in the previous results description (of table 9.5.4), where the variation around the mean value for all models is high (see also figure 9.5.9). Hence, deviations from the 1:1 line are more probable.

In conclusion, with respect to the 1:1 line, EFISCEN and Hybrid generate results of country R_s estimates, which match most closely the 1:1 line. The other model couples deviate strongly from the 1:1 line. With respect to R_s mutual correlation, EFISCEN and EuroBiota show the highest correlation coefficient of 0.28.

A general remark with respect to the results for calculated R_s described here is that even when higher correlations are observed between two models, these are not necessarily bound to generate the best estimate for R_s. The same is true with respect to the match of the trendline with the 1:1 line. The latter results merely indicate that some models generate results with are comparable at the R_s process description level (high R^2) or at the R_s value level (good match with the 1:1 line). A true test of the plausibility of the absolute R_s values generated by the models is a comparison with measured R_s fluxes. Since these do not exist at the country level, some if not all of the modellers actually test their models at the forest patch level using soil respiration measurements. Even then, no certainty exists that the comparison of R_s derived from measured data at patch level is representative for the country level R_s fluxes.

9.5.2.3 Discussion and conclusions

When carbon dioxide is exchanged between the atmosphere and vegetation by photosynthesis and respiration, the overall carbon balance can be obtained by summing up the gains and losses over a period of weeks or a year. To be able to make statements of the carbon balance of a continent, spatial scaling up must be performed. Typically mathematical models of empirical or of a more explicit deterministic nature are applied to reach this objective. In this chapter the results of four different models are presented, giving estimates of the NPP, NEP and soil respiration fluxes at the European continental level, with as basic spatial units the respective European countries. It has been stated earlier in this chapter that some of the models have the possibility to be applied at a finer spatial scale for example the 1-km^2 scale. The option has been taken however to resize the spatial units of three

models to the size of the model with the coarsest spatial unit e.g. the country level. This enabled the comparisons described in Chapters 9.5.3.1 and 9.5.3.2.

It has been illustrated that the basic forest cover maps for Europe still have a large uncertainty on forest area estimates and hence a large potential for improvement. The mere fact that different data sources of forest cover area are used in the LTEEFII large-scale models, represents a source of additional uncertainty for the estimates of NPP, NEP and soil respiration on top of the uncertainty introduced by differences in model design, the model basic theoretical concepts and the model input data quality. At least a mean uncertainty of 46 % on the forest surface area of Europe is to be taken into account when interpreting NPP, NEP and soil respiration flux results of the large-scale models. The method(s) used for performing forest area surveys, lead to forest area estimates, which elicit a strong numerical divergence. Many of the forest cover maps and basic data for Europe are based on remote sensing data. Hence, not only the land cover classification algorithms applied, but also the quality standards adopted in the satellite sensor pre-processing algorithms and pre-processing chains, as well as the spatial and multi-temporal resolutions selected by using different satellite sensors (NOAA/AVHRR, Landsat, SPOT/HRV), in short, all these factors play a crucial role in the final forest cover estimate accuracy. Typically a power law relationship between the magnitude and spatial scale of forest surface area variability is observed in figure 9.5.1, indicating that forest cover area is strongly and non-linearly spatially dependent. Hence, NPP, NEP and soil respiration fluxes can be expected to elicit the same non-linear behaviour in function of spatial scale. This is illustrated for NEP in figure 9.5.11. The relationship between the standard deviation on the country mean NEP value and country forest cover percentage, is highly non-linear and elicits a strong drop in variability with high country forest cover percentages. Figure 9.5.11 also implies that the most reliable estimates for NEP at the country level are obtained for those countries with the highest forest cover percentage, which intuitively makes sense. The two high forest cover countries, Sweden and Finland, have a country mean NEP of respectively 0.7 and 0.9 [Mg C/ha/y]. NPP is respectively 3.9 and 3.5 [Mg C/ha/y] and soil respiration respectively 3.2 and 2.6 [Mg C/ha/y]. This may indicate with a rather high probability, that these countries act as a sink to carbon on a yearly basis.

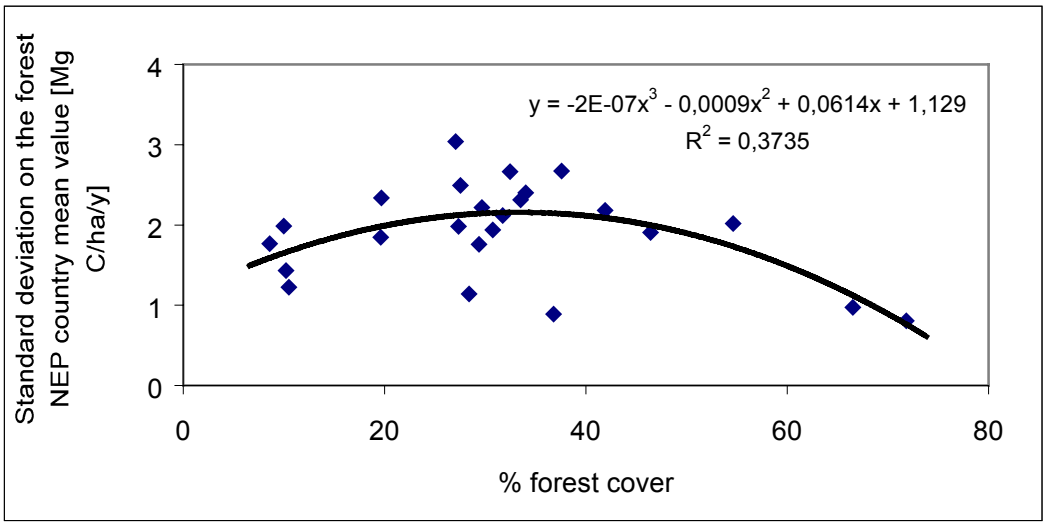

Figure 9.5.11: Standard deviation of country NEP in function of increasing forest cover percentage per country. The relationship is highly non-linear and elicits a strong drop in variability with high country forest cover percentages.

The overall mean NPP value for Europe is 5.4 [Mg C/ha/y] with an uncertainty of 25 %. This uncertainty drops to 23 % when Yugoslavia is left out of the dataset as an extreme outlier. The highest correlation is obtained between EFISCEN and EuroBiota with a R^2 of 0.28. Nevertheless the correlation is negative, hence when the EFISCEN NPP estimate increases, the EuroBiota NPP estimate decreases. This indicates a basic difference in behaviour of both models, under (environmental) conditions where NPP changes at the country level.

The overall mean value for European NEP is 1.7 [Mg C/ha/y] with an uncertainty of 42%. This uncertainty is significantly higher than for the NPP estimate. The uncertainty on the European NEP estimate does not drop much (to 41%) when Yugoslavia is left out of the dataset as an extreme outlier. One can conclude that none of the four models correlates mutually, to a satisfactory degree at the NEP level. The highest coefficient of determination is obtained for a weak NEP correlation between C-fix and Hybrid with a R^2 of 0.1. EFISCEN correlates weak and negatively with C-Fix and EuroBiota.

The overall mean value for European soil respiration is 3.7 [Mg C/ha/y] with an uncertainty of 32%. This uncertainty is in between that of NEP and NPP. When outliers are removed from the dataset the uncertainty remains unchanged. Highest correlations for R_s are obtained between EFISCEN and EuroBiota with a R^2 of 0.28 (but the correlation is negative though) and to a lesser extent between EFISCEN and Hybrid with a R^2 of 0.1. EFISCEN correlates negatively with C-Fix and EuroBiota but a positive trend function with a weak correlation is observed between EFISCEN and Hybrid. EuroBiota and Hybrid correlate poorly and negatively.

In conclusion, estimates of the basic carbon balance fluxes at the European level and at the country level have been made based on four different large-scale models. A strong scale dependency is observed for the forest area estimates as well as for the

carbon balance fluxes. The most reliable flux estimates are obtained for those countries with the highest percentage of forest cover. A European scale estimate has been generated as well, with an uncertainty on the fluxes which is high, due to a combination of strongly fragmented forests in Central, Eastern and Southern Europe, and hence, a strong scale dependency as well as an unsuitable (coarse) spatial resolution of the space borne sensors used to generate the forest cover estimates. Ideally, the spatial resolution of the model grid cells or RS observed *f*APAR should match that of the area estimates as well as that of the mean forest patch size in Europe, given the strong dependencies on spatial scale. Apparently, most published forest surface area data have been generated with unsuitable e.g., too spatially coarse sensor resolutions.

References

CORINE (Coordination de l'information sur l'Einvironment), 1997. Technical and Methodological Guide for Updating CORINE Land Cover, EEA/JRC; Brussels

ESA (European Space Agency), 1992. RemoteSensing Forest Map of Europe; ESA/ISY project report; ESTEC - European Space Research and Technology Centre; Noordwijk, The Netherlands

Häme T., Andersson K., Rauste Y., Väätäinen S., Lohi A., Stenberg, P, Sarkeala J, Kennedy P, Folving S. (1999): FIRS Forest Probability Map of Europe for 1997; AVHRR-based forest probability mapping and reference data collection; International Symposium on Digital Earth. Beijing, CN, 29 Nov. - 2 Dec. 1999. (CD). Science Press

Iremonger S., Ravilious C. Quinton T. (Eds.), 1997: A global overview of forest conservation; CD-ROM, WCMC and CIFOR, Cambridge U.K.

Loveland TR., Reed BC., Brown JF., Ohlen DO., Zhu J., Yang L., Merchant JW., 2000. Development of a Global Land Cover Characteristics Database and IGBP DISCover from 1-km AVHRR Data: International Journal of Remote Sensing, v. 21, no. 6/7, p.; 1,303-1,330. (See also http://edcdaac.usgs.gov/glcc/glcc.html)

Schelhaas, M.J., Varis, S., Schuck, A., Nabuurs, G.J., 1999. EFISCEN's European Forest Resource Database, European Forest Institute, Joensuu, Finland, http://www.efi.fi/projects/eefr/.

UN-ECE/FAO, 2000. Forest Resources of Europe, CIS, North America, Australia, Japan and New Zealand (industrialized temperate/boreal countries), UN-ECE/FAO Contribution to the Global Forest Resources Assessment 2000, Main Report, United Nations, New York and Geneva. 445 p.

10 Synthesis

Koen Kramer, Ilkka Leinonen & Frits Mohren

10.1 Introduction

The central objective of the LTEEF-II project, *Long-Term Regional Effects of Climate Change on European Forests: Impact Assessment and Consequences for Carbon Budgets*, was to assess long-term climate change impacts on European forests, in terms of water and carbon fluxes, regional differences, long-term effects, and the overall carbon budget for forests in Europe. The results of this assessment were aimed to be used to identify sustainable forest management strategies that account for these impacts, and that maximise carbon sequestration.

This was done by: A) Assessment and modelling of the long-term regional impacts of climate change on European forests, with emphasis on growth rates and water relations (drought), and on possible adaptive strategies for forest management, and by B) Upscaling of such regional responses to the European scale, to quantify the overall carbon budget and sustainable wood supply of European forests, at present and under future climate change.

The regional impact assessment includes: *i*) the assessment of likely responses of forests in the main climatic regions in Europe; *ii*) the quantification of changes in the timing and magnitude of fluxes of carbon and water between the vegetation and the atmosphere; *iii*) the assessment of possibilities of acclimation by means of self-regulating processes of existing forests; and *iv*) the identification of adaptive response strategies for forest management.

The upscaling to the European level include: *i*) maps of GPP, NPP and NEE of European forests on which national boundaries are superimposed; *ii*) an estimate of the carbon balance for the forest sector per country; and *iii*) assessments of timber production and forest carbon budgets per country under future climate scenarios, including estimates of carbon sink strength in case of aforestation.

10.2 Evaluation of process-based carbon balance models

For the study and quantitative analysis of probable effects of climate and other environmental changes on forests, and for the development of adaptive forest management strategies, mechanistic process-based models that include physiological processes sensitive to the effects of changes in temperature, precipitation, CO_2, nitrogen availability etc. are required. Models of this kind have been developed over the past decades, and are generally based on the carbon budget of the ecosystem, thereby distinguishing between tree biomass and soil carbon.

Evaluation of model performance consisted of the following tests:

(i) The calibration and testing of the model using process-based parameters from experimental work,
(ii) model comparison with eddy co-variance measurements,
(iii) comparison of predicted stand growth under current climatic conditions against long-term growth and yield data of permanent plots,
(iv) a sensitivity analysis to identify the climatic factors that critically determine the plants' growth given the physiological characteristics of the species, and
(v) an uncertainty analysis quantifying the forest response based on uncertainty in the inputs of the model.

In the following the testing of models against CO_2- and water flux data will be discussed; the short-term sensitivity of these fluxes to climate change scenario's; and the consequences of uncertainty in parameter values for the uncertainty of the model prediction of the fluxes. Next, the testing of the models against long-term growth and yield data will be discussed, as well as the sensitivity of the growth characteristics of the forest to climate change scenario's. No uncertainty analysis of input parameters was performed for long-term forest growth.

The database with ecophysiological parameters obtained from the EU-funded ECOCRAFT project was for use within the LTEEF community. This provided a rich source of independly estimated parameter values for many of the processes that are described by the process-based models used in LTEEF. For the model comparison it was aimed that models should have, whenever possible, the same parameter values obtained form this database. Another important source of information was made available by the EU-funded project EUROFLUX. The fluxes of CO_2 and water measured in this project for a number of forest sites throughout Europe enabled the detailed and independent testing of the process-based models at the stand level. Both the ECOCRAFT database and the EUROFLUX eddy covariance measurements made a critical testing and selection of the LTEEF models possible, and an assessment of which aspects of the models should be improved.

The results (see paragraph 4.3.1 and 4.4.1) indicated that there is generally a good correlation between the measured and predicted daily fluxes of net ecosystem exchange of carbon (NEE), but also that the goodness-of-fit systematically varied between sites. This is because the net carbon exchange is the result of two large fluxes, gross photosynthesis and total ecosystem respiration. The magnitude and trend in the response of these two fluxes to climatic variables, especially incoming radiation and temperature, are critical to assess the applicability of the models under changing environmental conditions. Several of the LTEEF-models were able to produce similar responses as observed. However, it should be noted that the quality of the eddy-covariance data and correction methods are still debated (see paragraph 4.3). Moreover, the datasets used do not represent all climatic conditions encountered all over Europe. There was no strong water stress influence in the data sets used. Thus the conclusions drawn from this exercise are limited to the boreal and northern temperate forests.

There was no independent source of information available on the impacts of climate change on the exchange of CO_2 and water between forests and the atmosphere. Therefore, a sensitivity analysis was performed by changing climatic parameters, including CO_2 and temperature, over pre-defined ranges to assess the sensitivity of the model's output to changes in these driving factors.

The results for the short-term sensitivity (see paragraph 4.3.4 and 4.4.2) of the CO_2 and water fluxes to climate change indicated that the responses critically depend on the parameter values of the photosynthesis and conductance submodels. These parameters determine the range of environmental conditions where photosynthesis at the leaf level is limited either by light or by CO_2 and thereby the response of the forest stand to changes in ambient CO_2 concentration. There are also critical differences in the temperature sensitivity of photosynthesis between species at the leaf level, that are directly integrated into differences in temperature sensitivity at the stand level (see also Ch 3). An accurate estimate of the photosynthetic parameters at the leaf level is therefore crucial for climate change impact assessments at much larger scales.

There is not only uncertainty in how climatic factors might change in the future, thereby affecting the future projection of the models, also the value input parameters are to some degree uncertain. E.g. due to natural variability, or due to the inability to measure the parameter with the required accuracy. However, uncertainty in different input parameters will not affect the model results to the same degree. An uncertainty analysis now aims to quantify the uncertainty of the forest response based on a estimate of the range of variation in the physiological parameters of the trees. As there are many parameters involved to describe a given process, this uncertainty analysis is preferably be done such that the relative importance of processes can be evaluated rather than that of single parameters. This analysis was done here for one species and by one model only.

The results of this analysis (paragraph 4.3.6 and 4.4.4) indicated that for the CO_2 flux, the output uncertainty depends mostly on uncertainty in the parameters that describe the CO_2- and light-responses of leaf-level photosynthesis (explaining 72% and 20% of the total output variability, respectively). For the water flux, the uncertainty in parameters characterising stomatal conductance is the major source of uncertainty (59%), followed by those characterising the CO_2 response of leaf photosynthesis (34%). Uncertainty in parameters characterising the dark respiration and temperature responses on photosynthesis explain less than 10% of the total uncertainty of both the CO_2 and water flux. However, it should be noted that the conclusions of such an uncertainty analysis are valid provided the accuracy of the range of parameter values. Moreover, there is unavoidably some degree of arbitrariness on how to lump parameters into groups.

As the models are aimed to be used to forecast long-term growth of forests they were tested under current climatic conditions by comparing the model output to long-term growth and yield data. This data is obtained in traditional forest growth and yield research and presented in local yield tables.

The result indicated (see paragraph 4.3.3 and 4.4.3) that most models are able to accurately predict the long-term evolution in number of trees, diameter at breast height, the basal area and height based on a given thinning regime. The prediction of the current annual increment (CAI) is problematic for those models that do not include age-related feedback in their description of the processes. For these models the CAI remains fairly constant over the entire simulation period, whereas CAI is known to decline with ageing of the forest. It should be noted that the models describe the development of a specific forest under specific climatic and site conditions, whereas the growth and yield tables present averaged values over many more or less similar forests.

The long-term consequences of changes of CO_2, temperature and precipitation on forest growth was evaluated by means of a sensitivity analysis. This was done for a number of models at one site. The variables evaluated include gross primary productivity (GPP), net primary productivity (NPP), current annual increment (CAI) and evapotranspiration (ET) .

The results indicated (paragraph 4.3.5 and 4.4.3) that most models are consistent in a positive response to an increase in atmospheric CO_2 concentration, and a negative response with declining precipitation. However, the sign of the response to temperature differs between models. This is due to differences between models in the sensitivity to temperature of photosynthesis and autotroph respiration. Models that include an age-related decline in productivity are also more likely to show a negative effect of temperature. The models differed in the predicted magnitude of the response of forest growth characteristics to the climatic factors. However, currently there is no data available to test the validity of the long-term responses.

10.3 Regional impact assessment

Effects of environmental changes on physiological processes and on seasonal pattern of growth rates were quantified, and integrated at both the forest level and the regional level over prolonged periods of time (years to decades). Three regions were characterised: boreal, temperate and Mediterranean, because there are regional differences in climate change over Europe that can be quantified using the current generation of global circulation models, and because growth of the forest types occurring in these regions differ in their control by climatic factors (e.g. temperature in the North of Europe; water availability in the South). For each region a limited number of forest types was characterised by the main tree species and the driving climatic factors on forest growth for each region (corresponding to the main forest types as used in national forest inventories in the region) and testing of relevant models for the defined forest types. Selected process-based models for each regions were used for the evaluation of forest growth and responses to climate change. Regional comparison of forest responses to both climate change scenarios and forest management strategies will then be performed, to quantify different flux control mechanisms and possibilities for adaptive forest management strategies.

This comprises:

(i) the use of regionally differentiated climate change scenarios (a/o through outcome of the LINK and ECLAT projects) and the forest management strategies per region and forest type;
(ii) regional impact assessment based on applying models to the selected forest types and to both climate change and management scenarios

The products provided by the regional impact assessment include:

(i) the assessment of likely responses of forests in the main climatic regions in Europe;
(ii) the quantification of changes in the timing and magnitude of fluxes of carbon and water between the vegetation and the atmosphere;
(iii) the assessment of possibilities of acclimation by means of self-regulating processes of existing forests; and
(iv) the identification of response strategies for forest management.

In the following, the applications of the process-based models in quantifying the effects of climatic change on the forest growth and carbon budgets at the site level are discussed. In Chapter 7, this was done with the focus on the separate physiological processes and selected species and sites, and in Chapter 8 by estimating the overall changes in growth rates over different regions of Europe.

The long-term changes in the climatic conditions have been predicted to affect forest growth for example through changes in the length of the growing season, allocation of carbohydrates, and the availability of water and nutrients (Chapters 7 and 8). These are also processes, the description of which differs strongly between the applied models (Chapters 2 and 3), and therefore are likely to be the source of the variation in the predicted growth responses. Since no systematic model comparison and evaluation at the level of these processes has been carried out, in many cases it is also not possible to evaluate the consistency of the predictions of growth changes between models.

In Chapter 8, the results of all applied models are presented separately for three regions: boreal, temperate and Mediterranean. For each of these regions, a limited number of representative forest types were used in modelling applications. Since the number of applied models varied between the sites, the results for each site and tree species were made comparable with each other by taking into account the systematic variation in the predictions of different models. The results showed that the specific climatic change scenario (Chapter 6), used in the model simulations, resulted predictions of increased forest growth at all these regions from year 1990 to 2070. Based on the corrected mean values of all sites, species and age classes, the highest growth increase was predicted for the boreal region (76 %). For the temperate and Mediterranean regions, the predicted increase was 53 and 62 %, respectively. Within each region, some variation in the model predictions between different sites was found. For example, at the northern boreal Scots pine site, the models predicted on average 85 % growth increase, while at the southern boreal site, the predicted increase for the same species was 61 %. However, compared to the variation

between sites, the variation between different models was much higher. For example, at the southern boreal Scots pine site, the applied 6 models produced a variation range of 106 percent units. At the northern boreal site (5 models applied), this range was even wider (128 percent units). In addition to the predicted growth rates, large variation between model predictions of the climatic change responses was found also in the case of other variables, such as maximum standing volume and litter production (Chapter 8.1-8.3).

The variation between the applied models in the predictions of the response of the processes of forest growth to the climatic change affects directly the upscaling results (Chapter 9). For example, in the upscaling method based on the forest inventory data and the large scale forest scenario model, the site-specific prediction of a single process-based model was extrapolated over larger area (Chapter 9.2). In this case, the predictions of the future forest carbon budgets for different regions and countries are strongly dependent on the selection of the applied process-based models. However, since the systematic variation in the model predictions is known, the model-related uncertainty in the upscaling results can also be quantified.

The discrepancy in the model predictions of the climatic change responses could not be expected on the basis of the results of model validation presented in Chapter 4. For example, when compared to the annual EUROFLUX estimates of GPP and respiration at the boreal Scots pine site, three models, COCA/FEF, FORGRO and HYDRALL, produced accurate estimates of these variables. In addition, all these models showed similar responses of daily carbon fluxes to temperature and radiation, and these responses were also in agreement with the measurements. Despite that, the predictions of these three models for the increase of stem growth of Scots pine at the southern boreal site from year 1990 to 2070 varied from 4 to 93%. Such results suggest that the model related uncertainty in the predictions of the climatic change impacts can not be considerably reduced by selecting the applicable models on the basis of short-term model validation.

Also in the comparison with long-term growth and yield tables (Chapter 4), the prediction of stem growth of several models was in agreement with the reference data. However, although these results can be used for validation of the age related growth changes, they are not sufficient to evaluate the reliability of the models when used for predictions of the climatic change responses, since the data from the growth tables do not include the effect of climatic variations.

The comparison of the regional differences in the variation of the model predictions shows that the best agreement between the models is found at the temperate region, where the average between-model variation in the predicted growth change was 67 percent units (Chapter 8.4). At the boreal and Mediterranean regions, this variation was considerable higher. These additional uncertainties are likely due to the ability of the models to predict the effects of air and soil temperature on the changes in the growing season length and nutrient availability at the boreal conditions. At the Mediterranean region, the predictions of the effects water availability are probably the most important factor causing differences between the models.

10.4 Upscaling to the European level

Upscaling from the regional to the European scale was performed to provide a dynamic carbon budget for European forests and to assess the possibility of increasing carbon storage, and the long-term wood supply in forest ecosystems, by means of silvicultural practices. Several methods of upscaling have been performed: based on national forest inventory data; based on biome scale modelling; and based on remote sensing data.
Upscaling forest inventory data to the European scale entails incorporating regional forest responses in the large scale forestry model, EFISCEN, by integrating and harmonising the outputs of the process-based models to adjust growth and yield curves in the EFISCEN model for the regional forest types considered. Subsequently, the current and future European carbon budget and wood production will be assessed based on the EFISCEN model, including total tree biomass, soil organic matter and wood products. Furthermore, forest management strategies aimed at mitigating possibly adverse impacts of climate change were defined and evaluated in term of European carbon budget and long-term wood supply.

Upscaling by biome scale modelling includes large scale vegetation modelling and how this is affected by temperature and atmospheric CO_2. Two approaches were applied: one that focusses on pools and fluxes of carbon and water through the soil-water-atmosphere continuum (EUROBIOTA), and one that focusses on the dynamic changes that occur in general vegetation types due to natural succession, and how this changes due to climatic change (HYBRID).

Upscaling by means of remote sensing will use the products of other European and international projects (FIRS, LINK) to derive surface conditions of incident radiation and climatic variables. These surface conditions will then be used to drive existing models capable of estimating gross primary productivity, GPP, net primary productivity, NPP, and net ecosystem gas exchange, NEE, of the selected forest types, with a resolution of 1 km^2.

The products promised by the upscaling to the European level contain:
(i) maps of GPP, NPP and NEE of European forests on which national boundaries are superimposed;
(ii) an estimate of the carbon balance for the forest sector per country;
(iii) simulated yield tables and timber production per country; and
(iv) an assessment of timber production and forest carbon budgets per country under future climate scenarios, including estimates of carbon sink strength in case of aforestration.

These products are described in detail in Chapter 9, whereas the approaches used are explained in chapter 5. In the following the results of upscaling by forest inventory data, GISMO's and RS will be outlined.

The effects of the climatic change on the forest carbon budgets at the European level were predicted by three models, EFISCEN, EuroBiota and Hybrid. Furthermore, EuroBiota and Hybrid provided also these results at the regional level and EuroBiota

at the country level. In the following, the results of these model concerning the predictions of net primary production, net ecosystem production, and tree and soil carbon stocks are discussed. Amongst the different scenarios applied in the connection of the EFISCEN model, the results of the Business as Usual scenario (no changes in the forest management or forest area) are presented here, since they are the most comparable with the results of other models. The results of Hybrid include all ecosystems, while other models have made predictions only for forests.

The results for the whole Europe show strong variation between different modelling approaches both in the predictions of the initial situation and in the effects of climatic change (Fig. 10.1). In the case of the net primary production, the lowest initial estimate is given by EFISCEN (400 Tg C/year [1005-200]) and the highest by Hybrid (1000 Tg C/year [1990]). In the predictions for the net ecosystem production, the situation is opposite. The estimate of EFISCEN is more than 5 times higher compared to the estimate of Hybrid. Thus, the variation in the model predicted heterotrophic respiration is much higher than the variation in the predictions of NPP. However, compared to all models the results of which are presented here, the most deviant prediction is made by the remote sensing approach (C-Fix model), which produced over 4 times higher estimate for the NEP of the European forest (year 1997) compared to the EFISCEN estimate (see Chapter 9.4)

Variation occurred also in the model estimates of carbon stock in Europe. In the case of the carbon stock in trees, EFISCEN and Hybrid produced the estimate of similar magnitude, while the estimate of EuroBiota was considerable higher. For the soil carbon stock, the EFISCEN estimate was much lower compared to both EuroBiota and Hybrid (Fig. 10.2).

All models predicted a slightly increasing trend in the changes of NPP from year 1990 to year 2050. The relative increase was highest in the prediction of EFISCEN (20 %). In the case of NEP for the same time period, EFISCEN predicted slight decrease, Eurobiota predicted no changes, whilst Hybrid predicted strong relative decrease (over 60 %).

The models predicted only small changes in the tree and soil carbon stocks from year 1990 to 2050. Relatively highest increase in the tree carbon stock was predicted by Hybrid (25 %). For the soil carbon stock, EFISCEN predicted the highest relative increase (8 %).

The effect of different forest management scenarios on the European carbon budgets were also included in the simulations carried out with the EFISCEN model. The results show that the differences between the Business as Usual management scenario and the Multifunctional scenario (see Chapter 9.2) in both NPP and NEP are considerable smaller compared to the changes caused by the climatic change.

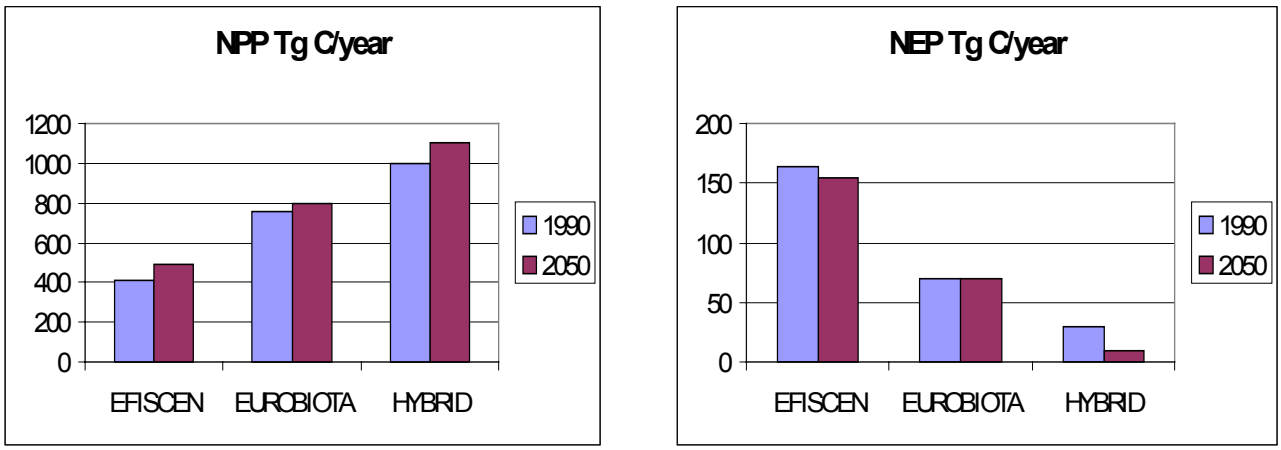

Figure 10.1. The predictions of the upscaling models for the net primary production and the net ecosystem production of European forests (EFISCEN and EuroBiota) and all European ecosystems (Hybrid) for years 1990 (EFISCEN results for years 1995-2000) and 2050.

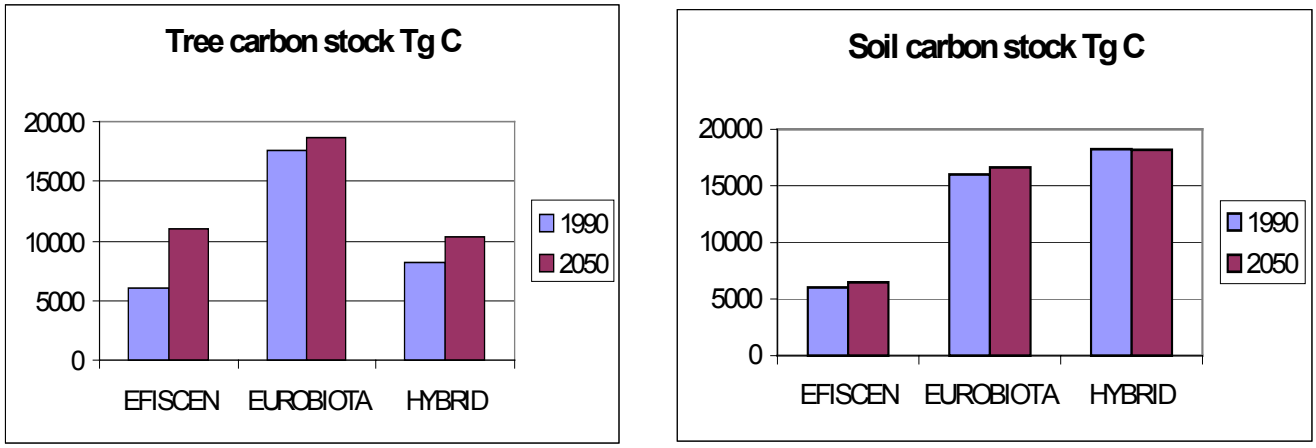

Figure 10.2. The predictions of the upscaling models for the tree and soil carbon stocks of European forests for years 1990 and 2050.

The models EuroBiota and Hybrid differed also in their predictions of the changes of regional carbon fluxes from year 1990 to 2050 (Chapter 9.3). Hybrid predicted the highest increase in NPP at the boreal region and strong decrease at the Mediterranean region as a result of the climatic change. The results of EuroBiota showed the highest NPP at the boreal and lowest at the temperate regions, with very low response to climatic change. For NEP, EuroBiota predicted slightly increasing trend at the boreal region and decrease especially at the Mediterranean region. In the results of Hybrid, the decrease of NEP at the Mediterranean region was considerably stronger and resulted to negative carbon budgets for this region.

The effects of the climatic change on the net ecosystem production was predicted at the country level by the EuroBiota model. For 18 countries, the NEP was predicted to increase and for 16 countries to decrease. Concerning the predicted future conditions, no comparison between other models at the country level could be carried out. However, the country level estimates of carbon exchange for the initial

(year 1990) situation from all large scale models (C-Fix, EFISCEN, EuroBiota and Hybrid) are presented in Chapter 9.5. Generally, there were large systematic differences between models in their country-specific predictions of NPP, NEP and heterotrophic respiration, and in pair-wise comparison, usually no correlation between models was found in the case of all these variables. The relative standard deviation between the country specific model predictions of NEP was on average 85 %, and for those countries where all models were applied, it varied between 67 % (United Kingdom) and 129 % (Yugoslavia). For NPP, the average standard deviation was 61 % and corresponding minimum and maximum 18 % (Luxembourg) and 102 % (Yugoslavia), respectively. Such strong variation in the estimates of the initial conditions can be considered to be one of the main sources for the uncertainties observed in the model prediction